
The University Of Sheffield.

# TERT-dependent senescence and inflammation in ageing, using zebrafish as a model

Raquel Rua Martins

A thesis submitted in partial fulfilment of the requirements for the degree of Doctor of Philosophy

The University of Sheffield
Faculty of Medicine, Dentistry and Health
Department of Oncology and Metabolism

May 2020

## Acknowledgements

This journey wouldn't have been possible without the support of key people that have been part of my life for the past 3 years and 8 months. Thus, I would like to acknowledge them.

To my supervisor, Dr. Catarina Henriques. Thank you for believing in me, for giving me the freedom to develop as a researcher and guiding me throughout this journey. It has been a great pleasure to work with such an enthusiastic, pragmatic and team-player person as you are!

To my second supervisor, Professor Ilaria Bellantuono. Thank you for being a good mentor, especially during the last and most challenging part of my PhD. Thank you for all the scientific discussions and career advices!

To collaborators that participated in this journey. Thank you, Dr. Ryan McDonald, for the opportunity of participating in a project on retina degeneration, which became a big part of my thesis and will lead to a publication; Dr. Micheal Rera, for trusting in me to validate the smurf assay in zebrafish by gavage, which led to a publication; Dr. will Norton, for kindly sharing your Ethovision software so that I could analyse the behavioural data of my project.

To the current and former members of the lab. Thank you for being part of this journey: Luke Mansfield, Nadiyah Mughal, Fatin Giman, Emily Thompson, Ricardo Novoa. A special thank you to Pam Ellis who has been a great partner in the lab and a very kind and patience teacher. Thanks for sharing your passion and expertise in molecular biology, and for all the scientific and less scientific discussions that contributed to keep my head up during my PhD!

To my dear friend Ana Faustino. Your enthusiasm, ambition, resilience, and genuine passion for science have been a true inspiration to me since I met you. Thank you for all your encouragement even before I started applying to my PhD. Thank you for being always there (since day -1!), for being so insightful, and for always having the right piece of advice to give!

To my friends and family. Thank you for your curiosity about my research, for listening, for sharing your own experiences, and for bringing so much joy into my life!

To my mum. Thank you for your unconditional support, for picking my calls at any time, for listening patiently even without fully understanding it, and for always persuading me to achieve my goals!

To my husband, João. Thank you for being always by my side, for motivating me to pursue my objectives, for helping me to overcome obstacles and for being always ready to celebrate every single achievement! And of course, thank you so much for patiently sharing your expertise in excel with me, that was really useful during my PhD.

## Declaration

I, the author, confirm that the Thesis is my own work. I am aware of the University's Guidance on the Use of Unfair Means (www.sheffield.ac.uk/ssid/unfair-means). This work has not been previously been presented for an award at this, or any other, university.

This thesis has been written in an alternative format ("Thesis including published works – or works formatted with the intention or possibility of publication), including one Chapter in article format (*Chapter 3*) and three Chapters in a "traditional" or monograph format (*Chapter 4* , *Chapter 5* and *Chapter 6*). The reason for this is that one chapter was already being written for publication purposes when this thesis was written. Details on authors contributions regarding *Chapter 3* can be found in *section 3.1*.

The work carried out during this project has led / will lead to the following publications and presentations:

Publications

- **Raquel R. Martins**, Pam S. Ellis, Ryan B. MacDonald, Rebecca J. Richardson, Catarina M. Henriques (2019). Resident Immunity in Tissue Repair and Maintenance: The Zebrafish Model Coming of Age. Front. Cell Dev. Biol. doi: 10.3389/fcell.2019.00012.
- **Raquel R. Martins**, Andrew W. McCracken, Mirre J. P. Simons, Catarina, M. Henriques, Micheal Rera (2018). How to Catch a Smurf? Ageing and Beyond...In vivo Assessment of Intestinal Permeability in Multiple Model Organisms. Bio-Protocols. doi: 10.21769/BioProtoc.2722.
- **Raquel R. Martins** (under review). Behaviour in Zebrafish. Book Chapter in Zebra Fish.
- Pam S. Ellis, **Raquel R. Martins**, Catarina M. Henriques (under review). Adult Zebrafish as a vertebrate model of ageing. Book Chapter in Zebra Fish.
- **Raquel R. Martins**, Ryan B. MacDonald, Catarina M. Henriques (in preparation). Deciphering the potential roles for telomere-associated senescence and inflammation in neurodegeneration - can zebrafish help? Review Article to be submitted in FEBS.

- **Raquel R. Martins**, Mazen Zamzam, Mariya Moosajee, Ryan Thummel, Catarina M. Henriques, Ryan B. MacDonald (in preparation). Age-related retinal degeneration is insufficient to stimulate the Müller glia regenerative response in zebrafish, leading to gliosis and loss of vision. To be submitted in ELife.

Abstracts

- **Raquel R. Martins**, Nadyiah Mughal, Ilaria Bellantuono, Catarina M. Henriques (2019). Telomerase-dependent senescence and inflammation with ageing in the zebrafish brain. Brain, Behavior and Immunity. doi.org/10.1016/j.bbi.2019.08.029

Oral presentations

- **Raquel R. Martins**, Pam S. Ellis, Nadyiah Mughal, Ilaria Bellantuono, Catarina M. Henriques. "Telomerase-dependent senescence and inflammation with ageing in the zebrafish brain". Blitz session at FENS regional meeting 2019, Belgrade, Serbia (July 2019).
- **Raquel R. Martins**, Pam S. Ellis, Nadyiah Mughal, Ilaria Bellantuono, Catarina M. Henriques. "Telomerase-dependent senescence and inflammation in the aged zebrafish brain". At the University of Sheffield Medical School Annual Research Meeting, Sheffield, UK (June 2019).
- **Raquel R. Martins**, Pam S. Ellis, Nadyiah Mughal, Ilaria Bellantuono, Catarina M. Henriques. "Telomerase-dependent senescence and inflammation in the aged zebrafish brain". At the PNIRS and GEBIN Meeting, Berlin, Germany (June 2019).
- **Raquel R. Martins**, Pam S. Ellis, Nadyiah Mughal, Ilaria Bellantuono, Catarina M. Henriques. "Telomerase-dependent senescence and inflammation in the aged zebrafish brain". At the Sinfonia Symposium, Sheffield, UK (March 2019).
- **Raquel R. Martins** and Catarina M. Henriques. "Senescence and inflammation in ageing, using zebrafish as a model". At the University of Sheffield Medical School Biological Services talk series, Sheffield, UK (October 2018).

- **Raquel R. Martins,** Pam S. Ellis, Nadyiah Mughal, Emily J. Thompson, Ilaria Bellantuono, Catarina M. Henriques. "Telomerase-dependent senescence and inflammation in the aged zebrafish brain". Bateson Centre BCORS talk series, Sheffield, UK (October 2018).
- **Raquel R. Martins,** Ilaria Bellantuono, Catarina M. Henriques. "Inflammation in ageing, using zebrafish as a model - is your 'gut feeling' making your brain old?" University of Sheffield Melanby Seminar talk series, Sheffield, UK (2017).

Poster presentations

- Ryan B. MacDonald, **Raquel R. Martins,** Mariya Moosajee, Catarina M. Henriques. "Age-related retinal changes in zebrafish mimics human disease pathogenesis". At the International Congress on Precise Medicine, Munich, Germany (October 2019).
- **Raquel R. Martins**, Pam S. Ellis, Nadyiah Mughal, Ilaria Bellantuono, Catarina M. Henriques. "Telomerase-dependent senescence and inflammation with ageing in the zebrafish brain". At the FENS Regional Meeting 2019, Belgrade, Serbia (July 2019).
- **Raquel R. Martins**, Pam S. Ellis, Nadyiah Mughal, Ilaria Bellantuono, Catarina M. Henriques. "Telomerase-dependent senescence and inflammation with ageing in the zebrafish brain". At the PNIRS and GEBIN Meeting, Berlin, Germany (June 2019).
- **Raquel R. Martins,** Pam S. Ellis, Nadyiah Mughal, Ilaria Bellantuono, Catarina M. Henriques. "Telomerase-dependent senescence and inflammation with ageing in the zebrafish brain". At the University of Sheffield Medical School Annual Research Meeting, Sheffield, UK (June 2018).
- **Raquel R. Martins,** Pam S. Ellis, Emily J. Thompson, Ilaria Bellantuono, Catarina M. Henriques. "Inflammation in ageing using zebrafish as a model - is your 'gut feeling' making your brain old?" At the University of Sheffield Medical School Annual Research Meeting, Sheffield, UK (September 2017).
- **Raquel R. Martins**, Pam S. Ellis, Emily J. Thompson, Ilaria Bellantuono, Catarina M. Henriques. "Inflammation in ageing using zebrafish as a model - is your 'gut feeling' making your brain old?" At the University of Sheffield Medical School Annual Research Meeting, Sheffield, UK (June 2017).

- **Raquel R. Martins**, Ilaria Bellantuono, Catarina M. Henriques. “Inflammation in ageing using zebrafish as a model - is your 'gut feeling' making your brain old?” At the University of Sheffield Annual Bateson Away Day, Sheffield, UK (November 2016).

Moreover, one side project where I participated during my PhD lead/ will lead to the following publications and has led to the following poster presentations:

Publications (work in progress)

- Pam S. Ellis, **Raquel R. Martins**, Asma Farhat, Emily J. Thomson, Ilaria Bellantuono, Stephen A. Renshaw, Catarina M. Henriques (in preparation). Zebrafish gut macrophages have telomerase-dependent “hyper-long” telomeres and require telomerase for function.

Poster presentations

- Pam S. Ellis, **Raquel R. Martins**, Asma Farhat, Emily J. Thompson, Bernard Corfe, Ilaria Bellantuono, Stephen A. Renshaw, Catarina M. Henriques. “Gut-associated leukocytes have telomerase-dependent hyper-long telomeres and require telomerase for function “. At the Fish Vaccination Workshop, Netherlands (April 2017).
- Pam S. Ellis, Asma Farhat, Emily J. Thompson, **Raquel R. Martins**, Bernard Corfe, Ilaria Bellantuono, Stephen A. Renshaw, Catarina M. Henriques. “Gut-associated leukocytes integrate the stem cell niche in the adult zebrafish gut and require telomerase for function”. At the University of Sheffield Annual Bateson Away Day, Sheffield, UK (November 2016).

## Abstract

Uncovering the mechanisms underlying ageing of the central nervous system (CNS) is crucial to identify therapeutic targets to promote healthy ageing. Although the CNS is considered predominantly post-mitotic, it has been suggested that telomerase, mostly known for its role in cell division through maintenance of telomere length, has a protective role against cellular senescence. However, the mechanisms underlying this remain unclear. Here, I aimed to determine telomerase-dependent mechanisms of ageing in the CNS, particularly in the retina and the brain. To do so, I used wild-type zebrafish alongside with the telomerase-mutant (*tert*$^{-/-}$) zebrafish model.

This study shows that zebrafish display retina degeneration and visual impairment with ageing, and that these occur in a telomerase independent manner. Despite preserving its regenerative capacity in response to acute damage until old ages, rather than regeneration, the aged zebrafish retina undergoes gliosis, like in humans. This highlights zebrafish as a suitable model to explore relevant mechanisms to neurodegeneration in the human retina, during ageing, pointing to gliosis as a key target to explore endogenous regeneration mechanisms.

When looking at the brain, this study shows an accumulation of senescence markers, specifically in the diencephalon and cerebellum. Contrasting with the retina, in the brain, these hallmarks were accelerated in the *tert*$^{-/-}$ model, suggesting that TERT exerts a protective role against accumulation of senescence in the aged brain. Here, I also identify a set of genes potentially involved in TERT-dependent senescence in the ageing brain, but further investigation is required to test whether the expression of these genes delay accumulation of senescence in the aged zebrafish brain.

Together, this opens new lines of investigation on telomerase-dependent and independent mechanisms of ageing, pointing to zebrafish as a valuable model to further explore potential therapeutic targets aiming to ameliorate retina and brain degeneration with ageing.

## Table of Contents

## List of Tables

## List of Figures

## Abbreviations

| ACRONYM | DEFINITION |
|---|---|
| **A2E** | N-retinylidene-N-retinylethanolamine |
| **AC** | Amacrine cell |
| **AD** | Alzheimer's disease |
| **ALS** | Amyotrophic lateral sclerosis |
| **AMD** | Age-related macular disease |
| **ATM** | Ataxia telangiectasia mutated |
| **B** | Blank |
| **BBB** | Blood-brain barrier |
| **BC** | Bipolar cell |
| **BCA** | Bicinchoninic acid |
| **BLM** | Bloom Syndrome |
| **BMK-1** | BimC subfamily of kinesin-1 |
| **BMS** | Biomedical Science |
| **BP** | Base-pair |
| **BRDU** | 5-BRomoDeoxyUridine |
| **BSA** | Bovine serum albumin |
| **CDK** | Cyclin-dependent kinase |
| **CDKI** | Cyclin-dependent kinase inhibitor |
| **CDKN1A** | Cyclin-dependent kinase inhibitor 1A, or p21 |
| **CDKN2A** | Cyclin-dependent kinase inhibitor 2A, or $p16^{INK4a}$ |
| **CE** | Cerebellum |
| **CK** | Cockayne Syndrome |
| **CMZ** | Ciliary marginal zone |
| **CNS** | Central nervous system |
| **CT** | Cycle threshold |
| **DAPI** | 4',6-diamidino-2-phenylindole |
| **DE** | Differentially expressed |
| **DDR** | DNA-damage responses |
| **DI** | Discrimination index |
| **DIE** | Diencephalon |
| **DKC** | Dyskeratosis congenita |
| **DKC1** | Dyskeratosis congenita 1 |
| **DL** | Dorsal lateral |
| **DPF** | Days post-fertilisation |

| | |
|---|---|
| **DQ** | Dasatinib and Quercetin |
| **DSB** | DNA Double-strand breaks |
| **DS CDNA** | Double-stranded cDNA |
| **EDU** | 5-Ethynyl-2'-deoxyuridine |
| **EDTA** | Ethylenediaminetetraacetic acid |
| **ENU** | N-Ethyl-N-nitrosourea |
| **FDR** | False discovery rate |
| **FISH** | Fluorescence in situ hybridisation |
| **FITC** | Fluorescein isothiocyanate |
| **FOV** | Field of View |
| **G** | Guanine |
| **GABA** | Gamma-aminobutyric acid |
| **GAR1** | GAR1 ribonucleoprotein |
| **GATA1** | GATA-binding factor 1 |
| **GBA** | Glucocerebrosidase |
| **GCL** | Ganglion cell layer |
| **GFAP** | Glial fibrillary acidic protein |
| **GFP** | Fluo-green fluorescent protein |
| **GOI** | Gene of interest |
| **GRO** | Growth Regulated Oncogene |
| **GS** | Glutamine synthetase |
| **G4** | Generation 4 |
| **G6** | Generation 6 |
| **$H_2O_2$** | Hydrogen peroxide |
| **HBSS** | Hanks' Balanced Salt solution |
| **HC** | Horizontal cell |
| **H&E** | Haematoxylin & eosin |
| **HGF** | Hepatocyte Growth Factor |
| **HPL** | Hours post-light damage |
| **HRP** | Horseradish peroxidase |
| **HSC** | Hematopoietic stem cell |
| **HUVEC** | Human umbilical vein endothelial cell |
| **IF** | Immunofluorescence |
| **IGF1** | Insulin-like growth factor 1 |
| **IGFBP** | Insulin-like Growth Factor-Binding Protein |
| **IHC** | Immunohistochemistry |
| **IHF** | Immunohistochemistry |

| | |
|---|---|
| **IL6** | Interleukin-6 |
| **IL8** | Interleukin-8 |
| **INL** | Inner nuclear layer |
| **IPF** | Idiopathic pulmonary fibrosis |
| **IPL** | Inner plexiform layer |
| **ISP** | Individual study plan |
| **KB** | Kilobase |
| **LMF** | Light Microscopy Facility |
| **LPS** | Lipopolysaccharide |
| **MCP-2** | Monocyte chemoattractant protein-2 |
| **MEF** | Mouse embryonic fibroblasts |
| **MG** | Müller glia |
| **$MGCL_2$** | Magnesium chloride |
| **MHC** | Major histocompatibility complex |
| **MIP-3A** | Macrophage Inflammatory Protein-3 |
| **MMP-1** | Matrix metalloproteinase 1 |
| **MMP-3** | Matrix metalloproteinase 3 |
| **MMP-12** | Matrix metalloproteinase 12 |
| **MO** | Medulla oblongata |
| **MS-222** | Tricaine mesylate-222 |
| **4-MU-CHITOTRIOSIDE** | 4–methylumbelliferyl–β-D-N, N', N"-triacetylchitotriose |
| **NAD** | Nicotinamide adenine dinucleotide |
| **NFKB** | Nuclear factor kappa B |
| **NHP2** | Nucleolar protein family A member 2 |
| **NOP10** | NOP10 ribonucleoprotein |
| **NOR** | Novel object recognition |
| **NOT** | Novel object test |
| **NPC** | Neural progenitor cell |
| **NSC** | Neural stem cell |
| **OB** | Olfactive bulb |
| **OCT** | Optimal cutting temperature |
| **OF** | Open field |
| **OHT** | Hydroxytamoxifen |
| **OKR** | Optokinetic response |
| **ON** | Overnight |
| **ONL** | Outer nuclear layer |
| **OPL** | Outer plexiform layer |

| | |
|---|---|
| **OT** | Optic tectum |
| **PADJ** | P-value adjusted |
| **PBS** | Phosphate buffered saline |
| **PC** | Purkinje cell |
| **PCA** | Principal component analysis |
| **PCL** | Purkinje cell layer |
| **PCNA** | Proliferating cell nuclear antigen |
| **PCR** | Polymerase chain reaction |
| **PD** | Parkinson's disease |
| **PDGF-AA** | Platelet-derived growth factor-AA |
| **PFA** | Paraformaldehyde buffered |
| **PGZ** | Periventricular grey zone |
| **PKC** | Protein kinase C |
| **PNA** | Peptide nucleic acid |
| **POT1** | Protection of telomere 1 |
| **PPI** | Protein-protein interaction |
| **PR** | Photoreceptor |
| **PUMA** | Mediated by p53 upregulated modulator of apoptosis |
| **P38MAPK** | p38 mitogen-activated protein kinases |
| **RAP1** | Repressor/activator protein 1 |
| **RB** | Retinoblastoma protein |
| **REF** | Reference |
| **RGC** | Retinal ganglion cell |
| **RIN** | RNA integrity number |
| **ROS** | Reactive oxygen species |
| **RNA SEQ** | RNA Sequencing |
| **RPE** | Retinal pigment epithelium |
| **RPESC** | Retinal pigment epithelium stem cell |
| **RT** | Room temperature (when in Chapter 2, only) |
| **RT** | Reverse transcriptase |
| **RT-QPCR** | Quantitative reverse transcription polymerase |
| **SA-β-GAL** | Senescence-associated β-Galactosidase |
| **SAMP8** | Senescence-accelerated mouse prone 8 |
| **SASP** | Senescence-associated secretory phenotype |
| **SEM** | Standard error of the mean |
| **SGZ** | Sub-granular zone |
| **SITRAN** | Sheffield Institute for Translational Neuroscience |

| | |
|---|---|
| **snoRNA** | Small nucleolar RNA |
| **SOCS** | Couple suppressor of cytokine signalling |
| **SPI1** | Transcription factor PU.1 |
| **SSC** | Saline-sodium citrate |
| **STEM** | Short Time-series Expression Miner |
| **SVZ** | Sub-ventricular zone |
| **T** | Test |
| **TE** | Tris-EDTA |
| **TEL** | Telencephalon |
| **TERC** | Telomerase RNA component |
| **TERT** | Telomerase reverse transcriptase |
| **TGFβ1** | Transforming growth factor β1 |
| **TIN2** | TRF1 and TRF2 interacting nuclear protein 2 |
| **TM** | Melting temperature |
| **TNFα** | Tumour necrosis factor alpha |
| **TOD** | Time of death |
| **TPP1** | Adrenocortical dysplasia protein homolog; RAP1 |
| **TRF** | Telomere restriction fragment |
| **TRF1** | Telomere repeat binding 1 |
| **TRF2** | Telomere repeat binding 2 |
| **TS** | Time spent |
| **TUNEL** | Terminal deoxynucleotidyl transferase dUTP nick end labelling |
| **UK** | United Kingdom |
| **VEGF** | Vascular endothelial growth factor |
| **VTA** | Ventral tegmental area |
| **VV** | Ventral nuclei of the ventral telencephalon |
| **WT** | Wild type |
| **WRM** | Werner syndrome |
| **γH2AX** | H2A histone family member X phosphorylated at serine 139 |

# Chapter 1.
# Introduction

## 1.1 Ageing

People are now living longer than ever before, as life expectancy has been increasing. In the European Union, life expectancy increased almost 10 years in the past 5 decades and it is predicted to increase another 7 years until 2060, reaching the 84 years of age in man and the 89 years of age in women (European Commission Directorate-General for Economic and Financial Affairs, 2015). In the United Kingdom (UK), the lifespan increase of the past decades has stalled since 2010. Whilst from 1980 to 2010 life expectancy in the UK increased 1 year every 6 years, nowadays it takes on average 21.5 years (15 in man and 28 in women) to increase life expectancy by 1 year (Michael et al., 2020). If this rate is to be maintained, then it is expected that life expectancy in the UK will increase by 2.8 years for man and 1.5 year for women, reaching the 82.4 and 84.7 years of age, respectively, by 2060.

The drawback of an increased life expectancy is that with ageing comes disease and therefore people are now living longer with the burden of age-associated diseases. Indeed, ageing can be defined as a gradual accumulation of damage that leads to a functional decline of the organism (López-Otín et al., 2013), increasing vulnerability to chronic diseases and probability of death (Barnett et al., 2012; Cutler & Mattson, 2006; Marengoni et al., 2014). In particular after the age of 65, the incidence of chronic diseases such as hypertension, dementia, arthritis, heart diseases, and visual impairments, increases dramatically (Alessandra et al., 2009; Partnership for Solution, 2004). Importantly, the percentage of over 65's with multimorbidity, i.e. co-occurrence of more than 1 disease (Fortin et al., 2004), reaches about 60% (Barnett et al., 2012; Vogeli et al., 2007). Chronic disease refers to a permanent, non-reversible condition that affects a person both physically and mentally, leading to an increased risk of disability and hampering the daily-life activities (Partnership for Solution, 2004). Hence, age-associated chronic diseases have a strong negative impact in the quality of life as well as in the medical care costs of the elderly. In fact, the European average of care expenditure *per capita* by age doubles between 65 and 90 years old (European Commission Directorate-General for Economic and Financial Affairs, 2015). Similarly, in the UK, it is estimated that the NHS care costs increase from ca.£1,000 to ca.£2,000-2,500, between the age groups of 65 and >85 (Angele, 2018).

Considering this, it is urgent to prevent age-related diseases in order to promote health in ageing, so that people may live healthier for longer ('healthspan') (Tinetti et al. 2012). Longer

healthspan would reduce the age-associated negative impact on people's quality of life and on the socio-medical economy. To achieve this, it is essential to understand the mechanisms underlying the ageing process and that predispose people to multiple chronic diseases of ageing. Highlighting this urge, the Corporate Plan 2014-2015 of the UK Department of Health set research into "ageing well" as one of the top-3 priorities (Unit & Health, 2014) and the Horizon 2020 (Work plan 2018-2020) framework is aiming to develop research and techniques to promote healthy ageing (Commission, 2018).

## 1.2 Hallmarks of ageing

With ageing, cells and tissues undergo several molecular alterations that contribute to the impairment of tissue homeostasis, leading to progressive tissue degeneration. These alterations include genome instability, epigenetic modifications, loss of proteostasis, and telomere shortening, known as primary hallmarks of ageing (López-Otín et al., 2013). Accordingly, premature ageing syndromes (progerias) are underlined by accumulation of DNA damage and impairment of DNA repair (Burtner & Kennedy, 2010; Mostoslavsky et al., 2006), aberrant DNA methylation (Heyn et al., 2013), loss of proteostasis (Alupei et al., 2018; Gabriel et al., 2016) and telomere dysfunction (Armanios et al. 2009; Zhong et al. 2011).

The primary hallmarks of ageing do not occur isolated and are instead known to interact with and affect each other in multiple ways. For example, the exposure to cellular extrinsic factors such as radiation and chemicals, as well as cellular intrinsic factors such as Reactive Oxygen Species (ROS) and DNA replication errors, threat genomic and mitochondrial DNA, contributing to accumulation of DNA damage and consequent genome instability (López-Otín et al., 2013; Moskalev et al., 2013; Ovadya & Krizhanovsky, 2014). Indeed, mutations in genes encoding for key enzymes involved in DNA repair and DNA maintenance cause progeroid syndromes such as Werner Syndrome (WRM), Bloom Syndrome (BLM), Cockayne Syndrome (CK) and Dyskeratosis congenita (DKC) (Burtner & Kennedy, 2010).

With ageing, there are also epigenetic alterations, including changes in DNA methylation patterns and chromatin remodelling (Talens et al., 2012), which contribute to structural and functional alterations in the genome, reinforcing this DNA damage cycle (Zhang et al. 2016; Moskalev et al. 2013). Moreover, with ageing, there is deterioration of the ability to regulate

protein homeostasis (proteostasis), which can either lead to a loss of function or gain of toxic function, affecting cell function and causing disease (Koga et al., 2012; Powers et al., 2009). De-regulated proteostasis may impair the DNA-repair machinery, promoting genomic instability and contributing to DNA damage accumulation (Jackson & Bartek, 2010). Importantly, due to its G-rich regions, telomeres are favoured sites for accumulation of DNA damage where, contrary to other DNA regions, DNA damage is not efficiently repaired (Hewitt et al., 2012). This means that ROS-induced DNA damage can cause telomere damage and rapid telomere attrition, contributing, in turn, to more DNA-damage responses (DDR). This can therefore create a positive feedback loop generating more genomic instability (Kim et al., 2016; Rossiello et al., 2014). Adding to this telomere damage, it is well described that telomeres shorten with age (Allsopp et al., 1995; Heidinger et al., 2012; Moyzis et al., 1988), which will be detailed in *section 1.2.1*.

### 1.2.1 Telomeres and telomerase: structure and function

Telomeres are specialised structures that constitute the tips of linear chromosomes in eukaryotes, comprising repetitive TTAGGG sequences of DNA (Moyzis et al., 1988). In humans, telomeres consist of 2-30 kilobase (kb)-long double-stranded DNA repeats, presenting a single-stranded 100-200 nucleotide-long 3' overhang, termed 3' Guanine- or G-overhang (Lange, 2004) (**Fig 1.1A, left**). Telomeres are associated with a protein complex, known as Shelterin, essential for telomere protection and function. This protein complex is organised in 6 distinct subunits, including telomere repeat binding 1 (TRF1), telomere repeat binding 2 (TRF2, or TRFA in zebrafish), protection of telomere 1 (POT1), repressor/activator protein 1 (RAP1), TRF1 and TRF2 interacting nuclear protein 2 (TIN2) and adrenocortical dysplasia protein homolog (TPP1) (Palm & Lange, 2008; Wagner et al., 2017) (**Fig 1.1A, left**). The Shelterin complex is highly conserved among vertebrates. Likewise, zebrafish present the same 6 subunits as mammals (Wagner et al., 2017).

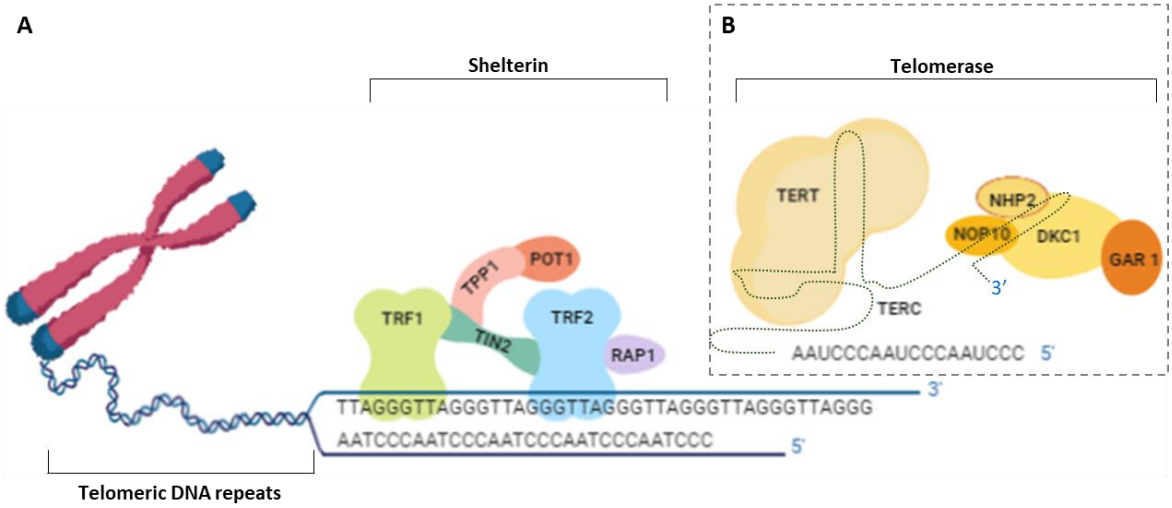


**Fig 1.1. Diagram illustrating the structure of telomeres, the associated Shelterin complex, and telomerase. (A)** Structure of telomeres, constituted by repetitive DNA sequences (TTAGGG), and associated protein complex, called Shelterin. TRF1: telomere repeat binding 1; TRF2: telomere repeat binding 2; TIN2: TRF1 and TRF2 interacting nuclear protein 2; POT1: protection of telomere 1; TPP1: adrenocortical dysplasia protein homolog; RAP1: repressor/activator protein 1. **(B)** Representation of telomerase constituted by TERT and TERC components. DKC1: dyskeratosis congenita 1; NHP2: nucleolar protein family A member 2; NOP10: NOP10 ribonucleoprotein; GAR1: GAR1 ribonucleoprotein. Image made in Biorender (https://biorender.com) and adapted from (Maciejowski & Lange, 2017).

Together with Shelterin, the 3' G-overhang form a loop-like structure at telomeres (termed T-loop), creating a protective "cap". This protective "cap" "hides" the end of linear chromosomes, preventing their recognition as DNA Double-Strand Breaks (DSBs) (Carneiro et al., 2010; Sullivan & Karlseder, 2010). However, because DNA polymerases are unable to complete DNA replication at the termini of the lagging strand (3' end), known as the 'end-replication-problem', telomeres shorten with each cell division (Levy et al., 1992). It is estimated that there is a loss of around 50-200 base-pairs (bp) in each cell division (Levy et al., 1992), at least in cell culture. As telomeres do not comprise any protein-encoding gene, telomere shortening offers a buffering-like system, protecting the protein-coding DNA against erosion with each cell division. Importantly, when telomeres become too short, they become "uncapped" (Ferreira et al., 2004), and this exposure of the DNA double strand end, leads to activation of DDRs (Levy et al., 1992; Sahin & Depinho, 2010).

Telomerase is the only known enzyme capable of counteracting telomere erosion, by elongating telomeres. Nonetheless, in humans, telomerase expression is restricted in most somatic cells. Telomerase is mainly expressed, albeit at limited levels, in stem cells, germ cells (Wright et al., 1996), cancer cells (Kim et al., 1994) and some activated immune cells (Gizard et al., 2011; Hiyama et al., 1995). Therefore, despite telomerase's ability to elongate telomeres, its limited expression in most cells is not sufficient to prevent telomere shortening over-time (Greider & Blackburn, 1985).

Telomerase is a ribonucleoprotein formed by a telomere-specific reverse transcriptase (TERT) and an RNA template (TERC) (Greider & Blackburn, 1985). The TERT component of telomerase uses the RNA template, TERC, to synthetize *de novo* telomeric tandem repeats at the 3' end of telomeres (Greider & Blackburn, 1985). This occurs in association with a core of 4 telomerase-associated proteins, including dyskeratosis congenita 1 (DKC1), nucleolar protein family A member 2 (NHP2), NOP10 ribonucleoprotein (NOP10), and GAR1 ribonucleoprotein (GAR1) (Armanios, 2010; Dey & Chakrabarti, 2018; Egan & Collins, 2012) (**Fig 1.1B**). These four proteins are known to interact with a box H/ACA domain, which resembles a H/ACA small nucleolar RNA (snoRNA), and is located at the 3'-terminal of TERC (Mitchell et al., 1999). The interaction between the H/ACA box and the four above mentioned telomerase-associated proteins is important to regulate RNA stability, maturation and

location, and it is therefore essential for telomere lengthening (Armanios, 2010; Mitchell et al., 2000).

Furthermore, the TERT component of telomerase has a complex structure, containing an RNA binding domain (or TERC binding domain) localised at the N-terminal, a reverse transcriptase (RT) domain localised at the C-terminal and a C-terminal extension (Armbruster et al., 2001; Lai et al., 2001). Both RNA binding and RT domains are required for telomere elongation (Lai et al., 2001). The C-terminus of TERT was also shown to be essential for telomere elongation, as the addition of an epitope tag at this site blocked its ability to prevent telomere shortening in human fibroblasts (Counter et al., 1998).

Therefore, telomerase is a complex protein and the correct assembly of its holoenzyme complex involves a multistep process that is crucial for telomerase activity at elongating telomeres.

#### 1.2.1.1 Telomerase functions: canonical versus non-canonical

Although telomere biogenesis is the most well-characterised function of telomerase (i.e. canonical functions), this ribonucleoprotein has been reported to have important functions that are independent of telomeres (i.e. non-canonical functions) (e.g. Goodman & Jain, 2011; Romaniuk et al., 2019; Ségal-bendirdjian & Geli, 2019; Sung, Ali, & Lee, 2014). These non-canonical functions of telomerase have been suggested to occur at the nucleus, cytoplasm and mitochondria. Despite this, work so far has been unable to discern which part of telomerase is responsible for which non-canonical function. It may be that they cannot be completely separated (Mukherjee et al., 2011). Further work genetically modulating different parts of telomerase in model organisms should help clarifying this. Modulating TERC or TERT components separately, or even modulating specific parts of the TERT component of telomerase (e.g. RNA-binding domain or reverse transcriptase), would help to dissect which components of telomerase are required for the different functions of telomerase.

At the nucleus, telomerase seems to have an important role on transcriptional regulation. By recognising the sequence ACCACCC, human TERC has been shown to interact with 2,198 sites of the genome, including with the MYC promoter and several genes from the Wnt pathway (Chu et al., 2012). Apart from these direct interactions, modulation of TERC has been

suggested to alter the expression of other important genes. For example, inhibition of *TERT* (using shRNA) in human induced pluripotent stem cells has been shown to reduce the differentiation of hematopoietic stem cells (HSCs), without affecting telomere length (Jose et al., 2018). Similarly, depletion of TERC (using a morpholino antisense oligonucleotide model) in zebrafish embryos was shown to lead to impairment of myelopoiesis. The authors showed that this occur independently of telomerase activity as TERT-knockout morpholino did not display any alteration in myelopoiesis (Alcaraz-pe et al., 2014). This evidence show that the telomerase role in HSCs differentiation and myelopoiesis is independent of its functions at telomeres (Alcaraz-pe et al., 2014; Jose et al., 2018). Although the mechanisms underlying this remain generally unclear, Alcaraz-pe et al. (2014) showed that the role of TERC in myelopoiesis may involve modulation of transcription factor PU.1 (SPI1) and GATA-binding factor 1 (GATA1) by TERC (Alcaraz-pe et al., 2014). Together, this suggest that the TERC component of telomerase can play roles independent of telomeres, possibly by modulating the expression of key transcription factors.

Apart from TERC functions at the nucleus, recently it was shown that this component of telomerase can also translocate to the mitochondria, where it is processed giving rise to a shorter form, TERC-53. This shorter form is then translocated to the cytoplasm where it can play roles independently of telomeres or telomerase activity (Cheng et al., 2018). *In vitro*, overexpression of TERC-53 in mouse embryonic fibroblasts (MEFs) was reported to accelerate cellular senescence, without affecting telomere length. Additionally, TERC-53 overexpression in mice led to reduced proliferation in the hippocampus and this was associated with accelerated cognitive decline (Zheng et al., 2019). The authors proposed that these functions of TERC-53 might be associated with regulation of gene expression at the nucleus; however, the mechanisms underlying these functions remain largely unknown (Zheng et al., 2019).

Like TERC, the TERT component of telomerase has also been reported to interact with several gene promoters, including promoters of genes associated with the Wnt pathway. Accordingly, TERT expression was shown to be essential for the development of the anterior-posterior axis in *Xenopus laevis*, through direct modulation of Wnt/β-catenin signalling pathway (Park et al., 2015). Moreover, the TERT component of telomerase can modulate the expression of other genes, through which TERT has been shown to play several other roles. Within those roles, TERT expression has been shown to be essential for cell proliferation and

cell survival. More specifically, TERT expression has been shown to promote proliferation in the mouse skin, particularly in keratinocytes and hair follicle stem cells. Importantly, this does not require TERC expression or catalytic telomerase activity, suggesting that this function of telomerase is independent of its activities at telomeres (Choi et al., 2008; Sarin et al., 2005). Accordingly, lack of TERT (using a morpholino model) was reported to lead to reduced haematopoiesis in zebrafish embryos, without affecting telomeres. Deficient haematopoiesis was rescued by the expression of the RNA-binding domain of TERT, but not by its RT domain (Imamura et al., 2008). This suggests that the function of TERT in haematopoiesis, in zebrafish, only requires specific domains of telomerase and does not require TERT functions at telomeres. Furthermore, TERT expression was also reported to protect human cells against p53-induced apoptosis, independently of telomerase activity or telomere length (Cao et al., 2002; Rahman et al., 2005).

Apart from its functions in cell proliferation and cell survival, TERT was shown to induce transcription of inflammatory-associated genes, including nuclear factor kappa B (NFkB) and tumour necrosis factor alpha (TNFα) (Deacon & Knox, 2018; Ghosh et al., 2012; Mattiussi et al., 2012). Additionally, increasing TERT expression in both nucleus and cytoplasm has shown to exert a protective effect against excitotoxicity in the mammalian brain, contributing to cell survival (Eitan et al., 2012). However, the mechanisms underlying this remain unclear.

Interestingly, TERT can translocate from the nucleus to the mitochondria site (Ahmed et al., 2008). Santos et al. have reported that TERT at the mitochondria promotes mitochondrial DNA damage and increased levels of apoptosis in several human cell lines (e.g. fibroblasts, breast epithelial cells and HeLa cells). The authors proposed that TERT disturbs the integrity of mitochondrial DNA, either by inducing DNA damage or by affecting DNA repair (Hertzog Santos et al., 2006; Hettzog Santos et al., 2004). However, more recent evidence has shown opposite results, by showing that TERT expression at the mitochondria has a protective role against DNA damage and oxidative stress, in human umbilical vein endothelial cells (HUVECs) and human fibroblasts (Ahmed et al., 2008; Haendeler et al., 2009). Ahmed et al. reported that TERT at the mitochondria leads to better function of the mitochondria and integrity of mitochondria DNA, reducing production of mitochondria superoxide and ROS (Ahmed et al., 2008). Supporting this evidence, mitochondria from TERT-deficient mice displays decreased respiratory chain activity, suggesting that TERT expression is important for mitochondria

function (Haendeler et al., 2009). Haendeler et al., (2009) identified that TERT can bind to mitochondrial DNA, particularly to ND1 and ND2 genes, hypothesising that this mechanism could contribute to reduced ROS production (Haendeler et al., 2009). However, the mechanisms underlying the potential protective role of telomerase against oxidative stress are still largely unknown.

In summary, telomerase has been proposed to have multiple functions, which seem to vary depending on its location, presence of the different components of telomerase, telomerase activity and possibly, cellular, and organismal context. Telomerase non-canonical functions have been revealed to be quite intricate and complex, and therefore the mechanisms associated with these functions are still largely unknown. Despite this, continuous efforts have been made to uncover the complex mechanisms underlying telomerase.

## 1.3 Cellular senescence

Most of the primary mechanisms driving ageing mentioned in *section 1.2* have in common the accumulation of DNA damage. In response to DNA damage accumulation, the machinery of DNA damage response is activated, promoting mechanisms of repair (Ovadya & Krizhanovsky, 2014; Sahin & Depinho, 2010). These mechanisms are thought to trigger a cascade of events that culminate in p53-mediated activation of p21 or, when persistent, $p16^{INK4a}$ activation. p21 and $p16^{INK4a}$ are two major cyclin-dependent kinase (CDK) inhibitors (encoded by CDKN1A and CDKN2A, respectively) that act by repressing target genes required for S-phase onset, leading to cell-cycle arrest (van Deursen, 2014). When a cell loses its division capacity in response to DNA damage, it can either enter apoptosis (programmed cell-death), mediated by P53 upregulated modulator of apoptosis (PUMA; Roos & Kaina 2006), or enter a senescence state, through a still not fully understood process mediated by p53, P21 and $p16^{INK4a}$ (e.g. Xue et al. 2007; Coppé et al. 2008; for review, see: van Deursen 2014).

The term senescence and, more specifically, “replicative senescence”, was first introduced by Hayflick when it was described that *in vitro* cultured human fibroblasts undergo a finite number of cell divisions (about 50 replications), after which they enter a non-proliferative state (Hayflick, 1965; Hayflick & Moorhead, 1961). Later, Bodnar and colleagues determined that replicative senescence is associated with telomere shortening (Bodnar et al., 1998). It is

thought that when telomeres reach a certain limit (established as 12.8 repeats of TTAGGG in human cells, Capper et al. 2007) termed the Hayflick limit, DDRs are elicited, leading to cell-cycle arrest. Depending on the cell type and model organismal, this may lead to senescence (Allsopp & Harley, 1995). Nonetheless, apart from telomere dysfunction that can lead to replicative senescence, there are other stimuli capable of inducing cellular senescence. For example, high levels of DNA damage and/or ROS can lead to stress-induced senescence and activated oncogenes can trigger oncogene-induced senescence (Campisi & d'Adda di Fagagna, 2007; van Deursen, 2014) (**Fig 1.2A**).

Today, senescent cells are known as non-proliferative but metabolically active cells (Coppé et al., 2008), that are resistant to apoptosis (Ryu et al., 2007). Additionally, senescent cells have been described to release the so-called senescence-associated secretory phenotype (SASP) (Coppé et al., 2008), which includes multiple pro-inflammatory cytokines, such as Interleukin-6 (IL-6); chemokines, such as Interleukin-8 (IL-8), Monocyte Chemoattractant Protein-2 (MCP-2), and Macrophage Inflammatory Protein-3 (MIP-3a); growth factors, such as Growth Regulated Oncogene (GRO), Hepatocyte Growth Factor (HGF) and Insulin-like Growth Factor-Binding Protein (IGFBP); and tissue remodelling factors such as matrix metalloproteinases (MMP-1, -3, -12) (Coppé et al. 2008; Campisi & d'Adda di Fagagna 2007; Ohtani & Hara 2013) (**Fig 1.2B**). Importantly, the presence of elevated levels of SASP, released by senescent cells themselves, can induce cellular senescence in the surrounding cells, by paracrine senescence (Acosta et al., 2013).

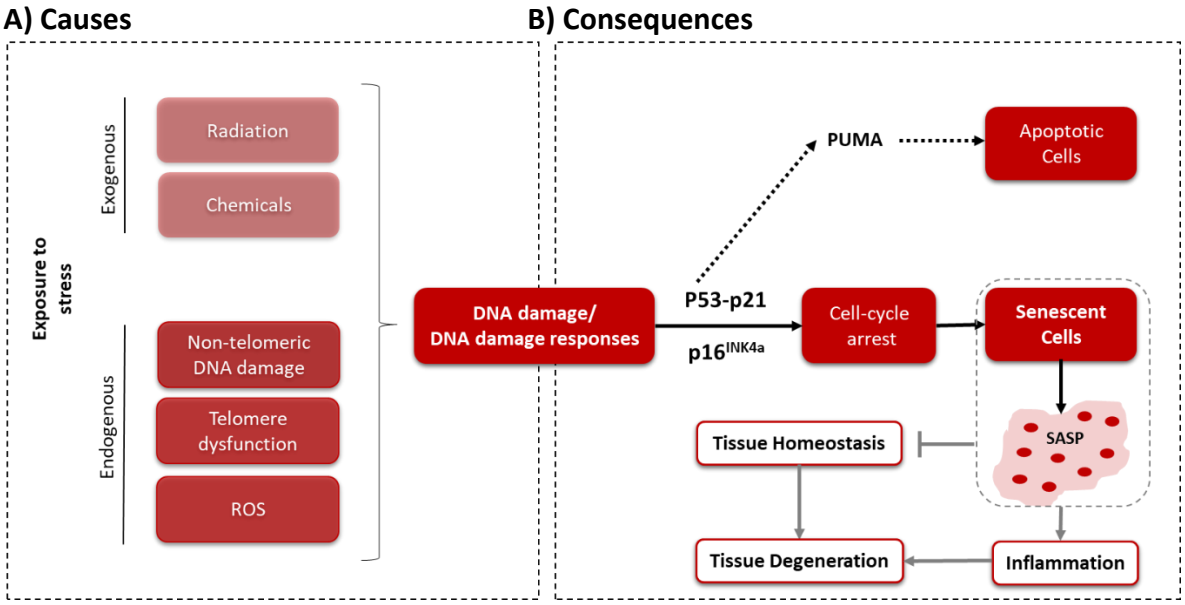


**Fig 1.2. Diagram illustrating putative causes and consequences of DNA damage accumulation with ageing**. **a)** Both exogenous (i.e. radiation and chemicals) and endogenous (i.e. DNA damage, telomere dysfunction, and ROS) stresses lead to an accumulation of DNA damage that triggers DNA damage responses. **b)** DNA damage responses activate a cascade of events that culminate in p53-mediated activation p21 and activation of $p16^{INK4a}$ and promote cell-cycle arrest. When a cell loses its proliferative ability, it can either enter in apoptosis, through p53-mediated PUMA activation, or enter in a senescent state, mediated by p53-p21 and $p16^{INK4a}$. Senescent cells secrete several cytokines, chemokines, and growth factors (SASP), which impairs tissue homeostasis, promotes inflammation and contributes to tissue degeneration.

Giving senescent cells' inability to proliferate, they were first considered to be a protective mechanism, by acting as tumour suppressors (Serrano et al., 1997). However, more recently it has been shown that, probably due to the different characteristics of the SASP phenotype (Coppé et al., 2010; Pérez-Mancera et al., 2014), accumulation of senescent cells can also contribute to tissue degeneration (Ovadya & Krizhanovsky, 2014).

### 1.3.1 From cellular senescence to *inflammageing*

Senescent cells play important roles in tissue repair (Krizhanovsky et al., 2008), wound healing (Demaria et al., 2014) and tumour suppression (Serrano et al., 1997). For example, hepatic stellate cells proliferate in response to liver damage (fibrosis) and eventually enter senescence, locating along the fibrotic scar. Senescence in these cells triggers a mechanism of immune clearance, part of the immunosurveillance phenomenon, recruiting natural killer cells which eliminate the senescent cells and contribute to tissue repair (Krizhanovsky et al., 2008). Additionally, the presence of senescent cells at the wound site seems to be important for fin regeneration after amputation, in adult zebrafish (Da et al., 2019). Demaria et al. (2014) have also described a transient increase in senescent cells in wound healing, particularly at the wound site, in the days following an injury, in mice (Demaria et al., 2014). In this context, the SASP factor Platelet-derived growth factor-AA (PDGF-AA) was identified to be crucial to promote the repair mechanism which, in turn, is delayed in the absence of senescent cells (Demaria et al., 2014). Furthermore, senescent pre-malignant hepatocytes secrete chemokines and cytokines that can recruit immune cells and promote their clearance from the tissue, through a T-cell mediated process (Kang et al., 2011), which was shown to play an important role in tumour suppression (Sagiv & Krizhanovsky, 2013). There is also evidence suggesting that a similar tumour suppression mechanism can also occur in liver carcinoma in both mice (Xue et al. 2007) and humans (Kang et al., 2011).

These studies suggest that, at least some types of senescent cells, in some contexts, can be cleared by the immune system, contributing to tissue repair and homeostasis. However, senescent cells have been reported to accumulate with ageing in different tissues of different organisms, including humans (Dimri et al., 1995), primates (Jeyapalan, 2007), rodents (Wang et al., 2009) and zebrafish (Carneiro et al., 2016; Henriques et al., 2013). On one hand, this

accumulation of senescence in old organisms suggests that there is a greater number of cells that are becoming senescent with ageing, possibly due to defects in DNA repair and/or SASP-factors released by surrounding cells. On the other hand, accumulation of senescent cells with ageing may also suggest that they are not being efficiently cleared from aged tissues. This is important because persistent accumulation of senescent cells with ageing can contribute to tissue degeneration and disease in at least two manners: (1) in a cell autonomous manner, by hampering cell proliferation, which contributes to the impairment of tissue homeostasis; and (2) in a non-cell-autonomous manner, through SASP, by contributing to a sterile, low-level inflammatory state, termed '*inflammageing*' (Franceschi & Campisi, 2014; Tchkonia et al. 2013; Freund et al. 2010; Campisi & d'Adda di Fagagna 2007). *Inflammageing* characterises aged tissues and underlies multiple diseases of ageing (Ovadya & Krizhanovsky, 2014; van Deursen, 2014) (**Fig 1.2B**).

Accordingly, the accumulation of senescent cells seems to be associated with many age-related diseases. In humans, senescent cells' accumulation has been identified in patients with cataracts, osteoporosis, cancer (Ovadya & Krizhanovsky, 2014), type 2 diabetes, glaucoma (Jeck et al., 2012), idiopathic pulmonary fibrosis (IPF) (Schafer et al., 2017), atherosclerosis (Childs et al., 2016), liver cirrhosis (Wiemann et al., 2019), Alzheimer's disease (AD) (Lukens et al., 2009) and Amyotrophic Lateral Sclerosis (ALS) (Salech et al., 2017). This is not human specific, as animal models also show an association between accumulation of cellular senescence and disease. For example, in mice, accumulation of senescent cells is associated with cachexia, lipodystrophy, kidney and cardiac dysfunction, cancer (Baker et al., 2016), tau-hyperphosphorylation in the brain and cognitive impairment (Bussian et al., 2018). In zebrafish, telomere dysfunction-induced senescence has been associated with sarcopenia, cachexia, infection, cancer and infertility (Carneiro et al., 2016; Henriques et al., 2013).

Importantly, recent ground-breaking studies in mice showed that clearance of senescent cells (by inducing apoptosis specifically in p16-expressing cells) ameliorates multiple age-related phenotypes and increases lifespan. More specifically, clearance of senescent cells in mice attenuated the appearance of lipodystrophy, glomerulosclerosis, kidney deterioration, cardiomyocyte hypertrophy and locomotion impairment, typically observed in aged mice (Baker et al., 2008, 2016; Bussian et al., 2018). This provided the first proof-principle evidence that senescent cells can cause disease, highlighting senescence as an important therapeutic target for multiple chronic diseases of ageing. Reinforcing this, initial phases of clinical trials now show that clearance of senescent cells in humans, using senolytics (drugs that selectively destroy senescent cells by promoting apoptosis of senescent cells), may also have positive effects. Treatment with Dasatinib and Quercetin (DQ) (3 days/week for 3 weeks) in a cohort of 14 patients with idiopathic pulmonary fibrosis (IPF) significantly ameliorated the physical function of the patients, improving their walking distance, pacing speed and chair-stands capacity (Justice et al., 2019). Moreover, a 3-day treatment with DQ in 9 patients with diabetic kidney disease, led to decreased number of macrophages and crown-like structures in adipose tissue, characteristics of patients with diabetes and obesity (Hickson et al., 2019). Despite these benefits, possible side effects of these treatments are still being explored. This is important, not only due to safety and toxicity issues but also because oral treatments are likely to affect non-target tissues as well, with unknown consequences. For example, Justice et al. (2019) reported that during treatment patients often presented cough, tiredness, nausea and headaches (Justice et al., 2019). Therefore, it is important to better understand the potential side effects of senolytic treatments and to explore alternative, more targeted therapies, to prevent or alleviate the accumulation of cellular senescence with ageing.

### 1.3.2 Markers of cellular senescence

Given the complex and heterogeneous profile of senescent cells, there is not a universal marker that can identify senescent cells. Because of this, cellular senescence is usually identified by a combination of markers.

SA-β-Gal is the most widely used marker of cellular senescence and it is defined as Senescence Associated β-galactosidase (SA-β-Gal) activity detected specifically at suboptimal

pH 6.0 (Dimri et al., 1995). SA-β-Gal activity is thought to result from increased lysosomal β-D-galactosidase expression, encoded by the *GLB1* gene. Although β-D-galactosidase expression is normally detected at optimal pH 4 – 4.5 in non-senescent cells, its activity can be detected at suboptimal pH 6.0 (called SA-β-Gal) specifically in senescent cells (Lee et al., 2006). Increased SA-β-Gal activity in senescent cells is therefore likely due to an enlargement of the lysosomal compartment or increased lysosomal activity (Lee et al., 2006). However, SA-β-Gal staining presents some limitations as it can also be detected in other conditions, including in quiescent cells, immortalised cells, cells exposed to hydrogen peroxide ($H_2O_2$), and cells under serum starvation (Severino et al., 2000; Yang & Hu, 2005). Additionally, SA-β-Gal activity can also be transiently expressed by activated immune cells, particularly by pro-inflammatory macrophages, which can lead to a false-positive signal (Hall et al., 2017). Hence, SA-β-Gal activity should only be used as a marker of cellular senescence when in combination with other markers.

Other markers of senescence include accumulation of DNA damage, commonly assessed by γH2AX foci (H2A histone family member X phosphorylated at serine 139), and consequent DDRs. DDR can include increased expression of p53, p21, and/or p16, together with hypo-phosphorylated retinoblastoma protein (RB) and hyper-phosphorylated ataxia telangiectasia mutated (ATM) (Hernandez-Segura et al., 2017; Hernandez-Segura et al., 2018). Being non-proliferative cells, resistant to apoptosis, senescent cells are also identified by the absence of proliferative (i.e. 5-BRomoDeoxyUridine, BrdU, and/or Proliferating Cell Nuclear Antigen, PCNA) and apoptosis markers (i.e. PUMA). Being metabolically active, senescent cells may also be detected by the presence of SASP-associated cytokines, chemokines, and growth factors. These can include IL6, IL8, MCP-2, MMP-1, MMP-3, MMP-12, IGFBP, among others (Coppé et al. 2008; Campisi & d'Adda di Fagagna 2007; Ohtani & Hara 2013). Furthermore, senescent cells have shown to suffer morphological alterations, including enlarged size, loss of LaminB1, appearance of cytoplasmatic chromatin fragments, changes in plasma membrane's composition and increased production of ROS (Hernandez-Segura et al., 2017, 2018). Thus, in an ideal scenario, these are additional markers that should be used to characterise cellular senescence.

However, it is important to note that not all senescent cells will express all the markers above mentioned. This depends on the type of senescence (i.e. replicative senescence, stress-

induced senescence, oncogene-induced senescence) as well as on the type of cells (i.e. fibroblasts, melanocytes). It is therefore important to stress that cellular senescence should be assessed by using a combination of markers. Nonetheless, it is often technically challenging or impossible to test all these markers in the same cell.

## 1.4 Accumulation of senescence with ageing in high versus low proliferative tissues

Interestingly, it has been reported that senescent cells accumulate with ageing in a time- and tissue-dependent manner (Carneiro et al., 2016; Henriques et al., 2013; Krishnamurthy et al., 2004). In rodents, it was shown that the duodenum, the kidney and the gonads are the tissues accumulating higher levels of senescence with ageing, assessed by p16 mRNA expression (from 2.5 to 26 months of age) (Krishnamurthy et al., 2004). Apart from the intestine and kidney, a more recent study also showed high accumulation of senescence in inguinal fat, liver, pancreas and spleen of aged mice (>30 months of age), characterised by elevated levels of p21 and p16 (Yousefzadeh et al., 2020). Similarly, zebrafish was reported to accumulate higher levels of cellular senescence, assessed by γH2AX and SA-β-Gal expression, in the kidney marrow, gut and gonads (from 3 to 24 months of age) (Carneiro et al., 2016).

Note that these are mainly high proliferative tissues. As tissues with high cell turnover present accelerated telomere erosion (Bodnar et al., 1998; Lee et al., 1998), they are more likely to accumulate replicative senescence over-time. Indeed, using the zebrafish premature ageing model *tert*$^{-/-}$, Henriques et al. (2013) showed that accumulation of senescence in the kidney marrow, gut and gonads occurs earlier and in greater level than in the muscle, a low proliferative tissue (3-6 compared with 12 months of age) (Henriques et al., 2013). Thus, this time- and tissue-dependent accumulation of senescent cells with ageing is likely influenced by the proliferative rates of the tissues, given that cell turnover leads to telomere shortening.

### 1.4.1 Accumulation of senescence in the aged gut

Early accumulation of critically short telomeres have been identified in high proliferative tissues such as the gut, in a *tert* knockout mice model (Lee et al., 1998). In agreement with this, more recent studies in zebrafish have reported that the gut is one of the first organs to accumulate extremely short telomeres, senescent cells and inflammation, with ageing

(Carneiro et al., 2016). Like in mice (Lee et al., 1998), this accumulation in zebrafish is anticipated and exacerbated in the absence of telomerase (Henriques et al., 2013), suggesting that telomerase restriction and consequent telomere shortening (an already mentioned hallmark of ageing) are important mechanisms driving this process. Since accumulation of senescence was shown to be associated with telomere shortening, aggravated in the absence of telomerase, this is likely to be replicative senescence.

These observations are in accordance with the concept of the gut as a 'motor' for multiple organ failure, first suggested in the late eighties. This hypothesis proposed that changes in the microbiota and/or the translocation of organisms through the gut barrier can contribute to the development of systemic infection (Marshall et al., 1988). Nowadays, there is evidence suggesting that the gut plays an important role in the pathogenesis and progression of systemic inflammation, which can lead to multiple organ failure and eventually death (de Jong et al., 2016). Accordingly, gut barrier permeability has been shown to increase with ageing in drosophila and zebrafish, and to be a good predictor of mortality, surpassing chronological age (Dambroise et al., 2016; Rera et al., 2012).

### 1.4.2 Accumulation of senescence in the aged central nervous system (CNS)

Despite being considered a predominantly non-dividing, post-mitotic tissue, growing evidence now shows that the CNS also accumulates cellular senescence with ageing. Indeed, some markers of senescence have been identified in the ageing brain and eye, in both mice and zebrafish (Arslan-Ergul et al. 2016; Baker et al., 2008; Jurk et al., 2012; Kishi et al., 2008; Van Houcke et al., 2019). Moreover, this phenomenon does not seem to be limited to the brain or the eye, as cellular senescence has also been reported in the mice peripheral nervous system (Jurk et al., 2012) and in the zebrafish spinal cord, with ageing (Kishi et al., 2008).

However, most of these studies did not assess multiple markers of senescence. Particularly Van et al. (2019) and Kishi et al. (2008), only measured SA-β-Gal in the zebrafish retina and spinal cord (Kishi et al., 2008; Van Houcke et al., 2019). Therefore, the knowledge about the nature of senescence in the CNS is still quite limited (see *section 1.3.2*).

#### 1.4.2.1 Senescence in the aged retina

Markers of senescence have been detected in the eye, with ageing. More specifically, increased expression of p16 has been reported in the eye of the progeroid mouse model (bubr1$^{-/-}$) (Baker et al., 2008), and increased SA-β-Gal expression has been identified in the retina of old zebrafish (Van Houcke et al., 2019).

It has been suggested that a specific region of the retina accumulates senescence with ageing – the retinal pigment epithelium (RPE). In culture, human RPE cells from a child donor underwent senescence over-time, displaying decreased cell proliferation and increased levels of SA-β-Gal (Matsunaga et al., 1999). Adult RPE cells (ARPE-19 line), in culture, were also shown to acquire elevated levels of DNA damage when exposed to concentrated N-retinylidene-N-retinylethanolamine (A2E) (Wang et al., 2018), a well-described constituent of lipofuscin in the RPE (Sparrow et al., 2003). Supporting the idea that cellular senescence may also occur *in vivo*, a 40 years old study has reported elevated levels of lipofuscin with ageing, in the human RPE (Wing et al., 1978). Studies in animal models also corroborate this idea, since A2E and lipofuscin have been reported to increase with ageing in the RPE of mice (Boyer et al., 2012), and accumulation of SA-β-Gal has been detected in the RPE of old primates (Mishima et al., 1999). Similarly, it was recently shown accumulation of SA-β-Gal in the aged zebrafish retina, particularly in the RPE (Van Houcke et al., 2019).

RPE is a layer of epithelial cells that, among other functions, has a crucial role in maintaining the integrity of the photoreceptors (J. Marshall, 1987; Nian & Lo, 2019; Salvi et al., 2006). Nonetheless, these cells are known to undergo degeneration with ageing, displaying morphological alterations and increased apoptosis, in both mice and humans (Majji et al., 2000; Priore et al., 2002). It is now thought that accumulation of cellular senescence in the RPE can lead to degeneration of these cells, which in turn affect the integrity of the photoreceptors (Holz et al., 2001). As degeneration of the RPE is a hallmark of age-related macular disease (AMD), a retinal disease that can lead to vision impairment or even vision loss, it has been postulated that accumulation of senescence in the RPE can be part of the etiology of this disease (Holz et al., 2001; Kozlowski, 2012; Blasiak, 2020). Nonetheless, further investigation is required to confirm whether accumulation of senescence with ageing can lead to visual impairment and/ or AMD.

Furthermore, other parts of the retina are known to undergo degeneration with ageing. Indeed, human retinal ageing affects several cell populations, being characterised by overall thinning of the retina (Eriksson & Alm, 2009), degeneration and death of photoreceptors (Nian & Lo, 2019), as well as neuronal loss (Aggarwal et al., 2007; Gao & Hollyfield, 1992; Nian & Lo, 2019). It remains unknown whether other cell populations of the retina, apart from the RPE, undergo senescence over-time and whether it contributes to overall retina degeneration and visual impairment with ageing.

#### 1.4.2.2 Senescence in the aged brain

With ageing, elevated levels of DNA damage (Baltanás et al., 2011; S. Zhu & Coffman, 2017) and SA-β-Gal (Arslan-Ergul et al., 2016; Jurk et al., 2012) have been identified in the mice and zebrafish brains. In addition, increased expression of CDKi, such as p21 and p16, and SASP factors, such as Insulin-like growth factor 1 (IGF1) and IL6, have been observed in the mice aged brain (Jurk et al., 2012). Importantly, this is not limited to animal models, as senescence-associated markers have also been reported in human neurodegenerative diseases. In particular, increased levels of DNA damage checkpoints such as p53, p21 and p16, as well as SASP factors have been observed in the spinal cord and brain of patients with ALS (De Felice et al., 2014) and AD (Bhat et al., 2012), respectively. Hence, the literature shows that despite being a low proliferative tissue, the CNS accumulates senescence, and that this may be associated with brain diseases of ageing. Causality between senescence and neurodegenerative diseases has not yet been established in human. However, mice models where senescent cells have been cleared (Bussian et al., 2018) show an improve of the cognitive decline in aged mice, suggesting that senescence can actively contribute to it. It remains to be determined which cell populations undergo senescence in natural ageing, in the CNS, and what type of senescence this is, i.e. replicative, telomere-dependent or stress-induced senescence.

It has been reported that several cell populations in the CNS can undergo senescence, depending on the context. Neural stem cells (NSCs) and neural progenitor cells (NPCs) have been shown to undergo stress-induced senescence when exposed to ionized radiation, characterised by increased SA-β-Gal (Mason, 2012) and p16 expression (Le et al., 2018). Endothelial cells and pericytes, two major components of the blood brain barrier (BBB), have

also been reported to undergo senescence with ageing in mice, *in vitro* and *in vivo*, expressing elevated levels of p16, p21 and SA-β-Gal (Yamazaki et al., 2016).

Microglia, specialised immune cells of the CNS, seem to undergo replicative senescence, *in vitro* and *in vivo* (Flanary & Streit, 2004; Raj et al., 2015). *In vivo,* this was demonstrated in a progeroid mice model where microglia displays short telomeres and modest increased expression of p21 and SASP-factors (Raj et al., 2015). Moreover, a mouse model of tau-dependent neurodegenerative disease ($MAPT^{P301S}$PS19) was shown to display senescence-associated markers, in comparison with age matched WT (Bussian et al., 2018), suggesting that senescence in aged microglia might be associated with tau-associated disease. Astrocytes, the most abundant glial cell in the CNS, also seem to undergo stress-induced senescence, in humans (Crowe et al., 2016; Mason, 2012), exhibiting high levels of SASP factors when exposed to irradiation (Mason, 2012), as well as SA-β-gal activity, increased expression of DNA damage checkpoints (Bitto et al., 2010) and SASP-factors (Crowe et al., 2016), when exposed to $H_2O_2$. However, *in vitro* studies have reported controversial results regarding whether these cells also undergo replicative senescence. Whilst Flanary & Streit (2004) did not identify replicative senescence in rat astrocytes (Flanary & Streit, 2004), another two studies reported that astrocytes from humans (Evans et al., 2003), mice and rats undergo replicative senescence (Evans et al., 2003). Oligodendrocytes are the glial cells responsible for producing the sheath of myelin around the neuronal axons. Post-mortem studies have reported increased DNA damage in the white matter, together with oxidative damage and SA-β-Gal in this cell population (Nasrabady et al., 2018).

Surprisingly, neurons, considered largely non-proliferative cells, have also been reported to undergo senescence. Le et al. showed increased expression of p16 in the hippocampus, sub-ventricular zone (SVZ) and cortex of mice, after irradiation (Le et al., 2018). Similarly, cortical neurons and Purkinje neurons of aged mice present DNA damage, SA-β-Gal and SASP factors. Curiously, myenteric ganglia also undergoes senescence in the aged mice, presenting DNA damage, together with activated P38MAPK p38 mitogen-activated protein kinases (p38MAPK), SA-β-Gal and ROS (Jurk et al., 2012).

Together, the literature shows that great part of the cell populations in the CNS undergoes senescence and, despite being a low-proliferative tissue, some of them even undergo

replicative senescence. This raises the question of whether there is evidence for telomere shortening and/or telomerase deficiency in the ageing CNS.

### 1.4.3 Potential association between cellular senescence, telomere shortening and decreased telomerase expression in the ageing CNS

#### 1.4.3.1 Telomerase, telomere shortening and senescence in the aged retina

RPE cells display the shortest telomeres within the cell populations occupying the neural retina (Desgarnier et al., 2016). However, it is still unclear whether this is due to a higher cell turnover or due to stress-induced damage that can lead to fast telomere erosion.

Cells from the RPE have been shown to undergo replicative senescence, at least in culture. After 57-58 passages, RPE cells from a 1-year old donor displayed critically short telomeres and elevated expression of SA-β-Gal (Matsunaga et al., 1999). It is important to note that these observations were from cells derived from one single donor, and therefore may not be representative of the population. Despite the limitations, these observations might be surprising as RPE cells are generally considered to be quiescent. Actually, it is thought that the mammalian retina lacks proliferative capacity (Jadhav et al., 2009; Ooto et al., 2004). Despite this, a few studies have suggested that there is a population of peripheral RPE cells, in mice, that retain their proliferative capacity throughout life and that are able to migrate to the central retina (Kokkinopoulos et al., 2011). Additionally, Salero et al. (2012) reported the existence of RPE stem cells (RPESCs), capable of dividing and differentiating, in human cell cultures (Salero et al., 2012). However, it is still unclear whether peripheral RPE cells and/ or RPESCs are able to replace dying RPE in the central retina. Moreover, it remains unclear whether a subpopulation of dividing RPE cells undergo replicative senescence with ageing, *in vivo*.

Furthermore, RPE cells have been reported to undergo stress-induced senescence. For example, exposure to cigarette smoke was shown to lead to increased ROS and accumulation of senescence (increased DNA damage, SA-β-Gal, p21, p16, and SASP factors), in a human RPE cell line (ARPE-19). The same cell line displayed increased levels of IL6, IL8 and vascular endothelial growth factor (VEGF) after exposure to $H_2O_2$. (Marazita et al., 2016). Additionally, in a cell culture of human RPE cells, photosensitisation to A2E was shown to lead to

accumulation of senescence, characterised by increased levels d DNA damage, accompanied by telomere shortening (Sparrow et al., 2003). Interestingly, a parallel study has showed that telomerase over-expression rescued A2E-induced cellular senescence in human RPE cells (Wang et al., 2018). This suggests that somehow telomerase may play a protective role against accumulation of senescence in the RPE layer of the retina. It remains unclear whether this potential protective role is associated with telomerase canonical or non-canonical functions.

One of the functions of the RPE cells is to phagocytose the discs of the photoreceptors' outer segment, when they start detaching. However, with ageing, the ability of degrading cell debris decreases and therefore the RPE cells tend to accumulate phagosome contents over-time. This is thought to lead to the accumulation of lipofuscin and oxidative stress in this cell population (Marshall, 1987; Nian & Lo, 2019; Salvi et al., 2006). Since there is accumulation of A2E and lipofuscin in the ageing mammalian RPE (Wing et al., 1978; Boyer et al., 2012) and that increased levels of A2E can contribute to accumulation of senescence (Sparrow et al., 2003), it is plausible to hypothesise that accumulation of lipofuscin and oxidative stress in the RPE cells, with ageing, can lead to cellular senescence.

Hence, it is still unclear whether accumulation of senescence in the aged retina is associated with increased lipofuscin and oxidative stress (i.e stress-induced senescence) or whether telomere shortening can also contribute for it (i.e. replicative senescence). Independently of this, telomerase may be important to prevent accumulation of cellular senescence in the ageing retina, as its over-expression was shown to reduce senescence in response to A2E (Wang et al., 2018). Supporting this, clinical trials have shown that telomerase reactivation alleviates the symptoms of AMD (Dow & Harley, 2016; Rowe-Rendleman & Randolph, 2004). This suggests that expression of telomerase may play a protective role against retina degeneration. Accordingly, the telomerase mutant zebrafish model (*tert*$^{-/-}$) has been reported to present accelerated retina thinning, in comparison to WT siblings (Anchelin et al., 2013). Therefore, telomerase seems to be important to maintain retina's health; however, the mechanisms underlying this remain unclear.

This encourages additional study to test whether telomerase expression has a protective effect against retina degeneration with ageing and consequent visual impairment, and what functions of telomerase (i.e. canonical versus non-canonical) are involved on this. This is

important because uncovering the mechanisms underlying retina degeneration would allow to find new therapeutic targets to prevent and/or delay vision impairment with ageing.

#### 1.4.3.2 Telomerase, telomere shortening and senescence in the aged brain

Telomere shortening has been identified in the brain, in human ageing, particularly in the cerebral white matter after the age of 60 (Nakamura et al., 2007). Similarly, there is telomere shortening with ageing in the mice (at 26 months) (Ain et al., 2018) and zebrafish brains (at 26-32.5 months) (Arslan-Ergul et al., 2016). As expected, telomere shortening with ageing occurs in an environment with really low levels of telomerase, which are not enough to prevent telomere erosion. In mice, there is a dramatic decrease in telomerase activity after the first postnatal week, being its activity in adulthood almost restricted to the SVZ and olfactory bulb (OB) (Caporaso et al., 2003). In zebrafish, there is an increase in telomerase expression in the brain and eye until 6-months of age, followed by a dramatic decrease until 30-months of age (Anchelin et al., 2011).

In humans, contrary to rodents and fish (Caporaso et al., 2003; Anchelin et al., 2011), telomerase expression in the brain does not seem to decrease with ageing (Allsopp et al., 1995). Nonetheless, it is important to take into account that the levels of telomerase are already very low from birth (Allsopp et al., 1995), and therefore any further changes in the levels of telomerase may be under the limits of detection. Nonetheless, it was shown that patients with ALS display lower telomerase expression when compared with age-matched controls (De Felice et al., 2014), suggesting once again that low expression of telomerase may be associated with age-associated brain disorders. Importantly, low expression of telomerase has reported to be associated with accumulation of senescent-associated markers, as patients with ALS present higher levels of p53 and p21 in the spinal cord when compared with healthy age-matched controls (De Felice et al., 2014). Hence, low levels of telomerase and consequent telomere shortening may contribute to age-associated brain disorders by promoting senescence. Nonetheless, it remains unknown whether the potential impact of telomerase on aged-associated brain diseases is telomere-dependent, since patients with Parkinson's disease (PD) (Hudson et al., 2011), ALS (Linkus et al., 2016) and AD (Lukens et al., 2009) do not present shorter telomeres in the brain, when compared with age-matched healthy controls.

Importantly, growing evidence in animal models now support that telomerase may play a protective role against senescence accumulation in the aged brain. This evidence comes mainly from telomerase-deficient animal models. For example, 4$^{th}$ generation (G4) of telomerase-deficient mice models lacking specifically the TERC component of telomerase (*Terc*$^{-/-}$), display accelerated telomere shortening and increased levels of senescence-associated markers in Purkinje neurons, cortical neurons (Jurk et al., 2012) and microglia (Raj et al., 2015), when compared with *Terc*$^{+/+}$ siblings. Furthermore, an ALS mouse model that lacks expression of TERC (*Terc*$^{-/-}$*; SOD1G93A*) has accelerated onset of ALS phenotypes and dies prematurely (Linkus et al., 2016). These studies suggest that the TERC component of telomerase can exert a protective role against accumulation of senescence in the aged brain and, possibly, a protective role against neurodegenerative diseases. It remains unknown whether this is a specific function of TERC or whether lack of TERT would also accelerate senescence accumulation in ageing. Jaskelioff et al., (2011) has shown that the G4 TERT-ER mouse model (in a *Tert*$^{-/-}$ background), lacking specifically the TERT component of telomerase, displays decreased levels of proliferation and increased expression of p53 when compared to *Tert*$^{+/+}$ siblings. This is a knock-in mouse model that reactivates ectopic TERT expression in the whole body, upon addition of 4-hydroxytamoxifen (4-OHT). After TERT reactivation, proliferative capacity is rescued and levels of p53 decrease, reinforcing the idea that TERT plays an important role in the brain (Jaskelioff et al., 2011). Further supporting evidence comes from showing that transient TERT activation is sufficient to delay the onset and progression of ALS disease in a mouse model. This was observed in the *SOD1* transgenic mouse model, a model that has a mutation in the Cu/Zn Superoxide Dismutase 1 gene, like around 20% of the cases of familial ALS (Eitan et al., 2012). Together, these studies suggest TERT may have important functions in the brain, by promoting cell proliferation and survival, and by delaying neurodegenerative diseases.

This encourages further investigation to determine TERT expression can prevent and/or delay senescence accumulation in the brain and, if so, which mechanisms are responsible for this. More specifically, it would be important to test whether protective functions of TERT are telomere dependent (i.e. canonical functions) or telomere independent (i.e. non-canonical function), and whether lack of TERT can drive brain diseases of ageing. It is relevant to test this because understanding the mechanisms underlying brain ageing would open new lines

of investigation aiming to find therapeutic approaches to promote healthy ageing and ameliorate quality of life in the elderly.

## 1.5 Zebrafish as a research model of ageing

Zebrafish (Danio *rerio*) is a freshwater teleost fish from the *Cyprinidae* family (Spence et al., 2008), originally from South Asia (Sterba, 1962). In the wild, zebrafish abundantly inhabits ditches, ponds and shallow lakes (Spence et al., 2006), with warm (26-31 ºC), clear (visibility up to 30 cm), shallow (1-100 cm depth), slow-moving waters (Spence et al., 2006). Zebrafish is also described as a gregarious species, living in shoals of <12 to >300 fish in its natural environment (Suriyampola et al., 2016).

Since George Streisinger brought, for the first time, zebrafish into the laboratory in the 70's (reported in Clarck, 1981), this species has become a popular research model. This is mainly due to their favourable embryologic and genetic features. Zebrafish have large number of offspring (>100 eggs) and can reproduce all year round. Danio *rerio* present a fast growth, as it is close to full development by the 5$^{th}$ day post-fertilisation (dpf) and reaches adulthood (sexual maturity) at 3 months of age. This, together with their small size (2-4cm long), makes them a cost-effective species to house. Additionally, the zebrafish genome has been entirely mapped and it presents a great similarity with human genome – 71% of the protein-coding human genes have orthologs in the zebrafish genome (Howe et al., 2013; Sassen & Köster, 2015), and there are now several sophisticated genetic tools available to zebrafish. Moreover, besides external embryo development, the zebrafish larvae are transparent until the 5$^{th}$ day post-fertilization, making it an exceptional model for live imaging.

Regarding the mechanisms of ageing, zebrafish was shown to present human-like telomeres size (6-15 bk) and to require telomerase expression to maintain a healthy lifespan (Anchelin et al., 2013; Carneiro et al., 2016; Henriques et al., 2013). G1 telomerase-deficient zebrafish is reported to develop age-related phenotypes and die prematurely, with a half-life 3x shorter (c.12 months) than WT siblings (c.30 months) (Anchelin et al., 2013; Carneiro et al., 2016; Henriques et al., 2013). This contrasts with the most commonly used laboratory mice (BALB/c or C57BL/6) that have 5- to 10-times longer telomeres (around 40-60 kb) than humans (Hemann & Greider, 2000) and require several consecutive inbred generations of

telomerase-deficient models, normally G4 to G6, until displaying accelerated development of age-related phenotypes and shorter lifespan (Ferron et al., 2009). Zebrafish is therefore an appropriate model to study telomere- and telomerase-dependent features of ageing.

In this project, apart from the WT zebrafish, I also used the *tert*$^{-/-}$ model, a model of premature ageing (Henriques et al. 2013). Apart from the shorter lifespan already mentioned, this model develops a progressive accumulation of critically short telomeres, cellular senescence and inflammation over a relatively short period of time compared with the naturally ageing WT (3-6 months in the *tert*$^{-/-}$ versus 12-18 months in the WT) (Carneiro et al. 2016). Hence, using the prematurely aged *tert*$^{-/-}$ model alongside with WT siblings provides a faster temporal analysis throughout the life course of the animal, allowing, at the same time, to uncover telomerase-dependent mechanisms.

Importantly, and relevant for this project, accumulation of senescence in the ageing zebrafish does not seem to be confined to peripheric tissues, as the zebrafish retina and brain also seem to accumulate senescent-associated markers over-time. Moreover, SA-β-Gal expression was also reported in the aged zebrafish telencephalon, accompanied by telomere shortening and decreased proliferation levels (Arslan-Ergul et al., 2016), suggesting that the zebrafish brain may undergo replicative senescence with ageing. It remains unknown whether limited expression of telomerase plays a role in accumulation of senescence in the aged zebrafish brain and, if so, which mechanisms are associated with this.

It is important to mention that the zebrafish retina presents a high regenerative capacity upon acute damage (Cameron, 2000; Richardson et al., 2017; Stenkamp, 2015). Nonetheless, it remains unclear what is the impact of this regenerative ability on ageing. If the zebrafish retina can regenerate until old age, then I would not expect that the zebrafish retina to degenerate with ageing. However, it was recently shown that the zebrafish retina undergoes neurodegeneration with ageing (Van Houcke et al., 2019). It remains unknown whether this degeneration is due to an impairment of its regenerative ability and whether telomerase, known to be essential for regeneration, is required to prevent and/or delay degeneration in the zebrafish retina.

Together, this suggest that zebrafish is a useful model to further explore the role of telomerase in retina and brain ageing.

## 1.6 Hypothesis and Aims

In this project I aimed to test the following hypotheses:

**Hypothesis 1.** "The zebrafish retina does not undergo degeneration with ageing due to Müller glia regenerative capacity, and this requires telomerase expression".

In order to test this hypothesis, this project has the following aims:

**Aim 1.** Determine whether the zebrafish retina undergoes age-associated degeneration and whether this is accelerated in the absence of telomerase.

**Aim 2.** Determine whether Müller glia maintain their regenerative capacity throughout the zebrafish lifespan.

**Hypothesis 2.** "There is accumulation of cellular senescence with ageing, in the zebrafish brain, in a TERT-dependent manner".

In order to test this hypothesis, this project has the following aims:

- **Aim 1**. Determine whether there is accumulation of cellular senescence in the naturally aged zebrafish brain.

- **Aim 2.** Determine whether lack of TERT expression leads to an accelerated accumulation of senescence in the ageing zebrafish brain.

**Hypothesis 3.** "Accumulation of TERT-dependent senescence in the aged zebrafish brain is associated with inflammation and impairment of tissue homeostasis".

In order to test this hypothesis, this project has the following aims:

- **Aim 1**. Determine whether accumulation of TERT-dependent senescence in the aged zebrafish brain is associated with inflammation, tissue dysfunction and behavioural alterations.

- **Aim 2.** Identify potential TERT-dependent mechanisms of ageing in the zebrafish brain that might be involved in accumulation of senescence.

**Hypothesis 4.** "TERT-dependent accumulation of senescence and inflammation in the aged gut (high proliferative tissue) precedes the brain (low proliferative tissue)".

In order to test this hypothesis, this project has the following aim:

- **Aim 1.** Determine whether there is accumulation of senescence and inflammation in the naturally aged zebrafish gut, and whether this is accelerated in the absence of TERT

- **Aim 2.** Determine whether accumulation of cellular senescence in the gut precedes the brain.

  These two aims were tested in the same animals used to test Hypothesis 2 and 3, in order to directly compare gut and brain.

# Chapter 2.
# Materials and methods

## 2.1 General experimental design

In this project, different tissues from the same fish were collected and/or analysed in parallel, for most of the experiments performed. For example, using paraffin sections of the whole fish allowed me to analyse the expression of several age-associated markers, by IF, in the retina, brain and gut of the same fish (**Fig 2.1**, Group 1). For different sets of experiments, I collected the brain and the gut from the same fish and processed the tissues in the same way in order to analyse other age-associated markers in both tissues. From one group of fish, brain and gut tissues were fixed, cryopreserved and cryosectioned to perform the SA-β-Gal assay (**Fig 2.1**, Group 2). From another two groups, brain and gut tissues were collected from same individuals, followed by RNA or protein extraction, to perform RT-qPCR and RNA Sequencing or enzymatic assays, respectively (**Fig 2.1**, Group 3 and 4).

This approached allowed me to directly compare ageing-associated phenotypes in different tissues, particularly low and high proliferative tissues, in the same animal. Ultimately, this enabled to assess whether the ageing-associated markers analysed in this project differ in a tissue-dependent manner and whether some tissues age earlier than others. This was one of the aims of *Chapter 6*. At the same time, this type of approach contributed to a lower use of animals, contributing to the 3R's policy (replacement, reduction, and refinement).

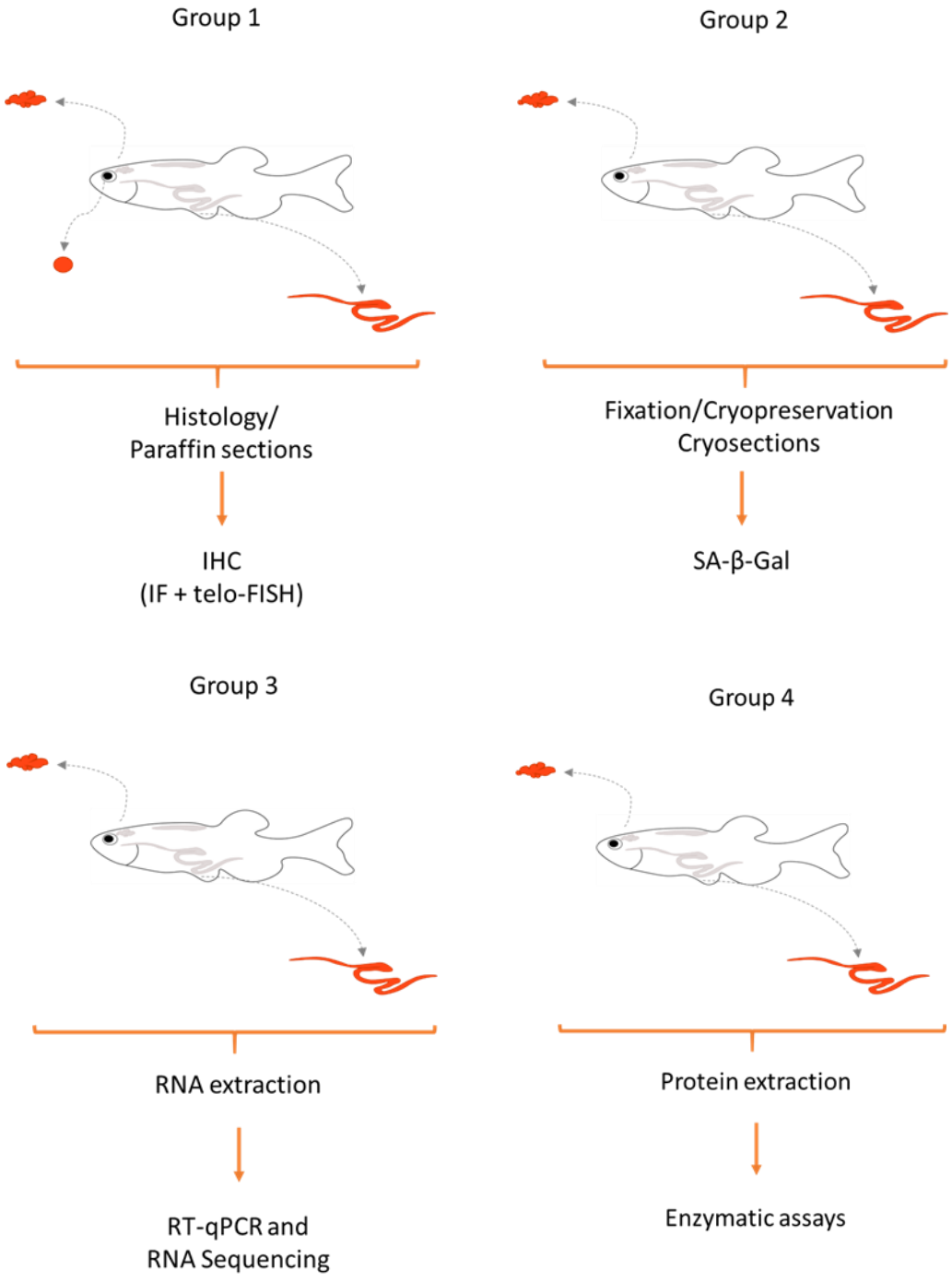


**Fig 2.1. Schematic figure showing the experimental design of most of the experiments performed in this project.** In this project, different organs of the same animals (retina, brain and gut) were used to perform most of the experiments. Each 'Group' illustrated here represent a set of fish used for one group of experiments. Each 'Group' therefore includes several WT and *tert*$^{-/-}$ fish, from different ages.

## 2.2 Zebrafish

### 2.2.1 Adult zebrafish husbandry

All the experimental procedures were carried out in accordance with the UK legislation – Animals (Scientific Procedures) Act 1986 – under the Project License 70/8681 held by Dr Catarina M. Henriques and the Personal License I1395945C held by Raquel Martins. All adult zebrafish were housed in aquaria at the Bateson Centre, University of Sheffield, and maintained with a 14h-light and 10h-dark cycles, at 27-28°C. All tests involving zebrafish manipulation were approved beforehand through the submission and respective approval (by the aquarium manager) of an Individual Study Plan (ISP).

### 2.2.2 Zebrafish lines

The telomerase mutant line (*tert* $^{hu3430}$) is available at the ZFIN repository (ZFIN ID: ZDB-GENO-100412-50) and was first described by Henriques et al. (2013). Briefly, it consists of a point mutation in the second exon of the *tert* gene that leads to an early stop codon, preventing RNA translation and consequent protein formation. This line was generated by N-Ethyl-N-nitrosourea (ENU) mutagenesis. For simplicity, the *tert* $^{hu3430}$ homozygous mutants will be referred to as *tert*$^{-/-}$. Due to the reduced infertility of the *tert*$^{-/-}$ zebrafish (Anchelin et al., 2013; Henriques et al., 2013) the telomerase-mutants used in this project derived from *tert*$^{+/-}$ in-crosses and all the fish used in this study are F1 animals.

The mpeg.mcherry.caax line is an immune reporter line where macrophages/microglia express a fluorescent protein (mcherry) and therefore can be easily identified (Ellett et al., 2011). This line was used in some experiments of this project in order to identify macrophages/microglia cells. For that, *tert*$^{+/}$; mpeg.mcherry progeny were incrossed to generate both *tert*$^{+/+}$; mpeg.mcherry and *tert*$^{-/-}$; mpeg.mcherry fish.

Whenever possible, when comparing *tert*$^{+/-}$ and *tert*$^{-/-}$, age-matched siblings were used. However, due to the limitation in numbers of fish at specific ages, occasionally age-matched non-siblings were used instead, including *tert*$^{+/+}$ and *tert*$^{-/-}$ reporter lines. Moreover, WT AB, non-mutant fish, were used for later ages (>30 months), due to unavailability of old *tert*$^{+/+}$ siblings at the time of experiments. Unless otherwise stated, WT refers to both *tert*$^{+/+}$ and WT fish.

## 2.3 Immunohistochemistry (IHC)

IHC was used to detect the expression of target proteins and respective spatial distribution in the brain and gut, throughout the adult zebrafish life. More specifically, I used IHC to detect specific cell populations within each tissue and to detect several senescence- and inflammation-associated markers.

### 2.3.1 Tissue fixation and processing: paraffin-embedded sections

Fish were culled by immersion in concentrated tricaine mesylate (MS-222, SIGMA-ALDRICH, St. Louis, MO, USA). After terminal anaesthesia, the animals were fixed by immersion in 50ml of 4% paraformaldehyde buffered at pH 7.0 (PFA, SIGMA-ALDRICH) at 4°C for 48-72h, and decalcified in 50ml of 0.5M Ethylenediaminetetraacetic acid (EDTA, SIGMA-ALDRICH), pH 8.0, for additional 48-72h. Then, the whole fish was paraffin-embedded in a series of formalin and ethanol washes, as follows: formalin (SIGMA-ALDRICH) for 10min, formalin (SIGMA-ALDRICH) for 50min, ethanol 50% for 1h, ethanol 70% for 1h, ethanol 95% for 1h 30min, ethanol 100% for 2h, ethanol 100% for 2h 30min, 50:50 of ethanol 100% : xilol for 1h 30min, xylene (SIGMA-ALDRICH) for 3h, xylene (SIGMA-ALDRICH) for 3h, paraffin for 3h and paraffin for 4h 30min. To do this, absolute ethanol (Thermo Fisher Scientific, Waltham, MA, USA) diluted in distilled water ($dH_2O$, VWR International) and paraffin histosec pastilles (Merck & Co, Kenilworth, NJ, USA) were used. Paraffin-embedded fish were sectioned by the histology staff at the SkeletAL lab, at the Medical School of the University of Sheffield (tUoS), using a Leica TP 1020 cryostat, and stored at room temperature (RT). Unless otherwise stated, the tissue sections were longitudinal (sagittal) 4µm-thick slices.

### 2.3.2 Standard immunofluorescence (IF) protocol

In order to perform IF, paraffin-embedded slices were deparaffinised and hydrated through the following sequence of washes: histoclear (Scientific Laboratory Supplies, Wilford, Nottingham, UK) 2x 5min, ethanol 100% 2x 5min, ethanol 90% 5min, ethanol 70% 5min, and $dH_2O$ 2x 5min. For this, absolute ethanol (Thermo Fisher Scientific) was diluted in $dH_2O$. After antigen retrieval in 0.01M citrate buffer at pH 6.0, made with Trisodium citrate dihydrate

(SIGMA-ALDRICH) – sub-boiling at 800W in a microwave for 10min –, the tissue sections were permeabilised in phosphate buffered saline (PBS, SIGMA-ALDRICH) 0.5% Triton X-100 (SIGMA-ALDRICH, for 10min) and blocked in blocking solution for 1h. The blocking solution consisted in 3% bovine serum albumin (BSA, SIGMA-ALDRICH), 5% Goat Serum (or Donkey Serum, both from SIGMA-ALDRICH), and 0.3% Tween-20 in PBS (SIGMA-ALDRICH).

The slides were then incubated overnight (ON) at 4°C, with the primary antibody, in a humidified box. This incubation period was followed by washes in PBS 0.1% Tween-20 (SIGMA-ALDRICH, 3x 10min) and secondary antibody incubation (1h at RT or ON at 4°C). All primary and secondary antibodies were diluted in blocking solution before incubation on the slides. Note that two primary antibodies can be added if both come from different species (e.g. a mouse monoclonal antibody with a rabbit polyclonal antibody) and if the secondary antibody is conjugated with different fluorophores (e.g. anti-mouse Alexa Fluor® 488 with anti-rabbit Alexa Fluor® 568). The primary and secondary antibodies used in this project are described in **Table 2.1** and **Table 2.2**, respectively.

Finally, the tissues were incubated in 1µg/ml of 4',6-diamidino-2-phenylindole (DAPI, Thermo Fisher Scientific), a nuclear staining, diluted in PBS (SIGMA-ALDRICH), for 10min at RT. After 3x 10min washes in PBS 1x (SIGMA-ALDRICH), the slides were mounted with vectashield (an antifade mounting medium, from Vector Laboratories, Burlingame, CA, USA), covered with a coverslip (Scientific Laboratory Supplies), and sealed with clear nail varnish.

The same IF protocol was used in cryosections, without the deparaffinisation step. LCP1 was the only antibody used in cryosections (see *section 2.4.1*). LCP1 and all the other antibodies described in were used in paraffin sections.

**Table 2.1 Primary antibodies used for immunostaining.**

| Antibody, species and type | Dilution factor | Catalogue number; Company, City, Country |
|---|---|---|
| yH2AX rabbit polyclonal | 1:500 | GTX127342; GeneTex, Irvine, CA, USA |
| PCNA mouse monoclonal | 1:500 | NB500-106; Novus Biologicals, Littleton, CO, USA |
| PCNA rabbit | 1:50 | GTX124496; GeneTex, Irvine, CA, USA |
| LCP1 (L-plastin) rabbit polyclonal | 1:200 | GTX124420; Novus Biologicals, Littleton, CO, USA |
| RFP mouse monoclonal | 1:500 | GTX82561; GeneTex, Irvine, CA, USA |

**Table 2.2 Secondary antibodies used for immunostaining.**

| Antibody, species and type | Dilution factor | Catalogue number; Company, City, Country |
|---|---|---|
| Goat anti-rabbit IgG Alexa Fluor® 488 | 1:500 | A11008; Invitrogen, Carlsbad, CA, USA |
| Goat anti-rabbit IgG Alexa Fluor® 568 | 1:500 | 10032302; Thermo Fisher Scientific, Waltham, MA, USA |
| Donkey anti-rabbit IgG Alexa Fluor® 647 | 1:500 | A31573; Thermo Fisher Scientific, Waltham, MA, USA |
| Goat anti-mouse IgG Alexa Fluor® 568 | 1:500 | 10348072; Thermo Fisher Scientific, Waltham, MA, USA |
| Goat anti-mouse IgG Alexa Fluor® 647 | 1:500 | A21235; Thermo Fisher Scientific, Waltham, MA, USA |

### 2.3.3 Telomere-fluorescence *in situ* hybridization (telo-FISH)

Telo-FISH allows the detection of telomeres by probing TTAGGG sequences with a peptide nucleic acid (PNA) telomere oligonucleotide. Relative telomere length, *in situ*, can then be quantitatively measured by probe signal intensity (intensity value of the mean, in arbitrary units).

This technique was performed in combination with IF, following the protocol described in *section 2.3.2*. After incubation with the secondary antibody and respective washes, the tissues were fixed in 4% PFA (SIGMA-ALDRICH) for 20min. Washes in PBS (SIGMA-ALDRICH, 3x 10min) were followed by a dehydration step consisting of washes with ice cold 70%, 90% and 100% ethanol (Thermo Fisher Scientific, 3min each). After this, the slides were left to dry for 45min to 1h. Once the slides were completely dried, 10µl of hybridisation solution (see **Table 2.3**) was pipetted on top of each tissue section and the slides were covered with a coverslip. The slides were incubated for 10min at 80°C for DNA denaturation, followed by incubation for 2h at RT, in the dark, to allow the probe to hybridise with the complementary DNA. After the incubation period, the coverslips were gently removed and the slides were washed for 10min in a solution made of 70% formamide (SIGMA-ALDRICH), 10% 2x saline-sodium citrate (SSC, SIGMA-ALDRICH) and 20% $dH_2O$. This was followed by two more washes of 10min each, in 2x SSC (SIGMA-ALDRICH). SSC was diluted from a 20x stock solution consisting 88.3g of Tri-sodium citrate dihydrate (SIGMA-ALDRICH) and 175.3g of NaCl (SIGMA-ALDRICH), diluted in $dH_2O$ to a total volume of 1L, adjusted to pH of 7.0 and autoclaved. Finally, the slides were washed in PBS (SIGMA-ALDRICH), incubated in DAPI (Thermo Fisher Scientific) for 10min and mounted as previously described in *section 2.3.2*.

**Table 2.3 Components of hybridisation solution used in Telo-FISH.**

| Reaction component | Volume per 100µl of reaction solution (10 samples) | Company |
|---|---|---|
| $MgCl_2$ buffer, pH 7.0 | 8.56µl | Lab-made, *see below* |
| Formamide | 70µl | Thermo Fisher Scientific |
| 1mM Tris, pH 7.5 | 1µl | SIGMA-ALDRICH |
| 1x blocking buffer | 5µl | Lab-made*, see below* |
| PNA probe (Telo-Cy3, zebrafish, 568) | 2µl | Cambridge Research Biochemicals, Cleveland, UK |
| Cent-Fam probe (488) | 2µl | Eurogentec, Liège, Belgium |
| $dH_2O$ | 11.44µl | - |

For the hybridisation solution, the following buffers were made. $MgCl_2$ (magnesium chloride) buffer, consisting in 25mM magnesium chloride (SIGMA-ALDRICH), 9mM citric acid (SIGMA-ALDRICH) and 82mM sodium hydrogen phosphate (SIGMA-ALDRICH). Blocking buffer, consisting in 10x blocking reagent (Merck & Co.) diluted to 1x in maleic acid (SIGMA-ALDRICH).

Note that the hybridisation solution contains both PNA (Telo-Cy3) and FAM-labelled centromere (Cent-FAM) probes, which allow the detection of telomeres and centromeres, respectively. Here, centromeres serve as the control for cell proliferation, as dividing cells present twice the number of telomeres and centromeres. Hybridisation solution without PNA and Cent-Fam probes was added in a few slides as a negative control, in order to control for unspecific binding and/or background.

After imaging (see details in *section 2.3.4*), Telo-FISH staining was quantified by the intensity of the mean. For this, a line was drawn around each nucleus and the intensity of the mean was measured in each channel. Then, the ratio 'telomeres/centromeres' was calculated by dividing the intensity of the mean of telomeres (568 channel) by the intensity of the mean of centromeres (488 channel). Like this, the telomeric probe signal was normalised for the centromeric probe signal within individual cells.

### 2.3.4 IF imaging

The IF staining in paraffin-embedded sections was imaged using the DeltaVision epifluorescence microscope at the Light Microscopy Facility (LMF) at Department of Biomedical Science (BMS) of tUoS. In order to obtain images with good resolution, all images were taken using the 40x objective. For each animal, an average of 5 images was acquired from the gut and 20 from the brain (approximately 4 images per macroarea). Each image contains approximately 15 slices, of 0.2µm each, making up to a total of 3µm. All the images were taken in the different channels: 405 (DAPI), 488 (Fluorescein isothiocyanate, FITC), 568 (RED) and 647 (Cy5). For the gut, images containing 2-3 entire villi were taken from the middle region of the gut. For the brain, the images were selected aiming to cover the maximum area of each macroarea possible. The selection of all images was made based on DAPI staining (tissue structure) and blind to the target antigens.

### 2.3.5 IF quantifications

After the acquisition, a z-projection was made for each field of view (FOV) and the raw images were quantified. For most of the markers, quantifications were performed by manual counting using the 'Cell Count' tool of ImageJ Fiji (v. 1.51). For both gut and brain, the total number of cells (based on DAPI staining) and the positive cells (for each antibody) in each FOV were counted separately, and the percentage of positive cells was calculated. For the brain specifically, the weighted average of all macroareas (i.e. by normalising the positive cells by the average number of cells in each macroarea) was then used to estimate the % of positive cells in the whole brain. For the γH2Ax staining, cells containing >5 foci in the nucleus were considered positive.

Finally, the images were processed with Adobe Illustrator 21.0.2 for display purposes.

## 2.4 Senescence-associated β-Galactosidase (SA-β-Gal) staining assay

SA-β-Gal activity was assessed to test whether there is an accumulation of senescent cells with ageing in the zebrafish brain and gut, and if so, in which regions of the tissues this accumulation occurs. Moreover, SA-β-Gal staining in cryosections was combined with IF in order to identify which cell populations are becoming senescent with ageing.

### 2.4.1 Tissue fixation and processing: cryosections

Fish were culled by immersion in concentrated MS-222 (Thermo Fisher scientific), followed by immediate decapitation (Schedule 1 method). The tissues were dissected, rinsed in cold L15 (Thermo Fisher Scientific) and fixed in neutral buffered formalin (SIGMA-ALDRICH) overnight at 4°C. Then, the tissues were washed in 3ml cold PBS (SIGMA-ALDRICH), and embedded in 3ml of 30% sucrose (in PBS, SIGMA-ALDRICH) overnight at 4°C for cryopreservation. Before embedding in mounting media (optimal cutting temperature, OCT, compound, VWR International), the tissues were immersed in a 50:50 solution of 30% sucrose : OCT for 30min at 4°C. Finally, the tissues were mounted in a base mould (Electron Microscopy Sciences, Hatfield, PA, USA), with OCT, snap-frozen in dry ice, and stored at -20°C. Prior to use, the tissues were sectioned in 13µm-thick coronal sections, using a Leica CM1860 cryostat.

### 2.4.2 SA-β-Gal assay

The Senescence-Associated β-Galactosidase Staining Kit (Cell Signalling Technology, Danvers, MA, USA) was used to detect SA-β-Gal, following manufacturer's instructions. This technique consists in staining the tissue with X-gal substrate, known to be cleavaged by galactosidase. The cleavage of X-gal results in a blue colouration and therefore the levels of galactosidase in the tissue can be assessed by measuring the blue staining.

Briefly, after rinsing the cryosections in 1x PBS for 5min (SIGMA-ALDRICH), 200µl of β-Gal mix solution (see **Table 2.4**) was added in each slide. In parallel, β-Gal mix solution without the X-gal was added in some slides as a negative control. The slides were coverslipped and incubated at 37°C overnight in a humidified chamber box. On the next day, the slides were rinsed in 1x PBS (SIGMA, ALDRICH, 3x 1min) and mounted in glycergel mounting medium (Agilent, Santa Clara, CA, USA).

In order to combine IF with SA-β-Gal Staining, the following steps were performed. After SA-β-Gal Staining, the slides were washed in 1x PBS (SIGMA-ALDRICH, 3x 10min) and fixed in neutral buffered formalin (SIGMA-ALDRICH) for 10min at RT. The fixative was then washed in 1x PBS (SIGMA-ALDRICH) and the IF standard protocol was followed as described in *section 2.3.2* (antigen retrieval followed by permeabilisation, blocking and incubation with primary antibodies ON). After SA-β-Gal Staining, the secondary antibodies were incubated ON at 4°C instead of 1h at RT as in the standard IF protocol. This protocol was performed in order to detect SA-β-Gal staining and immune cells in the same sections, by using the LCP1 rabbit polyclonal primary antibody and the goat anti-rabbit IgG Alexa Fluor® 488 as the secondary antibody. The details of these antibodies and respective dilutions are described in **Table 2.1** and **Table 2.2**.

**Table 2.4 Components of the Senescence-Associated β-Galactosidase Staining Kit.**

| Reaction component | Volume per 1ml of reaction solution (5 slides) |
|---|---|
| 1x staining solution (pH 6.0) | 930µl |
| 100x solution A | 10µl |
| 100x solution B | 10µl |
| 20mg/ml 5-bromo-4-chloro-3-indolyl β D-galactopyranoside (X-gal) | 50µl |

### 2.4.3 SA-β-Gal imaging

The SA-β-Gal staining was imaged using the Olympus BX60 microscope or Leica DM6 microscope. Random slices were imaged in both microscopes and quantifications were compared. No differences were identified between images taken in the different microscopes (data not shown).

IF, when combined with SA-β-Gal staining, was imaged using an additional microscope, the Leica DM6 microscope, which allows the acquisition of images of the same FOV in different channels, simultaneously, including brightfield and fluorescent channels – DAPI, FITC and RED (Fluo-DAPI, Fluo-green fluorescent protein or GFP, and Fluo-Y3, respectively). Furthermore, Leica DM6 microscope has the option of generating an overlay image, combining the different staining in one single image. Alternatively, this overlay can be performed directly in ImageJ Fiji. This technique enabled the detection of the co-localisation of SA-β-Gal with immune cells. For the gut, approximately 4 images were taken per fish, containing at least 3 villi each. For the brain, approximately 6-9 images were taken per fish; 2-3 images from the anterior, middle and posterior part of the brain.

### 2.4.4 SA-β-Gal quantification

After capture, the raw images were analysed using ImageJ Fiji as follows. First, I defined the perimeter of the relevant section and measured its total area (**Fig 2.2A**). Then, the 'Color Threshold' tool was used to identify the SA-β-Gal-positive regions (or blue regions) within the perimeter, using the same set of settings across all images (hue: 116-192; saturation: 117-255; brightness: 0-255). The blue regions were selected, and their total area was measured (**Fig 2.2B, C**). The blue density was finally estimated by comparing the blue area with the total area of the section, obtaining the percentage of blue area per section.

As the different sections of the brain (anterior, middle and posterior) have different volumes, the weighted average of these 3 sections was calculated in order to have an approximate measure of the SA-β-Gal-positive area in the whole brain. This was done by normalising the blue area by the relative size of each brain section (anterior, middle and posterior). In order to analyse each macroarea individually, it was considered the arithmetic average of all the images taken from that specific macroarea.

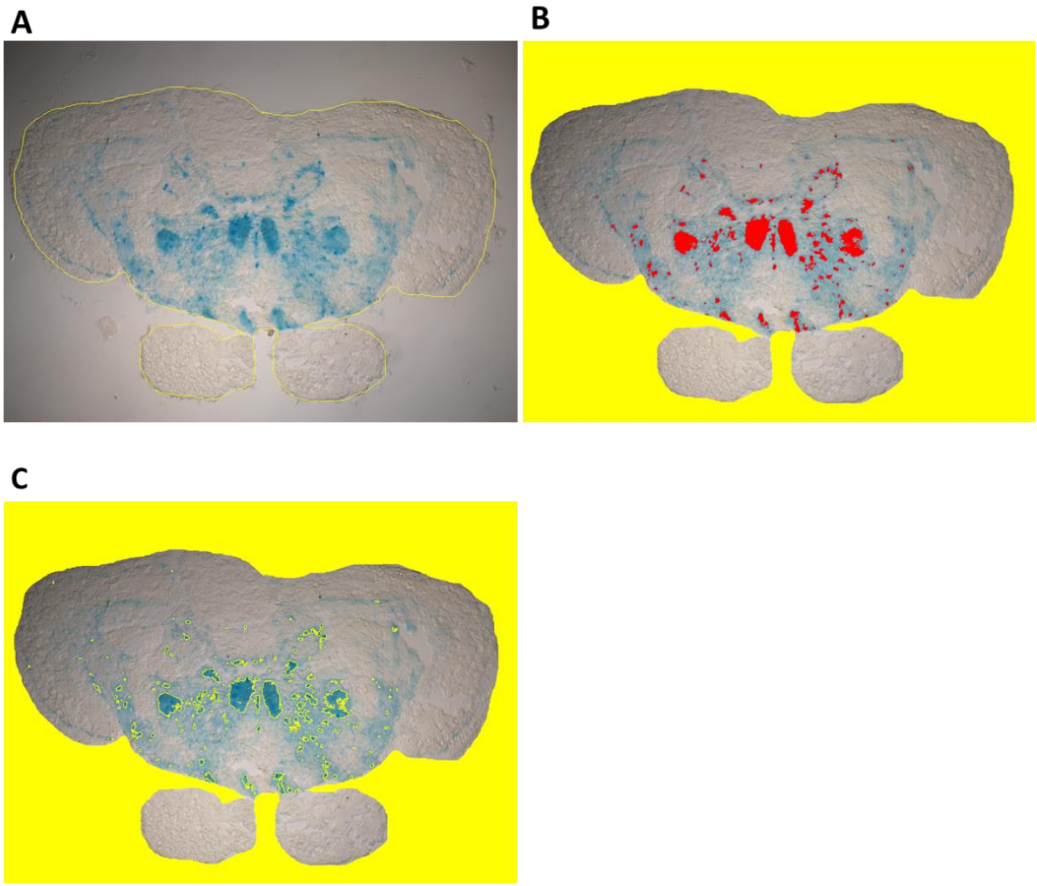


**Fig 2.2. Representation of how the SA-β-Gal-positive area (blue stained area) was identified and measured. (A)** First, the perimeter of the section was delimited, and the area of the section was measured. **(B)** Then, the blue areas were identified using the 'Color Threshold' tool in ImageJ Fiji (shown in red). **(C)** Finally, the SA-β-Gal-positive areas were delimited (shown by the yellow lines) and their area was measured.

## 2.5 Nucleic acid extraction and Quantitative Reverse Transcription Polymerase Chain Reaction (RT-qPCR)

RT-qPCR was used in this project to quantify the relative amount of specific mRNA transcripts. More specifically, I used RT-qPCR to analyse the relative expression of senescence-associated markers in the brain and gut, throughout zebrafish life.

All the RNA work was performed using nuclease-free plasticware and filter tips.

### 2.5.1 RNA extraction

Fish were culled by Schedule 1 method (as previously described in *section 2.5.1*). The tissues were rapidly dissected in cold PBS (SIGMA-ALDRICH), transferred to a microcentrifuge tube containing 100µl of Trizol (Thermo Fisher Scientific), snap-frozen in dry ice, and stored at -80°C until RNA extraction.

To isolate the RNA, the tissue was homogenized with a mechanical homogenizer (VWR International) and a 1.5 pestle (Kimble Chase, Vineland, NJ, USA), after adding extra 50µl of fresh Trizol (Thermo Fisher Scientific). After 5min incubation at RT, 30µl of chloroform (1:5, VWR International) was added and the solution mixed. The samples were then incubated for further 3min at RT and centrifuged (at 13,000g for 30min at 4°C). The resulting upper aqueous phase was transferred to a new microcentrifuge tube, and isopropanol (Thermo Fisher Scientific) was added (approximately 83% of the amount of aqueous phase) and mixed with the sample. After an incubation of 10min at RT, the samples were centrifuged (13,000g for 15min at 4°C) and the resulting supernatant was discarded. The pellet was twice washed in 250µl of ice cold 75% ethanol and then left to air-dry. Once dried, the pellets were resuspended in 14µl of nuclease-free water (VWR International).

All the samples were analysed on a Nanodrop 1000 Spectrophotometer in order to measure the concentration of RNA and to assess RNA purity. The RNA purity was analysed by the 260/230 and 260/280 ratios; samples with values >1.8 were considered acceptable while samples with values ≤1.8 were discarded. From each batch of RNA extracted, some of the samples with an acceptable RNA purity were further analysed in a bioanalyzer Agilent 2100 (Agilent, Santa Clara, CA, USA), to assess RNA integrity. When RNA integrity number (RIN) >8

was observed, all samples from that batch were considered good to be further used (except the ones with not acceptable RNA purity, which were discarded). When these samples had a RIN ≤8, all the samples from that batch were analysed by bioanalyzer (Agilent) and only samples with RIN >8 were used. Finally, all the RNA samples were stored at -80°C until further use.

### 2.5.2 Complementary DNA (cDNA) synthesis

cDNA synthesis was performed using the SuperScript II RT Kit (Thermo Fisher Scientific), following the manufacturer's instructions. Briefly, each RNA sample (300ng) was mixed with 0.5µl of 500µg/ml random primers (Promega, Madison, WI, USA), 1µl of 10mM dNTP Mix (Life Technologies) and nuclease-free water up to 12µl, in a microcentrifuge tube. Afterwards, this mix was incubated at 65°C for 5min. After cooling on ice, 4µl of 5X First-Strand Buffer, 2µl of 0.1M DTT, and 1µl of RNAse inhibitor (New England Biolabs Inc., Ipswich, MA, USA) were added and the contents were mixed. This was followed by a 2min incubation at 25°C, after which 1µl of SuperScript II RT was added. The samples were then incubated consecutively at 25°C for 10min, 42°C for 50min and 70°C for 15min. Finally, the resulting cDNA was stored at -20°C until use.

### 2.5.3 RT-qPCR

Contrarily to standard PCRs, RT-qPCR enables the quantification of mRNA expression. This is performed by using a fluorescent dye (SYBR Green), which intercalates with the double-stranded DNA. Therefore, the fluorescence intensity increases with the increasing number of gene copies, allowing a real-time quantification of the PCR product. The results are then analysed by the cycle threshold (Ct) values, where a Ct is defined as the number of cycles necessary to detect fluorescent signal (above the threshold, i.e. background). The primers used in this study are described in **Table 2.5.**

**Table 2.5 RT-qPCR primers used in this project.**

| Gene | Primer sequences | References |
|---|---|---|
| *beta-actin* | forward – 5’ TTCACCACCACAGCCGAAAGA 3’<br>reverse – 5’ TACCGCAAGATTCCATACCCA 3’ | (Henriques et al., 2013) |
| *p53* | forward – 5’ GGTGCTGAATGGACAACTGTGCT 3’<br>reverse – 5’ GCAACTGACCTTCCTGAGTCTCC 3’ | (Henriques et al., 2013) |
| *cdkn1α* | forward – 5’ ATGCAGCTCCAGACAGATGA 3’<br>reverse – 5’ CGCAAACAGACCAACATCAC 3’ | (Henriques et al., 2013) |
| *cdkn2α* | forward – 5’ ATTATTTTAAGATATAATATTTTGATAAA 3’<br>reverse – 5’ CTACTACTATAATCA ATTCATCCTC 3’ | (Farmen, Hultman, Anglès, & Erik, 2014) |
| *cyclin g1* | forward – 5’ GTGATGAAGATTCAGCCCAAGC 3’<br>reverse – 5’ CACTGGCCAGAGGGACATTTTTCT 3’ | (Henriques et al., 2013) |

Prior to the primers use, each set of primers was optimised. Firstly, a range of cDNA concentrations was tested (1:10, 1:20, 1:40, 1:80, 1:160, 1:320, 1:640 and 1:1,280) using the same primer concentrations and, at least, 3 different melting temperatures (Tm). Secondly, a standard curve was designed, and the slope of the curve was analysed. A slope between −3 and -3.9 was considered good. Thirdly, the dissociation curve of the RT-qPCR was analysed in order to ensure the existence of a single peak – multiple peaks might indicate non-specific binding and/or primer dimers. Once an optimal primer efficiency and dissociation curve were found, the lowest successful cDNA concentration falling within the linear range of standard curve (15-30 Cts), as well as the optimal Tm, were used in the subsequent reactions.

To perform RT-qPCR, a 384-well plate (Greiner Bio-One, Kremsmünster, AT) was prepared with 6µl of SYBR Mix (PerfeCTa SYBR Green FastMix, ROX, from VWR International), 0.5µl of primers (forward and reverse, at a final concentration of 0.5µM each) and 5µl of cDNA, *per* sample. Triplicates of each sample were used in each RT-qPCR plate. Then, the plate was covered with a micro-seal B PCR plate sealing film (Bio-Rad, Hercules, CA, USA) and spun down at 13,000 rpm for 1min. The ABI 7900HT Sequence Detection System (Applied Biosystems, CA, USA) was used to run the RT-qPCRs, with the following program: 95°C for 10min; 40 cycles of 95°C for 30sec followed by optimal Tm for 1min; and dissociation stage. The dissociation stage aimed to generate a melting curve profile and consisted in a heating to 95ºC for 15sec, followed by cooling to Tm for 1min, and heating again to 95ºC for 15sec.

The results were analysed as follows. First, the standard error of the triplicates (of each sample) was calculated and all the samples with triplicates presenting a standard deviation ≥1 were excluded. Second, the fold change expression for each gene was calculated, using the ΔΔCt method (derived from the Livak & Schmittgen (2001)). For this, the mRNA expression of each target gene was first normalised to the reference gene (*beta-actin*), by subtracting the Ct value of the reference gene ($Ct_{ref}$) from the Ct value of the gene of interest ($Ct_{GOI}$) (**Formula 1**). The result of this equation is commonly called ΔCt. Then, the ΔCt of the 'control' group ($\Delta Ct_{control}$) was subtracted from the ΔCt of the 'test' group ($\Delta Ct_{test}$), obtaining the ΔΔCt value (**Formula 2**). Finally, the fold change was calculated using **Formula 3**. Unless otherwise stated, the 'control' group refers to the WT young group.

The ΔΔCt method was considered valid to analyse the data in this project because the efficiency curve of target and reference genes were relatively similar. The calculation of the

average ΔCt between the reference gene and each target gene in a dilution series, revealed efficiency curves with a slope of ≤0.13 (*p53*: 0.089; *p21*: 0.134; *p16*: 0.132; *cyclin g1*: 0.079).

**Formula 1** $$\Delta\mathrm{Ct} = Ct_{GOI} - Ct_{ref}$$

**Formula 2** $$\Delta\Delta\mathrm{Ct} = \Delta Ct_{test} - \Delta Ct_{control}$$

**Formula 3** $$\text{Fold change} = 2^{-\Delta\Delta\mathrm{Ct}}$$

## 2.6 RNA Sequencing (RNA Seq)

RNA was extracted as described *in section 2.5.1*. The RNA samples used in RNA Seq were first analysed by bioanalyzer (Agilent) and all of them presented a RIN ≥9.

The RNA Seq was performed by Matthew Wyles (BSc, MPhil), at the *Genomics and Sequencing facility* of Sheffield Institute for Translational Neuroscience (SITraN). I observed all the procedure and did the subsequent analysis.

### 2.6.1 mRNA isolation and fragmentation

mRNA was prepared from total RNA by removal of rRNA, non-coding RNA and degraded RNA. This was performed using the Oligo dT Beads approach, in which only RNA that contains poly(A) tails (mature mRNA) can bind to the magnetic beads.

NEBNext Poly(A) mRNA Magnetic Isolation Module (New England Biolabs Inc) was used to isolate the mRNA, following manufacturer's instructions. Therefore, unless otherwise stated, all the reagents used during the protocol were provided by this Kit.

Briefly, a total of 500ng of RNA *per* sample was diluted in nuclease-free water to a final volume of 50µl and mixed with 50µl of Oligo dT Beads (Agencourt AMPure XP, Beckman Coulter, Indianapolis, IN, USA). To facilitate the binding of mRNA to the beads, the RNA was denatured by incubating the solution at 65°C for 5min and then cooling it down to 4°C (with the lid set at >75°C to prevent evaporation). To allow binding of mRNA to the beads, the solution was then incubated at RT for 5min and then placed in a magnetic rack, still at RT,

until the solution became clear (≈2min). To remove unbound RNA, the supernatant was removed and discarded without disrupting the beads; and the beads were washed twice with 200µl of Wash Buffer. Every wash consisted of placing the solution in the magnetic rack until the solution was clear and then removing and discarding the supernatant. For the first elution of the mRNA from the beads, 50µl of Tris Buffer was added to each sample, and the resultant solution was heated at 80°C for 2min, then cooled to 25°C (with lid set at >90°C). To re-bind the mRNA to the beads, 50µl of RNA binding buffer (2x) was added to the beads. After an incubation period of 5min at RT, the buffer was washed out and the beads were washed one final time with Wash Buffer.

Later, the purified mRNA was eluted from the beads and fragmented. To do this, 11.5µl of First Strand Synthesis Reaction Buffer and Random Primer Mix (2x) (40% and 10% each, respectively) were added into each sample and incubated at 94°C for 15min (with the lid set at 105°C), before cooling down to 4°C. The resulting solution was placed in the magnetic rack and the unbound fragmented mRNA was collected (10µl in total).

### 2.6.2 First- and second-strand cDNA synthesis

To synthesise the first strand of cDNA, the 10µl of fragmented mRNA was mixed with 8µl of NEBNext Strand Specificity Reagent and 2µl of NEBNext First-Strand Synthesis Enzyme Mix (total of 20µl). These reagents are part of the kit above mentioned. The solution was incubated for 10min at 25°C, followed by 15min at 42°C, 15min at 70°C and then held at 4°C.

To synthesise the second strand of cDNA, the 20µl of first-strand synthesis product was mixed with the following: 8µl of NEBNext Second Strand Synthesis Reaction Buffer with dUTP Mix (10x), 4µl NEBNext Second Strand Synthesis Enzyme Mix and 48µl of nuclease-free water (total of 80µl). The resulting solution was then incubated at 16°C for 1h. All the reagents are part of the kit above mentioned.

The double-stranded cDNA (dscDNA) was then purified in order to remove any enzymes, buffers or primers from the solution. To do this, the second strand synthesis reaction product was incubated with 144µl of NEBNetx Sample Purification Beads, for 5min at RT, placed in the magnetic rack and washed. This was followed by three washes in 200µl of 80% ethanol; the beads were then air-dried. Finally, the dscDNA was eluted from the beads by incubating the

solution with 53µl of 0.1x Tris-EDTA (TE) Buffer for 2min at RT in the magnetic rack. All the reagents are part of the kit above mentioned. After this, the dscDNA (total of 50µl) was collected and stored at -20°C.

### 2.6.3 Library preparation

To prepare the library, the NEBNext Ultra Directional RNA Library Prep Kit (Illumina) was used, following manufacturer's instructions. Unless otherwise stated, all the reagents used in this protocol were provided by this Kit.

### 2.6.4 Adaptor ligation

First, the dscDNA was prepared for adaptor ligation. The 50µl of dscDNA was mixed with 7µl of NEBNext Ultra II End Prep Reaction Buffer (10x) and 3µl of NEBNext Ultra II End Prep Enzyme Mix (total of 60µl). The solution was incubated as follows: at 20°C for 30min, at 65°C for 30min and then hold at 4°C (always with the lid set at >75°C). This process generates an end-repair/ dA-tailing in the extremities of the dscDNA to enable the ligation of the adaptors (that have single T overhangs).

For the adaptor ligation, 60µl of product from the previous step were mixed with 2.5µl of adaptor (after 5-fold dilution in Adaptor Dilution Buffer), 1µl of NEBNext Ligation Enhancer and 30µl of NEBNext Ultra II Ligation Master Mix. Together, this solution is called 'Ligation Reaction' and contains the dscDNA with the adaptors. After incubating the Ligation Reaction at 20°C for 15min, the USER Enzyme was added, and the resulting solution was incubated at 37°C for 15min (the lid set at >45°C). This step removes uracil nucleotides from the dscDNA, making it accessible for PCR.

In order to remove enzymes and excess adaptor, the Ligation Reaction was purified with 87µl of Oligo dT Beads (Agencourt AMPure XP). The beads were then washed 3x in 200µl of ethanol 80% and air-dried. Finally, purified dscDNA was eluted from the beads by adding 17µl of 0.1x TE. The final 15µl of dscDNA were transferred to a new tube in order to prepare the libraries.

### 2.6.5 PCR enrichment of libraries

The library PCR enrichment is an important step that enables an increase in the library yield and incorporation of the barcodes in each sample. The NEBNext Multiplex Oligos for Illumina (Index Primers Set 1, New England Biolabs Inc) was used for the PCR reaction. In this kit, each set of primers contains a universal primer and an index primer which includes a barcode. This means that during the PCR, a unique barcode will be added to each sample, enabling all the samples to be sequenced together and then demultiplexed for analysis. The PCR reaction and program used are presented in **Table 2.6** and **Table 2.7**, respectively.

The PCR product (≈50µl) was then purified using 45µl of Oligo dT Beads (Agencourt AMPure XP), followed by three washes with ethanol 80%. After air-drying, the dscDNA was eluted by adding 23µl of 0.1x TE, and the resulting 20µl of the library were collected.

Before proceeding with the sequencing, the quality of each library was assessed by bioanalyzer (Agilent 2100). The presence of peaks at ≈80bp or ≈128bp suggest primers and adaptor-dimer carryover, respectively. To remove the excess adaptor, the samples were washed once again with Oligo dT Beads (Agencourt AMPure XP). After this wash, all the libraries displayed good electropherograms and therefore were used for sequencing.

### 2.6.6 Sequencing

The sequencing was run on an Illumina HiScan SQ sequencer, using a high output run and sequencing by synthesis V3 chemistry on a single 100bp run. The sequencing process was monitored in real-time using Sequencing Analysis Viewer v1.8.37 Software, and therefore quality control was performed during and after sequencing.

Then, the data was imported into a .FASTQ file format in order to perform the analysis.

**Table 2.6 Components for the PCR reaction used to prepare the libraries for RNA Seq.**

| Component | Volume per library |
|---|---|
| Adaptor ligated dscDNA (resulting from step described on section 2.6.4) | 15µl |
| Master | 25µl |
| Universal PCR Primer/ i5 Primer | 5µl |
| Index (X) Primer/ i7 Primer | 5µl |

**Table 2.7 PCR program used to prepare the libraries for the RNA Seq.**

| Cycle Step | Temperature | Time | Cycles |
|---|---|---|---|
| Initial Denaturation | 98°C | 30sec | 1 |
| Denaturation | 98°C | 10sec | 8 |
| Annealing/Extension | 65°C | 75sec | |
| Final Extension | 65°C | 5min | 1 |
| Hold | 4°C | ∞ | |

### 2.6.7 RNA Seq analysis

Dr Mark Dunning (Director of the Bioinformatics Core at the University of Sheffield) performed the initial analysis of the RNA-Seq data, including alignment quality control and normalisation. The remaining analysis was performed by me.

The experimental aim was to identify the differentially expressed (DE) genes, being up- and down-regulated in a consistent way over-time, in the zebrafish brain. In order to identify those genes, a time-series analysis was performed using the Short Time-series Expression Miner (STEM) software (v1.3.12) (Ernst & Bar-joseph, 2006). During this analysis, all time-points were normalised for the earlier time-point (2 months), which in turn was transformed to start at 0 (as baseline). For analysis purposes, the settings were used as follows. For filtering the data, I used a maximum number of missing values of 0, a minimum correlation between repeats of 0.6 and a minimum absolute expression change of 0.6. For the model profiles, a significance level of 0.05 was considered and Bonferroni test was used as the correction method. All the genes presenting a p-value adjusted (padj) <0.05 were considered DE genes and were therefore selected for further analysis.

After identifying the DE genes with ageing in each tissue, enrichment analysis was performed in order to determine the functions to which the genes were associated with. Enrichment analysis was performed in Metascape (Zhou et al., 2019) using a minimum overlap of 3, a p-value cut-off of 0.01 and a minim enrichment of 1.5. The enrichment terms identified in this software were compared and confirmed by using an extra resource tool, the Gene Ontology enRIchment anaLysis and visualization, known as GOrilla (Eden, Navon, Steinfeld, Lipson, & Yakhini, 2009). In GOrilla, a p-value cut-off of 0.01 was also considered.

Networks of genes were analysed using STRING v11.0 (Szklarczyk et al., 2019) and Cytoscape v3.7.2 (Shannon et al., 2003) software. More specifically, STRING software was used to perform a first assessment of the networks, determining the genes interacting with other genes (minimum interaction score of 0.4) and eliminating any disconnected nodes. Gene interactions were based on textmining, experiments previously performed, databases, co-expression, neighbourhood in the genome, gene fusion and co-occurrence in publications. The networks identified in STRING were then deeper analysed in Cytoscape, where it was possible to determine the key characteristics of the networks such as the number of nodes,

edges (or degree) or neighbourhood connectivity, among others. In order to identify small, strongly connected and meaningful networks, the 10 genes with the highest degree (highest number of interactions with other genes) from each group of genes were selected. Later, STRING software was also used in order to assess specific interactions between genes within each network, as well as to make the networks used for display purposes.

Finally, venn diagrams were performed using the Venny v2.1.

## 2.7 Protein extraction and enzymatic assays

Enzymatic assays were used in order to analyse chitotriosidase activity, an inflammatory-associated marker, in the ageing brain and gut.

### 2.7.1 Protein extraction

Fish were culled by Schedule 1 method as described in *section 2.3.* Tissues were dissected rapidly, transferred to a microcentrifuge tube and immediately snap-frozen in liquid nitrogen. The samples were stored at -80°C until protein extraction.

The tissue was homogenised in 100µl of ultra-pure water using a mechanical homogenizer (VWR International) and RNAse-free disposable pestles (Thermo Fisher Scientific) for approximately 30sec, on ice. Then, the samples were spun down at 4°C, at 2,000rpm, for 5min. After transferring the supernatant to a new tube, samples were stored at -80°C until further use.

### 2.7.2 Protein quantification

Protein extracts were quantified by the bicinchoninic acid (BCA) method, using the Pierce™ BCA Protein Assay Kit (Thermo Fisher Scientific). The BCA assay is a colorimetric method that consists in a biuret reaction that leads to a reduction of copper ($Cu^{+2}$ to $Cu^{+1}$) in the presence of an alkaline solution. The chelation of 2 molecules of BCA to $Cu^{+1}$ result in a purple-coloured product, which can be measured by a plate reader.

In order to perform the BCA assay, a standard curve was prepared with a range of 0.2-2µm of BSA (from the kit), along with a blank control (containing ultra-pure water only). At the same time, 5µl of each protein extract was mixed with 1ml of BCA (from the kit), in microcentrifugation tubes, and incubated at 37°C for 10min in a water bath. After adding an additional 20µl of copper sulphate (from the kit), the solution was mixed and incubated at 37°C for 20min. Then, 200µl of each sample (or BSA standard curve) were transferred to a Corning™ Costar™ Brand 96-Well EIA/RIA Plate (Thermo Fisher Scientific), in duplicates, and absorbances were read in a Varioskan Plate Reader (at Sheffield RNAi Screening Facility) at a wavelength of 562nm.

Sample concentrations were calculated as follows. Firstly, the blank duplicates were averaged and subtracted from all of the other optical densities. Secondly, the total amount of protein from each sample was interpolated from the standard curve using GraphPad Prism 7.0 software ('linear regression' -> interpolate unknowns from standard curve'). Finally, the protein concentration of each sample was calculated.

### 2.7.3 Chitotriosidase activity assay

In order to measure chitotriosidase activity levels, I used the same protocol previously described in zebrafish by Keatinge et al., (2015). This method allows to assess the hydrolyse capacity of 4–methylumbelliferyl–β-D-N, N', N"-triacetylchitotriose (4-MU-chitotrioside), by chitotriosidase enzyme. Chitotriosidase activity assay was performed as follows.

A total of 10µl of protein extract per sample was mixed with 100µl of substrate solution and incubated at 28°C for 60min. A blank control containing 10µl of ultra-pure water was prepared alongside with the samples. Substrate solution consisted in 4-MU-chitotrioside (SIGMA-ALDRICH) diluted in McIlvaine solution at pH 5.2 (1.73mg of 4-MU-chitotrioside per 100 ml of McIlvaine solution). To make the McIlvaine solution, stock solutions of 0.1M citric acid (SIGMA-ALDRICH) and 0.2M di-sodium hydrogen phosphate (SIGMA-ALDRICH) were mixed at a ratio of 45% and 55%, respectively, obtaining a final pH of 5.2.

After incubation, 1ml of stop solution (0.25M glycine buffer, pH 10.4, containing 0.01% Triton X-100 (SIGMA-ALDRICH)) was added to each sample (and blank control), and 200µl of the final solution was transferred to a Corning™ Costar™ Brand 96-Well EIA/RIA Plate (Thermo

Fisher Scientific). Duplicates of each sample were used. An extra microcentrifuge tube was prepared with 200µl of standard solution (5µm 1,4-Methylumbelliferone, SIGMA-ALDRICH) and 900µl of stop solution. A volume of 200µl of the final solution was transferred to the 96-well plate, in duplicates. The fluorescence was then read in a Varioskan Plate Reader (excitation: 365nm; emission: 450nm).

Finally, the chitotriosidase activity was calculated in nM/h/ml, using **Formula 4**.

**T**, fluorescence of test samples

**B**, fluorescence of blank

**Std**, standard

**Formula 4**

$$\frac{(T-B)}{std} X \frac{60}{incubation\ time\ [min]} X \frac{1000}{volume\ [\mu l]}$$

## 2.8 *In vivo* assays

In this study*, in vivo* assays were performed in order to test BBB and gut barrier permeability with ageing, in zebrafish.

### 2.8.1 Testing BBB permeability

To test BBB permeability, a total of 5µl of 0.1% IRDye 680RD Dextran (LI-COR Biosciences, Lincoln, NE, USA) diluted in Hanks' Balanced Salt solution (HBSS, Thermo Fisher Scientific) were injected by IP. Two different sizes of the compound were tested, with the following molecular weights: 4kDa and 70kDa. A group of fish injected with 5µl of HBSS alone was used as a vehicle control group. The fish were culled 3h after IP, and the brains were collected and imaged using a LI-COR Odyssey CLx machine (LI-COR). The brain fluorescence was then quantified using the Image Studio 4.0 Software for Odyssey CLx (LI-COR).

### 2.8.2 Testing gut barrier permeability: "Smurf" assay

In this project, the "smurf" assay was used to test gut permeability with ageing. This assay involves feeding the animal with a blue food colourant and then observe changes in the skin colouration. In a young, healthy animal, the food colourant is not expected to cross the gut barrier and no blue should be observed in the skin. However, if there is increased gut permeability, as it is predicted with ageing, there should be increased blue colouration in the skin (Dambroise et al., 2016). The "smurf" assay was performed by water immersion, as described in Dambroise et al. (2016). Briefly, the fish were immersed in aquarium water containing 2.5% of filtered blue food colourant (Blue #1 stock solution, Erioglaucine disodium salt, Acros Organics, Thermo Fisher Scientific), for 30min. Then, fish were rinsed in clear water until excess surface blue colouration was removed (**Fig 2.3**). After the "smurf" assay, fish were culled by Schedule 1 and pictures of the whole-body were taken.

**Fig 2.3. Illustrative pictures of the "smurf" assay by water immersion.** The fish were exposed to blue dye (food colourant) diluted in water, for 30min (top image). Then, the fish were rinsed in clear water (middle image) until the blue colouration wore off (bottom image). The rinsing time was the same for all the experimental groups.

At the end of the protocol, fish skin colouration was quantified by the median intensity of the mean, using ImageJ Fiji software. This was done in the white stripes of the skin only, as the blue stripes of the zebrafish skin could be a confounding factor.

## 2.9 Behavioural assays

Behavioural assays were performed to test whether age-associated cellular and molecular dysfunctions occur at the same time as age-related behavioural alterations.

### 2.9.1 Open field (OF) and novel object (NO) tests

OF and NO tests were used to test locomotion and anxiety-like behaviour in zebrafish, with ageing. These tests were performed at the behaviour room (BMS Department of the tUoS).

Before the experiment, all fish were acclimatised to the behaviour room for at least 1h. During this period, fish were maintained in crossing tanks containing approximately 2.5L of water, in groups of 3 fish. OF and NO tests were performed one after the other, using a 27x14x14cm tank (length x width x height) containing 7cm of water depth. The walls of the test tank were covered in white paper in order to avoid external visual stimuli (**Fig 2.4A**). A fish was gently placed into the test tank with a net and the recording of the test behaviour started immediately, using a top camera. After 10min of OF test, the fish was transferred to the holding tank for 2min. During this interval, a red 3x1.5x1.5cm object (length x width x height) was placed in the centre of the test tank (**Fig 2.4B, C**). The fish was gently placed again in the test tank for additional 10min (NO test). In the end, the fish was returned to its tank. During the 20min trial, the fish behaviour was recorded for later data analysis. The test was carried for one fish at each time. The water in the test tank was replaced in between every fish.

The assays were performed for 3 consecutive days and 10 to 20 fish were tested per day. The day and time of experiment were semi-randomly determined so that all the fish from each group were equally distributed for the morning and afternoon sessions of each day of experiment. This aimed to avoid confounding factors related to the day and schedule of the experiment.

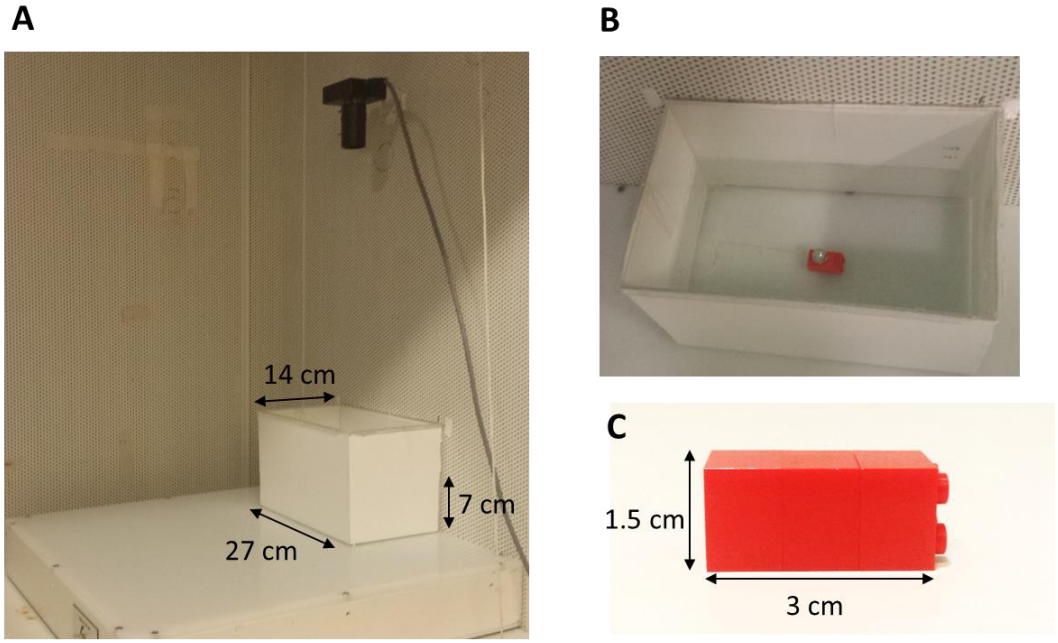


**Fig 2.4. Representative images of the setup used to perform OF and NO tests. (A)** Picture of the tank and top camera used to record the fish behaviour. **(B)** Top view of the test tank with novel object placed in the centre. **(C)** Close picture of the object used for the NOT.

Later, fish behaviour was analysed using the video tracking software EthoVision XT (Noldus Information Technology Inc., Lessburg, VA, USA). This analysis was performed at the University of Leicester, in the laboratory of Dr William Norton, who generously lent me the software with respective key.

Locomotion behaviour was analysed by measuring the total distance swam during the OF test. Anxiety-like behaviour was analysed in both OF and NO tests. In the OF test, anxiety-like behaviour was assessed by the time spent on the edge versus the centre of the tank – the preference for staying in the edges of the tank is called thigmotaxic behaviour and can be used as a measure of anxiety in zebrafish (Allan Kalueff et al., 2013). In the NO test, anxiety-like behaviour was measured by the time spent near the novel object. Poor exploratory activity regarding the object is considered a signal of anxiety in zebrafish (Allan Kalueff et al., 2013). Two times the width of the fish was the measure used to delimit the area considered as the 'edges of tank' in the OF test, and the area considered to be 'near the object' in the NO test.

### 2.9.2 Novel object recognition (NOR) test

The NOR assay aimed to test cognition, more specifically working memory, with ageing, in zebrafish. This test was also performed in the behaviour room of the BMS Department of the University of Sheffield. This test consists in 2 phases. In Phase 1 (exploratory phase) the fish are exposed to two different objects and are allowed to explore them. In Phase 2 (test phase), one of the previous objects is replaced by a new one (novel object) and therefore the fish can explore two objects – the novel *versus* the familiar object. It is considered that the fish can distinguish the novel from the familiar object when the fish shows a preference for one of the objects during the test phase. This preference is evaluated by the time spent near the objects.

Before the experiment, all the fish were acclimatised to the behaviour room for at least 1h as described in section 2.8.1. The NOR test was performed in a 32x17.5x17.5cm tank (length x width x height) containing 7cm of water depth (**Fig 2.5**).

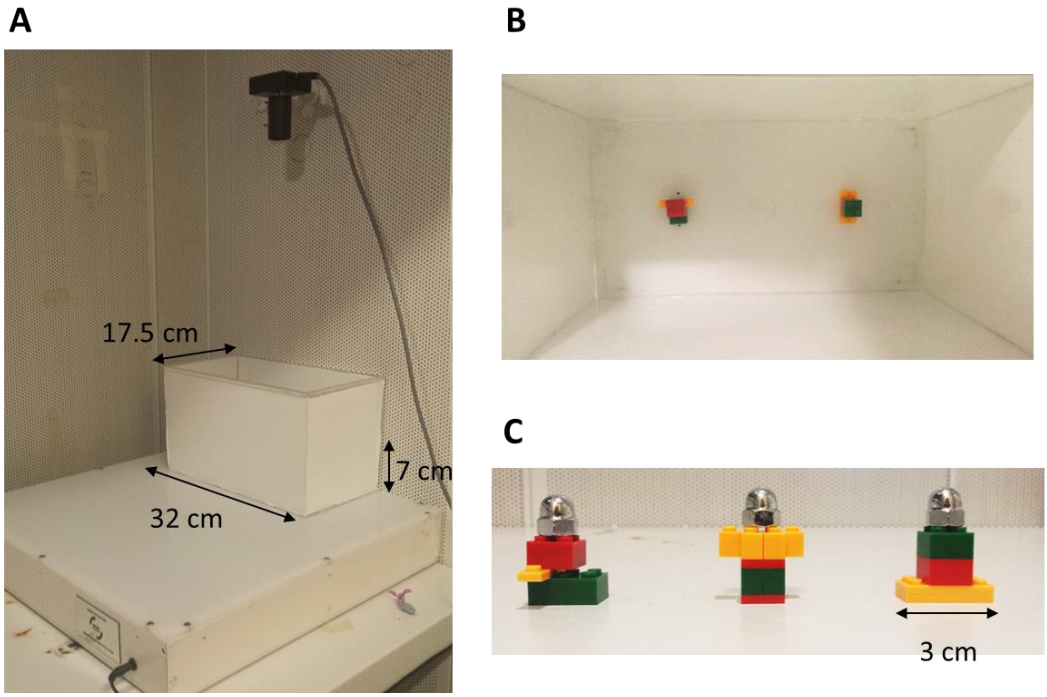


**Fig 2.5. Representative images of the setup used to perform the NOR test. (A)** Picture of the tank and top camera used to record the fish behaviour. **(B)** Top view of the test tank with two equidistant objects. **(C)** Close picture of the 3 different objects used in the NOR test.

In Phase 1, the test tank contained two equidistant objects (Object A and Object B), of approximately 3x3cm each. A fish was gently placed into the test tank and its behaviour was recorded for 10min. After Phase 1, the fish were placed in a holding tank for 2min and then returned to the test tank for Phase 2. In Phase two, the test tank contained two equally distant objects, Object A (familiar object) and Object C (novel object). In the end, the fish was returned to its tank. During the 20min trial, the fish behaviour was recorded for later data analysis. Like in the OF and NO tests, in the NOR test each fish was tested at a time and the water of the test tank was replaced between every fish.

The NOR test was performed for 3 consecutive days, where 10 to 20 fish were semi-randomly assigned to each morning/afternoon to test an equal number of fish from each group in the different days of experiment. Moreover, the designation (A, B or C) of the 3 objects available and their location (left or right) in the test tank were semi-randomly assigned in each day of experiment in order to avoid bias towards a possible favourite object or tank location.

Fish behaviour was analysed by measuring the time spent near the familiar and novel objects. Object discrimination was accessed by **Formula 5**, where positive values indicate a preference for the familiar object and negative values indicate a preference for the novel object. A mean value statistically significant from 0 was considered a successful discrimination between the two objects.

**TS**, time spent

**DI**, discrimination index

**Formula 5** $$DI = TS_{Familiar\ Object} - TS_{Novel\ Object}$$

## 2.10 Statistical analysis

All the statistical analysis was performed with GraphPad Prism v7.00, except for the random effect ANOVA which was analysed with the IBM SPSS Statistics v25.

Normality was assessed by the Shapiro-Wilk test. Unpaired t-test or Mann Whitney test were used to compare 2 data points, depending on whether the samples presented a Gaussian distribution or not, respectively. One-way ANOVA or two-way ANOVA followed by post-hoc tests with Bonferroni post-correction were used in order to compare more than 2 data points in 1 or 2 groups from the same tissue, respectively. Kruskal-Wallis followed by Dunn's post-hoc test replaced the One-Way ANOVA for non-normally distributed data.

Telomere length (or telomere/centromere ratio) was analysed by random effects ANOVA. Here, the intensity value of the mean (per cell) was used as the biological identity and the animals within each experimental group were analysed as a random variable. By doing so, the intensity value of the mean of each cell was taken into consideration within each animal. To perform a random effects ANOVA, linear mixed models were applied using the following script.

**Telo_Centro**, dependent variable (intensity values of the mean)
**Genotype**, independent variable of genotype (WT versus *tert*$^{-/-}$)
**Age**, independent variable of age (young versus old)
**Animal**, random variable, containing all the animals used in this study.

**Script:**

```
MIXED Telo_Centro BY Genotype Age Animal
  /CRITERIA=CIN(95) MXITER(100) MXSTEP(10) SCORING(1) SINGULAR(0.000000000001)
HCONVERGE(0,
    ABSOLUTE) LCONVERGE(0, ABSOLUTE) PCONVERGE(0.000001, ABSOLUTE)
  /FIXED=Genotype Age Genotype*Age | SSTYPE(3)
  /METHOD=REML
  /PRINT=DESCRIPTIVES
  /RANDOM=Animal | COVTYPE(VC)
  /EMMEANS=TABLES(Genotype)
  /EMMEANS=TABLES(Age)
  /EMMEANS=TABLES(Genotype*Age)
  /EMMEANS=TABLES(Genotype*Age) COMPARE(Age) ADJ(LSD)
  /EMMEANS=TABLES(Genotype*Age) COMPARE(Genotype) ADJ(LSD).
```

Moreover, Wilcoxon signed-ranked test against the hypothetical value of 0 was used to assess object discrimination during the NOR test. This is because a discrimination index close to 0 indicate that there is no discrimination between familiar and novel object. The higher the discrimination index, the better discrimination between the two objects.

A critical value for significance of $p<0.05$ was used throughout the study. Unless otherwise stated: p-value≥0.05; *p-value<0.05; **p-value<0.01; and ***p-value<0.001.

Finally, power calculations were performed in order to calculate the sample sizes required for each experiment. To do so, I calculated the effect sized following the 3R guidelines (http://www.3rs-reduction.co.uk/html/6__power_and_sample_size.html), using **Formula 6**.

**M1**, mean of group 1

**M2,** mean of group 2

**SE**, Standard error

**Formula 6**

$$Effect\ size = \frac{M1 - M2}{SE.}$$

Then, it was identified the minimum sample size required to detect a 25% difference with 90% power and 5% significance level in a two-sided test, using a reference table (available in the link above mentioned).

# Chapter 3.
# Age-related retinal degeneration is insufficient to stimulate the Müller glia regenerative response in zebrafish, leading to gliosis and loss of vision

# Title: Age-related retinal degeneration is insufficient to stimulate the Müller glia regenerative response in zebrafish, leading to gliosis and loss of vision

**Authors**
Raquel R. Martins[1,2], Mazen Zamzam[3], Mariya Moosajee[4, 5, 6, 7], Ryan Thummel[3], Catarina M. Henriques[1,2§], Ryan B. MacDonald[4§]

Affiliations:
1. Bateson Centre, University of Sheffield, Sheffield, UK, S10 2TN
2. Department of Oncology and Metabolism, University of Sheffield, UK,
3. Department of Ophthalmology, Visual and Anatomical Sciences, Wayne State University School of Medicine, Detroit, MI 48201, USA
4. Institute of Ophthalmology, University College London, London, UK, EC1V 9EL
5. Moorfields Eye Hospital NHS Foundation Trust, London, EC1V 2PD, UK
6. Great Ormond Street Hospital for Children NHS Foundation Trust, London, WC1N 3JH, UK
7. The Francis Crick Institute, London, NW1 1AT, London

§Co-corresponding authors: c.m.henriques@sheffield.ac.uk and ryan.macdonald@ucl.ac.uk

**Keywords:** retina, Müller glia, ageing, proliferation, degeneration, gliosis, zebrafish, telomerase, regeneration

**Article to be submitted to eLife**

## 3.1 Details on authors contributions

I have contributed to all figures and tables of this manuscript, except Fig 3.5; by participating in the experimental design as well as by performing the experiments and analysing the respective data. Moreover, I have co-written the article together with Catarina M. Henriques and Ryan B. McDonald.

Other authors: Catarina M. Henriques and Ryan B. MacDonald have contributed to conceive and design the experiments of the project, leading and supervising this project. Mazen Zamzam, supervised by Ryan Thummel, performed the experiments from Fig 3.5 and respective analysis. Mariya Moosajee generously lent us a behavioural setup in order to perform the optokinetic response test. Ryan Thummel and Mariya Moosajee have given intellectual input to this project.

## 3.2 Abstract

Ageing is a significant risk factor for developing retinal degenerative diseases and vision loss. Regenerative therapies offer great promise in the treatment of these devastating blinding conditions, but it remains unclear how old age impacts retinal homeostasis and its' ability to regenerate in response to chronic damage. We used the zebrafish model to characterise retinal ageing in the wild type and the premature ageing telomerase mutant (*tert*$^{-/-}$) model. We show that the zebrafish retina undergoes thinning due to an overall neuronal degeneration with ageing, which is largely telomerase independent. Despite its well-documented regenerative potential after damage, this neurodegeneration with ageing is insufficient to stimulate the Müller glia (MG) regenerative response. This occurs even though MG do maintain their regenerative capacity until old age following an acute retinal damage. In contrast, chronic neurodegeneration with ageing results in a gliotic response, thereby recapitulating several hallmarks of human retinal degeneration with ageing. Our work identifies gliosis as a key difference between chronic and acute damage, a key consideration for targeting endogenous regeneration mechanisms to treat human retinal disease.

### 3.2.1 Graphical abstract

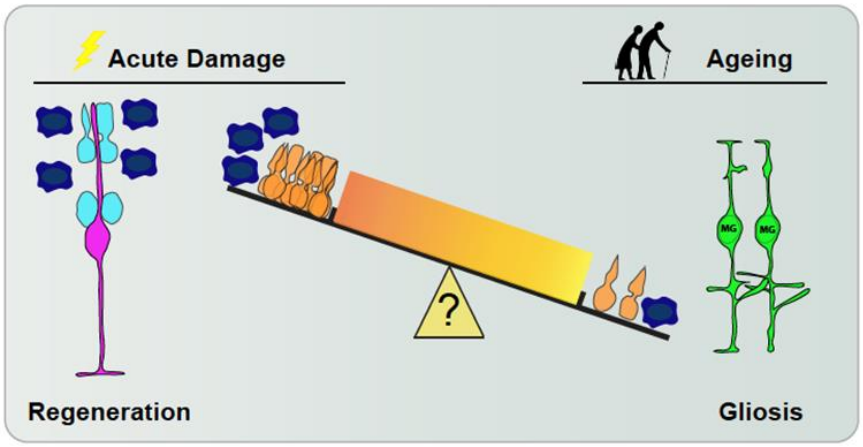


Our data suggest that the mechanisms driving regeneration in response to acute damage versus chronic, age-related damage, are different. It may be that either the number of cells dying in natural ageing is not enough to stimulate MG to proliferate, or the low number of microglia and respective signals released are not sufficient to trigger MG proliferation

## 3.3 Introduction

Ageing is a significant risk factor for human retinal degenerative disease, such as age-related macular degeneration (AMD) and vision loss. As the population is ageing worldwide, the identification and potential treatment of the underlying cellular and molecular dysfunctions will be critical for global health going forward. Regeneration-based therapies, such as stimulating endogenous regenerative mechanisms, offer great promise for the treatment of many human blinding diseases. Intensive efforts have been made to uncover the molecular mechanisms regulating the retinas' endogenous regenerative responses in lower vertebrates (Fischer & Reh, 2001; Lenkowski & Raymond, 2014; Raymond et al., 2006; Thummel et al., 2008; Wan & Goldman, 2016). While the mammalian retina lacks significant regenerative capacity (Jadhav et al., 2009; Ooto et al., 2004), re-introduction of key molecular signals into Müller glia (MG) has shown great promise to stimulate the genesis of new neurons after damage (Jorstad et al., 2017, 2020; Karl et al., 2008). However, these studies in lower vertebrates and mammals are typically carried out in young adults. As advanced age is strongly associated with the pathogenesis of many retinal degenerative conditions, understanding the effects of ageing on the regenerative potential in the retina is an important consideration for the efficacy of such treatments going forward.

The zebrafish is a well-established model to study retinal development, disease and regeneration (Cameron, 2000; Eastlake et al., 2017; Richardson et al., 2017; Stenkamp, 2015). In the retina, the principal cells tasked with supporting retinal circuits throughout life are the MG. MG do this by providing a myriad of support functions to neurons, including trophic support, neurotransmitter recycling and energy metabolism (Reichenbach & Bringmann, 2013). While these functions are critical to the maintenance of healthy retinal function, MG also play a prominent role in disease and after neuronal insult. In the mammalian retina, degeneration results in a MG gliotic response. This leads to the up-regulation of stress proteins and morphology changes, which are thought to be neuroprotective initially, but may ultimately culminate in dysfunction (Bringmann et al., 2009). In contrast to mammals, after damage, the MG in the zebrafish retina will undergo a brief reactive gliosis-like phase that transitions into a de-differentiation and proliferation of the MG progenitor cell to generate new neurons (Eastlake et al., 2017; Thomas et al., 2016; Thummel et al., 2008). While MG may be the primary source of neurons after injury in teleosts, regeneration can also occur

from the ciliary marginal zone (CMZ) (Raymond et al., 2006). CMZ is a population of progenitors found in the peripheral retina that is thought to contribute to retinal growth throughout life (**Fig 3.1A**). Additionally, rods can originate from rod-specific progenitors (Johns & Fernald, 1981; Julian et al., 1998) found in the outer retina. Rod-specific progenitors are derived from MG that slowly divide in the WT retina (Bernardos et al., 2007; Otteson et al., 2001; Raymond et al., 2006). Multiple acute injuries do not appear to reduce the overall regenerative response of MG; however, there does appear to be chronic inflammation after successive rounds of injury (Ranski et al., 2018). It should be noted that studies of MG-derived regeneration are often carried out in young adult animals, and it remains unclear how ageing impacts regenerative potential throughout the life course. While the zebrafish retina has been shown to display decreased cell density and increased cell death with increasing age (Van Houcke et al., 2019), it remains unclear if this age-related cell death stimulates endogenous regeneration and repair mechanisms, or how natural age impacts the regenerative potential of the MG. We hypothesised that the zebrafish retina loses its steady state regenerative capacity with ageing, thereby leading to degeneration and vision loss.

Recent studies have shown that zebrafish display key human-like hallmarks of ageing in most tissues. Depending on the tissue, this includes telomere shortening and consequent DNA damage, decreased proliferation, and increased apoptosis or accumulation of senescence (Anchelin et al., 2013; C. Carneiro et al., 2016; Henriques et al., 2013). Zebrafish thus offer an attractive model to study regeneration in a human-like, ageing model. Telomere shortening is a hallmark of ageing implicated in many age-related diseases (López-Otín et al., 2013). Telomeres, a protective cap in linear chromosomes, shorten significantly with each cell division, in proliferative tissues, due to the end-replication problem and consequent oxidative damage of the lagging end (Levy et al., 1992). Progressive shortening of telomeres can have damaging effects, such as cellular senescence, which is characterized by permanent cell cycle arrest and persistent DNA damage response. Telomerase is the enzyme with the ability to correct this end-replication problem, but most somatic cells maintain a low level of telomerase expression (Forsyth et al., 2002; Henriques & Ferreira, 2012). Given that telomerase activity correlates to a cell's proliferation potential, this enzyme is perceived as a positive aspect in the context of regeneration. In fact, telomerase has been shown to be essential for tissue regeneration, namely in the mammalian liver (Lin et al., 2018) and in the

zebrafish heart (Bednarek et al., 2015). Furthermore, there is some evidence that telomerase is important for retina's health. In humans, age-related diseases of the retina, such as AMD, have been reported to be alleviated by telomerase reactivation (Dow & Harley, 2016; Rowe-Rendleman & Randolph, 2004), suggesting that limited expression of telomerase may play a role in retina ageing. Accordingly, the telomerase mutant zebrafish model (*tert*$^{-/-}$), known to age and die prematurely (Carneiro et al., 2016; Henriques et al., 2013), have been reported to display accelerated retina thinning (Anchelin et al., 2013). As it has been shown that cellular proliferation is a key factor in retinal homeostasis (Van Houcke et al., 2019), and that telomerase and telomere stability play an important role in cell proliferation, we sought to determine whether retinal degeneration and vision impairment with ageing is telomerase-dependent.

Here, we used zebrafish as a model to determine how ageing impacts the retina's steady-state homeostasis and whether this is telomerase-dependent. Our work shows that zebrafish retina ageing is characterised by structural and morphological alterations in the central retina, resembling human retina ageing. These include retina thinning, neuronal loss and disorganisation of the photoreceptors, culminating in visual impairment. Interestingly, retina ageing and consequent vision loss is not significantly accelerated by lack of telomerase expression. Importantly, contrary to what occurs in situations of acute damage, we observed no compensatory proliferation in response to age-related neuronal degeneration. Despite lack of regeneration in response to chronic, age-related damage, MG retain their capacity to proliferate and restore lost neurons in response to an acute damage until old age. In contrast, with chronic age-related degeneration, in MG cells undergo a gliosis-like phenotype, including characteristic changes in morphology and localisation of glial fibrillary acidic protein (GFAP) intermediate filaments. Together, our work suggests key molecular differences between chronic and acute damage in the retina.

## 3.4 Results

### 3.4.1 Zebrafish retina ageing is characterised by telomerase-independent central retina thinning, morphological alterations, and neurodegeneration

Similar to humans, the zebrafish retina consists in three nuclear layers separated by two plexiform layers. The nuclear layers consist in the outer nuclear layer (ONL) containing photoreceptors; the inner nuclear layer (INL) containing bipolar cells (BCs), amacrine cells (ACs), horizontal cells (HCs) and Müller glia (MG); and the ganglion cell layer (GCL) mainly containing retinal ganglion cells (RGCs) (**Fig 3.1A**). Furthermore, the zebrafish retina can be divided into discrete regions based on age (Fu, Nagashima, Guo, Raymond, & Wei, 2018). Here, we characterise two regions: the central retina containing the oldest cells, born during early development; and the peripheral retina containing the ciliary marginal zone (CMZ) and the immediately adjacent tissues, comprising the newest born cells (**Fig 3.1A**).

A key hallmark of human retinal ageing is the thinning in the central retina (Eriksson & Alm, 2009). Previously it was shown that the linear cell density in the central region of the adult zebrafish retina also declines with age, with exception of rods (Van Houcke et al., 2019). However, it remained unclear whether telomerase played a role on this. As such, we quantified retinal thickness in the central and peripheral adult zebrafish retina by DAPI stain at defined time-points of adulthood. Our results show that the WT retina progressively thins with ageing in the central region (**Fig 3.1B, B'**), as previously shown. Retina thinning is not accelerated in the prematurely aged *tert*$^{-/-}$ model when compared to its WT counterpart at any age analysed, suggesting that thinning of central retina with ageing is independent of telomerase (**Fig 3.1B, B'**; **Supplementary Fig 1A**). Proliferation in the central retina is low but it still decreases significantly with ageing (**Fig 3.1D, D'**). However, this is not accelerated in the absence of telomerase (*tert*$^{-/-}$), suggesting different mechanisms other than telomere shortening to be the limiting factor for proliferation in this region.

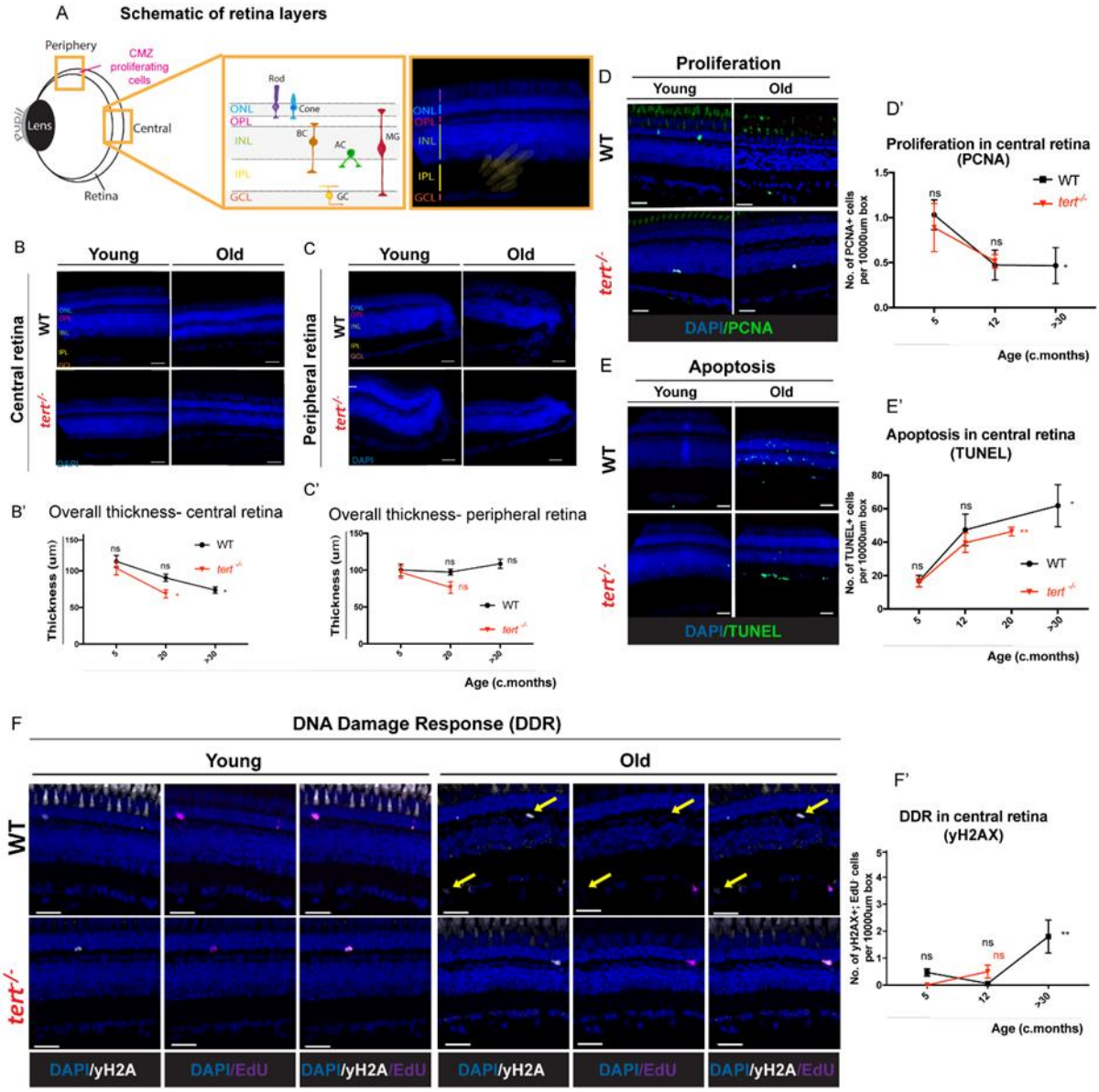
A
Schematic of retina layers
Periphery
CMZ proliferating cells
Lens
Central
Retina
Rod
Cone
BC
AC
MG
GC
ONL
OPL
INL
IPL
GCL
B
Young
Old
Central retina
WT
tert-/-
C
Peripheral retina
B'
Overall thickness- central retina
C'
Overall thickness- peripheral retina
Thickness (um)
Age (c.months)
D
Proliferation
DAPI/PCNA
D'
Proliferation in central retina (PCNA)
No. of PCNA+ cells per 10000um box
E
Apoptosis
DAPI/TUNEL
E'
Apoptosis in central retina (TUNEL)
No. of TUNEL+ cells per 10000um box
F
DNA Damage Response (DDR)
DAPI/yH2A
DAPI/EdU
DAPI/yH2A/EdU
F'
DDR in central retina (yH2AX)
No. of yH2AX+; EdU cells per 10000um box

**Fig 3.1. Zebrafish retina ageing is characterised by thinning of the central retina, accompanied by decreased proliferation and increased apoptosis and DNA damage. This occurs independently of telomerase.** (A) Schematic figure of the zebrafish retina with respective layers and cell types. (B) Representative images of the central and (C) peripheral retina in both WT and *tert*$^{-/-}$, at young (5 months) and old ages (>30 months in WT and 20 in *tert*$^{-/-}$). The staining was performed in 4µm-thick paraffin sections. Bars: 20µm. (B'-C') Quantifications of the overall retina thickness (in µm) using DAPI staining, in (B') central and (C') peripheral retina. The black line represents WT and the red line represents *tert*$^{-/-}$. Error bars represent the standard error of the mean (SEM). N=3. (D-F) Representative images of central retina immunolabelled with (D) PCNA (proliferative cells, in green), (E) TUNEL (apoptotic cells, in green) and (F) γH2AX; EdU (DNA damage, in white, and proliferating cells, in purple), in the central retina of both WT and *tert*$^{-/-}$, at young (5 months) and old ages (>30 months in WT and 12 or 20 in *tert*$^{-/-}$). Bars: 20µm. The staining was performed in (E, F) 16µm-thick or (E) 4µm-thick paraffin sections. (F) Yellow arrows highlight γH2AX+; EdU- cells, putative senescent cells. (D'-F') Quantifications of the number of (D') PCNA+ cells, (E') TUNEL+ cells and (F') γH2AX+; EdU- cells, per area (10 000 µm$^2$). The black line represents WT and red line represents tert$^{-/-}$. Error bars represent the SEM. (D') N=6-12; (E', F') N=3-4. Statistics: two-way ANOVA (WT vs *tert*$^{-/-}$ at young versus old ages) and one-way ANOVA (WT and *tert*$^{-/-}$ over-time). Differences between genotypes are indicated above each time-point, whereas differences over-time in each genotype are indicated in the end of the lines, in black WT, in red *tert*$^{-/-}$. P-value: * <0.05; ** <0.01; *** <0.001.

Contrary to the central retina, there is no obvious overall thinning of the peripheral retina with natural ageing nor in the absence of telomerase (**Fig 3.1C, C'** and **Supplementary Fig 1B**). Although the CMZ is known to be proliferative, its proliferation activity decreases with ageing (**Supplementary Fig 1C**) and seems to be insufficient to drive telomere-dependent arrest of cell cycle. Reduced proliferation with ageing is therefore unlikely to be the driving mechanisms for retinal degeneration, whereas cell death is likely to play a more important role.

Increased activated caspase-3 has been shown in the aged zebrafish retina (Van Houcke et al., 2019). However, this was not quantified, and it remains unclear whether this was associated with telomerase-dependent DNA damage. Moreover, there are other forms of cell death that are not caspase-3 dependent. We therefore used a more generalised early cell death marker which labels DNA breaks, Terminal deoxynucleotidyl transferase dUTP nick end labeling (TUNEL). We found that there is significantly increased cell death in the aged central retina (**Fig 3.1E, E'**). Again, cell death occurs independently of telomerase, as increased number of dying cells was not accelerated in the *tert*$^{-/-}$ model when compared with their WT counterpart.

Cellular senescence, which is characterised by a permanent cell cycle arrest and persistent DNA damage response (reviewed in Tchkonia et al., 2013), has also been suggested to increase in the aged retina, in mammals and zebrafish (Majji et al., 2000; Van Houcke et al., 2019; Wing et al., 1978). Our results show that the decrease in cell proliferation with ageing is accompanied by accumulation of strong γH2AX nuclear foci, a molecular marker for DNA damage, in non-proliferating cells (EdU-negative) (**Fig 3.1F, F'**), potentially representing senescent cells. We now show that this increase in DNA damage also occurs in a telomerase-independent manner, as no differences are identified between genotypes at any time-point analysed.

Together, these data show that aging in the retina is characterized by decreasing proliferation, accompanied by increasing DNA damage and cell death. These events are likely to contribute to the retinal thinning observed in the aged retina. Importantly, although this DNA damage is likely underpinning the previously reported increase in SA-β-gal (Van Houcke et al., 2019), we show that this is unlikely to be a telomere-dependent and therefore unlikely to be replicative senescence.

#### 3.4.1.1 Morphological alterations and neurodegeneration

Besides its role in cellular proliferation, telomerase has been shown to have telomere-independent (i.e. non-canonical functions), including in zebrafish (Alcaraz-pe et al., 2014). For instance, in the central nervous system, it has been suggested that telomerase has a neuroprotective role against oxidative damage (Ahmed et al., 2008; Haendeler et al., 2009). In fact, telomerase activity is identified in post-mitotic neurons in the adult zebrafish retina (Wui-Man Lau et al., 2008), where telomerase could exert telomere-independent functions. We therefore tested whether telomerase played a role in age-related morphological alterations and neurodegeneration in the zebrafish retina. To test this, we carried out cell labelling using immunohistochemistry for several molecular markers (**Supplementary Table 1**) throughout the lifespan of zebrafish, in the presence and absence of telomerase (*tert*$^{-/-}$).

The loss of photoreceptor integrity is one of the key features of human retina ageing and disease, including decreased photoreceptor number and integrity (Nian & Lo, 2019) and this has been shown to also happen with ageing in the zebrafish retina (Van Houcke et al., 2019). Rhodopsin immunolabelling confirmed that, like in humans, rod photoreceptor outer segments in the zebrafish retina undergo dramatic structural changes with ageing, losing their long and rectangular characteristic shape (**Fig 3.2A**). Qualitative analysis of rhodopsin shows that 100% of young WT fish present long and aligned outer segments whereas 100% of old WT fish present short and misaligned outer segments (**Fig 3.2A'**). Like for other phenotypes, these defects are not accelerated in the *tert*$^{-/-}$ at the comparable age tested of 5 months old, suggesting this is likely a telomerase-independent phenomenon (**Fig 3.2A'**). The structural changes we observe in the rods' outer segments are accompanied by disruption of the tight junction protein zonula occludens (ZO-1) (**Fig 3.2B**), a marker for the outer limiting membrane thought to be involved in photoreceptor degeneration (Fu et al., 2018). Qualitative analysis shows that whereas the majority of young WT fish show a continuous ZO-1 line underlying the photoreceptors, all of the old WT fish present breaks in the ZO-1 (**Fig 3.2B'**). These defects are also not accelerated in the *tert*$^{-/-}$ at the comparable age tested of 5 months old, suggesting this is likely a telomerase-independent phenomenon.

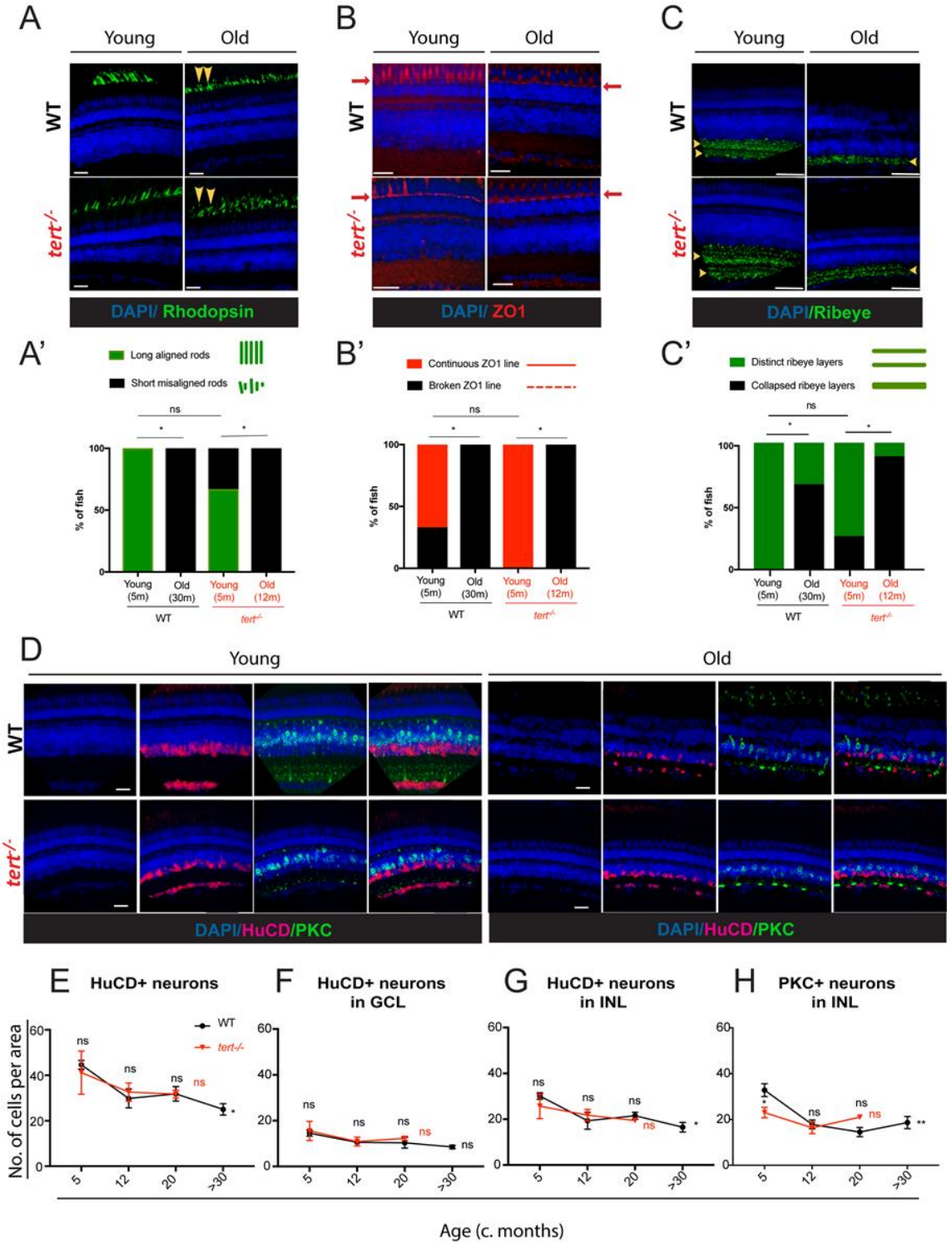
A
Young
Old
WT
tert-/-
DAPI/ Rhodopsin
B
Young
Old
WT
tert-/-
DAPI/ ZO1
C
Young
Old
WT
tert-/-
DAPI/Ribeye
A'
Long aligned rods
Short misaligned rods
ns
*
*
100
50
0
% of fish
Young (5m)
Old (30m)
Young (5m)
Old (12m)
WT
tert-/-
B'
Continuous ZO1 line
Broken ZO1 line
ns
*
*
100
50
0
% of fish
Young (5m)
Old (30m)
Young (5m)
Old (12m)
WT
tert-/-
C'
Distinct ribeye layers
Collapsed ribeye layers
ns
*
*
100
50
0
% of fish
Young (5m)
Old (30m)
Young (5m)
Old (12m)
WT
tert-/-
D
Young
Old
WT
tert-/-
DAPI/HuCD/PKC
DAPI/HuCD/PKC
E
HuCD+ neurons
F
HuCD+ neurons in GCL
G
HuCD+ neurons in INL
H
PKC+ neurons in INL
No. of cells per area
WT
tert-/-
60
40
20
0
ns
*
**
5
12
20
>30
Age (c. months)

**Fig 3.2. Retina thinning with ageing is accompanied by structural and morphological alterations, and neurodegeneration, which occur independently of telomerase.** (A-C) Representative images of central retina immunolabelled with (A) rhodopsin (photoreceptors outer segments, in green), (B) ZO1 (outer limiting membrane, in red) and (C) ribeye (pre-synaptic ribbons, in green), in both WT and *tert*$^{-/-}$, at young (5 months) and old ages (>30 months in WT and 12 months in *tert*$^{-/-}$). The staining was performed in 4µm-thick paraffin sections. The red arrows in panel B point to the outer limiting membrane (ZO-1-expressing line). Bars: 20µm. (A'-C') Quantification of the percentage of fish presenting defects in (A') rhodopsin (short and misaligned outer segments), (B') ZO1 (broken outer limiting membrane) and (C') ribeye (collapsed ribeye layers). The black line represents WT and the red line represents *tert*$^{-/-}$. Error bars represent the SEM. (A'-B') N=3-6; (C') N=4-9. (D) Representative images of central retina immunolabelled with HuCD and protein kinase C, or PKC (amacrine in magenta and bipolar cells in green, respectively), in both WT and *tert*$^{-/-}$, at young (5 months) and old ages (>30 months in WT and 12 months in *tert*$^{-/-}$). The staining was performed in 16µm-thick paraffin sections. Bars: 20µm. (E-H) Quantifications of the number of HuCD-positive neurons (E) in the overall retina, (F) in the GCL (ganglion cells) and (G) in the INL (amacrine cells). (H) Quantifications of the number of PKC-positive neurons in the INL (bipolar cells). (E-H) The black line represents WT and red line represents *tert*$^{-/-}$. Error bars represent the SEM. N=3-4. The quantifications were performed per area of the retina (10 000 µm$^2$). CMZ: ciliary marginal zone; BP: bipolar cell; AC: amacrine cell; MG: müller glia; RGC: retinal ganglion cell; GCL: granular cell layer; IPL: inner plexiform layer; INL: inner nuclear layer; OPL: outer plexiform layer; ONL: outer nuclear layer; PR: photoreceptor. Statistics: (A'-C') Qui-square; (E-H) two-way ANOVA (WT vs *tert*$^{-/-}$ at young versus old ages) and one-way ANOVA (WT and *tert*$^{-/-}$ over-time). Differences between genotypes are indicated above each time-point, whereas differences over-time in each genotype are indicated in the end of the lines, in black WT, in red *tert*$^{-/-}$. P-value: * <0.05; ** <0.01; *** <0.001.

The RGCs, ACs and BCs are neurons that come together to make connections in the major synaptic neuropil, called the inner plexiform layer (IPL). We confirmed alterations in the synaptic IPL layer with ageing. Usually, the IPL is characterised by 6 distinct layers of pre-synaptic ribbons, as observed in zebrafish young ages (**Fig 3.2C**). However, this structure is collapsed in the aged zebrafish retina, where IPL displays decreased number and disorganisation of pre-synaptic ribbons (**Fig 3.2C'**). This pre-synaptic ribbon pathology is not accelerated in the *tert*$^{-/-}$ at the comparable age tested of 5 months old, suggesting this is likely a telomerase-independent phenomenon. Such alterations in the synapses of the IPL are known to influence neurotransmission in the retina. We therefore investigated the potential role of telomerase in more subtle alterations in the number of RGCs in GCL, and BCs and ACs in INL (**Fig 3.2D**). As expected, there is an overall neuronal loss with ageing in the zebrafish retina (**Fig 3.2E**). Importantly, this neuronal loss is not due to a decreased number of HuC/D-expressing RGCs in the GCL (**Fig 3.2F**), but due to a decreased number of HuC/D-expressing ACs (**Fig 3.2G**), and PKC-expressing BCs in the INL layer (**Fig 3.2H**). Additionally, in the aged zebrafish retina, BCs display disorganised axon terminals in the IPL. However, once again, neuronal loss is not accelerated in the absence of telomerase, suggesting that this is also a telomerase-independent phenomenon.

### 3.4.2 MG do not proliferate in response to chronic retinal neurodegeneration with ageing

Our data show there is significant accumulation of cell death and neuronal loss accompanying retinal thinning with ageing. However, it remains unclear whether these age-related degenerations are being counteracted to some degree by compensatory proliferation and, in particular, by the well-described regenerative response of MG in the retina. PCNA staining in the central retina suggested that there was no compensatory proliferation in this region (**Fig 3.1E, E'**). To characterise the steady state regenerative capacity of the retina until old age, we carried out a 3-day pulse of EdU followed by 0- and 30-days chase, in young and old WT and *tert*$^{-/-}$ zebrafish (**Fig 3.3A**). It is known that acute injury elicits a compensatory proliferation response in the zebrafish retina. We therefore hypothesised that the observed age-associated neuronal degeneration and cell death (**Fig 3.3B**) would lead to compensatory proliferation.

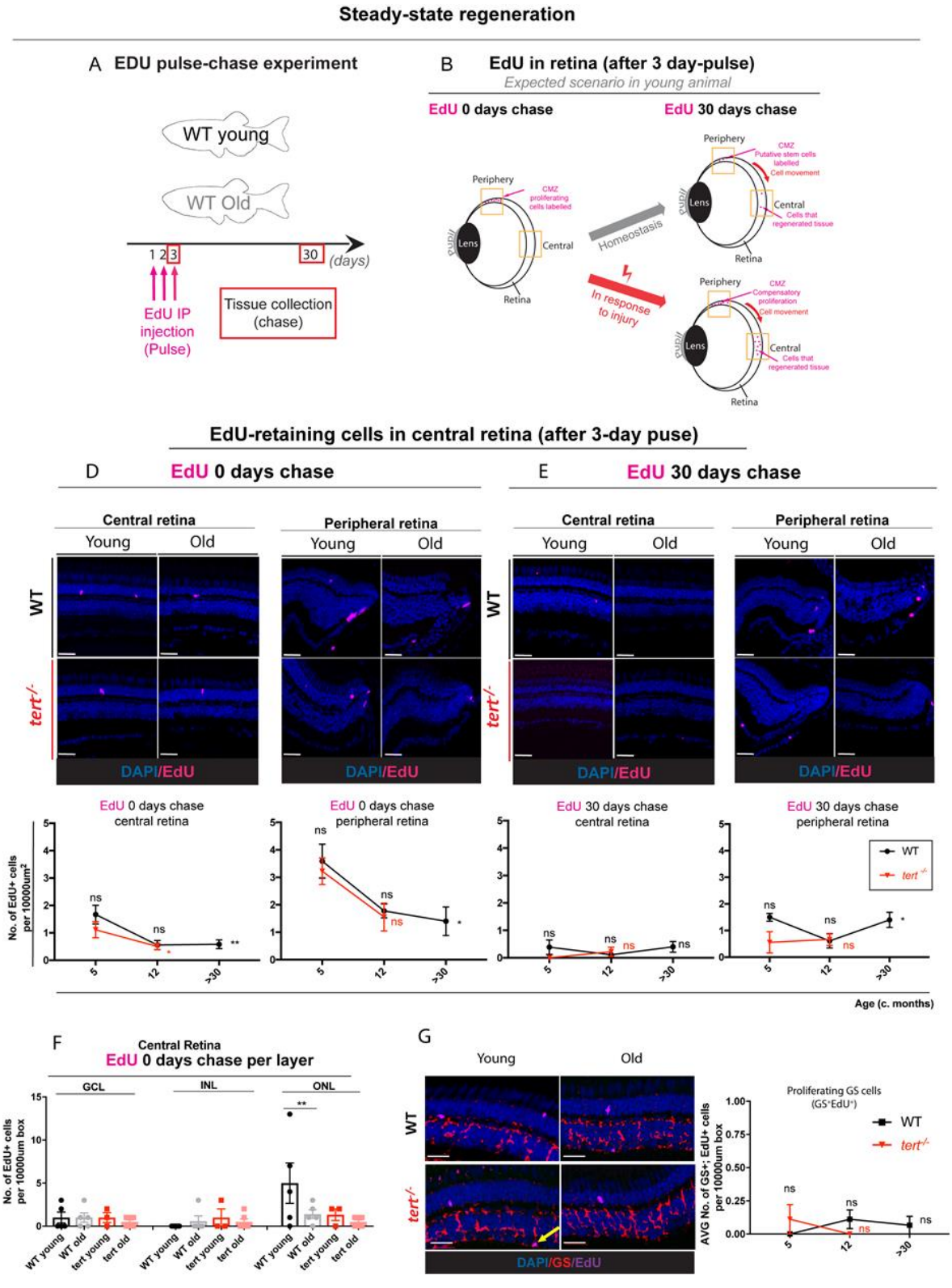
Steady-state regeneration
A EDU pulse-chase experiment
WT young
WT Old
1 2 3
30
(days)
EdU IP injection (Pulse)
Tissue collection (chase)
B EdU in retina (after 3 day-pulse)
Expected scenario in young animal
EdU 0 days chase
EdU 30 days chase
Periphery
CMZ proliferating cells labelled
Lens
Central
Retina
Homeostasis
In response to injury
CMZ Putative stem cells labelled Cell movement
Central Cells that regenerated tissue
CMZ Compensatory proliferation Cell movement
EdU-retaining cells in central retina (after 3-day puse)
D EdU 0 days chase
E EdU 30 days chase
Central retina
Peripheral retina
Young
Old
WT
tert-/-
DAPI/EdU
EdU 0 days chase central retina
EdU 0 days chase peripheral retina
EdU 30 days chase central retina
EdU 30 days chase peripheral retina
No. of EdU+ cells per 10000um2
ns
Age (c. months)
F
Central Retina
EdU 0 days chase per layer
GCL
INL
ONL
No. of EdU+ cells per 10000um box
WT young
WT old
tert young
tert old
G
Young
Old
WT
tert-/-
DAPI/GS/EdU
Proliferating GS cells (GS+EdU+)
AVG No. of GS+; EdU+ cells per 10000um box

**Fig 3.3. Aged zebrafish retina does not show signs of regeneration in response to spontaneous cell death and neuronal loss.** (A) Schematic figure of the experimental design: 3-day pulse of EdU, by IP injection, followed by 0- or 30-day chase; (B) and respective expected results. We anticipated that in a healthy young fish, the retina has some cells proliferating in the CMZ, which, over-time, will replace older cells in the central retina. In the case of injury, we anticipate that there will be elevated levels of proliferation in peripheral and central retina in order to replace the death cells. (C-D) Representative images of central and peripheral retina immunolabelled with EdU (in purple), at (C) 0- and (D) 30-days chase, in WT at young (5 months), middle (12 months) and old ages (>30 months), and *tert*$^{-/-}$ young (5 months) and old (12 months). The staining was performed in 16µm-thick paraffin sections. Bars: 20µm. (C', C'', D', D'') Quantifications of the number of EdU-retaining cells per area (10 000 µm$^2$), in the overall (C') central and (C'') peripheral retina at 0-days chase and in the overall (D') central and (D'') peripheral retina at 30-days chase. (E) Quantifications of the number of EdU-retaining cells per area (10 000 µm$^2$), per layer of the retina, at 0-days chase. Error bars represent SEM. N=3-6. (F) Representative images of central retina immunolabelled with GS (müller glia, in red) after a 3-day pulse of EdU, by IP injection, at 0-days chase, in WT at young (5 months) and old ages (>30 months). The staining was performed in 16µm-thick paraffin sections. Bars: 20µm. (F') Quantifications of the number of GS+; EdU+ cells per area (10 000 µm$^2$). Error bars represent SEM. N=3-6. CMZ: ciliary marginal zone. Statistics: Two-way ANOVA (WT vs *tert*$^{-/-}$ at young versus old ages) and one-way ANOVA (WT and *tert*$^{-/-}$ over-time). Differences between genotypes are indicated above each time-point, whereas differences over-time in each genotype are indicated in the end of the lines, in black WT, in red *tert*$^{-/-}$. P-value: * <0.05; ** <0.01; *** <0.001.

However, we observe few EdU positive cells and, instead of a compensatory proliferation response, we detect less EdU positive cells with ageing, suggesting overall reduced proliferative capacity (**Fig 3.3C, C'**). These levels are also reduced after a 30-days chase (**Fig 3.3D, D'**), suggesting that there are very few cells proliferating at all in the aged central retina. As the CMZ is known to be the most proliferative area in the adult retina, we tested whether we could detect more EdU-retaining cells in the peripheral retina in both young and old zebrafish. In the peripheral retina, at 0-days chase, we see double of the EdU-retaining cells than in the central retina (**Fig 3.3C, C', D, D'**). Nevertheless, as in the central retina, proliferation decreases with ageing (see also PCNA staining in **Supplementary Fig 1C**), suggesting that there is no compensatory proliferation in response to the observed increased cell death in natural ageing.

To test whether there was any compensatory proliferation with ageing occurring from rod-specific progenitors found scattered throughout the ONL of the retina (Johns & Fernald, 1981; Stenkamp, 2015), we quantified levels of EdU positive cells in the ONL. These progenitors are derived from slowly dividing MG (Bernardos et al., 2007; Lenkowski & Raymond, 2014; Otteson et al., 2001; Raymond et al., 2006). These rod precursors undergo a terminal mitosis to generate new rod photoreceptors (Johns & Fernald, 1981). Although we observe $EDU^{+}$ cells in the central ONL of 5 months WT (likely to be rod precursors dividing), there are barely any detected in >30 months old aged WT. Once again, removing telomerase (*tert*$^{-/-}$) had no further effect (**Fig 3.3E**). This shows that there is also no compensatory proliferation occurring in this region in response to the increased cell death with ageing, in the presence nor absence of telomerase.

Finally, as proliferation of MG is the primary source of neurons after injury in fish (Bernardos et al., 2007), we sought to determine whether there was any compensatory proliferation occurring in this cell population. To do so, we co-labelled cells with the classical marker of MG, glutamine synthetase (GS), and EdU, and identified the GS-positive; EdU-positive cells. We detected very few GS-positive; EdU-positive cells in the central retina in both WT and *tert*$^{-/-}$, at any time-point throughout their lifespan (**Fig 3.3F, F'**), suggesting MG are also not proliferating in the central retina at old ages. Together, our data show that there is no compensatory proliferation in response to age-related degeneration in the zebrafish retina, by any of the known sources of regeneration and neurogenesis: CMZ, rod precursor

cells and MG. Perhaps not surprisingly given the very low levels of proliferation in the first place and the fact that there is no compensatory proliferation, removing telomerase (*tert*$^{-/-}$ mutants) has no further effect. In summary, contrary to acute damage, our data show that age-related chronic cell death does not trigger proliferation of MG cells.

### 3.4.3 Zebrafish vision declines with ageing, independently of telomerase

Loss of visual acuity and contrast sensitivity with advancing age in humans has been well documented (Marshall, 1987; Salvi et al., 2006). As we observe pathological cellular changes in the aged zebrafish retina, we next wondered if vision is affected in the aged zebrafish. Visual testing in the zebrafish has been used to screen for mutants with defects in retinal development and function (Brockerhoff et al., 1995; Gross et al., 2005; Lessieur et al., 2019; Neuhauss et al., 1999). However, it is unclear if zebrafish show age-associated changes in visual acuity. In order to determine age-related changes in vision in naturally aged adult WT, we used the optokinetic response (OKR) assay. The OKR is a well-established assay to measure innate visual responses and provides a readout of visual acuity (Brockerhoff et al., 1995; Tappeiner et al., 2012) (**Fig 3.4A**). Our results show a decreased number of eye rotations per minute in aged fish (**Fig 3.4B**), suggesting that zebrafish vision declines with ageing. As it was previously shown that telomerase expression is important for macular function in humans (Dow & Harley, 2016; Rowe-Rendleman & Randolph, 2004), we used the *tert*$^{-/-}$ zebrafish model to test whether reduced telomerase expression with ageing could underpin changes in vision. Our data show that, in comparison with its WT counterpart, the *tert*$^{-/-}$ zebrafish does not display and accelerated reduced visual acuity at 5 months or 12 months of age, close to the end point of *tert*$^{-/-}$ life (**Fig 3.4B**). Together, our data show that the zebrafish retina displays significant age-related decrease of visual acuity. Importantly, these phenotypes are occurring in an age-dependent but telomerase-independent manner, as is the case for all key hallmarks of retina ageing measured so far (**Supplementary Table 1**). Telomerase seems therefore not required for the maintenance of the key retina steady state homeostasis hallmarks tested here.

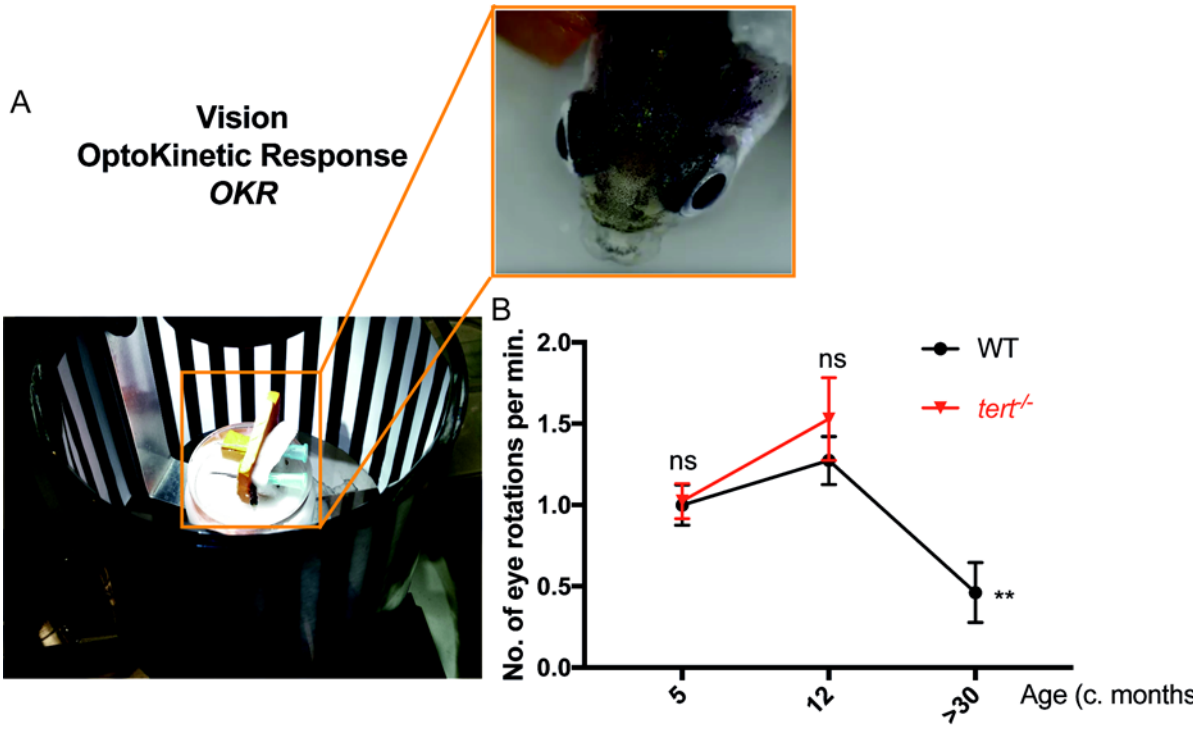
A
Vision
OptoKinetic Response
OKR
B
No. of eye rotations per min.
2.0
1.5
1.0
0.5
0.0
ns
ns
**
WT
tert-/-
5
12
>30
Age (c. months

**Fig 3.4. Zebrafish vision declines with ageing, independently of telomerase.** (A) OKR assay was performed by immobilising the fish in between soft sponges, inside a petri dish containing water, placed in the centre of a rotation chamber. The walls of the rotation chamber had 0.8 mm-thick black and white stripes and the chamber was maintained at a constant velocity of 12 rpm throughout the experiment. (B) The number of eye rotations per minute was manually quantified by video observation. The black line represents WT and the red line represents *tert*$^{-/-}$. Error bars represent the SEM. N=5-8. Statistics: two-way ANOVA (WT vs *tert*$^{-/-}$ at young versus old ages) and one-way ANOVA (WT and *tert*$^{-/-}$ over-time). Differences between genotypes are indicated above each time-point, whereas differences over-time in each genotype are indicated in the end of the lines, in black WT, in red *tert*$^{-/-}$. P-value: * <0.05; ** <0.01; *** <0.001.

### 3.4.4 MG retain the ability to regenerate the light damaged retina in aged zebrafish

It is well described that retinal cell death in response to acute injury leads to a regenerative response in zebrafish. However, in the context of chronic damage with ageing, we do not observe a MG proliferative regenerative response. Therefore, we next sought to determine whether the observed retinal degeneration could be due to the MG cells losing their capacity to regenerate in old age. In acute damage models it has been shown that several damage paradigms induce retinal neuron death and elicit a regenerative response in young or adult zebrafish (Bernardos et al., 2007; Cameron, 2000; Hanovice et al., 2019; Ranski et al., 2018). In adults, specifically between 9-18 months of age, repeated light-damage treatments result in MG continuously re-entering the cell cycle and proliferate to regenerate lost neurons, although they do show signs of chronic activation (Ranski et al., 2018). It remains unknown whether this regenerative capacity is maintained until old age. Nevertheless, retinal regeneration studies typically focus on adult retinas, not taking into account old age on regenerative response. To test this, we used the light-damage model where aged zebrafish were treated with light to elicit photoreceptor damage. To detect increased proliferation of MG in response to damage, a 3-day pulse of BrdU was performed, followed by a 28-days chase period (**Fig 3.5A**). After a 3-day pulse, BrdU should label both MG and their daughter cells, the newly-formed progenitors (**Fig 3.5B**). Our results show that light-lesion in the retina elicits an initial damage response characterized by the strong recruitment of microglia. These microglia are preferentially localized near the ONL, suggesting photoreceptors are worst affected, a typical feature of this damage model (**Fig 3.5C**). The recruitment of microglia to the retina reaches comparable levels across all ages tested. Moreover, there are no differences in the incorporation of BrdU with ageing on any layer, at 72 hours post-light damage (hpL), when the initial regenerative response is mounted, or at 28 dpL, when the number of MG that initially re-entered the cycle can be identified. Both the unaltered immediate timing of MG response and the overall capacity to regenerate each neuronal layer are maintained with increased age. Together these results suggest that the regenerative response remains intact throughout zebrafish lifespan. Therefore, the lack of compensatory proliferation in response to chronic, age-associated cell death in the ageing zebrafish retina is not due to a loss of capacity for MG to proliferate *per se*, but likely due to the absence or insufficient levels of the required stimuli for MG engagement.

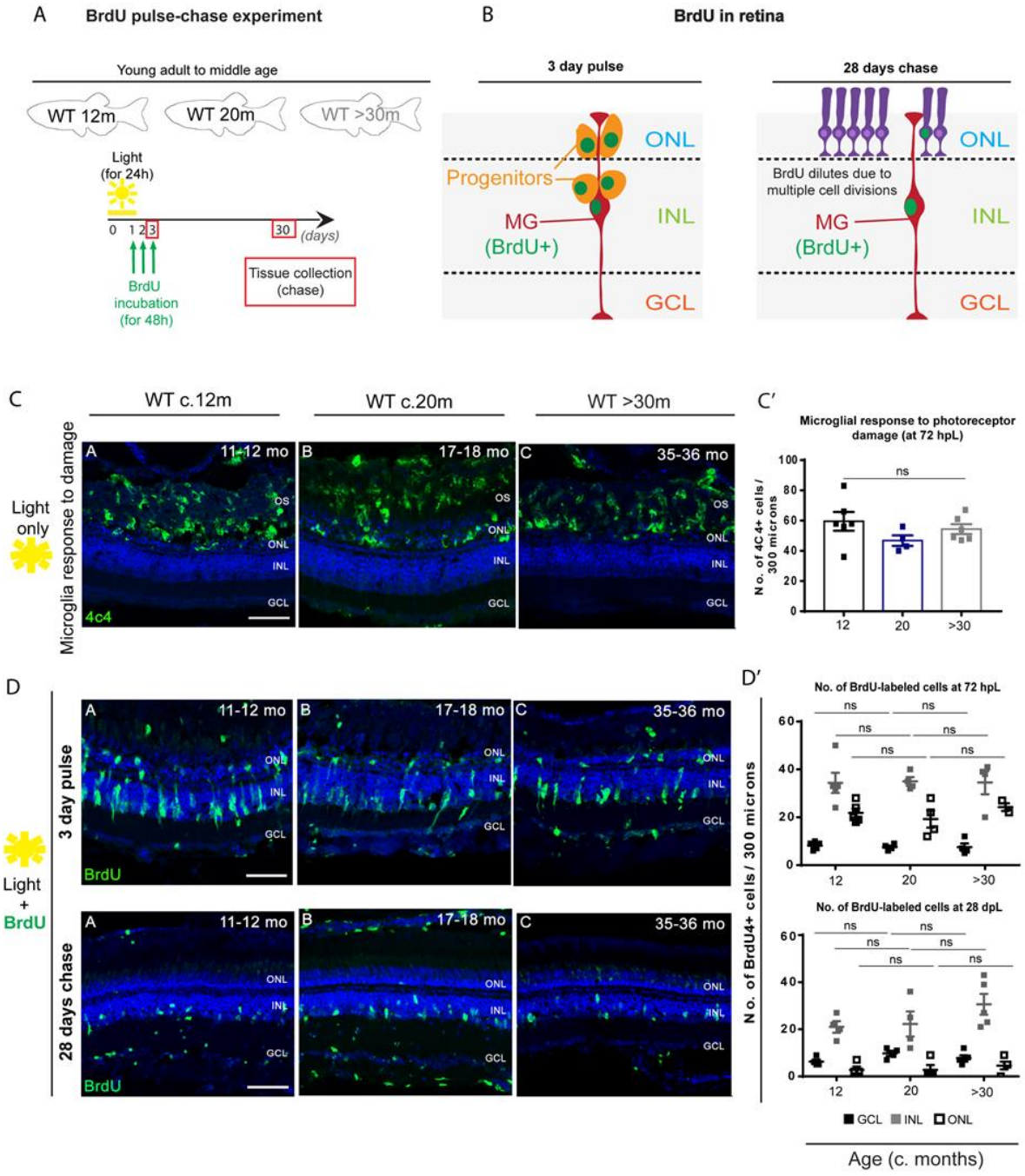
A
BrdU pulse-chase experiment
Young adult to middle age
WT 12m
WT 20m
WT >30m
Light
(for 24h)
0 1 2 3
30
(days)
BrdU
incubation
(for 48h)
Tissue collection
(chase)
B
BrdU in retina
3 day pulse
Progenitors
MG
(BrdU+)
ONL
INL
GCL
28 days chase
BrdU dilutes due to
multiple cell divisions
C
WT c.12m
WT c.20m
WT >30m
Light
only
Microglia response to damage
11-12 mo
17-18 mo
35-36 mo
OS
ONL
INL
GCL
4c4
C′
Microglial response to photoreceptor
damage (at 72 hpL)
No. of 4C4+ cells /
300 microns
ns
12
20
>30
D
Light
+
BrdU
3 day pulse
28 days chase
BrdU
D′
No. of BrdU-labeled cells at 72 hpL
No. of BrdU-labeled cells at 28 dpL
No. of BrdU4+ cells / 300 microns
GCL INL ONL
Age (c. months)

**Fig 3.5. Zebrafish MG regenerative capacity upon acute damage is maintained until old ages.** (A) Schematic image of the experimental design. To damage the retina and induce a regenerative response we place zebrafish in 30 minutes of direct light from a UV light source. The zebrafish are then immediately placed in light from Halogen lights for up to 4 days. A retinal section at 0 hours of light shows the undamaged retina. At 48 hours after the onset of light a majority of the photoreceptors (green) are destroyed. (B) Schematic image of the expected results. (C) Representative images of the central retina labelled with 4C4 (microglia, in green), after light onset, in young (12 months), middle aged 20 months) and old (>30 months) albino zebrafish. The majority of the microglia response to damage occurs within the outer segments (OS) and nuclear layer (ONL) of the retina, where a debris field is present due to photoreceptor degeneration. (C') Quantification of the number of microglial cells which responded to photoreceptor damage in the different aged groups (young represented in black, middle aged in blue and old in grey). (D) Representative images of the central retina 72 hours after light onset, immunolabeled with BrdU (proliferation, in green). (D'). Quantification of the number of cells proliferating in the ganglion cell layer (GCL, represented in black squares), inner nuclear layer (INL, represented in grey squares), and outer nuclear layer (ONL, represented in white squares) in each age group. (E) Representative images of the central retina 28 days after light onset. Fish were light treated for 24 hours and BrdU incorporation occurred between 24-72 hrs (green), which allowed for BrdU to be washed out the proliferating progenitors, leaving only MG which re-entered the cell cycle to be labelled. (E'). Quantification of the number of BrdU+ cells observed in the GCL, INL, and ONL of each aged group. Error bars represent the SEM. N=4-5. Stats: One-way ANOVA followed by Turkey post-hoc tests.

### 3.4.5 The zebrafish retina shows signs of gliosis, not regeneration, with ageing

In the mammalian retina, including human, gliosis is commonly observed in ageing and in response to neuronal damage. Gliosis in the retina typically involves two main glial cells, MG and microglia, which are the innate immune cells found in the nervous system. Microglia are key players in maintaining tissue homeostasis throughout life. They are activated in many neurodegenerative diseases, with increased number at sites of damage, including in the photoreceptor layer in many forms of retinal degeneration, reviewed in (Telegina et al., 2018). We therefore asked whether the age-dependent degeneration we described so far was accompanied by alterations in the number of microglia (4C4-positive cells) in the aged zebrafish retina. Surprisingly, despite there being no difference in numbers of microglia (4C4-positive cells) in the aged WT (**Fig 3.6A, B**), we observe an increased number of microglia co-labelling with TUNEL ($4C4^+$ $TUNEL^+$ cells) in natural WT ageing (**Fig 3.6A, C**). This suggests that there is an increased number of microglia encompassing staining for DNA double-strand breaks, potentially indicating microglia death or the engulfment of a dying cell.

MG respond to damage or injury in most, if not all, neurodegenerative diseases. The typical mammalian response is gliosis, whereby MG change shape and upregulate structural proteins like GFAP to promote a neuroprotective effect (Bringmann et al., 2009; Reichenbach & Bringmann, 2013). In the zebrafish retina, the initial regenerative response is similar to mammalian gliosis (Ranski et al., 2018; Thomas et al., 2016), which can be enhanced if proliferation is blocked (Thummel et al., 2008). Here, we identified MG using GS immunolabeling and characterized MG reactivity using the gliosis marker GFAP. We do not observe an overall change in MG number with ageing (**Fig 3.6D, D'**). Despite this, there is a significant change in the structure/morphology of the MG cells in the WT aged retina. Aberrations in the aged MG cells include disruptions in the radial morphology along the synaptic IPL and basal lamina (**Fig 3.6E, E'**), which are known hallmarks of gliosis in retina degeneration (Telegina et al., 2018). Qualitative assessment show that while all young fish display long and aligned intermediate filaments, 100% of the old fish present short, misaligned intermediate filaments, a marker of gliosis. Thus, similarly to humans, chronic neurodegeneration with ageing elicits a gliotic response in the zebrafish retina rather than the regeneration typically observed after acute injury.

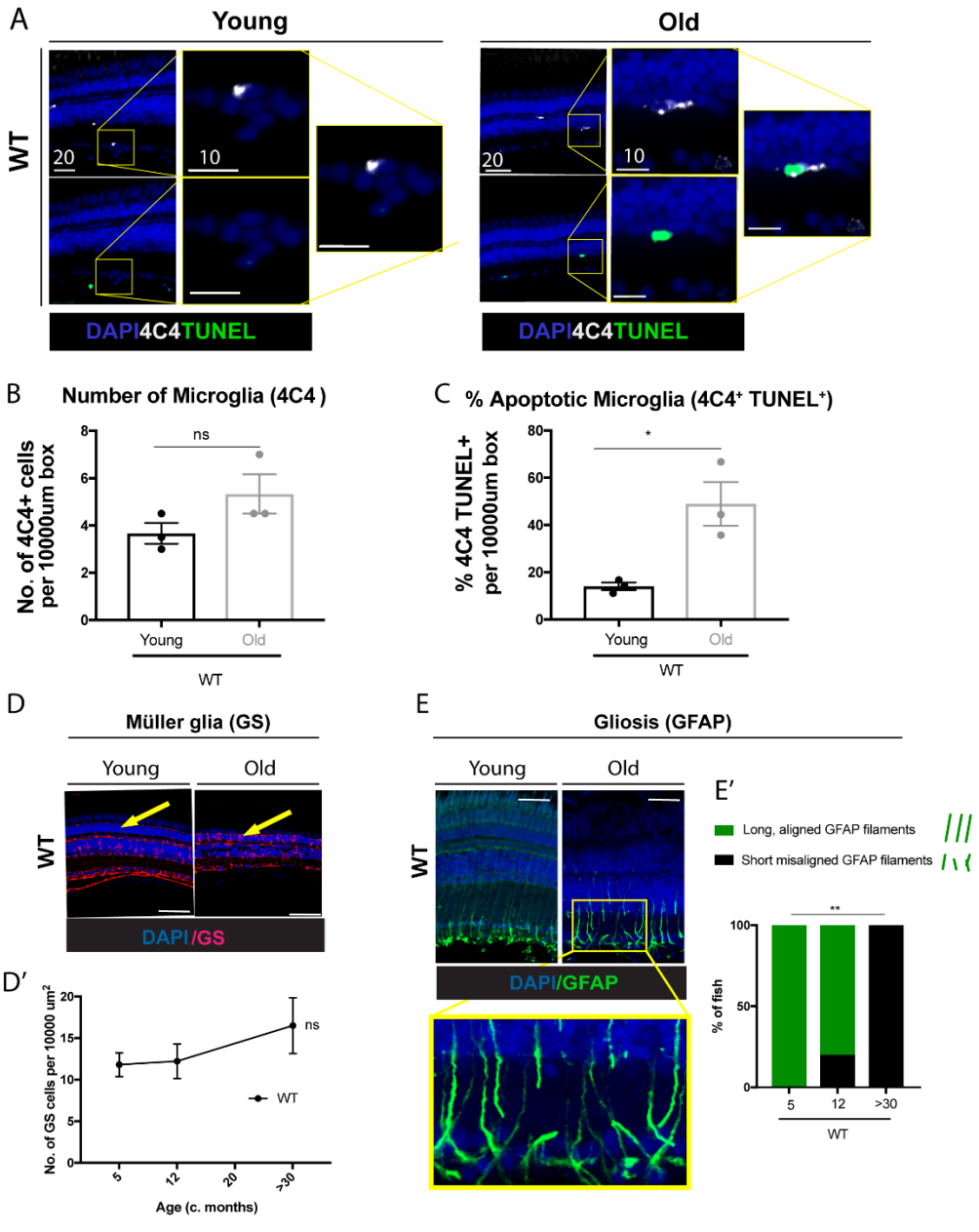
A
Young
Old
WT
20
10
DAPI4C4TUNEL
B
Number of Microglia (4C4 )
No. of 4C4+ cells per 10000um box
ns
Young
Old
WT
C
% Apoptotic Microglia (4C4+ TUNEL+)
% 4C4 TUNEL+ per 10000um box
*
D
Müller glia (GS)
DAPI/GS
D′
No. of GS cells per 10000 um2
Age (c. months)
E
Gliosis (GFAP)
DAPI/GFAP
E′
Long, aligned GFAP filaments
Short misaligned GFAP filaments
% of fish
**

**Fig 3.6. Zebrafish retina undergoes neuro-inflammation and gliosis with ageing.** (A) Representative images of central retina immunolabelled with 4C4 (microglia, in white) and TUNEL (apoptotic cells, in green), in WT, at young (5 months) and old ages (>30 months). The staining was performed in 4µm-thick paraffin sections. (B-C) (B-C) Quantification of the number of (B) 4C4-positive cells (microglia) and (C) 4C4-positive; TUNEL-positive cells (microglia entering apoptosis), per area (10 000 $\mu m^2$). Each dot represents one animal. Error bars represent the SEM. N=3. (D, E) Representative images of the central retina immunolabeled with GS (müller glia, in red) and (E) GFAP (reactive MG, in green), in WT at young (5 months), middle (12 months) and old ages (>30 months). Bars: 20µm. The staining was performed in (D) 4µm-thick paraffin sections or (E) 13µm-thick cryosections. (D'-E') Quantifications of the number of (D') GS-positive cells (MG) per area (10 000 $\mu m^2$), and (E') percentage of fish presenting disorganised GFAP filaments (gliosis-like phenotype). N= 3-6. Statistics: (B-C) unpaired t-tests; (D') one-way ANOVA followed by Bonferroni post-hoc tests; (E') chi-square. P-value: * <0.05; ** <0.01; *** <0.001.

## 3.5 Discussion

Using a combination of different cell labelling strategies from adulthood into old age in the zebrafish retina, we show that the zebrafish retina undergoes degeneration with ageing in a telomerase-independent manner. Contrasting to the acute damage contexts, ageing-induced cell death is insufficient to stimulate the MG regenerative response to replace lost cells. Instead, with ageing, MG develop a gliosis-like phenotype, more similar to the cellular changes observed in the aged human eye.

### 3.5.1 Telomerase dependent and independent hallmarks of retina zebrafish ageing

Previous work has shown that there are aspects of the human retina particularly sensitive to telomere shortening with ageing. Specifically, the RPE is known to be highly proliferative and thus have short telomeres. Accordingly, reactivation of telomerase has been described to ameliorate symptoms of AMD (Dow & Harley, 2016; Rowe-Rendleman & Randolph, 2004) and telomerase activators are currently in clinical trials (e.g. NCT02530255). However, retina homeostasis requires more than RPE maintenance. It also requires a steady-state level of proliferation of different cell types involved in multiple aspects of retina function. As in other proliferative tissues (Anchelin et al., 2013; Carneiro et al., 2016; Henriques et al., 2013), it would make sense that telomerase levels would influence zebrafish retina homeostasis. We therefore hypothesised that the zebrafish retina would degenerate in a telomerase-dependent manner, leading to vision loss. However, our data suggest that most age-related changes we observe in the retina, including vision loss are largely telomerase independent, since depletion of telomerase (*tert*$^{-/-}$) does not accelerate or exacerbate any of these phenotypes. Telomere dysfunction is well known to affect mostly highly proliferative tissues (reviewed in Henriques & Ferreira, 2012), and our data show that in the region most affected by ageing phenotypes, the central retina, there is very low levels of proliferation to start with. Even in the most proliferative region of the retina, the peripheral region containing the CMZ, proliferation is still not high enough to be affected by depletion of telomerase. Importantly, proliferation decreases further with ageing in both regions, so it makes sense that removing telomerase has no further additive effect. This suggests that replicative exhaustion of telomeres is not a limiting factor in the age-associated degeneration of the central retina.

Instead, it is likely that chronic exposure to damaging agents such as oxidising UV radiation is the key driver of degeneration in the retina. However, we cannot exclude that telomere-associated damage may still be a contributing factor to the observed increased levels of DNA damage and cell death or senescence in the central retina. Telomeres are known to be damaged by oxidative stress and can act as sinks of DNA damage, irrespectively of length and levels of telomerase (Hewitt et al., 2012). In fact, this is a likely contributor to RPE damage with ageing (Wang et al., 2018), potentially explaining why depleting telomerase has no effect on the proliferation of the ONL, where photoreceptors reside, nor does it accelerate vision loss.

### 3.5.2 Chronic vs. acute damage in MG responses to natural ageing

Regenerative mechanisms in the retina are an area of intense study and offer great hope for treatment of human disease. As the incidence of retina degeneration increases with age, regenerative capacity in the aged retina is a significant consideration for the efficacy of these therapies. Our results show that zebrafish develop vision loss with ageing and that this is underpinned by retinal neurodegeneration and gliosis. This could seem counter-intuitive, given that it is well established that the zebrafish retina is capable of regenerating after acute damage. Therefore, our data demonstrating a lack of regeneration after age-related cell death suggest that there are critical differences between chronic ageing and repair after an acute injury. Further supporting this, we show that this lack of regeneration in the context of ageing is not due to an intrinsic inability of MG to proliferate *per se*, as we show they are still capable of doing so in response to an acute injury in old animals.

Several tissues in the zebrafish retain the ability to regenerate throughout the lifespan of the zebrafish, including the fin and the heart (Itou et al., 2012; Pinto-teixeira et al., 2015). Likewise, the optic nerve crush paradigm has shown that there is successful recovery and function in the zebrafish retinotectal system (Van houcke et al., 2017) suggesting that regeneration is still possible at advanced age in the retina. The regenerative capacity of vertebrate tissues tends to decrease after repeated injury and as animals advance in age. This is likely due to reduced progenitor cell proliferation potential and subsequent differentiation (Collins et al., 2007). In the context of the central nervous system, this is aggravated by gliosis,

a reactive change in glial cells in response to damage. In the mammalian retina, MG cells undergo gliosis in response to damage and in many retina degenerative diseases (Bringmann et al., 2009). However, in the zebrafish retina MG cells undergo the initial reactive gliotic response after damage but quickly shift to the regenerative pathway. Here, we show that while we observe morphology alterations in MG cells in response to age-related neurodegeneration, MG in the aged retina retain their ability to regenerate in response to acute damage of photoreceptors. It is unclear if alternative damage models will also lead to similar regenerative response.

These observations raise a question about what mechanisms drive the behavioural switch of MG cells, from gliotic response to repair, and why they fail to be engaged in aging related retinal damage. Previous research in the context of acute damage to the zebrafish retina has uncovered some of the mechanisms. For instance, proliferation appears to be a key mechanism for the initiation of the regenerative response, as blocking proliferation after damage in the zebrafish retina results in MG gliosis and a lack of regeneration, similarly to mammals (Thummel et al., 2008). As retinal neurons and their synapses degenerate with age, this may result in a loss of neurotransmitter release, such as gamma-aminobutyric acid (GABA), which has been shown to facilitate the initiation of MG proliferation (Rao et al., 2017). Thus, dysregulation of neurotransmitters upon neurodegeneration could inhibit the key molecular pathways regulating regeneration. Alternatively, the initial inflammatory response has also been shown to be determinant for the repair process. Upon light-induced retinal damage, overexpression and subsequent release of TNFα by apoptotic photoreceptors seems to induce MG proliferation (Iribarne et al., 2019; Thomas et al., 2016). It remains unknown whether there is increased levels of TNFα with natural ageing and how this levels compared with the levels observed in response to acute damage. Additionally, not only there is an increased number of microglia upon retina's injury (Mitchell, et al., 2019) but also its presence has been shown to be essential for retina's regeneration (Conedera et al., 2019). Conversely, we show that the number of microglia in the retina does not increase with age. However, it remains unknown whether the unaltered number of microglia identified in the ageing retina is compromising the regenerative response.

Finally, it remains unclear what is the consequence of the gliotic-like response on retinal neurons in the aged retina, as gliosis is classically thought of as "Janus-faced", with both pro-

and anti- neuroprotective functions (Bringmann et al., 2009). Importantly, the kinetics of this gliosis relative to the neurodegeneration may provide further clues to the precise cellular breakdown in the retina resulting in widespread neuronal death and retinal dysfunction. More specifically, it is unclear whether ageing first affect the MG support functions for neurons, and therefore significantly contribute to the neuronal death, or whether it is purely a response to the damage. A higher temporal resolution of retina stages throughout life and novel markers for glial support functions may provide an answer.

### 3.5.3 Our proposed model: A molecular "tipping point" required to stimulate regeneration in ageing

Regeneration studies so far have relied on several damage paradigms, including phototoxic (Ranski et al., 2018) and ouabain induced lesions (Mitchell et al., 2019), which induce rapid cell death post-insult. While acute damage models are suitable to explore the cellular and molecular mechanisms underpinning the regenerative potential of the retina, they do not allow testing whether this regenerative response is also occurring with natural ageing in the retina. "Natural ageing" and associated stress-induced neuronal death play out over months or even years and we now show that they do not elicit the same regenerative response. This may be because the slow degeneration is not producing a strong enough signal in a short amount of time to induce MG to undergo the cellular and molecular process of regeneration (**Fig 3.7; proposed model**).

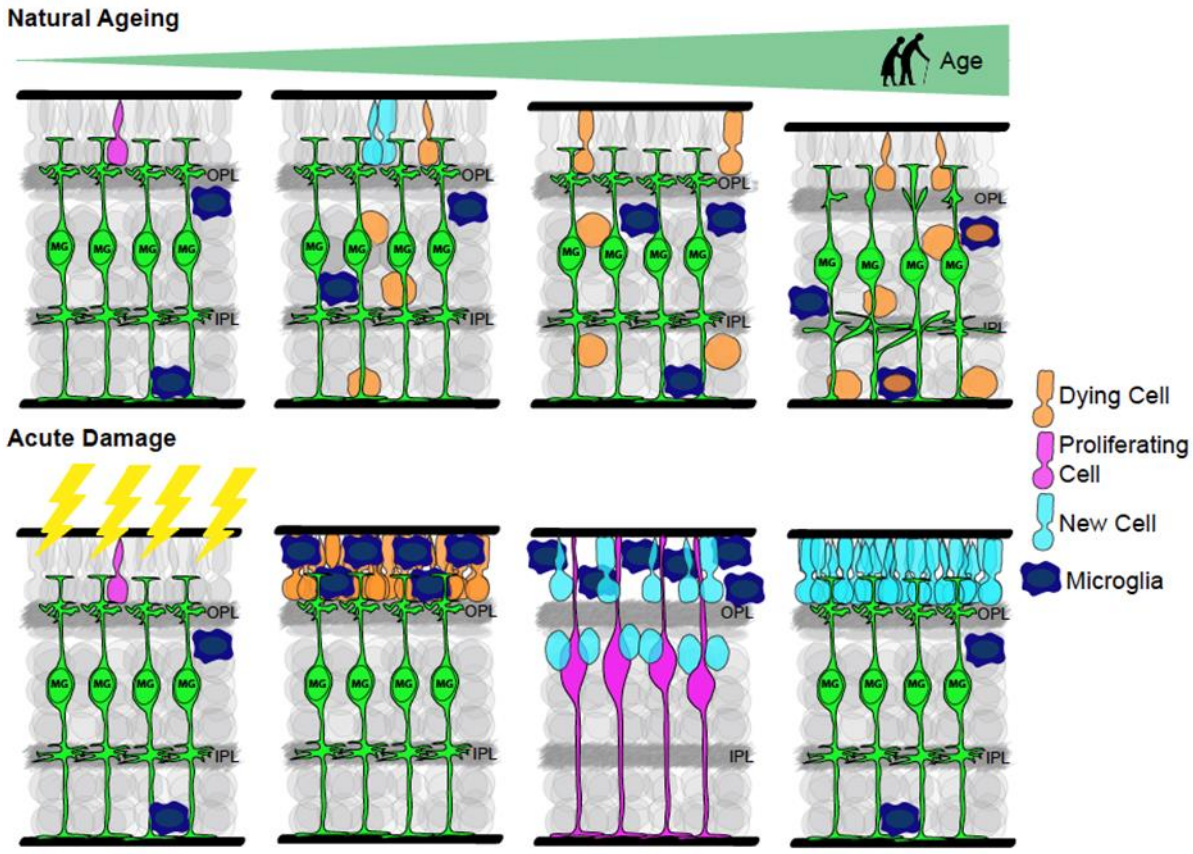
Natural Ageing
Age
OPL
IPL
MG
Acute Damage
Dying Cell
Proliferating Cell
New Cell
Microglia

**Fig 3.7. While zebrafish can regenerate the retina upon acute damage until late ages, its regenerative capacities do not prevent cell death, degeneration and consequent retina thinning with natural ageing.** Schematic figure with the working model. In natural ageing, zebrafish retina undergoes degeneration characterised by increased cell death and neuronal loss. Our current findings show that the proliferation levels are low in young ages and decrease even more with advancing age (represented in magenta). Moreover, the number of microglia, a key play in retina regeneration, is maintained stable throughout lifespan, with a potential increased number of microglia dying. The lack of Müller glia (MG) proliferation in response to chronic, age-related damage seems to lead to retina thinning with ageing, where death cells are not replaced. Middle: In contrast, in response to acute damage where there is a great number of dying cells followed by recruitment of microglia, MG proliferates, generating new neuronal cells, which replace the dying ones. Our current findings show that zebrafish is able to regenerate its retina in response to acute damage until late ages (>30 months), suggesting that the lack of regeneration in response to chronic damage is not due to MG's inability of proliferate**.**

Supporting this, it has been shown that the level of cell death can induce a differential response of MG cells. Whilst a large amount of rod death causes a regenerative response, small amounts do not (Montgomery et al., 2010; Thomas et al., 2012). In support of this concept, recent work suggests that there may be key signalling differences underpinning the difference between a "regenerative" or a "reparative" response to injury (Conedera et al., 2019). Thus, we propose that there are yet-to-be determine molecular pathways involved in the "tipping point" required to elicit a regenerative response in ageing. Such signal may derive from microglia, which are known to stimulate MG proliferation. Indeed, an acute damage in the retina is followed by an increased number of microglia, which are recruited to the injury site (Mitchell et al., 2019; White et al., 2017). Moreover, recruitment of microglia to the injury site has been shown to be crucial for tissue regeneration (White et al., 2017). Is it clear that while we detect a great number of microglial cells in the injury site upon light damage, in both young and old fish, we detect low numbers of microglia in a normal condition, which is maintained throughout zebrafish life-course. It may be that the low-level of damage observed in the aged retina is not enough to trigger key signalling pathways that would, in turn, be responsible for the microglial recruitment. In parallel, we observed increased number of microglia expressing TUNEL staining with ageing, suggesting that microglia might be dying with ageing. Nonetheless, it is important to consider that this technique has some limitations and therefore co-labelling of 4C4 and TUNEL could also represent a dying cell or cell fragments (containing DNA) inside microglial cells. Thus, we cannot exclude the possibility that microglial cells have increased, but de-regulated phagocytic capabilities with ageing, or alternatively, that microglial cells accumulate cell content over-time due to a failure in degrading phagocytosed cells.

### 3.5.4 Conclusions

Our work demonstrates that in response to age-induced neuronal degeneration the MG in the zebrafish retina respond by undergoing a response more akin to gliosis, rather than regeneration. This resembles what happens in the aged human retina, thereby demonstrating it as a suitable model to explore cellular and molecular mechanisms relevant to neurodegeneration in the human retina during ageing and disease. Importantly, we show that there are key differences between chronic and acute tissue damage, particularly involving

gliosis. Thus, gliosis is an important mechanism to consider for targeting endogenous regeneration mechanisms, aiming to prevent and/or delay human retinal degeneration and visual impairment.

## 3.6 Materials and Methods

### 3.6.1 Zebrafish husbandry

Zebrafish were maintained at 27-28ºC, in a 14:10 hour (h) light-dark cycle and fed twice a day. The OKR was performed in the UCL Institute of Ophthalmology and the phototoxic lesions and regeneration experiments were performed at Wayne State University School of Medicine (USA). All other experiments were performed in the University of Sheffield. All animal work was approved by local animal review boards, including the Local Ethical Review Committee at the University of Sheffield (performed according to the protocols of Project Licence 70/8681) and the Institutional Animal Care and Use Committee at Wayne State University School of Medicine (performed according to the protocols of IACUC-19-02-0970).

### 3.6.2 Zebrafish strains, ages, and sex

Three strains of adult zebrafish (Danio rerio) were used for these studies: wild-type (WT; AB strain), *tert*$^{-/-}$ (tert$^{AB/hu3430}$), and albino (slc45a2b4/b4). *tert*$^{-/-}$ zebrafish is a premature model of ageing and therefore, age and die earlier than the naturally aged zebrafish. While *tert*$^{-/-}$ fish have a lifespan of 12-20 months, WT fish typically die between 36-42 months of age (Carneiro et al., 2016; Henriques et al., 2013). In order to study age-related phenotypes in the zebrafish retina, here we used young (5 months) WT and *tert*$^{-/-}$ fish, alongside with middle aged (12 months) WT fish, and old WT and *tert*$^{-/-}$ fish. 'Old' was defined as the age at which the majority of the fish present age-associated phenotypes, such as cachexia, loss of body mass and curvature of the spine. These phenotypes develop close to the time of death and are observed at >30 months of age in WT and at >12 months in *tert*$^{-/-}$ (Carneiro et al., 2016; Henriques et al., 2013). In addition, we used adult albino zebrafish for retinal regeneration studies (described in detail below). Importantly, none of the animals included in this study

displayed visible morphological alterations in the eyes (e.g. cataracts). Whenever possible, males where chosen to perform the experiments

### 3.6.3 OKR assay

Fish were anaesthetised in 4% tricaine methanesulfonate (MS-222; Sigma-Aldrich) and placed in a small bed-like structure made of sponge, located inside a small petri dish containing fish water. During the experiment, fish were maintained still by the strategic use of needles that sustained the sponges close to the fish so that the fish could not move. The petri dish was then placed inside a rotation chamber with black and white striped walls (8 mm-thick stripes). After fish recovered from anaesthesia, the trial began, and the walls of the chamber started rotating at 12 rpm (for 1min to the left side followed by 1 min to the right side). The eyes' movement was recorded using a camera throughout the experiment.

After the experiment, the number of eye rotations per minute was measured by video observation and manually counting. The counting was performed blindly by two independent researchers. In the end, the results were normalised for the WT young from the same day / batch, in order to control for different days of experiment.

### 3.6.4 Intense light-damage paradigm with BrdU incorporation

A photolytic damage model in adult albino zebrafish was utilized to destroy rod and cone photoreceptors and elicit a regenerative response (Thomas et al., 2012). Briefly, adult albino zebrafish were dark-adapted for 10 days prior to a 30 min exposure to ~100,000 lux from a broadband light source. Next, fish were exposed to ~10,000 lux of light from four, 250 W halogen lamps for 24 hrs. Following 24 hrs of light treatment, fish were transferred to a 1L solution containing 0.66 g of NaCl, 0.1 g Neutral Regulator (SeaChem Laboratories, Inc. Stone Mountain, GA, USA), and 1.5 g BrdU (5mM; B5002; Sigma-Aldrich) for 48 hrs. This timeframe for BrdU incubation was based on previous studies in order to label MG cell-cycle re-entry (Ranski et al., 2018). Following a 48 hour incubation in BrdU, the fish were split into two groups: one group was euthanized by an overdose of 2-Phenoxyethanol and eyes were processed for immunohistochemistry as described below; the second group returned to

normal husbandry conditions for an additional 25 days (or 28 days after light onset) prior to euthanasia and tissue collection. During this time, BrdU incorporation dilutes in actively dividing cells, allowing for clear visualization of the number of MG in the INL that only divide a single time. It also serves as an indirect measure of regenerative capacity (i.e. an equal loss of BrdU-positive cells at 28 dpL between experimental groups would indicate similar numbers of progenitor cell divisions earlier in the regenerative process).

### 3.6.5 Tissue preparation: paraffin-embedded sections and cryosections

Adult fish were culled by overdose of MS-222, followed by confirmation of death. Whole fish or dissected eyeballs were then processed for paraffin-embedded sections or for cryosections, as follows:

Paraffin-embedded sections. Whole fish were fixed in in 4% paraformaldehyde (PFA) buffered at pH 7.0, at 4ºC for 48-72h, decalcified in 0.5M EDTA at pH 8.0 for 48-72h, and embedded in paraffin by the following series of washes: formalin I (Merck & Co, Kenilworth, NJ, USA) for 10 min, formalin II for 50min, ethanol 50% for 1h, ethanol 70% for 1h, ethanol 95% for 1h 30min, ethanol 100% for 2h, ethanol 100% for 2h 30min, 50:50 of ethanol 100% : xilol for 1h 30min, xylene I for 3h, xylene II for 3h, paraffin I for 3h and paraffin II for 4h 30min. Paraffin-embedded whole fish were then sliced in sagittal 4 µm-thick or coronal 16 µm-thick sections, using a Leica TP 1020 cryostat.

Cryopreservation and cryosections. Dissected eyeballs were fixed in 4% PFA at 4ºC, overnight (ON). Then, they were washed in cold 1x PBS and immersed in 30% sucrose in phosphate-buffered saline (PBS), ON at 4ºC, for cryopreservation. Single cryopreserved eyeballs were then embedded in mounting media – optimal cutting temperature compound (OCT, VWR International), snap-frozen at −80°C, and stored at -20ºC until cryosectioning. Cryosections were sliced at a 13µm thickness using a Leica Jung Frigocut cryostat or a Leica CM1860 cryostat.

### 3.6.6 Immunohistochemistry (IHC)

Before immunofluorescence (IF) staining, cryosections were hydrated in PBS at room temperature (RT) for 10 min, and paraffin-embedded sections were deparaffinised and hydrated as follows: histoclear (Scientific Laboratory Supplies, Wilford, Nottingham, UK) 2x for 5min, followed by ethanol 100% 2x for 5 min, ethanol 90% for 5min, ethanol 70% for 5min, and distilled water 2x for 5 min. After antigen retrieval in 0.01M citrate buffer at pH 6.0 for 10min, the sections were permeabilised in PBS 0.5% Triton X-100 for 10min and blocked in 3% bovine serum albumin (BSA), 5% Goat Serum (or Donkey Serum), 0.3% Tween-20 in PBS, for 1h. The slides were then incubated with the primary antibody at 4°C ON. After washes in PBS 0.1% Tween-20 (3x 10 min) to remove excess to primary antibody, the sections were incubated with secondary antibody at RT for 1h. Finally, the slides were incubated in 1 µg/ml of 4',6-diamidino-2-phenylindole (DAPI, Thermo Fisher Scientific) at RT for 10 min, washed in PBS 1x, and mounted with vectashield (Vector Laboratories, Burlingame, CA, USA). The primary and secondary antibodies used in this study are described in **Table 3.1** and **Table 3.2**, respectively.

**Table 3.1 Primary antibodies used for immunostaining.**

| Antibody, species and type | Dilution factor | Catalogue number; Company, City, Country |
|---|---|---|
| yH2AX rabbit polyclonal | 1:500 | GTX127342; GeneTex, Irvine, CA, USA |
| p53 rabbit polyclonal | 1:200 | AS-55342s; Labscoop, Little Rock, AR, USA |
| PCNA mouse monoclonal | 1:500 | NB500-106; Novus Biologicals, Littleton, CO, USA |
| PCNA rabbit polyclonal | 1:50 | GTX124496; GeneTex, Irvine, CA, USA |
| 7.4.C4 (4C4) mouse monoclonal | 1:100 | A gift from A. McGown |
| HuCD mouse monoclonal | 1:100 | A21271; Thermo Fisher Scientific, Waltham, MA, USA |
| PKCβ1 rabbit polyclonal | 1:100 | Santa Cruz, Dallas, TX, USA |
| Ribeye rabbit polyclonal | 1:10,000 | A gift from Teresa Nicholson |
| GFAP rabbit polyclonal | 1:200 | Z0334, Agilent DAKO, Santa Clara, CA, USA |
| GFAP mouse monoclonal | 1:100 | zrf1, ZIRC |
| Glutamine Synthase (GS) mouse monoclonal | 1:150 | mab302, Merck, Kenilworth, NJ, USA |
| Rhodopsin rabbit | 1:5,000 | A gift from David Hyde |
| BrdU rat | 1:200 | OBT0030A, Accurate Chemical & Scientific, Westbury, NY, USA |

**Table 3.2 Secondary antibodies used for immunostaining.**

| Antibody, species and type | Dilution factor | Catalogue number; Company, City, Country |
|---|---|---|
| Goat anti-rabbit IgG Alexa Fluor® 488 | 1:500 | A11008; Invitrogen, Carlsbad, CA, USA |
| Goat anti-rat IgG Alexa Fluor® 488 | 1:500 | A11006; Thermo Fisher Scientific, Waltham, MA, USA |
| Goat anti-rabbit IgG Alexa Fluor® 568 | 1:500 | 10032302; Thermo Fisher Scientific, Waltham, MA, USA |
| Donkey anti-rabbit IgG Alexa Fluor® 647 | 1:500 | A31573; Thermo Fisher Scientific, Waltham, MA, USA |
| Goat anti-mouse IgG Alexa Fluor® 488 | 1:500 | A11001; Thermo Fisher Scientific, Waltham, MA, USA |
| Goat anti-mouse IgG Alexa Fluor® 568 | 1:500 | 10348072; Thermo Fisher Scientific, Waltham, MA, USA |
| Goat anti-mouse IgG Alexa Fluor® 647 | 1:500 | A21235; Thermo Fisher Scientific, Waltham, MA, USA |

### 3.6.7 Terminal deoxynucleotidyl transferase dUTP nick end labelling (TUNEL) staining

In paraffin-embedded sections, TUNEL was performed using the *In Situ* Cell Death Detection Kit, Fluorescein (Merck & Co), following the manufacturer's instructions. Briefly, after deparaffinisation, hydration, antigen retrieval and permeabilization, as described above, the slides were incubated in enzyme and label solution (1:10) at 37ºC for 1h. The slides were then washed in 1x PBS (2x 10 min) before blocking and incubation with primary antibody.

In cryosections, the slides were washed 1x PBS for 5 min and fixed in 4% PFA at RT for 15 min. The PFA was washed off in 1x PBS for 5 min and the slides were then incubated in 20 µg/mL Proteinase K (Fermentas stock #K0721) at RT for 8 min and washed in 1x PBS for 5min. The slides were post-fixed in 4% PFA at RT for 5min, rinsed in 1x PBS and stained with *In situ* cell death detection Kit, TMR Red from ROCHE (Cat#12 156 792 910) at 37°C for 1.5hr. Finally, the slides were washed in 1x PBS for 5 min and mounted with Vectashield Hard Set medium with DAPI (#H-1500).

### 3.6.8 5-Ethynyl-2'-deoxyuridine (EDU) labelling

EdU labelling was detected using the Click-iT® EdU Imaging Kit (Thermo Fisher Scientific), following manufacturer's instructions. Briefly, fish were injected with 5µl of 10mM EdU diluted in dimethyl sulfoxide (DSMO), by intraperitoneal (IP) injection, for 3 consecutive days (3-day pulse). In order to differentiate proliferating cells and low-proliferative EdU-retaining cells, the fish were separated into two groups: 0-day chase and 30-days chase groups. The fish from the first group were culled 2h30min after the last injection of Edu, whereas the fish from the second group were culled 30 days after the last injection of EdU. After culling, whole fish were processed for paraffin-embedded sections as described above.

In order to detect EdU labelling in paraffin-embedded sections, the slides were deparaffinised, hydrated, underwent antigen retrieved, were permeabilized and washed in 1x PBS. The slides were incubated in freshly made EdU-labelling solution (per 1 ml of solution: 860µl of 1x Click-iT®EdU reaction buffer, 40µl $CuSO_4$, 2.5µl Alexa Fluor® 647 azide working solution and 100µl 10x EdU reaction buffer additive) at RT for 30min. Finally, the slides were washed in 1x PBS before blocking and incubation with primary antibody (ON, at 4ºC). The incubation in secondary antibody was performed as previously described.

### 3.6.9 Imaging and quantifications

Paraffin-embedded sections were imaged by epifluorescence microscopy, using a DeltaVision microscope with a 40x oil objective. Cryosections were imaged by laser scanning confocal imaging, using a Leica SP5 microscope or a Nikon A1 Confocal microscope, with a 40x oil objective. In both cases, multiple 0.2-0.6 µm thick z-stacks were acquired in order to capture the whole section. For each staining, a total of 4 images were taken per retina, 2 from central and 2 from peripheral retinal.

In order to quantify the staining, after making a z-projection, 3 boxes of 100x100 µm were drawn in each field of view (FOV). The total number of positive cells was then manually counted for each labelling. Rhodopsin, ZO1, ribeye and GFAP staining were an exception to this, for which a qualitative assessment was performed instead. To do so, structural and morphological defects were identified as follows. For the rhodopsin staining, as young WT retinas usually display long and aligned outer segments, all short and/or misaligned outer segments were considered defective. For the ZO1 staining, the average number of breaks in the ZO1-labelled membrane per animal was quantified. The average of breaks in the WT young animals was used as a reference, and any fish presenting an average number of breaks bellow this average was considered to present defects in the membrane. For the ribeye staining, young retinas usually present two distinguished layers of pre-synaptic ribbons. Thus, staining where the two layers of pre-synaptic ribbons are not distinguished, was considered defective. GFAP staining usually reveals long and aligned filaments in young WT retinas, and therefore broken, short and/or misaligned GFAP filaments were considered defective. Through this qualitative assessment it was calculated the percentage of fish per group presenting structural and morphological defects.

Finally, raw images were used for quantification purposes. The images were then processed with Adobe Illustrator 21.0.2 for display purposes.

### 3.6.10 Statistical analysis

Statistics were performed using the GraphPad Prism v7.00. Normality was assessed by Shapiro-Wilk test. For normally distributed data unpaired t-test was used to compare 2 data points and one-way ANOVA followed by Bonferroni post-hoc test was used to compare more

than 2 data points. For non-normally distributed data, Mann-Whitney test and Kruskal-Wallis test followed by Dunn's post-hoc test were used instead. Two-way ANOVA was used in order to compare more than 2 data points in 2 groups different groups (genotypes). Chi-square was performed to analyse structure and morphological changes in the retina based on qualitative assessment, having into account the number of animals per group displaying defects versus not displaying defects. A critical value for significance of $p<0.05$ was used throughout the analysis.

## 3.7 Acknowledgements

Thanks to Alex McGowen for 4c4, Teresa Nicholson for ribeye. Part of this work was supported by grants from the National Institutes of Health (NEI R01EY026551 and R21EY031526 to RT). Histology and imaging core resources were supported by vision core grants (P30EY04068) and an unrestricted grant from Research to Prevent Blindness to the Department of Ophthalmology, Visual and Anatomical Sciences (RT). This work was generously funded by a University of Sheffield PhD studentship to RRM, a Sheffield University Vice Chancellor's Research Fellowship and a Wellcome Trust/Royal Society Sir Henry Dale Fellowship (UNS35121) to CMH and a Welcome Trust Seed Award (210152/Z/18/Z) and a BBSRC David Phillips Fellowship (BB/S010386/1) to RBM.

## 3.8 Competing interests

The authors declare no competing interests.

## 3.10 Supplementary figures

**Fig 3.8. [Supplementary figure 1] Retina thinning in the aged zebrafish central and peripheral retina, per layer, and decreased proliferation in the zebrafish aged peripheral retina.** (A-B) Quantifications of the retina thickness (in µm) using DAPI staining, in (A) central and (B) peripheral retina, in young and old WT and *tert*$^{-/-}$. Error bars represent the SEM. N=3-5 (C) Representative images of the peripheral retina immunolabeled with PCNA (proliferation, in green), in both WT and *tert*$^{-/-}$, at young (5 months) and old ages (>30 months in WT and 20 in *tert*$^{-/-}$). The staining was performed in 16µm-thick paraffin sections. Bars: 20µm. (C') Quantifications of the number of PCNA+ cells per area (10 000 µm$^2$). The black line represents WT and red line represents *tert*$^{-/-}$. Error bars represent the SEM. N=6-12. Statistics: (A-B) Unpaired t-tests; (C') two-way ANOVA (WT vs *tert*$^{-/-}$ at young versus old ages) and one-way ANOVA (WT). Differences between genotypes are indicated above each time-point, whereas differences over-time in each genotype are indicated in the end of the lines, in black WT, in red *tert*$^{-/-}$. p-value: * <0.05; ** <0.01; *** <0.001.

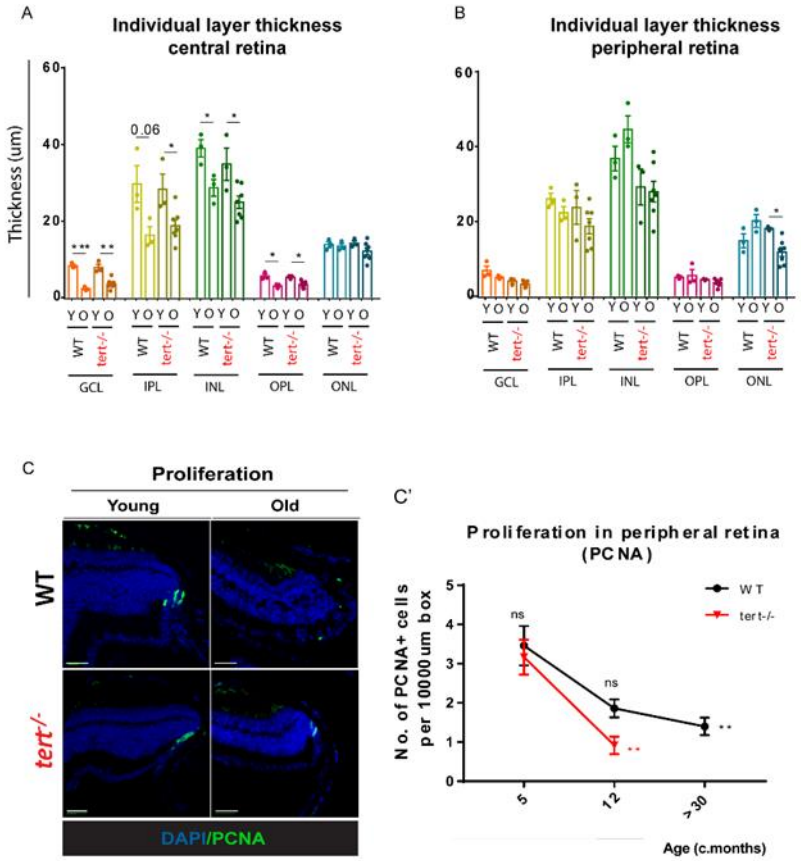

**Table 3.3 [Supplementary table 1] Summary of the phenotypes observed in the aged zebrafish retina, and which phenotypes are telomerase-dependent or independent.**

| Phenotype of WT aged | | Anticipated in *tert*$^{-/-}$? | | |
|---|---|---|---|---|
| | | **At 5 months** | **At 12 months (end life for *tert*$^{-/-}$)** | **Likely to be telomerase dependent?** |
| Visual impairment | | No | No | No |
| Thinning of the central retina | GCL | No | N/A | No |
| | IPL | No | N/A | No |
| | INL | No | N/A | No |
| | OPL | No | N/A | No |
| | ONL | No | N/A | No |
| Neuronal degeneration in central retina | Rods morphology | No | N/A | No |
| | ZO-1 membrane | No | N/A | No |
| | Pre-synaptic ribbons (Ribeye) | No | N/A | No |
| | BCs (PKC in INL) | Yes | No | No |
| | ACs (HuCD in INL) | No | No | No |
| | GCs (HuCD in GCL) | No | No | No |
| Hallmarks of cellular ageing In central retina | Apoptosis | No | No | No |
| | DNA damage/ senescence | No | No | No |
| | Proliferation | No | No | No |

**Fig 3.9. [Supplementary figure 2] Aged zebrafish retina does not show signs of regeneration in response to spontaneous cell death, neuronal loss and gliosis, in the peripheral retina. Moreover, this occurs in a telomerase-independent way.** (A-B) Representative images of EdU-positive cells (purple) after a 3-day pulse of EdU, by IP injection, (A) at 0- and (B) 30-days chase, in the peripheral retina of both WT and *tert*$^{-/-}$, at young (5 months) and time of death (TOD, >30 months in WT and 12 months in *tert*$^{-/-}$). The staining was performed in 16µm-thick paraffin sections. Bars: 20µm. (A'-B') Quantifications of the number of EdU+ cells per area (10 000 µm$^2$), at (A') 0- and (B') 30-days chase. The black line represents WT and the red line represents the *tert*$^{-/-}$. N=3-6. Error bars represent SEM. Statistics: two-way ANOVA (WT vs *tert*$^{-/-}$ at 5m and 12m months) and one-way ANOVA (WT over-time). p.value: * <0.05; ** <0.01; *** <0.001

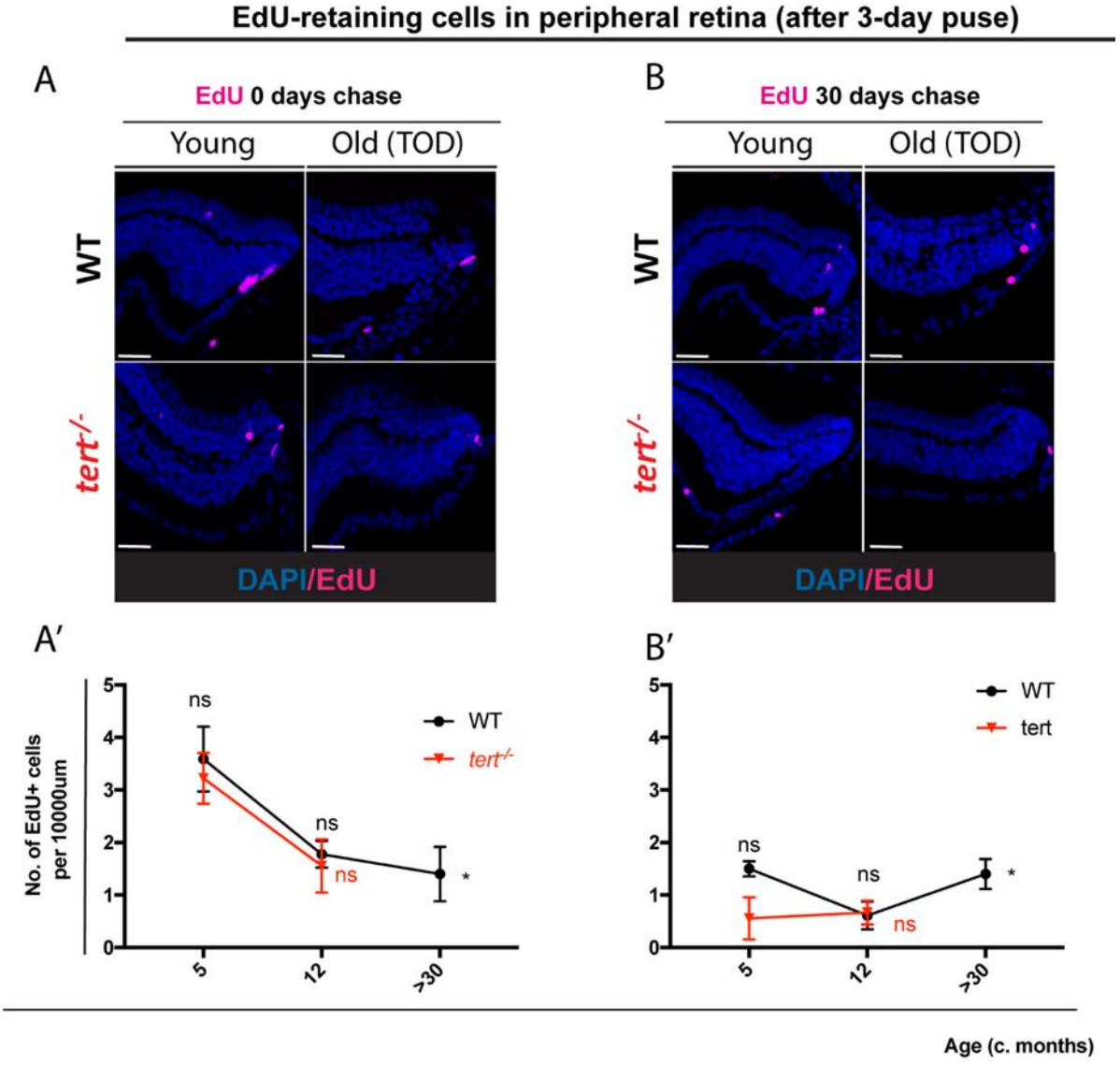

# Chapter 4.
# Exploring if TERT restriction contributes to accumulation of cellular senescence in the zebrafish aged brain

## 4.1 Introduction

Despite being considered predominantly a post-mitotic tissue, the brain displays telomere shortening with ageing in humans, rodents (rat and mouse) and fish (Arslan-Ergul et al., 2016; Bitto et al., 2010; Flanary & Streit, 2004). As expected, these species present low or undetectable levels of telomerase in the adult brain, which is a favoured environment for telomere shortening (Allsopp et al., 1995; Anchelin et al., 2011; Caporaso et al., 2003).

Importantly, G4 TERC-deficient mice (*Terc*$^{-/-}$) display increased levels of senescent-associated markers in neurons (Jurk et al., 2012) and in microglia (Raj et al., 2015), compared with age-matched *Terc*$^{+/+}$. This suggests that telomerase plays a protective role against accumulation of senescence in the ageing brain, via its role at telomeres. However, it remains unknown if the TERT component of telomerase also plays a protective role against senescence in the brain, either via its telomere-dependent (i.e canonical) or -independent functions (i.e. non-canonical). Understanding whether telomerase restriction contributes to cellular senescence in the brain and identifying the mechanisms behind it would potentially uncover new therapeutic targets to the promotion of healthy brain ageing.

Evidence suggests that the TERT component of telomerase plays an important role in the brain, particularly in enabling cell proliferation capacity. *In vitro*, neural stem cells (NSCs) derived from TERT-deficient G4 TERT-ER mice (knock-in model where endogenous TERT expression is induced upon addition of 4-OHT) display impaired proliferation capacity and present increased p53 expression, which are rescued upon TERT restoration (Jaskelioff et al., 2011). *In vivo,* TERT reactivation restores proliferation in the SVZ (Jaskelioff et al., 2011), suggesting that TERT expression affects proliferative regions of the brain. It is still unclear whether this is due to telomere length maintenance or non-canonical functions of telomerase, since reports suggest that telomerase can promote proliferation independently of telomere maintenance (Choi et al., 2008; Sarin et al., 2005). Furthermore, it remains to be investigated if TERT expression has any impact on cellular senescence, and whether it also affects non-proliferative regions of the brain. As it was shown that the zebrafish brain presents low levels of TERT in the adult brain, which tend to decrease with ageing (Sprungala, 2009), I hypothesise that limited expression of TERT in the aged zebrafish brain contributes to the accumulation of senescence with ageing.

To test this hypothesis, in this Chapter I aimed to determine if the zebrafish brain accumulates cellular senescence with natural ageing and, if so, whether this is accelerated in the absence of TERT expression. More specifically, I have assessed if the zebrafish brain accumulates senescence with ageing in the presence (WT) and absence (*tert*$^{-/-}$) of Tert, in an *in vivo* setting. To do so, I have assessed several senescence-associated markers, using complementary techniques, in the whole zebrafish brain as well as in the different brain macroareas.

## 4.2 Measuring cellular senescence in the naturally aged zebrafish brain

In order to test whether there is accumulation of senescence in the zebrafish brain, with natural ageing, I have assessed several senescence-associated markers throughout zebrafish lifespan. To do this, I used fish of different ages, from young (4-6 months) to old (>30 months).

As mentioned in *Chapter 1*, SA-β-Gal expression is a biomarker of cellular senescence, at least in most of the cell types tested (Dimri et al., 1995). Apart from accumulating SA-β-Gal, senescent cells are known to display increased levels of DNA damage, commonly identified through accumulation of γH2AX foci, as well as up-regulation of p53, cdkn1α (p21), cdkn2α (p16-like) and cyclin g1 genes (Campisi & d'Adda di Fagagna, 2007; van Deursen, 2014). Thus, these markers were assessed by using complementary techniques, including IHC and RT-qPCR.

### 4.2.1 Assessing SA-β-Gal expression in the naturally aged WT brain

SA-β-Gal expression was analysed by X-gal staining at pH 6.0, as described in *section 2.4.2.* To validate the assay, I tested whether the blue staining observed in the sections was specifically due to the cleavage of X-gal by galactosidase, and not due to an artefact. To test this, adjacent sections of the brain were stained with and without X-gal substrate. Only the brain sections incubated with X-gal substrate presented the blue chromogenic staining, indicating the presence of galactosidase, specifically at pH 6.0 (**Fig 4.1**). This assay was therefore considered viable to assess SA-β-Gal expression in the zebrafish brain.

In order to test whether there is an increased expression of SA-β-Gal with ageing in the zebrafish brain, SA-β-Gal staining was performed in cryosections of young (4-6 months) and old (>30 months) WT brains. The percentage of area containing SA-β-Gal staining was then quantified in the whole brain, using the method described in *section 2.4.4.*

The results showed a significant increase in SA-β-Gal expression with natural ageing in the whole zebrafish brain ($p=0.0009$, **Fig 4.2A, B**). It was also observed that SA-β-Gal staining did not accumulate in all regions of the brain, which suggests that some regions might be more prone to develop cellular senescence over-time. This will be further analysed in *section 3.3.*

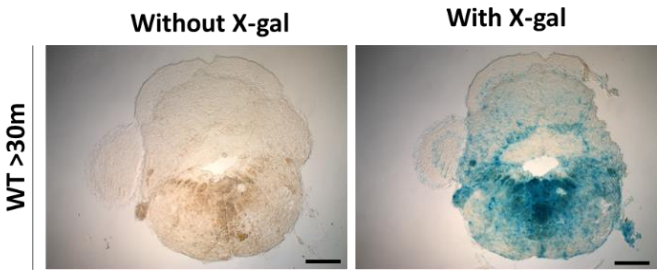


**Fig 4.1. Control experiment showing that blue staining is specific of X-gal cleavage by galactosidase.** Representative images from two adjacent brain sections of an old WT fish (rhombencephalon region), after SA-β-Gal staining. Without X-gal substrate (left) there is no blue staining in the section. The blue staining is only visible in the presence of X-gal substrate (right). Scale bar: 200µm.

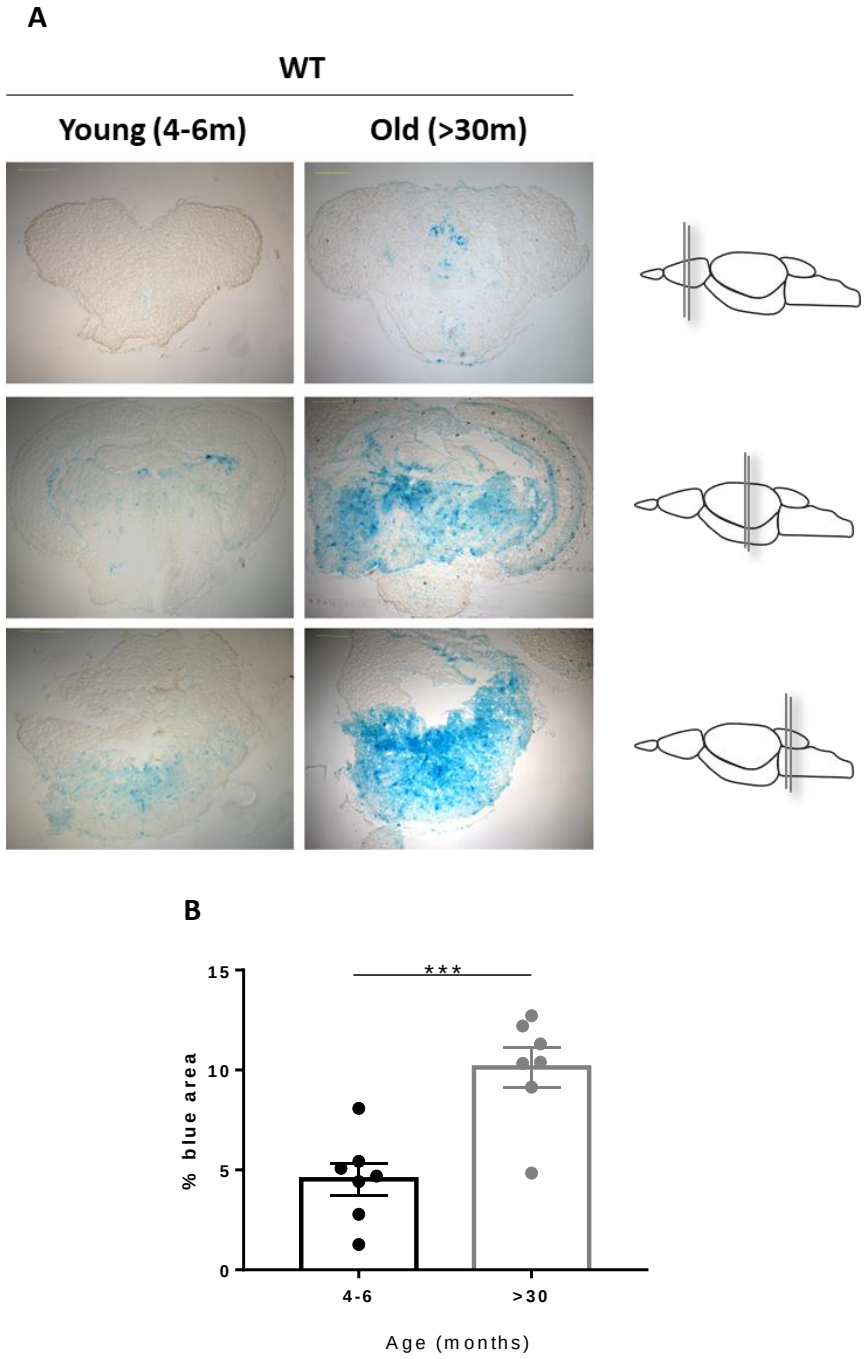


**Fig 4.2. SA-β-Gal expression in the whole zebrafish brain with natural ageing. (A)** Representative images of the SA-β-Gal staining in different regions of the brain, in young (4-6 months) and old (>30 months) WT zebrafish. **(B)** Quantifications of SA-β-Gal staining, in % of blue area, as described in *section 2.4.4*. Graphs: X-axis, age in months; Y-axis, % of blue area. N=7 per group. Each dot represents one animal. Error bars represent SEM. Unpaired t-test: * p<0.05; ** p<0.01; *** p<0.001.

### 4.2.2 Assessing DNA damage in the naturally aged WT brain

Senescent cells are known to have high levels of DNA damage, commonly measured by the accumulation of γH2AX foci. Hence, in order to test whether there is accumulation of DNA damage with ageing in the zebrafish brain, I compared the number of γH2AX foci in paraffin sections of young (9-17 months) and old (>30 months) WT fish. γH2AX foci were detected by IF, using the anti-γH2AX antibody, as described in *section 2.3.2*. This antibody had already been tested in the laboratory and previously published (Carneiro et al., 2016). The percentage of cells containing >5 γH2AX nuclear foci in sections of the whole zebrafish brain was then assessed as described in *section 2.3.5*.

The results showed a small increase in the number of γH2AX-positive cells in the zebrafish whole brain, over-time, that did not reach statistical significance (p=0.075, **Fig 4.3A, B**). Similar results were identified when assessing the number of non-proliferative cells expressing DNA damage (PCNA-negative; γH2AX-positive cells – data not shown), suggesting that these cells are likely to be putative senescent cells.

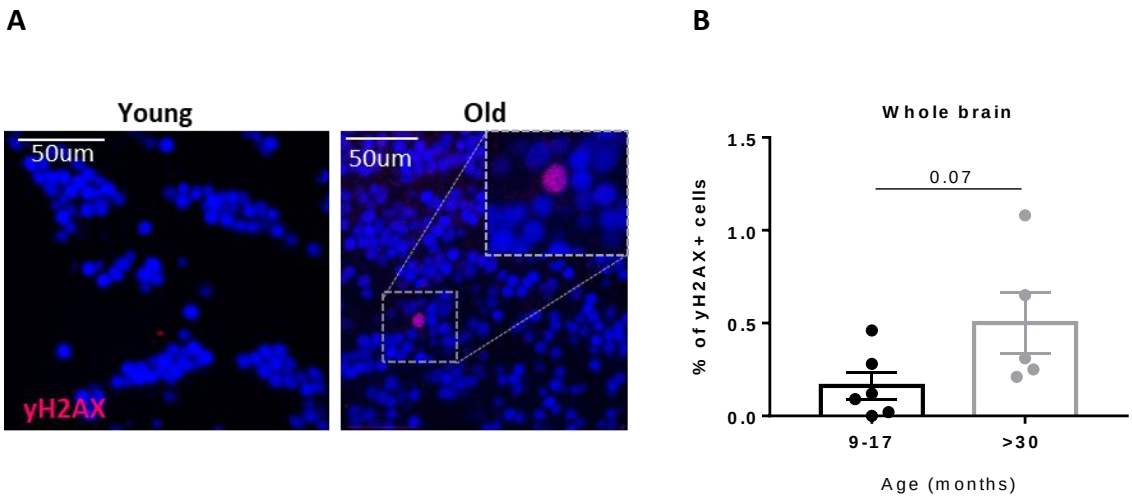


**Fig 4.3. DNA damage foci in the whole zebrafish brain with natural ageing. (A)** Representative image of yH2AX staining by IF, in young (9-17 months) and old (>30 months) adult zebrafish brain. **(B)** Quantification of the percentage of yH2AX$^{+}$ cells with ageing in the whole brain. Graphs: X-axis, age in months; Y-axis, percentage of yH2AX$^{+}$. N=5-6 *per* group. Each dot represents one animal. Bar errors represent the SEM. Unpaired t-test: * <0.05; ** <0.01; *** <0.001.

### 4.2.3 Assessing the expression of senescence-associated markers downstream of yH2AX, in the naturally aged WT brain

In response to increased DNA damage, senescent cells commonly display up-regulation of *p53*, *p21* and *p16*, accompanied by down-regulation of target genes essential for cell-cycle (Coppé et al., 2008; van Deursen, 2014). Since I had observed a trend for increased DNA damage in the aged brain, I then sought to measure the gene expression of *p53*, *p21* and *p16-like*, in order to further characterise which pathways of senescence are being activated in the naturally aged WT zebrafish brain. Here, I also analysed the expression of *cyclin g1*, a cyclin-dependent kinase known to be a target of *p53* in zebrafish (Danilova et al., 2010).

In order to measure gene expression of *p53*, *p21*, *p16-like* and *cycling g1* over-time in the zebrafish brain, mRNA expression was analysed by RT-qPCR, as described in *section 2.5.3*. The mRNA analysed in this experiment was derived from whole brain tissue from young (6-9 months), middle aged (22-24 months) and old (>30 months) fish. The mRNA expression of the genes of interest was then normalised for *beta-actin* (reference gene) and analysed using the ΔΔCt method, as described in *section 2.5.3*.

Prior to the experiment, the primers were optimised, as described in *section 2.5.3,* with all sets of primers presenting slopes between 3.206 and 3.397 (**Fig 4.4A-E**). Moreover, no non-specific amplifications were observed during the melting curve of the tested primers (**Fig 4.4F**).

As shown in **Fig 4.5A-D**, the results revealed no significant differences in the expression of *p53* (6-9m vs 22-24m: p=0.551; 6-9m vs >30m: p=0.769), *p21* (6-9m vs 22-24m: p=0.142; 6-9 vs >30m: p=0.863), *p16-like* (6-9m vs 22-24m: p=0.127), or *cyclin g1* (6-9m vs 22-24m: p=0.999; 6-9 vs >30m: p=0.999), in the whole zebrafish brain with natural ageing.

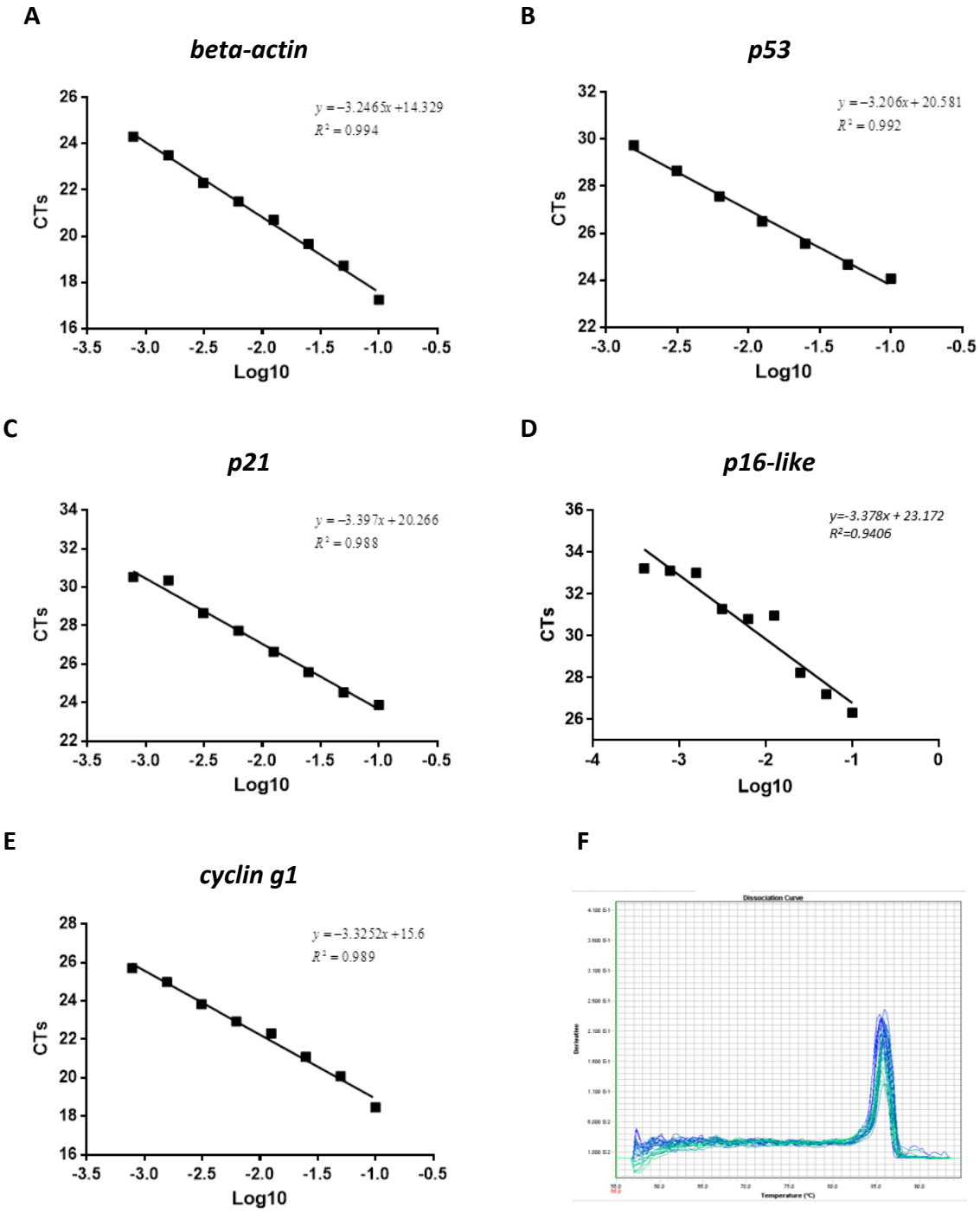


**Fig 4.4. Optimisation of primers.** Efficiency curves for all the genes optimised: (**A**) *beta-actin*, (**B**) *p53*, (**C**) *p21*, (**D**) *p16-like* and (**E**) *cyclin g1*. (**F**) Representative image of a melting curve; this is referent to *beta-actin* gene.

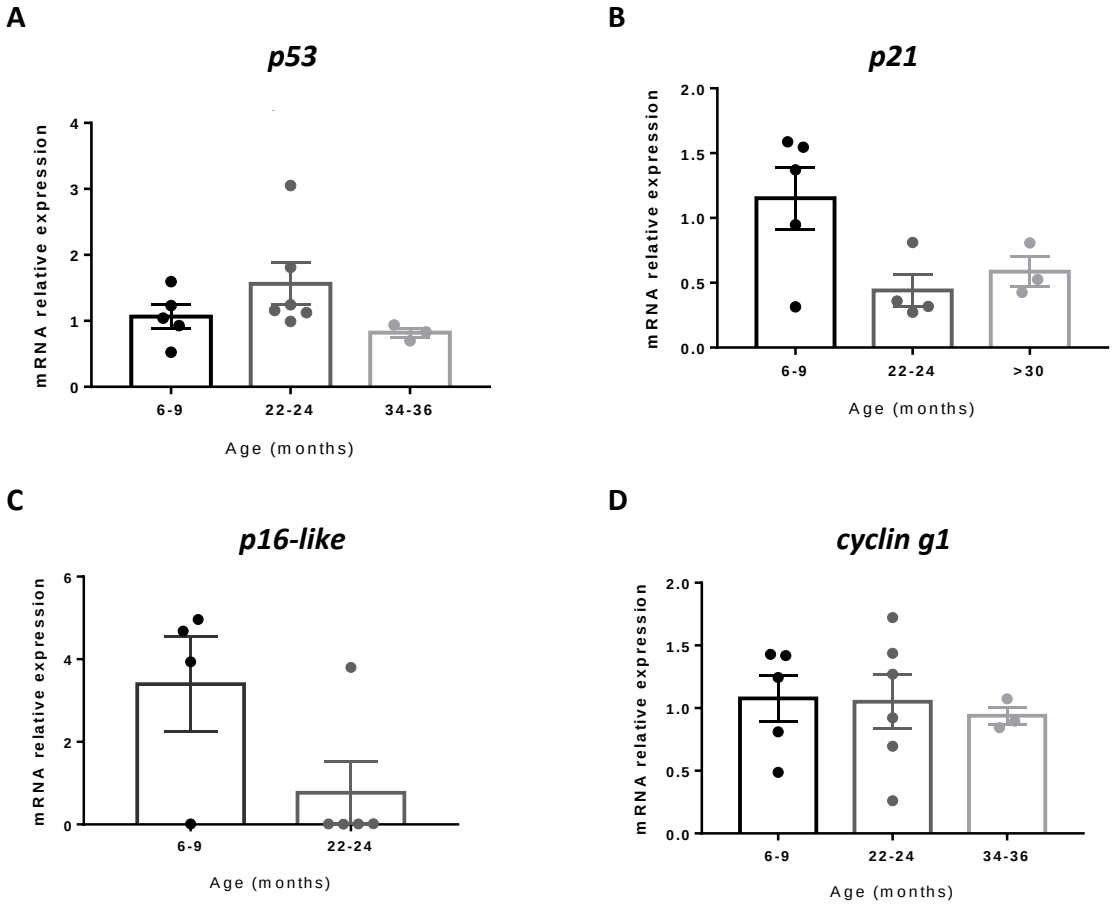


**Fig 4.5. mRNA relative expression of key downstream effectors of γH2AX in the whole zebrafish brain.** mRNA relative expression of (**A**) *p53*, (**B**) *p21*, (**C**) *p16*-like and (**D**) *cyclin g1* genes, in the young (6-9 months), middle aged (22-24 months) and old (>30 months) zebrafish brain. For this, the mRNA expression of each target gene was normalised to the reference gene (*beta-actin*) and analysed using the ΔΔCt method, as described in *section 2.5.3*. Graphs: X-axis, age in months; Y-axis, mRNA relative expression normalised to the WT 6-9 months of age, as described in *section 2.5.3*. N=3-6 *per* group. Each dot represents one animal. Bar errors represent the SEM. Statistics: (**A, B, D**) Kruskal-Wallis test followed by Dunn's post-hoc test or (**C**) Mann-Whitney test. * <0.05; ** <0.01; *** <0.001.

## 4.3 Determining the role of TERT in senescence accumulation in the zebrafish brain

If accumulation of senescence in natural WT ageing were telomerase (TERT) dependent, then one would predict that removing TERT would accelerate it. To test this, I compared the levels of senescence in the WT brain with the telomerase mutant zebrafish (premature ageing model *tert*$^{-/-}$), over-time. As mentioned in *Chapter 1*, the *tert*$^{-/-}$ model ages faster and dies prematurely, at around 12-18 months of age as compared to >30 months in WT. Thus, here I compared young (4-6 months) *tert*$^{-/-}$ versus WT brain, and old *tert*$^{-/-}$ (12-17 months) versus WT (>30 months) brain.

As I previously observed that SA-β-Gal expression accumulates differently between the different regions of the brain (see **Fig 4.2**), instead of assessing the whole brain, here I sought to determine which specific regions of the brain accumulate cellular senescence with ageing. To do this, I quantified senescence-associated markers in the 5 main macroareas of the zebrafish brain, at different ages throughout their life-course. The macroareas analysed included the telencephalon (Tel), the optic tectum (OT), the diencephalon (Die), the cerebellum (Ce) and the medulla oblongata (MO).

### 4.3.1 Assessing SA-β-Gal expression in the *tert*$^{-/-}$ brain

In order to test whether increased expression of SA-β-Gal with ageing is accelerated in the absence of TERT, SA-β-Gal staining was performed in brain cryosections of young (4-6 months) *tert*$^{-/-}$ fish, and compared with young (4-6 months) and old (>30 months) WT fish. SA-β-Gal was assessed by X-gal staining at pH 6.0, as described in *section 2.4.2.* The percentage of blue area (SA-β-Gal staining) in each macroarea of the brain was then quantified as described *in section 2.4.4*.

SA-β-Gal staining was detected in both WT old and *tert*$^{-/-}$ young fish in specific regions of the forebrain, midbrain and hindbrain. In particular, in the forebrain, SA-β-Gal staining was observed along the midline of the telencephalon (**Fig 4.6A-B, C1**) and, in abundance, throughout all the diencephalon with exception of the hypothalamus (**Fig 4.6A-B, C2-3**). In the midbrain, SA-β-Gal staining was detected in the periventricular grey zone (PGZ) and stratum opticum (SO) of the optic tectum (**Fig 4.6A-B, C2-3**). In the hindbrain, SA-β-Gal staining was observed in discrete spread zones of the cerebellum, appearing to be more

prominent in the Purkinje cell layer (PCL) (**Fig 4.6A-B, C4**), as well as in the medulla oblongata. The medulla oblongata was the macroarea that presented the highest levels of SA-β-Gal, displaying blue staining everywhere, with the strongest staining being identified close to the medullary canal (**Fig 4.6A-B, C4-5**).

Quantification of the SA-β-Gal staining per macroarea revealed no statistically significant differences in SA-β-Gal expression over-time, in the WT telencephalon and optic tectum (Tel: p=0.182; OT: p=0.359) (**Fig 4.7A, B**). SA-β-Gal expression was not accelerated in the absence of telomerase in the optic tectum, as no differences were detected between WT and *tert*$^{-/-}$ at 4-6 months in this region (p=0.859). Nonetheless, there was a small increase in SA-B-Gal expression in the young *tert*$^{-/-}$ telencephalon, when compared with the age-matched WT, that did not reach statistical significance (p=0.061).

In contrast with the telencephalon and optic tectum, the results showed a significant increase of SA-β-Gal expression over-time in the WT diencephalon (p=0.028, **Fig 4.7C**) and a small increase in the cerebellum, that did not reach statistical significance (p=0.075, **Fig 4.7D**). Interestingly, 4-6 months old *tert*$^{-/-}$ already presented higher levels of SA-β-Gal than its WT counterpart, in both macroareas (Die: p=0.028; Ce: p=0.036).

Finally, in the medulla oblongata, SA-β-Gal staining was already observed in some young WT fish (4-6 months), and no increasing SA-β-Gal expression was identified with natural ageing (p=0.258, **Fig 4.7E**), or in the absence of TERT (p=0.600).

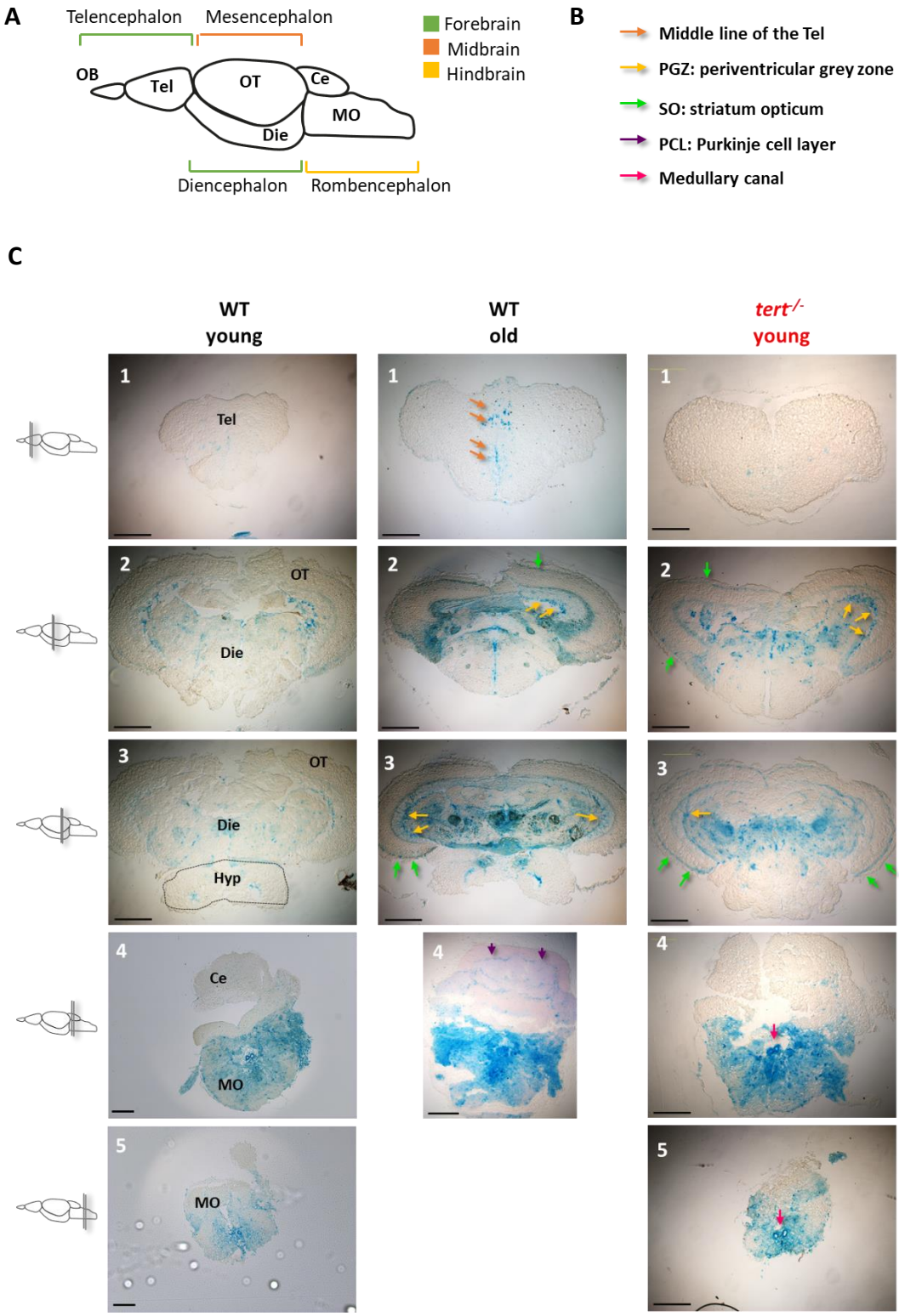


**Fig 4.6. Representative images of SA-β-Gal staining in the different brain macroareas, in young and old WT fish, and *tert*$^{-/-}$ young fish. (A)** Schematic figure of the zebrafish brain and respective macroareas. **(B)** Key for coloured arrows. **(C)** Representative images of SA-β-Gal staining in the different macroareas of the brain, in young (4-6 months) and old (>30 months) WT and young (4-6 months) *tert*$^{-/-}$. Scale bar: 200µm. Numbers 1 to 5 represent different locations of the brain, from the anterior to the posterior part of the brain. Abbreviations: OB, Olfactive Bulb; Tel, Telencephalon; OT, Optic Tectum; Die, Diencephalon; Hyp, Hypothalamus; Ce, Cerebellum; MO, Medulla Oblongata.

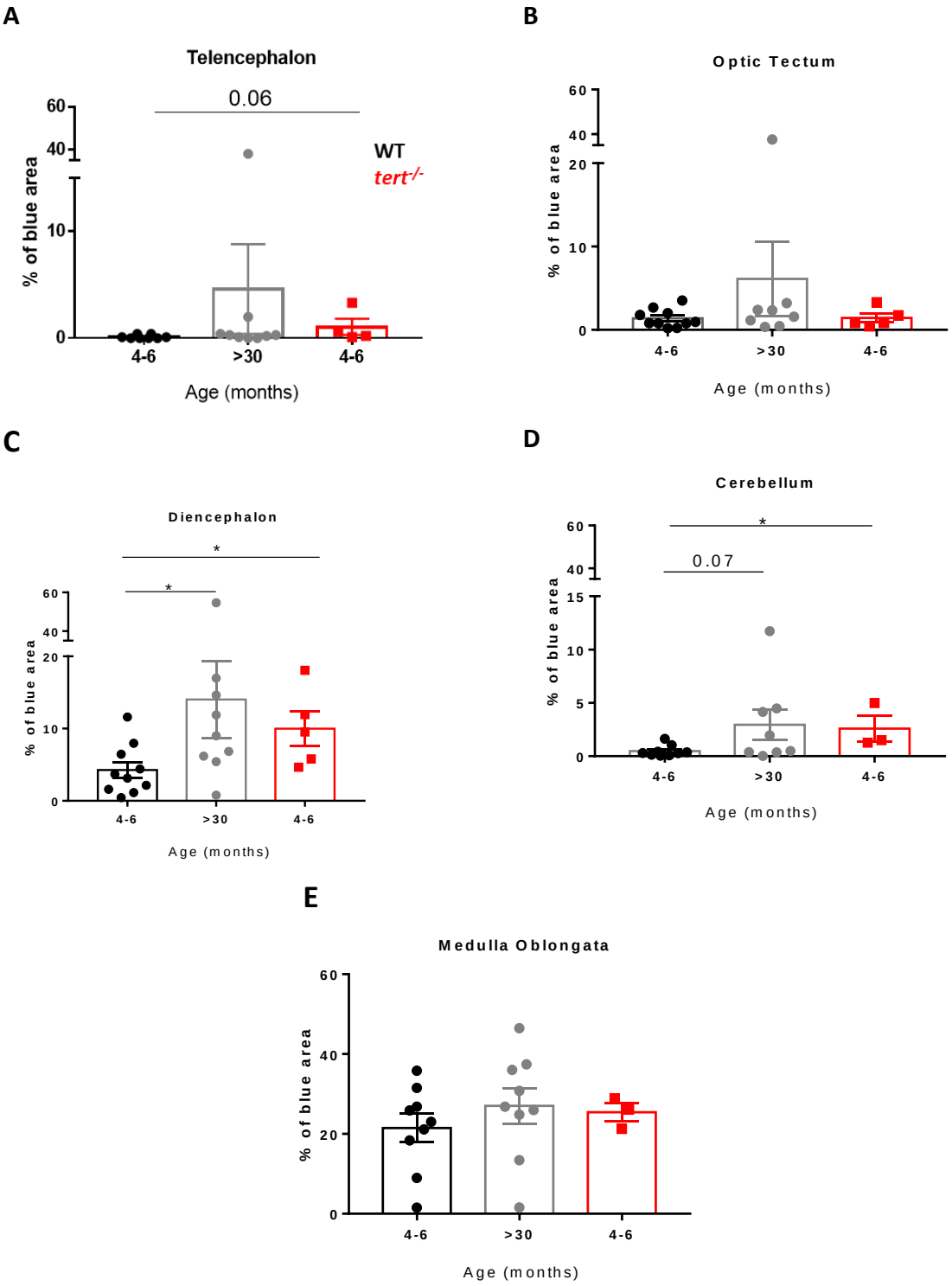


**Fig 4.7. Telomerase-dependent accumulation of SA-β-Gal in the ageing brain in the different brain macroareas.** Quantifications of SA-β-Gal staining, as described in *section 2.4.3*, in the **(A)** telencephalon **(B)** optic tectum, **(C)** diencephalon, **(D)** cerebellum and **(E)** medulla oblongata. Graphs: X-axis, age in months; Y-axis, % of blue area. N=3-10 per group. Each dot represents one animal. Error bars represent the SEM. Mann Whitney test: * p<0.05; ** p<0.01; *** p<0.001.

### 4.3.2 Assessing DNA damage in the *tert*$^{-/-}$ brain

In order to test whether accumulation of DNA damage with ageing is accelerated in the absence of TERT, DNA damage was quantified in paraffin sections of young (4-5 months) and old (9-17 months) *tert*$^{-/-}$ fish, and compared with young (4-5 months), middle aged (9-17 months) and old (>30 months) WT fish. DNA damage was assessed by the presence of γH2AX foci, detected by IF, as described in *section 2.3.2*. The percentage of γH2AX-positive cells in each macroarea of the brain was then quantified as described in *section 2.3.5*.

The results showed no significant change in the percentage of γH2AX-positive cells with natural ageing, in the telencephalon and optic tectum (WT: Tel: p=0.156; OT: p=0.567) **(Fig 4.8A, B**). Moreover, accumulation of DNA damage in these macroareas was not accelerated in the absence of TERT, as no differences were detected between *tert*$^{-/-}$ and WT at any time-point tested (Tel, 4-6m: p=0.999; 9-17m: p=0.999; OT, 4-6m: p=0.999; 9-17m: p=0.228).

In contrast, there was an increased percentage of γH2AX-positive cells with natural ageing in the diencephalon and cerebellum (Die: p=0.006, Ce: p=0.0003 **Fig 4.8C, D**). In the diencephalon this was specifically observed between the ages of 9-17 and >30 months (p=0.016). Moreover, *tert*$^{-/-}$ model presented higher levels of DNA damage in both macroareas at the age of 9-17 months, when compared with its WT counterpart (Die: p=0.025, Ce: p=0.031).

Due to technical issues it was not possible to obtain slides with tissue from the medulla oblongata in WT and *tert*$^{-/-}$ groups, and therefore DNA damage in this macroarea was not analysed.

Overall, the results showed an accumulation of DNA damage in brain, with natural ageing, specifically in the diencephalon and cerebellum, the same regions where it was identified accumulation of SA-β-Gal. Furthermore, accumulation of DNA damage and SA-β-Gal in these regions, but not in other regions of the brain, was accelerated in the *tert*$^{-/-}$ model. Together, these data show that there is accumulation of cellular senescence in the zebrafish diencephalon and cerebellum, with natural ageing, and that this is accelerated in the absence of TERT.

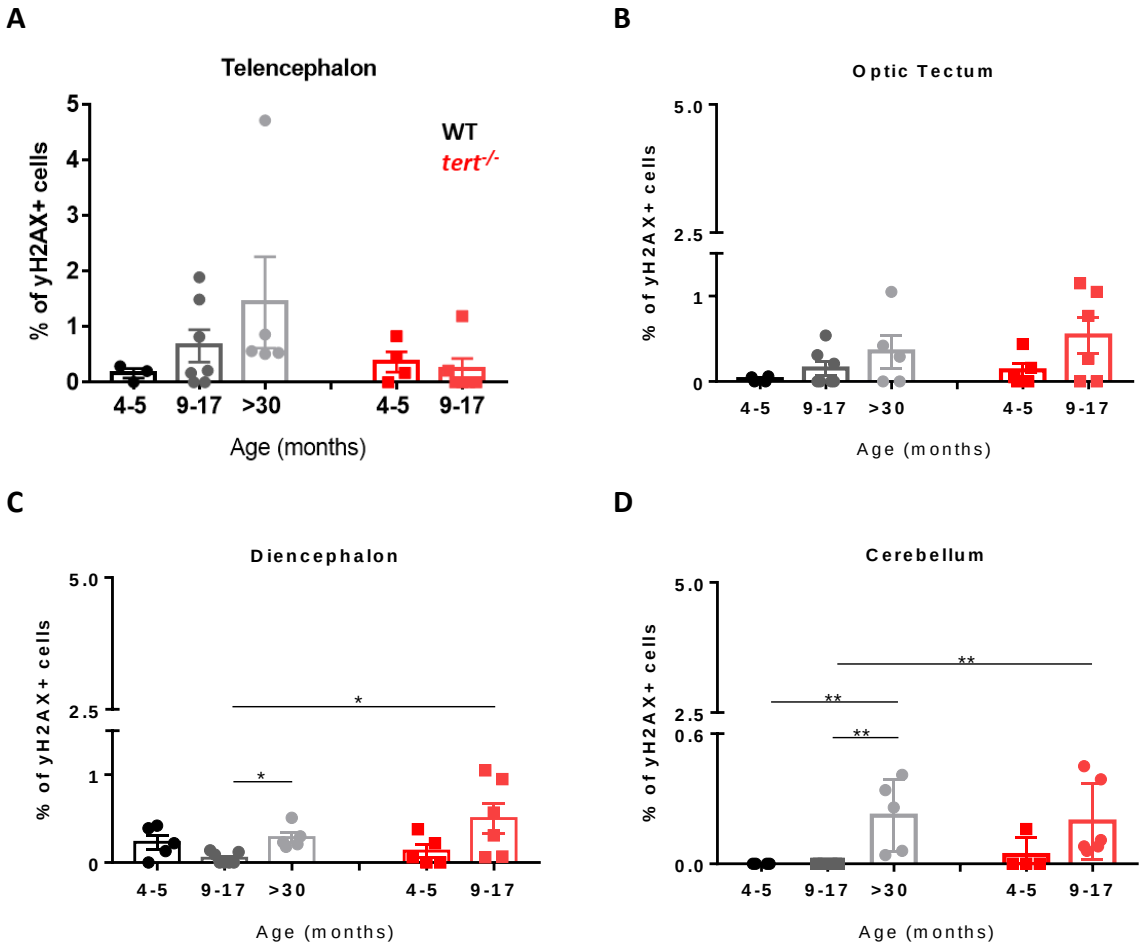


**Fig 4.8. Age-dependent accumulation of DNA damage with ageing in the different brain macroareas, in the presence and absence of telomerase.** Quantifications of γH2AX-positive cells in different macroareas of the zebrafish brain: **(A)** telencephalon **(B)** optic tectum, **(C)** diencephalon and **(D)** cerebellum. Graphs: X-axis, age in months; Y-axis, % of γH2AX-positive cells. N=3-7 per group. Each dot represents one animal. Error bars: SEM. Statistics: two-way ANOVA test was used to compare WT versus *tert*$^{-/-}$ at 4-5m versus 9-17m; Kruskal-Wallis followed by Dunn's post-hoc test was used to analysis WT over-time. * p<0.05; ** p<0.01; *** p<0.001.

## 4.4 Assessing potential replicative senescence in the aged zebrafish brain

Cells that undergo replicative senescence are characterised by a lack of proliferative activity and by the presence of critically short telomeres (Hayflick, 1965; Hayflick & Moorhead, 1961). Therefore, to test whether the accumulation of SA-β-Gal and DNA damage in the ageing brain are associated with replicative senescence, I measured proliferation levels and telomere length in the ageing zebrafish brain, in WT and *tert*$^{-/-}$. Using the *tert*$^{-/-}$ here allowed to have a control for what it can be considered short telomeres and associated replicative senescence, as it has been previously described in other tissues (Anchelin et al., 2013; Carneiro et al., 2016; Henriques et al., 2013).

### 4.4.1 Assessing proliferation levels in the ageing WT and *tert*$^{-/-}$ brain

Given that senescent cells are non-proliferative cells, as cellular senescence accumulates in the tissue, one would expect decreased number of proliferating cells. In order to test whether there is decreased cell proliferation with ageing in the zebrafish brain, and whether this is accelerated in the absence of TERT (i.e. telomerase-dependent), proliferation levels were quantified in paraffin sections of young (4-5 months) and old (14-17 months) *tert*$^{-/-}$ fish, and compared with young (4-5 months), middle aged (14-17 months) and old (>30 months) WT fish. Proliferation was detected by IF, using an antibody against PCNA, an antigen that label cells during S-phase, as described in *section 2.3.2*. This antibody had already been tested in the laboratory and previously published in zebrafish (Carneiro et al., 2016; Henriques et al., 2013). The percentage of PCNA-positive cells (proliferating cells) was counted as described in *section 2.3.5* and used as a measure of proliferative activity.

The results did not show any differences in proliferation with natural ageing, in the telencephalon and optic tectum (Tel: p=0.448; OT: p=0.694) (**Fig 4.9A-C**). Moreover, decreased levels of proliferation in these macroareas were not accelerated in the absence of TERT, as no differences were detected between WT and *tert*$^{-/-}$ at any time-point tested (Tel: 4-5m: p=0.999 14-17m: p=0.999; OT: 4-5m: p=0.999, 14-17m: p=0.999).

In the diencephalon, there was a small decrease in proliferation over-time in natural ageing that was borderline significant (p=0.058, **Fig 4.9D**). Moreover, in the cerebellum, there was a reduced percentage of cells dividing with natural ageing (p=0.022, **Fig 4.9E**). Decreased

proliferation levels were not accelerated in the absence of TERT as no differences were identified between WT nor *tert*$^{-/-}$ at any time-point tested, either in the diencephalon (4-5m: p=0.999, 14-17m: p=0.999) or in the cerebellum (4-5m: p=0.999, 14-17m: p=0.999).

Proliferation levels were not assessed in the medulla oblongata due to technical issues. In fact, this macroarea was missing in the majority of the analysed sections.

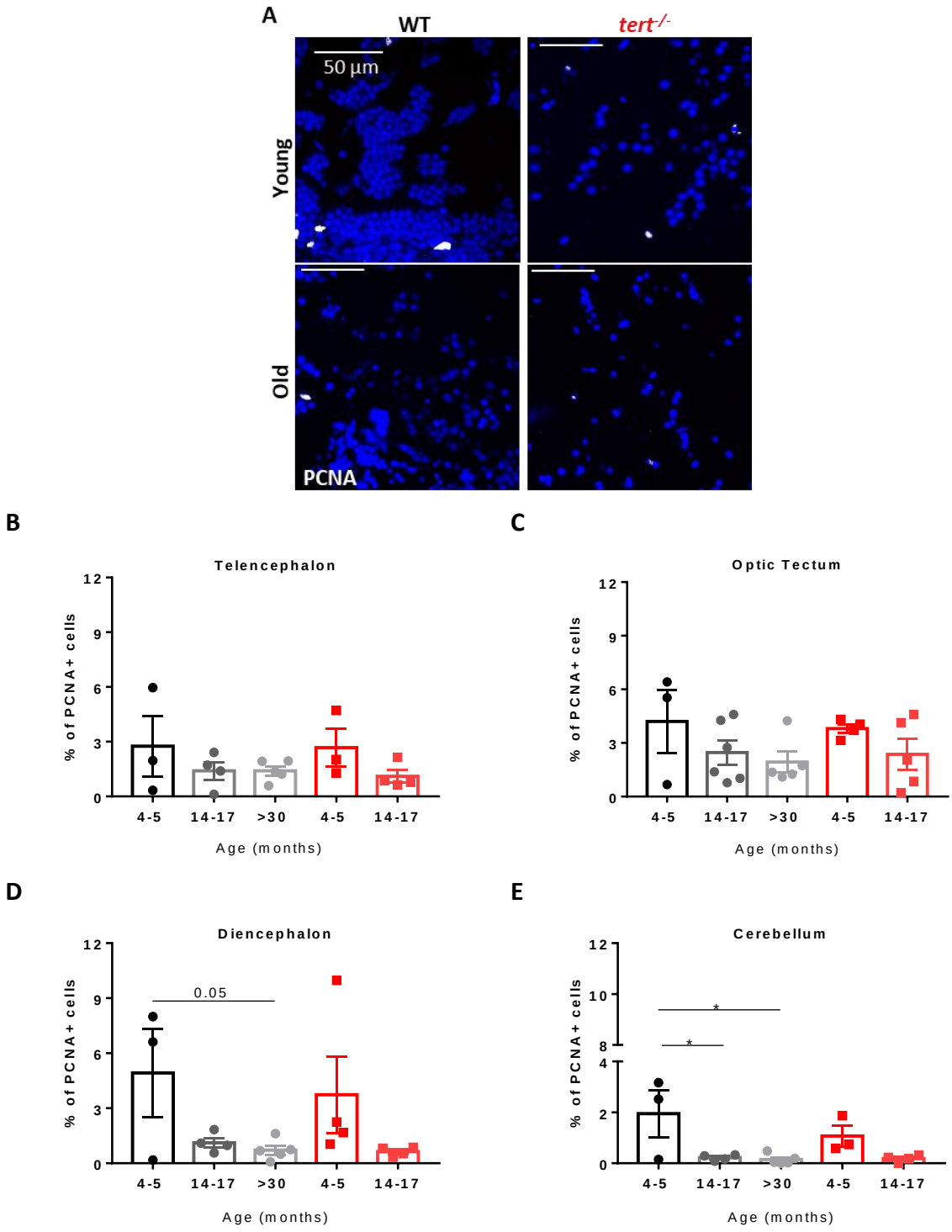


**Fig 4.9. Proliferation in the ageing brain zebrafish brain, per macroarea, in the presence (WT) and absence of telomerase (*tert*$^{-/-}$). (A)** Representative images of PCNA staining in the diencephalon of adult zebrafish. **(B-E)** Quantifications of % of PCNA-positive cells in the different macroareas of the zebrafish brain, including: **(B)** telencephalon, **(C)** optic tectum, **(D)** diencephalon and **(E)** cerebellum. Graph: X-axis, age in months; Y-axis, % of PCNA-positive cells. N=3-6 per group. Each dot represents one animal. Bar errors represent the SEM. Statistics: two-way ANOVA test was used to compare WT versus *tert*$^{-/-}$ at 4-5m versus 9-17m; Kruskal-Wallis followed by Dunn's post-hoc test was used to analysis WT over-time: * <0.05; ** <0.01; *** <0.001.

### 4.4.2 Measuring relative telomere length in the aged WT and *tert*$^{-/-}$ brain

Accumulation of cellular senescence with natural ageing, assessed by SA-β-Gal and DNA damage, was particularly detected in the diencephalon and cerebellum (see **Fig 4.7**, **Fig 4.8**), and this was accompanied by decreased proliferation levels (see **Fig 4.9**). Therefore, I then sought to test whether accumulation of cellular senescence was associated with critically short telomeres, which would suggest this would be replicative senescence. If this were to be replicative senescence, then it would be telomerase dependent, and therefore removing TERT would accelerate it. To test this, I measured relative telomere length, *in situ*, in brain tissue of young and old *tert*$^{-/-}$ fish (3-5 versus 12-17 months), and compared it against young and old WT fish (3-5 versus >30 months).

Relative telomere length was assessed *in situ*, by telo-FISH, by hybridising the tissues with a PNA telomere oligonucleotide, as described in *section 2.3.3*. The probe signal intensity was then measured as described in *section 2.3.3*. A centromere-specific probe was used alongside, and its signal intensity was used to calculate the telomeres/centromeres ratio, ensuring that telomere length was controlled for proliferation state. This technique had already been tested in the laboratory.

The results showed no significant differences in telomere length in the WT brain over-time ($p=0.146$) (**Fig 4.10A, B**). Nonetheless, there was a small decrease in telomere length in the *tert*$^{-/-}$, in comparison with its WT counterpart, at 3-5 months of age, that did not reach statistical significance ($p=0.058$).

**A**

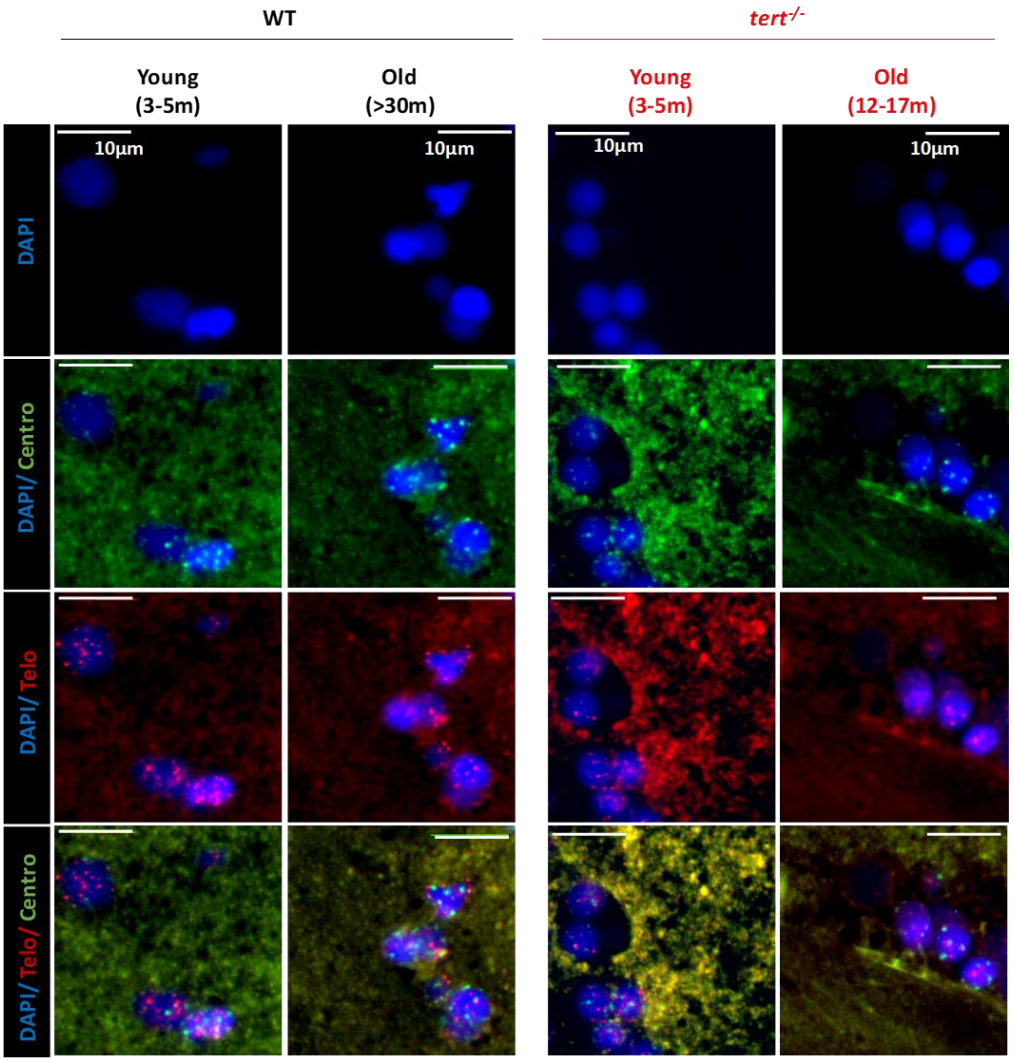


**B**

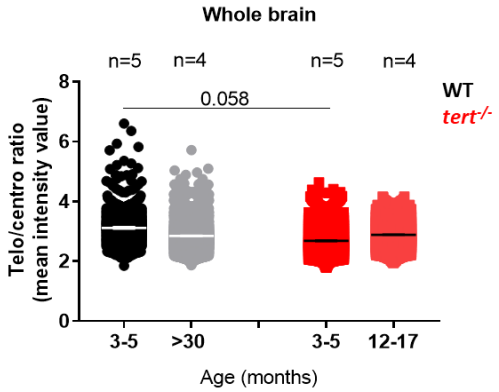


**Fig 4.10. Relative telomere length in the whole zebrafish brain with ageing. (A)** Representative images of telomeres and centromeres in the diencephalon of adult zebrafish. **(B)** Quantification of telomeres/centromeres ratio analysed as described in *section 2.3.3*. Graphs: X-axis age in months; Y-axis, telomeres/centromeres ratio, expressed in mean intensity value. N=4-5 per group. Each dot represents a cell. Bar errors represent the SEM. Random effects ANOVA: * <0.05; ** <0.01; *** <0.001.

Replicative senescence is likely to accumulate in proliferative zones, where there is accelerated telomere attrition. Therefore, I decided to test whether telomere shortening occurs in specific areas of the brain. To do this, telomere length was measured in all the individual macroareas of the brain. This was performed in paraffin sections of young (3-5 months) WT and *tert*$^{-/-}$ fish, and compared with old WT (>30 months) and old *tert*$^{-/-}$ (14-17 months) fish.

The results showed a decrease in telomere length with natural ageing in the telencephalon, optic tectum and cerebellum (Tel: p=0.034, OT: p=0.027, Ce: p=0.046) (**Fig 4.11A, B, D**). In contrast, telomere shortening with natural ageing was not observed in the diencephalon and medulla oblongata (Die: p=0.215, MO: p=0.327) (**Fig 4.11C, E**). Additionally, the *tert*$^{-/-}$ model displayed already shorter telomeres than its WT counterpart at the age of 3-5 months in the optic tectum (p=0.009). A small decrease in telomere length was also observed in the *tert*$^{-/-}$ model when compared with WT (3-5 months), in the telencephalon (p=0.076), diencephalon (p=0.077) and medulla oblongata (MO: p=0.054). However, this did not reach statistical significance. In contrast, no differences between genotypes were identified at 3-5 months of age in the cerebellum (p=0.106), or at 12-17 months of age in any of the macroareas (Tel: p=0.337, OT: p=0.840, Die: p=0.836, Ce: p=0.715, MO: p=0.616).

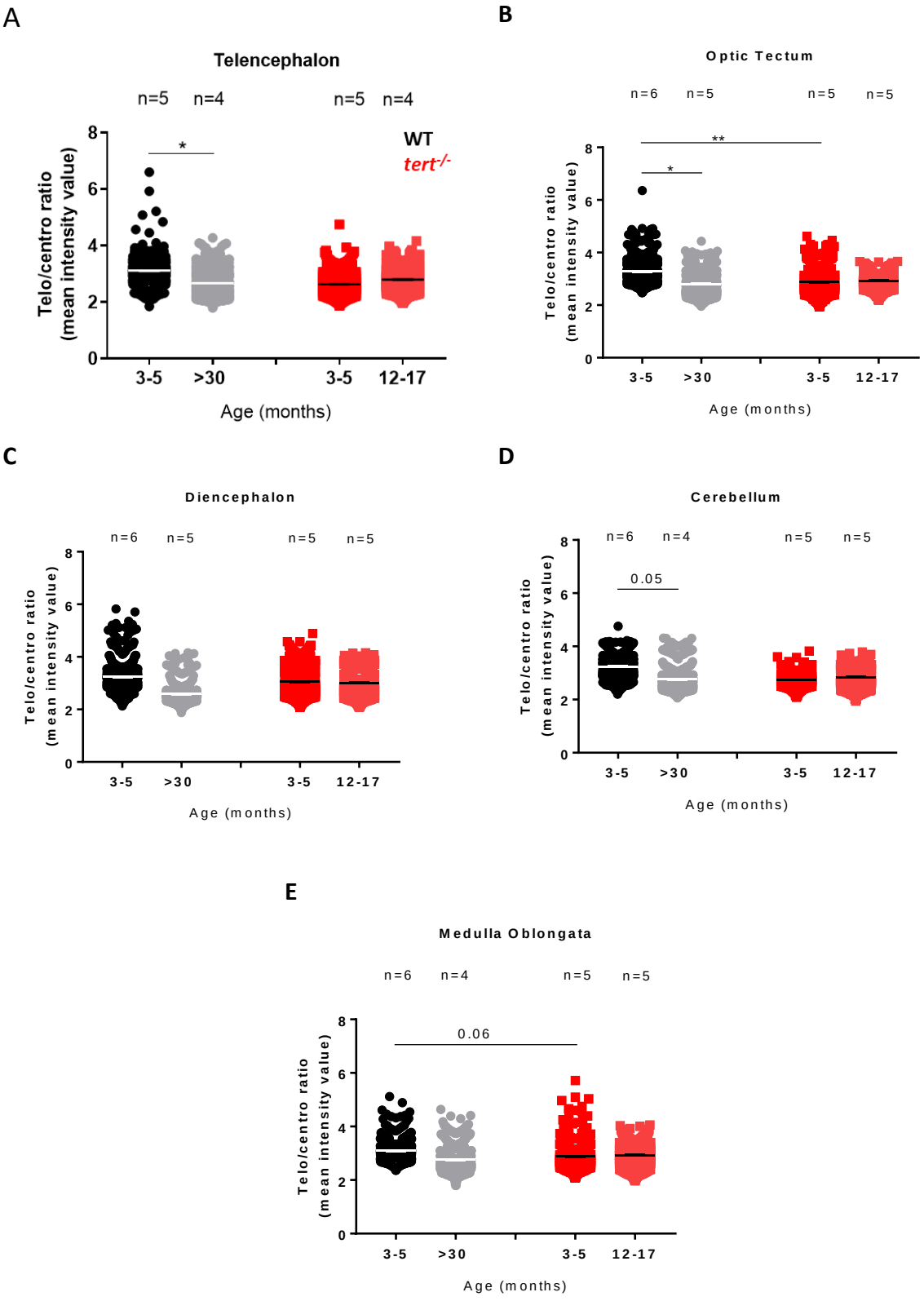


**Fig 4.11. Relative telomere length in the ageing zebrafish brain, per macroareas. (A-E)** Quantification of telomeres/centromeres ratio analysed as described in *section 2.3.3,* per macroareas: **(A)** telencephalon, **(B)** optic tectum, **(C)** diencephalon, **(D)** cerebellum and **(E)** medulla oblongata. Graphs: X-axis, age in months; Y-axis, telomeres/centromeres ratio, expressed in mean intensity value. N=4-6 per group. Each dot represents a cell. Bar errors represent the SEM. Random effects ANOVA: * <0.05; ** <0.01; *** <0.001.

## 4.5 Discussion

This Chapter aimed to determine whether TERT expression plays a role in protecting the ageing zebrafish brain against accumulation of cellular senescence. If so, whether this was due to its role at telomeres. In order to test this, I aimed to determine whether: (1) the zebrafish brain accumulates senescence with ageing and whether this is accelerated in the absence of TERT, and (2) whether accumulation of TERT-dependent senescence is accompanied by telomere shortening and therefore likely to be replicative senescence.

### Accumulation of cellular senescence in the naturally aged zebrafish brain

In order to test if there is accumulation of cellular senescence in the zebrafish brain, with natural ageing, and whether this is accelerated in the absence of telomerase, I assessed different markers of senescence in the WT and *tert*$^{-/-}$ zebrafish, throughout their lifetime. My initial study of the whole brain (i.e. without looking at any specific macroareas) identified increased SA-β-Gal expression in the brain, with natural ageing, accompanied by a small increase in DNA damage that did not reach significance. Similarly, a previous study in zebrafish had already identified accumulation of DNA damage in the whole brain from 12 months of age onwards (S. Zhu & Coffman, 2017). Moreover, accumulation of cellular senescence in the ageing brain is not an exclusive characteristic of zebrafish, as mice also display increased levels of SA-β-Gal and γH2AX in the aged brain, at least in some cell populations (Jurk et al., 2012). Nonetheless, this project failed in identifying any alteration in gene expression of down-effectors of γH2AX, commonly associated with cellular senescence, including *p53*, *p21* and *p16*. Although it remains unknown if these genes are up-regulated in the aged zebrafish brain, up-regulation of these genes has been identified in the aged mice brain, at least in some cell populations. These cell populations include endothelial cells (*p16* and *p21*) (Yamazaki et al., 2016), microglia (*p21*) (Raj et al., 2015), and cortical and Purkinje neurons (*p53*) (Jurk et al., 2012). It is important to note, though, that the SA-β-Gal staining hinted at potential accumulation of cellular senescence in specific macroareas, which could explain the lack of results when assessing whole brain expression of *p53*, *p21* and *p16* genes. Indeed, further analysis showed this to be the case.

Analysis per macroareas of the brain revealed that accumulation of cellular senescence does not occur homogeneously throughout the brain. Instead, this accumulation seems to occur specifically in the diencephalon and cerebellum, the only regions of the brain displaying increased levels of SA-β-Gal and DNA damage foci with natural ageing (see **Table 4.1**).

The fact that the small increase in SA-β-Gal expression in the aged cerebellum was borderline significant may be due to the reduced sample size used. Effect sizes showed that this experiment was underpowered, and it would be required a minimum of 34 animals per group, warranting further investigation with an increased number of animals.

Moreover, the fact that accumulation of senescence was only identified in two macroareas of the brain may explain the lack of differences observed in the expression of *p53*, *p21*, and *p16* in the aged zebrafish brain. As gene expression was analysed in RNA extracted from whole brain, the signal from a low number of senescent cells (which is expressed only in certain regions of the brain) is likely to have been masked by non-senescent cells in the surrounding. The analysis of *p21*, *p16* and *p53* expression in the whole brain tissue therefore revealed to be a technical limitation in this project. In the future, it would be important to confirm these results by analysing individual macroareas, or even specific cell populations after cell sorting.

**Table 4.1 Summary of the brain macroareas that display accumulation of senescence, reduced proliferation and telomere shortening with ageing in WT and *tert*$^{-/-}$ zebrafish.** In WT, the age represents the time-point from which differences started being observed. In *tert*$^{-/-}$**,** the age represents the time-point where differences are detected in comparison with their WT counterpart. Age is represented in months. Tel: Telencephalon, OT: Optic tectum, Die: Diencephalon, Ce: Cerebellum, MO: Medulla oblongata.

| | SA-β-Gal | | DNA damage | | Proliferation | | Telomere length | |
|---|---|---|---|---|---|---|---|---|
| | **WT** | ***tert*$^{-/-}$** | **WT** | ***tert*$^{-/-}$** | **WT** | ***tert*$^{-/-}$** | **WT** | ***tert*$^{-/-}$** |
| Tel | - | ↑ 4-6m* | - | - | - | - | ↓ >30m | ↓ 3-5m* |
| OT | - | - | - | - | - | - | ↓ >30m | ↓ 3-5m |
| Die | ↑ >30m | ↑ 4-6m | ↑ >30m | ↑ 9-17m | ↓ >30m* | - | - | ↓ 3-5m* |
| Ce | ↑ >30m* | ↑ 4-6m | ↑ >30m | ↑ 9-17m | ↓ >14-17m | - | ↓ >30m* | - |
| MO | - | - | - | - | - | - | - | ↓ 3-5m* |

*Borderline significance

## The role of TERT in accumulation of cellular senescence in the zebrafish brain

Importantly, accumulation of senescence in the diencephalon and cerebellum, but not in other macroareas of the brain, was accelerated in the *tert*$^{-/-}$ (versus the WT). A slight but non-significant increase in SA-β-Gal was also observed in the telencephalon of *tert*$^{-/-}$ at 4-6 months of age (versus young WT). However, in the absence of DNA damage it is not possible to conclude that there is increased senescence in this region of the brain. This is because, as mentioned in *section 1.3.2*, SA-β-Gal alone cannot be considered a universal marker of senescence and, ideally, should be used in combination with other markers of senescence. Together, the data shown here suggest that there is accumulation of cellular senescence in the zebrafish diencephalon and cerebellum, with natural ageing, as assessed by increased levels of DNA damage and SA-β-Gal. Importantly, this is accelerated in the absence of TERT, suggesting that the TERT component of telomerase plays a protective role against accumulation of cellular senescence in the aged zebrafish brain.

Contrary to what was found in this project, a previous study in WT zebrafish had reported an increased expression of SA-β-Gal in the telencephalon at >26 months of age (Arslan-Ergul et al., 2016). However, in that study the authors did not assess other markers of senescence (Arslan-Ergul et al., 2016). Considering that in some contexts SA-β-Gal can be expressed in non-senescent cells (Severino et al., 2000; Yang & Hu, 2005), and that no other marker of senescence was not used in the study, it is not possible to conclude with certainty that there is accumulation of cellular senescence in the aged zebrafish telencephalon. To my knowledge, there are no other studies in zebrafish assessing cellular senescence in the different regions of the brain. Nevertheless, some studies in mice have reported accumulation of cellular senescence with ageing in different brain regions.

Similarly to what was observed in this project, increased SA-β-Gal and γH2AX foci are identified in the aged mice cerebellum, particularly in Purkinje cells (PCs) (Jurk et al., 2012). Additionally, this is aggravated in the absence of TERC (G4 TERC$^{-/-}$) (Jurk et al., 2012). Cerebellar PCs are thought to be one of the most sensitive neuronal populations in the brain, suffering several age-associated changes that lead to loss of function (Zhang, Zhu, & Hua, 2010). In mammals, degeneration of this neuronal population has been associated with impairment of motor skills, spatial orientation and associative learning (Bernard & Seidler, 2014; Zhang et al., 2010). As zebrafish cerebellum is functionally similar to mammals (Knogler

et al. 2019; Matsui et al., 2014), PCs dysfunction with ageing may also contribute to motor and cognitive decline in zebrafish. As growing evidence now suggests that accumulation of cellular senescence may affect PCs, it is reasonable to hypothesise that accumulation of senescence in the cerebellum may contribute to motor and/or cognitive impairment in ageing. Additionally, as this project identified accelerated accumulation of senescence in the cerebellum in the absence of TERT, it might be that this component of telomerase is required for cerebellum-dependent behaviours. Lee et al. showed that even though WT mice displayed decreased spontaneous locomotion (a cerebellum-dependent behaviour) with ageing, this was not accelerated in the G4 *Tert*$^{-/-}$ mice model (Lee et al., 2010). This suggests that TERT is unlikely to affect locomotive behaviour in mice. However, it remains unexplored whether it affects other cerebellum-dependent behaviours, both in mammals and in zebrafish.

Apart from the cerebellum, markers of senescence have also been identified in the cortex, hippocampus (Bussian et al., 2018; Jurk et al., 2012), substantia *nigra*, ventral tegmental area (VTA), (Shaerzadeh et al., 2020), and SVZ of old mice (Molofsky et al., 2006). To my knowledge, it has not been tested whether lack of TERT expression is associated with cellular senescence in most of these regions of the brain. Nonetheless, some evidence now implies that this component of telomerase may be associated with senescence in the SVZ, a neurogenic niche in the mammalian brain, containing NSCs (Gage, 2000). More specifically, *in vitro*, mice-derived NSCs display higher levels of p53 accompanied by impaired proliferation capacity in the absence of TERT, which is rescued by telomerase reactivation (Jaskelioff et al., 2011). *In vivo*, the authors reported decreased proliferation activity in the SVZ of G4 *Tert*$^{-/-}$ mice in comparison to their G4 *Tert*$^{+/+}$ counterparts, which again was rescued by telomerase reactivation (Jaskelioff et al., 2011). It remains unknown whether there is increased expression of p53 together with other markers of senescence in the SVZ, *in vivo*, and whether this is accelerated in the absence of TERT.

The dorsal pallium in the zebrafish telencephalon is thought to be a rudimentary cortex, homologous to the mammalian isocortex. Within the dorsal pallium, the dorsal lateral region (Dl) is considered to be the homologous of the mammalian hippocampus, a structure with an important role in memory (Mueller et al., 2011; O'Connell & Hofmann, 2011). Contrary to what was observed in mice (Bussian et al., 2018; Jurk et al., 2012), this study did not show accumulation of senescence in the zebrafish dorsal pallium, or specifically in the Dl region.

Nonetheless, it is important to mention that the hippocampus, more specifically the sub-granular zone (SGZ) in the dentate gyrus, constitutes one of the neurogenic niches in the mammalian brain (Ming & Song, 2011). Proliferative cells in the hippocampus may therefore be more vulnerable to cellular senescence in comparison to other, non-proliferative regions of the brain. Accordingly, the second neurogenic niche in the mammalian brain, the SVZ, has been also shown to display markers of senescence in the aged mice (Molofsky et al., 2006). I also did not find increased expression of SA-β-Gal in the ventral nuclei of the ventral telencephalon (Vv), considered the homologous to the SVZ (Schmidt et al., 2013). In opposition to mammals where neurogenesis is constrained to two niches (Ming & Song, 2011), zebrafish present several proliferative regions (Grandel et al., 2006; Schmidt et al., 2013). The so far described proliferative areas of the zebrafish brain include the outer layer of the telencephalon, but not specifically the Dl or the Vv (Grandel et al., 2006; Schmidt et al., 2013). The differences in proliferation rate between mice hippocampus and zebrafish Dl, or between mice SVZ and zebrafish Vv, may therefore explain the differences in accumulation of senescence observed between the species. Further investigation would be required to test this hypothesis.

Substantia *nigra* and VTA are known as the core of the mammalian dopaminergic system, which is mainly involved in reward and motivation. These brain regions constitute an intense area of research in PD, a neurodegenerative disease mainly associated with degeneration and death of dopaminergic neurons. Unlike mammals where dopaminergic neurons are mainly distributed in the substatia *nigra* and VTA, zebrafish display a population of tyrosine hydroxylase (TH)-expressing neurons, thought to be dopaminergic neurons in zebrafish, in the posterior tuberculum of the diencephalon (Rink & Wullimann, 2001). This population of neurons is thought to project their axons to the subpallium region of the telencephalon, homologous to the mammalian striatum, constituting the 'dopaminergic system' in zebrafish. In addition, other clusters of TH-expressing neurons ('dopaminergic neurons') are also identified in other regions of the zebrafish diencephalon, including the pretectum, the ventral thalamus and the hypothalamus (Rink & Wullimann, 2001). In mice, it was recently reported that microglia undergo cellular senescence with ageing in the substancia *nigra* and VTA, possibly affecting the dopaminergic system (Shaerzadeh et al., 2020). If the same was to occur in zebrafish, then I would expect to see an increased number of microglia accumulating

senescence in the diencephalon region and, possibly, in the subpallium region of the telencephalon. Indeed, although this project did not identify increased senescence in the subpallium, accumulation of senescence was found widely spread in the diencephalon with exception of the hypothalamus. It remains unknown if microglia are undergoing senescence in the zebrafish diencephalon, over-time, and whether these cells are located near TH-expressing neurons. It would be interesting to explore these questions in a future experiment.

Of note, apart from the posterior tuberculum (a structure involved in the 'dopaminergic system' in zebrafish), the zebrafish diencephalon is constituted by the hypothalamus, prethalamus, thalamus and habenula, structures shared with mammals (Mueller, 2012). As I identified a large area of the diencephalon expressing SA-β-Gal in this project, it is likely that some of these structures also accumulate cellular senescence with ageing. Nonetheless, a more detailed analysis would be necessary to determine which structures and nuclei of the diencephalon accumulate senescence over-time. Additionally, it also remains unexplored whether these diencephalon-associated structures accumulate senescence in the mammalian brain. Overall, the diencephalon is one the most complex structures of the brain, containing multiple nuclei that serve as bridges between the cortex and subcortical regions, and interacting with various systems (sensorial, motor, endocrine, limbic) (Mueller, 2012). Thus, the diencephalon constitutes a relevant area to further study accumulation of senescence with ageing and to explore what are the putative consequences of accumulation of senescence in this region of the brain.

It is important to note that this project identified elevated expression of SA-β-Gal in the medulla oblongata from young ages, in both WT and *tert*$^{-/-}$ fish, with no further increase over-time. Nonetheless, it remains unclear whether this reflects real cellular senescence given that it was not possible to assess DNA damage in this macroarea due to technical issues. If the SA-β-Gal staining were indeed representing cellular senescence in the medulla oblongata, it would be fair to hypothesise that accumulation of senescence occurs at an earlier age than the ones analysed (<4-6 months). In zebrafish, the medulla oblongata contain the nuclei of 6 out of 12 cranial nerves, constituting a privileged place of communication between the brain and the periphery, known to be bidirectional (Moens & Prince, 2002). Part of this bidirectional communication occurs through the *vagus* nerve, which has been shown to be part of the gut-brain axis in the last few years (Carabotti, et al. 2015; Matteoli et al., 2014). Importantly, this

route of communication (through the *vagus* nerve) has been implicated in neurodegenerative diseases such as PD (Sampson et al., 2016). Considering this, it would be highly relevant to confirm whether the medulla oblongata already presents high levels of senescence at the age of 4-6 months and whether accumulation of senescence in the medulla oblongata precedes other macroareas of the brain. If this were to be the case, then it would be interesting to test how accumulation of senescence in this macroarea correlates with senescence in other tissues. It could well be that senescence in the medulla oblongata is contributing to accumulation of senescence not only in other parts of the brain but also in peripheral tissues. Alternatively, it could also be that peripheral tissues are contributing to accumulation of senescence in the medulla oblongata.

## Potential mechanisms underlying the protective role of TERT against accumulation of senescence

After identifying that there is accumulation of senescence in the aged zebrafish brain, specifically in the diencephalon and cerebellum, and that this is anticipated in the absence of telomerase, I tested whether senescence in the brain was associated with telomere shortening (i.e. replicative senescence). In order to test this, telomere length was assessed in both WT and *tert*$^{-/-}$, throughout their life course. If cellular senescence observed in the aged brain were associated with replicative senescence, then I would expect to see telomere shortening in the same macroareas where I observed accumulation of senescence. Within the macroareas accumulating cellular senescence with ageing, telomere shortening was identified in the WT cerebellum but not in the diencephalon, at >30 months of age (**Table 4.1**). In addition, as accumulation of cellular senescence in the diencephalon and cerebellum was accelerated in the *tert*$^{-/-}$ model, I expected to see the same pattern in telomere shortening. Nonetheless, although *tert*$^{-/-}$ model presented shorter telomeres in the diencephalon than their WT counterparts, at 3-5 months of age, no differences between genotypes were observed in the cerebellum. Furthermore, decreased telomere length was also observed in regions of the brain where accumulation of senescence was not observed. The inconsistency of these results in particular, together with a possible lack of sensitivity of the telo-FISH technique (see *section 6.5* for details), did not enable to take any relevant conclusions.

So far, these results raise two main hypotheses. (1) If TERT-associated senescence in the aged brain occurs in proliferative regions and is associated with telomere shortening, then it is likely that the protective role of telomerase against senescence is associated with its functions at telomeres (i.e. canonical functions). (2) If, instead, TERT-associated senescence in the aged brain occurs in non-proliferative regions and is independent of telomere length, then it is likely that the protective role of telomerase against senescence is associated with functions of telomerase that are independent of telomeres (i.e. non-canonical functions).

This project identified accumulation of SA-β-Gal, with ageing, not only in regions known to be proliferative areas in the adult zebrafish brain, but also in non-proliferative regions (**Fig 4.12**). Intriguingly, accelerated accumulation of SA-β-Gal in the absence of telomerase was also observed mainly in non-proliferative regions of the brain. These findings may suggest that TERT expression plays a protective role against accumulation of cellular senescence even in non-proliferative areas. Since telomerase is best known to be essential for proliferation, these results are unexpected at first glance. Nonetheless, TERT expression has been identified in the adult zebrafish brain in both proliferative and non-proliferative regions, and its overall expression reduced with ageing (Sprungala, 2009). This suggests that telomerase is likely to play other important roles in the brain, independently of its functions at telomeres. Hence, it would be important to confirm whether TERT-associated accumulation of senescence in the aged zebrafish brain is associated with proliferation and telomere shortening. This could be done by assessing cellular senescence in specific cell populations (for example, NSCs versus mature neurons) and by confirming the results in relation to telomere length. Ideally, this could be done by micro-dissecting specific cell types and assessing their telomere length using a more quantitative and sensitive technique. Such technique would involve a telomere specific RT-qPCR or Telomere Restriction Fragment (TRF) analysis by Southern blot. Both these techniques present technical challenges, but together, they would offer a better insight into this phenomenon.

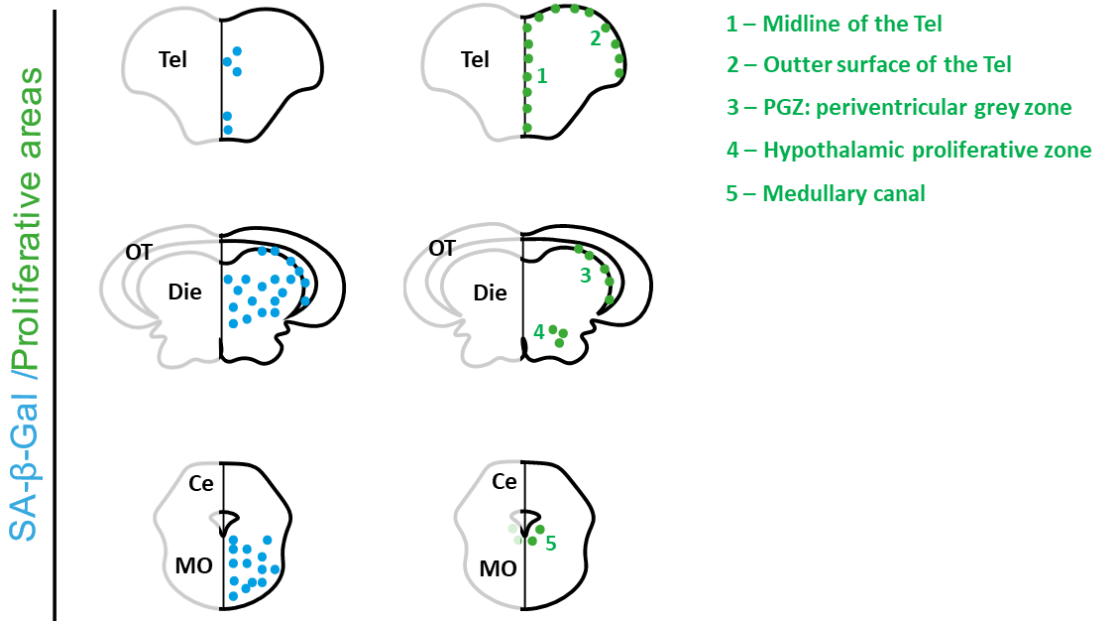


**Fig 4.12. Schematic figure illustrating the regions of the brain where I identified accumulation of SA-β-Gal and the regions that have been reported to be proliferative in the zebrafish adult brain, accordingly to Grandel et al., (2006).** Abbreviations: Tel, Telencephalon; OT, Optic Tectum; Die, Diencephalon; Ce, Cerebellum; MO, Medulla Oblongata.

## Conclusion

In summary, this Chapter shows that there is accumulation of senescence with ageing in the zebrafish brain, specifically in the diencephalon and cerebellum. Importantly, this accumulation is accelerated in the absence of TERT, suggesting that this component of telomerase play a protective role against senescence in the zebrafish brain. Nonetheless, it remains unclear whether this protective role is associated with canonical or non-canonical functions of telomerase and further investigation is required to address this question.

# Chapter 5.
# Exploring TERT-dependent mechanisms of ageing in the zebrafish brain

## 5.1 Introduction

In the previous chapter I observed that accumulation of cellular senescence with ageing in the zebrafish diencephalon and cerebellum occurs at earlier ages in the absence of Tert, suggesting that Tert activity exerts a protective effect against accumulation of senescence in these regions of the brain. Although this accumulation of senescence was detected in proliferative and non-proliferative regions of the brain, it was not possible to conclude whether the protective effect of Tert in the aged brain was associated with canonical or non-canonical functions of telomerase. Better understanding the mechanisms behind the accumulation of cellular senescence may help to find more targeted therapies to prevent accumulation of senescent cells with ageing and respective consequences. Hence, it is important to further explore what are the Tert-associated mechanisms that are affecting the aged brain and which of these mechanisms are involved in the protective effect of Tert against cellular senescence.

Within its non-canonical functions, telomerase has been reported to play a role in transcriptional regulation of inflammatory-associated genes (Choi et al., 2008; Ghosh et al., 2012). Moreover, cellular senescence has been associated with inflammation. On one hand, in some contexts, immune cells have been shown to be recruited to sites of cellular senescence (Demaria et al., 2014; Krizhanovsky et al., 2008). On the other hand, senescent cells have been shown to release pro-inflammatory factors (part of SASP), which can contribute to paracrine senescence (Acosta et al., 2013) as well as to tissue inflammation (Franceschi & Campisi, 2014; Campisi & d'Adda di Fagagna 2007). It could well be that the protective effects of Tert in the aged zebrafish brain are associated with inflammation, through its role at transcriptional regulation of inflammatory genes.

In this Chapter, I aimed to test whether there is increased inflammation in the zebrafish brain, with ageing, in a Tert dependent manner, and whether increased inflammation in the aged brain is correlated with accumulation of senescence. To test this, I assessed inflammation levels by IHC and enzymatic assays, in both WT and *tert*$^{-/-}$ zebrafish, throughout their lifetime. In addition, I sought to uncover other potential Tert-dependent mechanisms of ageing that affect the brain and be involved in cellular senescence. To do so, whole brains from WT and *tert*$^{-/-}$ zebrafish of different ages were analysed by RNA Sequencing. Network

analysis was performed in the RNA Sequencing data in order to find key sets of genes associated with Tert-dependent ageing in zebrafish brain.

## 5.2 Determining the role of TERT in inflammation in the aged zebrafish brain

Here, I sought out to test whether there is increased inflammation in the zebrafish brain, with ageing, and whether this is accelerated in the absence of TERT. To test this, I quantified the overall number of immune cells and assessed chitotriosidase activity, as a measure of immune activation, over-time, in the presence (WT) versus in the absence of Tert (*tert*$^{-/-}$).

### 5.2.1 Measuring the number of immune cells in the WT and *tert*$^{-/-}$ aged brain

In order to test whether there is increased number of immune cells in the brain, with natural ageing, I determined the percentage of immune cells from young (4-5 months), middle aged (9-17 months) and into old age (>30 months) WT brain. Immune cells were detected by IF, using the pan-leukocyte marker L-plastin (anti-LCP1 antibody), known to label all immune cell populations (see *section 2.3.2*). This antibody had already been tested in the laboratory. The percentage of immune cells was then counted as described in *section 2.3.5*.

The results showed an increased percentage of immune cells in the naturally aged brain ($p=0.004$, **Fig 5.1A, B**), more specifically at the age of >30 months (4-5m versus >30m: $p=0.009$, 9-17m versus >30m: $p=0.017$).

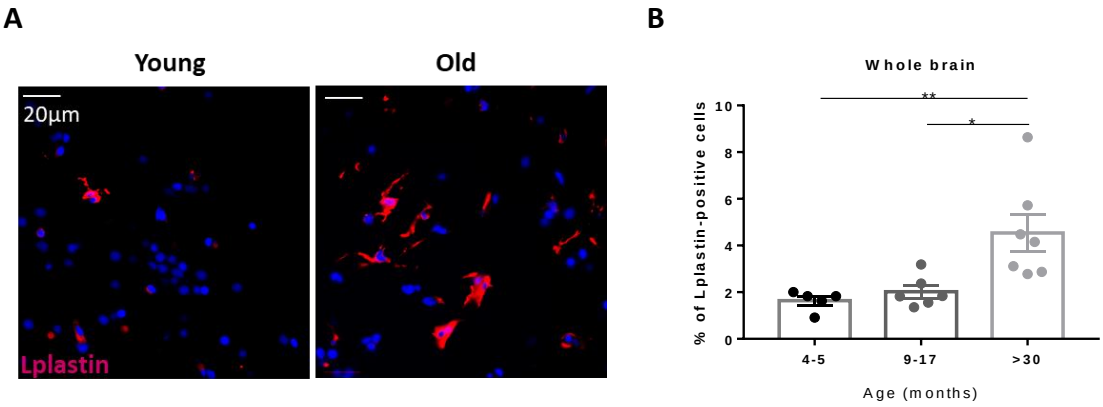


**Fig 5.1. Percentage of immune cells with natural ageing in the whole zebrafish brain. (A)** Representative images of L-plastin staining in the diencephalon of adult zebrafish. **(B)** Quantifications of percentage of L-plastin-positive cells in the whole zebrafish brain with natural ageing. Graph: X-axis, age in months; Y-axis, % of L-plastin-positive cells. N=5-7 per group. Each dot represents one animal. Error bars represent the SEM. One-way ANOVA followed by post-hoc test with Bonferroni correction: * $p<0.05$; ** $p<0.01$; *** $p<0.001$.

This increased number of immune cells in the whole zebrafish WT brain at >30 months, is occurring at the same age where I previously detected increased cellular senescence (see **Fig 4.2**). I therefore sought out to quantify whether accumulation of senescence was locally associated with increased number of immune cells. Since I previously determined that accumulation of senescence was accelerated in the absence of telomerase (*tert*$^{-/-}$), specifically in the cerebellum and diencephalon (see **Fig 4.6**), I then tested whether the increased percentage of immune cells was also TERT-dependent, in the same macroareas. To test this, I quantified the percentage of immune cells in each macroarea individually, in young (4-5 months) and old (9-17 months) *tert*$^{-/-}$, and compared with young (4-5 months), middle aged (9-17 months) and old (>30 months) WT fish. Immune cells were identified and counted as previously described (see *sections 2.2.2* and *2.2.5*).

The results showed that all the macroareas of the brain presented an increased percentage of immune cells with natural ageing, more specifically at >30 months of age (Tel: p=0.005, OT: p=0.002, Die: p=0.017, Ce: p=0.001, MO: p=0.005) (**Fig 5.2A-E**). The region with the higher number of immune cells was the medulla oblongata, followed by the optic tectum and diencephalon. Moreover, increased number of immune cells in the aged brain was not accelerated in the absence of Tert, as no differences were detected between WT and *tert*$^{-/-}$ model in any of the macroareas, at 4-6 months (Tel: p=0.999; OT: p=0.999; Die: p=0.999; Ce: p=0.999; MO: p=0.692) or at 9-17 months of age (Tel: p=0.999, OT: p=0.607; Die: p=0.622; Ce: p=0.215; MO: p=0.444).

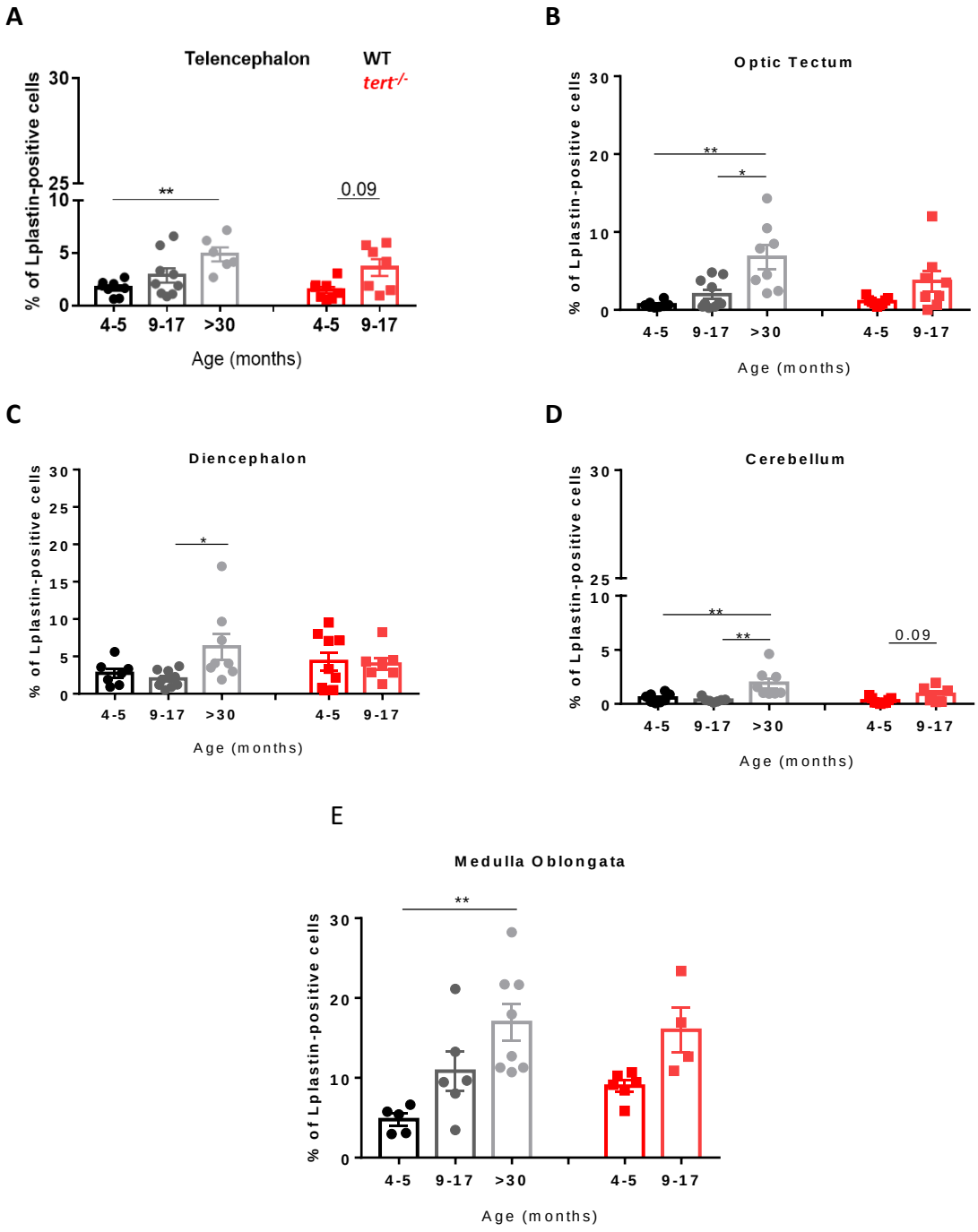


**Fig 5.2. Increased percentage of immune cells in the ageing brain is not explained by any specific macroarea of the brain.** Quantifications of L-plastin-positive cells in the different macroareas of the brain: **(A)** telencephalon, **(B)** optic tectum, **(C)** diencephalon, **(D)** cerebellum, **(E)** medulla oblongata. Graphs: X-axis, age in months; Y-axis, % of L-plastin-positive cells. N=4-9 per group. Each dot represents one animal. Error bars represent the SEM. Statistics: two-way ANOVA test was used to compare WT versus *tert*$^{-/-}$ at 4-5m versus 9-17m. Non-parametric Kruskal-Wallis followed by Dunn's post-hoc test was used to analysis WT over-time. * $p<0.05$; ** $p<0.01$; *** $p<0.001$.

### 5.2.2 Measuring the number of microglia/macrophages in the WT and *tert*$^{-/-}$ aged brain

Although no correlation was identified between location of general immune cells (L-plastin$^{+}$ cells) and senescent cells, I cannot exclude the possibility that there may be a subpopulation of immune cells associated with senescence. Therefore, I decided to look at specific immune cell populations. Microglia are known to be important for CNS immune surveillance and clearance. Therefore, I set out to test whether there is increased number of microglia/macrophages, specifically, in the ageing brain, and whether this is accelerated in the absence of telomerase.

To differentiate microglia/macrophages from other immune cells in the brain (e.g. neutrophils, T-cells, B-cells), the *mpeg-mcherry.caax* immune reporter line was used. Anti-RFP antibody was used to detect the mpeg-positive cells by IF, as described in *section 2.3.2*. To test the specificity of the anti-RFP antibody, cells were co-labelled with anti-LCP1 (L-plastin) and anti-RFP antibody. As shown in **Fig 5.3**, only a subpopulation of L-plastin-positive cells express *mpeg*, showing that the anti-RFP antibody detects only microglia/macrophages in the *mpeg-mcherry.caax* immune reporter line. This thus allowed the distinction between microglia/macrophages and other immune cell types.

The results showed that increased number of immune cells in the ageing brain is primarily due to an increased number of microglia/macrophages rather than other immune cell populations. This is because I detected an increased number of L-plastin-positive; mpeg-positive cells (p=0.049, **Fig 5.4A, B**), but not of L-plastin-positive; mpeg-negative cells (p=0.086, **Fig 5.4A, B'**), in the whole brain of naturally aged zebrafish. Furthermore, this increase in microglia/ macrophages is accelerated in the absence of TERT. Specifically, in the *tert*$^{-/-}$ brain the number of L-plastin-positive; mpeg-positive cells at the age of 4-5 months was already higher than its WT counterparts (p=0.009).

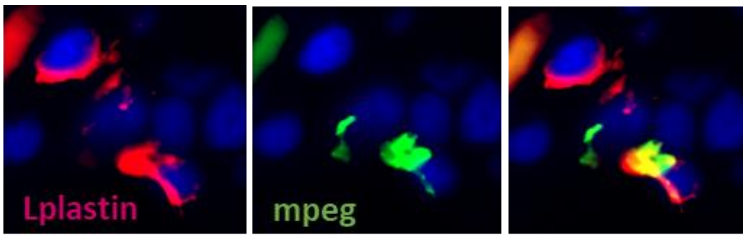


**Fig 5.3. Testing the anti-RFP antibody by IF.** Representative images of cells co-labelled with anti-LCP1 (L-plastin) and anti-RFP antibodies.

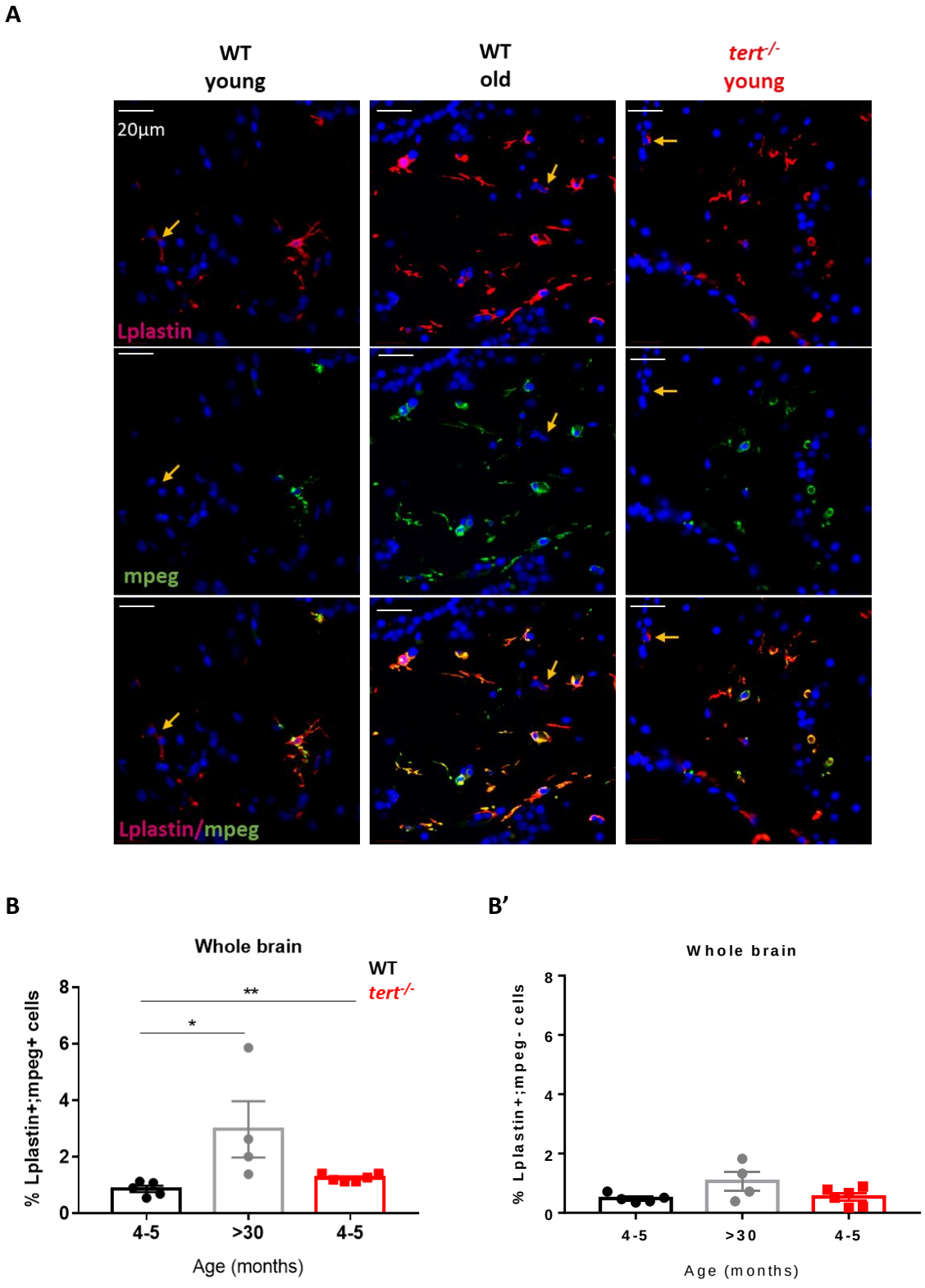


**Fig 5.4. Increased percentage of immune cells in the ageing (whole) brain is associated with increased number of mpeg-positive cells**. **(A)** Representative images of mpeg and L-plastin staining in the diencephalon of adult zebrafish. The yellow arrow highlights a Lplastin$^{+}$; mpeg$^{-}$ cell. **(B)** Quantifications of L-plastin-positive; mpeg-positive cells and **(B')** L-plastin-positive; mpeg-negative cells in the whole zebrafish brain. N=3-6 per group. Each dot represents one animal. Error bars represent the SEM. Unpaired t-tests: * p<0.05; ** p<0.01; *** p<0.001.

Next, I sought to test whether the increased number of microglia/macrophages (L-plastin-positive; mpeg-positive cells) in the ageing brain is occurring in the same regions where I previously detected cellular senescence (diencephalon and cerebellum). When looking at each macroarea individually, the results showed an increased percentage microglia/ macrophages in natural ageing in the telencephalon (p=0.016), optic tectum (p=0.017), cerebellum (p=0.057) and medulla oblongata (p=0.021) but not in the diencephalon (p=0.109) **Fig 5.5A-E**). Furthermore, there was no significant difference in the percentage of microglia/ macrophages in the young (4-5 months) *tert*$^{-/-}$, when compared to its WT counterpart, in the telencephalon (p=0.227), optic tectum (p=0.161) and cerebellum (p=0.792). However, I observed a higher number of microglia/ macrophages in the *tert*$^{-/-}$ model at 4-5 months of age, when compared with its WT counterpart, particularly in the diencephalon (p=0.044) and medulla oblongata (p=0.011).

On the other hand, there was no change in the percentage of L-plastin-positive; mpeg-negative cells (which would represent all immune cells apart from microglia/ macrophages) with natural ageing in the telencephalon (p=0.185), optic tectum (p=0.08), diencephalon (p=0.266) or cerebellum (p=0.09) (**Fig 5.6A-D**). Only the medulla oblongata showed a slight increase in the number of L-plastin-positive; mpeg-negative cells over-time, borderline significant (p=0.046) (**Fig 5.6E**). Moreover, no differences were detected between WT and *tert*$^{-/-}$ at 4-5 months in any of the macroareas analysed (Tel: p=0.861; OT: p=0.167; Die: p=0.779; Cer: p=0.345; MO: p=0.656).

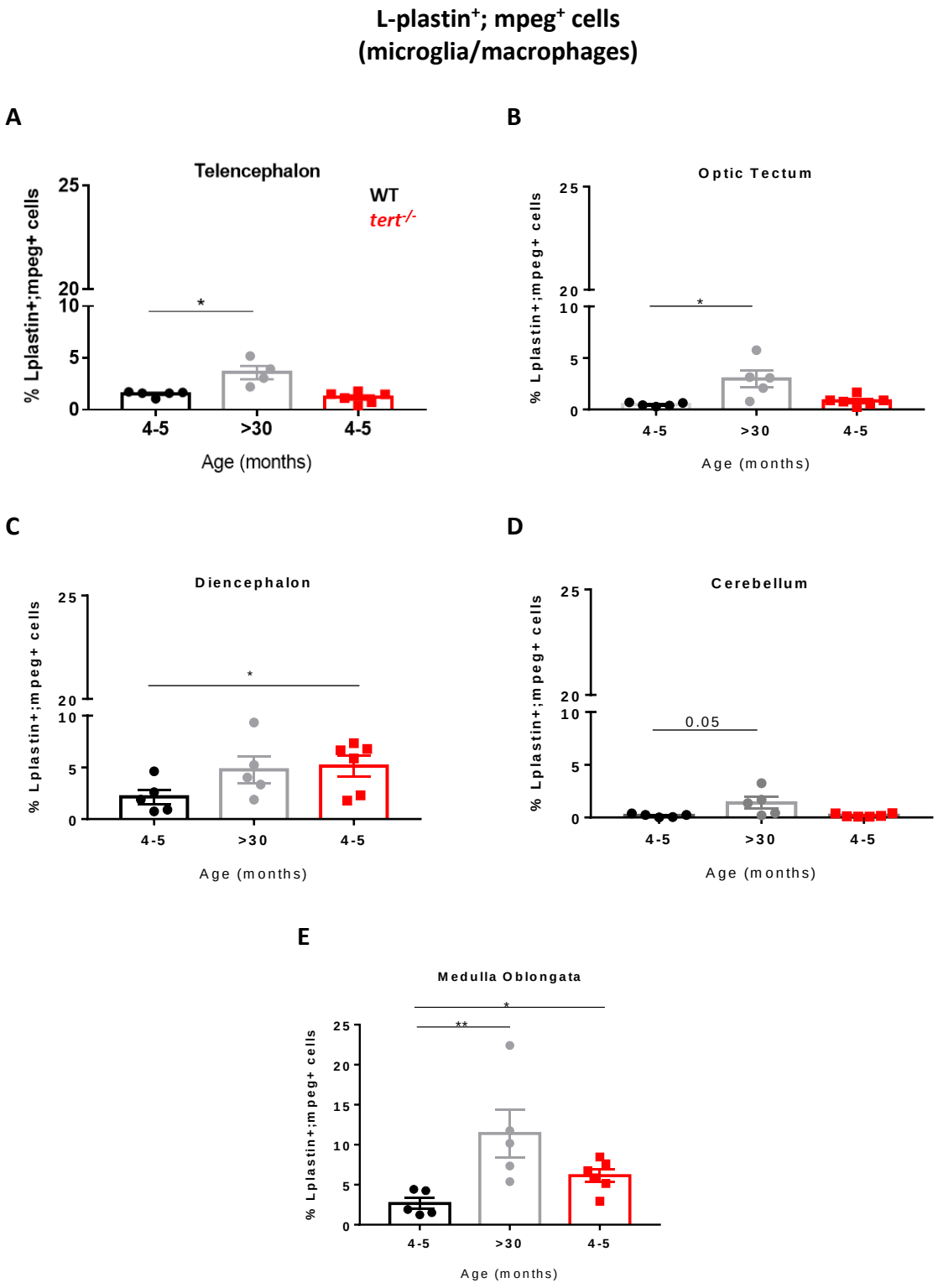


**Fig 5.5. Percentage of L-plastin$^{+}$; mpeg$^{+}$ cells in the aged zebrafish brain.** Quantifications of L-plastin; mpeg cells in the **(A)** telencephalon, **(B)** optic tectum, **(C)** cerebellum, **(D)** diencephalon, and **(E)** medulla oblongata. N=3-6 per group. Each dot represents one animal. Error bars represent the SEM. Unpaired t-tests (**B, C, E**) or Mann Whitney (**A, D**) test: * p<0.05; ** p<0.01; *** p<0.001.

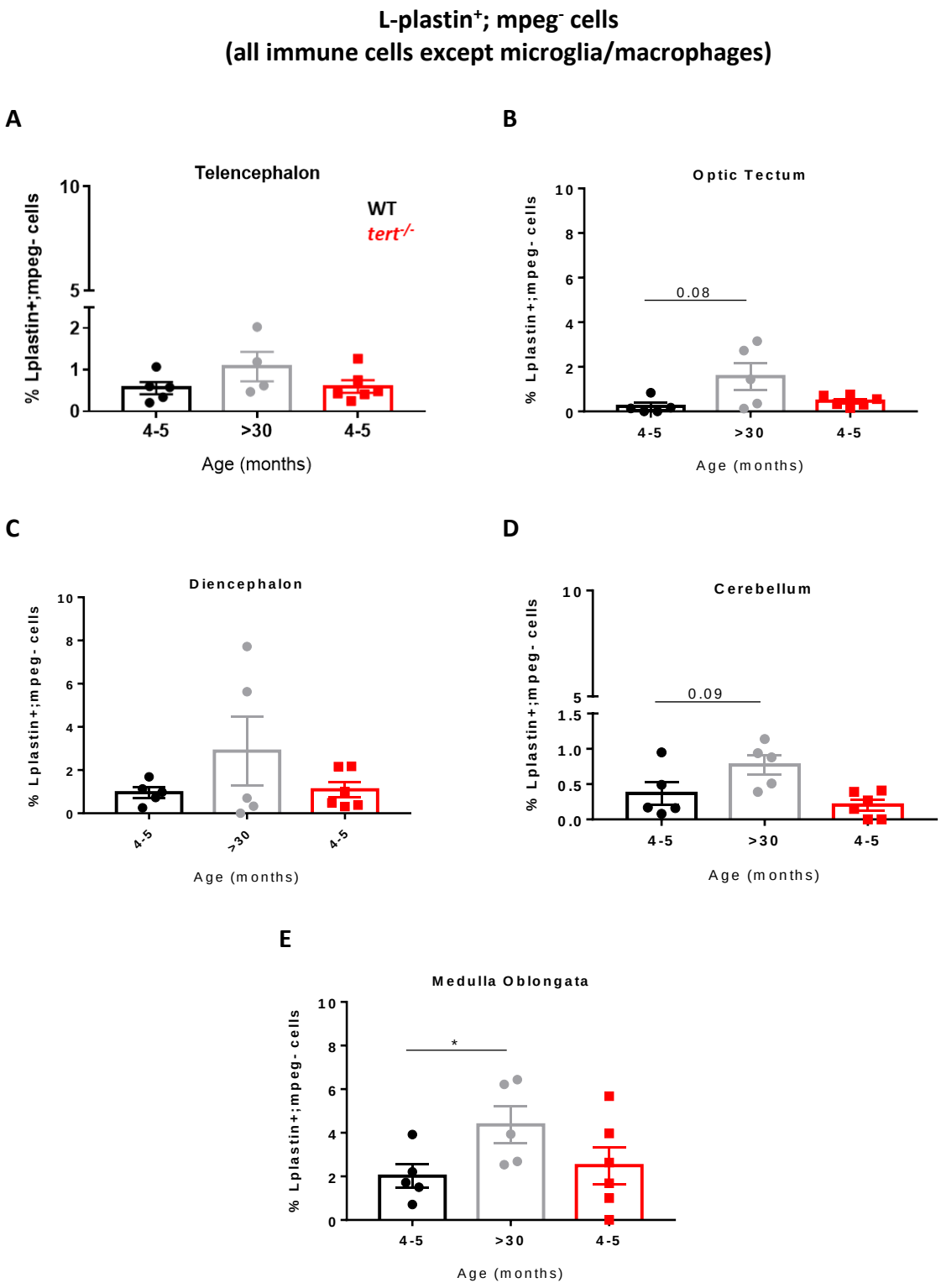


**Fig 5.6. Percentage of L-plastin$^{+}$; mpeg$^{-}$ cells in the aged zebrafish brain.** Quantifications of L-plastin$^{+}$; mpeg$^{-}$ cells in the **(A)** telencephalon, **(B**) optic tectum, **(C)** cerebellum, **(D)** diencephalon, and **(E)** medulla oblongata. N=3-6 per group. Each dot represents one animal. Error bars represent the SEM. Unpaired t-tests (**A, C, D, E**) or Mann Whitney (**B**) test: * p<0.05; ** p<0.01; *** p<0.001.

Altogether, these data suggest that the increased number of immune cells in the ageing brain is associated with an increased number of microglia/ macrophages (mpeg-positive cells) in all the macroareas. Nonetheless, there are other immune cell populations apart from microglia/ macrophages that are contributing, at least in part, to the increased number of immune cells in the ageing medulla oblongata and, to a lesser extent, the ageing cerebellum. Additionally, these data suggest that there is no correlation between the location of senescent cells and mpeg-positive immune cells (microglia/macrophages) or mpeg-negative immune cells (e.g. neutrophils, T-cells).

Interestingly, the increased number of immune cells in the natural ageing brain does not seem to be explained by increased proliferation of these cells, since I did not observe any differences in the number of immune cells proliferating over-time in any of the brain macroareas (Tel: p=0.428, OT: p=0.581, Die: p=0.874, Ce: p=0.403, MO: p=0.378) (**Fig 5.7**). Furthermore, there was also no difference in the proliferation of immune cells in the absence of TERT, in most of the macroareas, as no differences were identified between WT and *tert*$^{-/-}$ at 4-5 or 9-17 months of age, in the telencephalon (4-5m, p=0.954; 9-17m,p=0.999), optic tectum (4-5m, p=0.999; 9-17m,p=0.658), cerebellum (4-5m, p=0.999; 9-17m,p=0.999) or diencephalon (4-5m, p=0.999; 9-17m,p=0.999). The medulla oblongata was an exception to this. Whilst no differences between genotypes were identified at 4-5 months of age (p=0.999), at 9-17 months of age *tert*$^{-/-}$ presented higher number of proliferating immune cells than its counterpart WT (p=0.0001).

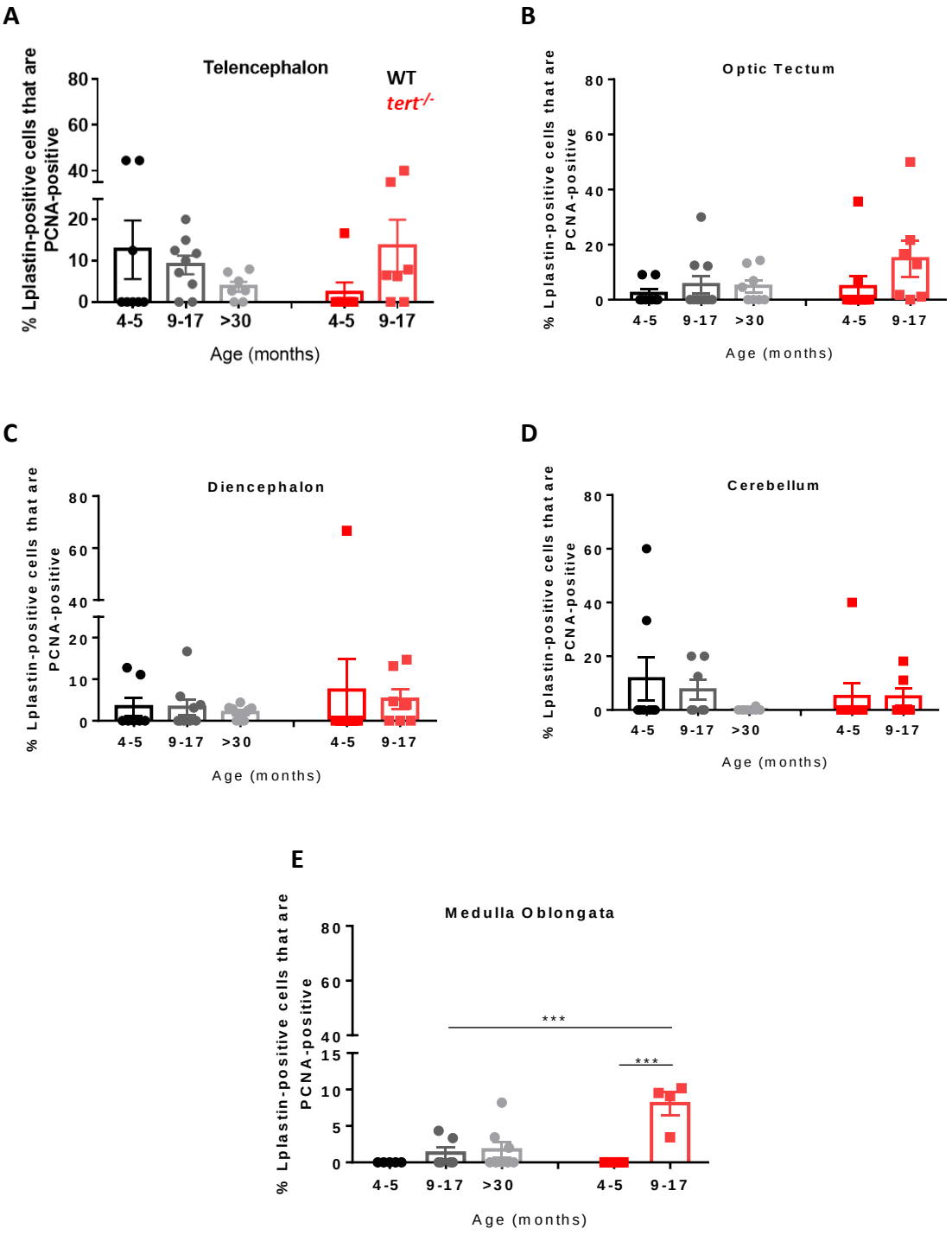


**Fig 5.7. Percentage of immune cells proliferating with ageing, in the different brain macroareas.** Quantification of L-plastin-, PCNA-positive cells in the different macroareas of the brain: **(A)** telencephalon, **(B)** optic tectum, **(C)** diencephalon, **(D)** cerebellum, **(E)** medulla oblongata. Graphs: X-axis, age in months; Y-axis, % of L-plastin-positive that are proliferating (PCNA-positive). N=4-10 per group. Each dot represents one animal. Error bars represent the SEM. Statistics: two-way ANOVA test was used to compare WT versus *tert*$^{-/-}$ at 4-5 versus 9-17 months. Non-parametric Kruskal-Wallis followed by Dunn's post-hoc test was used to analysis WT over-time. * $p<0.05$; ** $p<0.01$; *** $p<0.001$.

### 5.2.3 Measuring chitotriosidase activity in the WT and *tert*$^{-/-}$ aged brain

Inflammation is not only characterised by increased number of immune cells but also by increased immune activation. Therefore, then I set out to test whether there is increased immune activation in the ageing brain and whether this is accelerated in the absence of telomerase. To do this, chitotriosidase activity was measured in the whole WT and *tert*$^{-/-}$ brain at different time-points, as described in *section 2.7.3*. Chitotriosidase is an enzyme expressed by activated macrophages and other phagocytic cells and therefore it is a good biomarker of microglia/macrophages activation.

In this experiment, the glucocerebrosidase 1 deficient (*GBA*$^{-/-}$) zebrafish model was used as a positive control. This is a model that presents a mutation in the *glucocerebrosidase 1* gene (Keatinge et al., 2015), leading to Gaucher's disease. This disease is a lysosomal storage disorder, characterised by extremely high levels of chitotriosidase activity, making it a good reference model for extremely high level of chitotriosidase.

The results showed increased chitotriosidase activity over-time in the naturally aged brain, identified at >30 months of age ($p=0.005$, **Fig 5.8**). Although no differences in chitotriosidase activity were identified between WT and *tert*$^{-/-}$ at the age of 5 months ($p>0.999$), *tert*$^{-/-}$ animals at the age of 14-16 months presented higher chitotriosidase activity than their WT counterparts ($p=0.008$).

Overall, the data suggest that there are increased levels of chitotriosidase in the naturally aged brain and that this is accelerated in the absence of telomerase. Interestingly, although there is increased chitotriosidase activity with ageing in both WT and *tert*$^{-/-}$, the maximum activity detected is ≈40% lower than in the *GBA*$^{-/-}$.

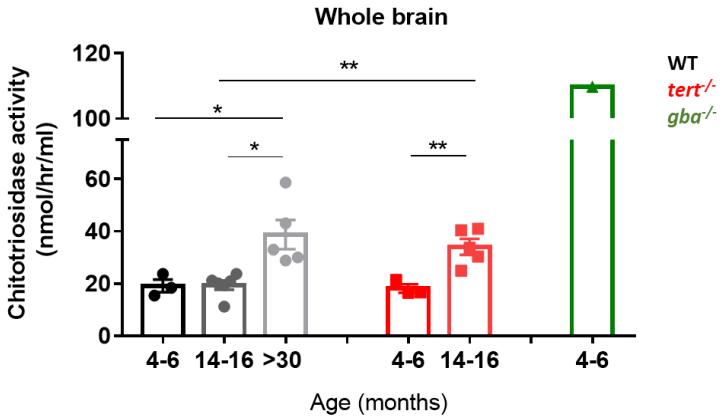


**Fig 5.8. Chitotriosidase activity in the whole brain.** Graphs: X-axis, age in months; Y-axis, chitotriosidase activity in nmol/h/ml, analysed as described in *section 2.7.3*. Statistical analysis: WT versus *tert*$^{-/-}$ of 4-6 versus 14-16 months of age were analysed by two-way ANOVA followed by planned comparisons with Bonferroni corrections. Additionally, one-way ANOVA was performed to compared WT over-time, including >30 months of age. N=3-6 *per* group. Each dot represents one animal. Bar errors represent the SEM. * <0.05; ** <0.01; *** <0.001.

## 5.3 Assessment of BBB permeability in WT and *tert*$^{-/-}$ aged zebrafish brain

As shown in **Fig 5.5** and **Fig 5.7**, I previously identified increased number of immune cells in the ageing zebrafish brain, which is not explained by increased proliferation of immune cells. Hence, I then tested whether infiltration of peripheral immune cells in the aged brain could explain the increased number of immune cells observed. Immune cells should not cross the BBB and invade the brain in a healthy condition unless the BBB is compromised. I therefore sought out to test the BBB integrity in young and old zebrafish. It has been described that zebrafish presents a functional BBB from the 10$^{th}$ dpf (Fleming et al., 2013), from which age molecules such as horseradish peroxidase (HRP, 44,000Da), evans blue (961Da), and sodium fluorescein (376Da) do not cross this barrier (Fleming et al., 2013; Jeong et al., 2008). However, it remained unknown whether zebrafish BBB becomes leaky with ageing. Here, a BBB permeability assay was performed in both WT and *tert*$^{-/-}$ at the ages where increased number of immune cells were identified in the brain, >30 months and 14-17 months, respectively. As described in *section 2.8.1*, in this assay I used an infrared fluorescent dye (0.1% IRDye 680RD Dextran diluted in HBSS), injected by IP. This dye had never been tested in zebrafish before and therefore I firstly tested if this compound is suitable to test BBB permeability in adult zebrafish: if it spreads easily throughout the body after IP injection, reaching the brain; and if it is quantifiable in an accurate way.

First, I performed a pilot study where I used the IRDye 680RD Dextran (fluorescent dye) conjugated with two molecules of different weights: 70kDa and 4kDa. In order to detect the fluorescent dextran, live fish were anaesthetised and imaged at several time-points after IP injection (30min, 1h, 2h, 3h). After an incubation period of 3h, the fish were culled, and the bodies were imaged in order to test for the presence of the dextran dyes. As shown in **Fig 5.9**, the 4kDa dextran (in green) was detected in the 800 channel while the 70kDa dextran (red) was detected in the 700 channel. The 4kDa dextran spread throughout the body in 30min, becoming stronger 3h after IP injection. The 70kDa dextran was only identified in the peritoneal area 30min after injection and, although it spread slowly during the 3h period, it did not reach the head in all the animals. If the dye does not spread well throughout the body to reach the brain, it does not constitute a good tool to test BBB permeability. Therefore, the 4kDa dextran was considered a better tool to test BBB permeability and chosen to do so.

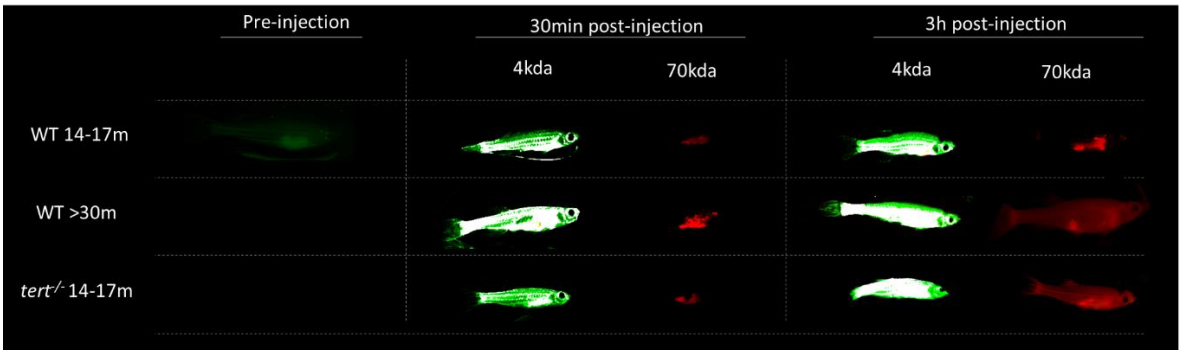


**Fig 5.9. Pilot experiment showing whole-body fluorescence after IP injection of 4kDa and 70kDa dextran.** Whole-body fluorescence before IP injection, and 30min and 3h after IP injection with 4kDa (green) and 70kDa (red) dextran, in WT and *tert*$^{-/-}$ at different ages.

To test BBB permeability, animals were injected with 4kDa, by IP. Three hours after injection, the fish were culled, the brains dissected and the fluorescence in the brains was measured to assess the BBB permeability. The results showed increased dextran-associated fluorescence in the naturally aged zebrafish brain at >30 months, when compared to 14-17 months brains (p=0.0001) (**Fig 5.10**). Importantly, the fluorescence levels at >30 months, but not at 14-17 months, were significantly higher than the age-matched vehicle control animals (experimental vs vehicle control group, at 14-17m: p=0.161; at >30m: p<0.001). In the *tert*$^{-/-}$ model, there was a small increase in fluorescence at 14-17 months when compared to their WT counterparts, but this did not reach statistical significance (p=0.08). Nevertheless, 14-17 months old *tert*$^{-/-}$ brains already presented higher levels of dextran-associated fluorescence when compared to the age-matched vehicle control animals (p=0.046).

These findings suggest that there is increased BBB permeability in the naturally aged brain, at >30 months of age, and that this is accelerated in the *tert*$^{-/-}$, where BBB disruption is detected at 14-17 months of age. Furthermore, the results suggest that increased BBB permeability occur at the same age or at a later age as increased number of microglia/macrophages and elevated chitotriosidase activity is observed (at >30m in WT and 4-5m in *tert*$^{-/-}$).

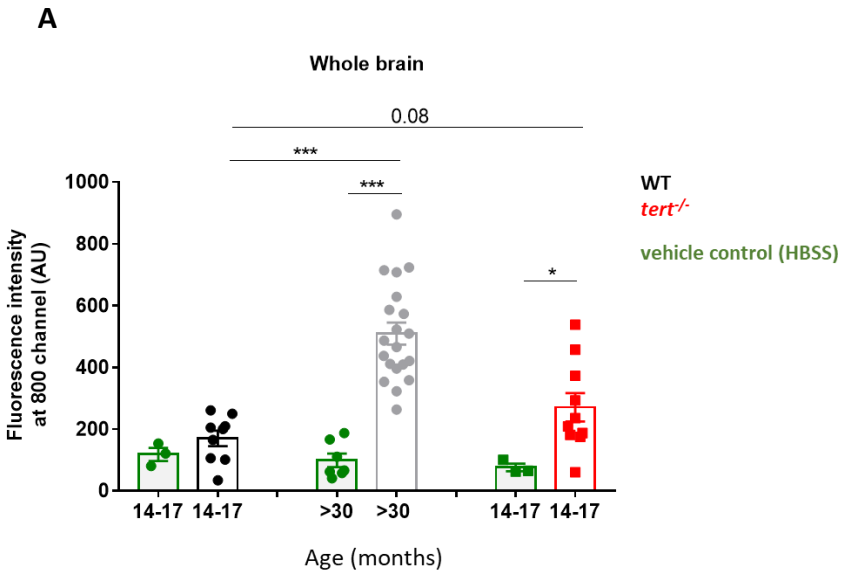


**Fig 5.10. BBB permeability in the zebrafish aged brain, in the presence and absence of telomerase. (A)** Whole brain fluorescence 3h after IP injection of 4kDa dextran, in WT and *tert*$^{-/-}$ at different ages. Graphs: X-axis, age in months; Y-axis, fluorescence intensity (AU). N=9-20 per group in the tested animals; N=3-6 per group in the vehicle control animals. Each dot represents one animal. Bar errors represent the SEM. Statistics: unpaired t-tests. * $p<0.05$; ** $p<0.01$; *** $p<0.001$.

## 5.4 Analysis of behavioural alterations in the WT and *tert*$^{-/-}$ aged zebrafish

It is known that both ageing and inflammation can influence behaviour. For example, natural ageing has been reported to be accompanied by several behavioural alterations in both mammals and fish, including reduced locomotion and impairment of memory and learning abilities (Altun et al., 2007; Shoji et al., 2016; Yu et al., 2006). Moreover, lipopolysaccharide (LPS)-induced peripheral inflammation has been shown to lead to behavioural alterations in rodents, in a dose-dependent manner, including decreased locomotion activity and increased anxiety-like behaviour (Bassi et al., 2012; Tarr et al., 2012; Zhu et al., 2019). Therefore, I set out to test whether there are age-related behavioural alterations in zebrafish at the same age as it is identified increased inflammation. Locomotion, anxiety-like behaviour and short-term memory were assessed, as described in *sections 2.8.1* and *2.8.2*.

Locomotion behaviour was assessed through an open-field test. The results showed decrease distance swam by WT fish at the age of >30 months (versus 14-17 months, p=0.018) (**Fig 5.11**). These findings suggest that zebrafish present reduced locomotion behaviour with ageing, more specifically at the age when increased inflammation and BBB permeability are identified. If TERT were to have a protective effect towards impaired locomotion, then removing TERT would further exacerbate or accelerate this behavioural dysfunction. To test this, I determined locomotion behaviour of *tert*$^{-/-}$ fish in parallel to WT counterparts. However, I found no significant differences between WT and *tert*$^{-/-}$ at 14-17 months of age (p=0.473).

Anxiety-like behaviour was assessed by the open-field and novel object tests. The open field test showed that, with ageing, WT fish tend to spend more time in the central area of the tank (14-17 versus >30m: p=0.009) (**Fig 5.12A**). Similarly, with ageing, fish spent more time near the object during the novel object test (14-17 versus >30m: p=0.014), (**Fig 5.12B**). Increased time spent in the central area of the tank and/or exploring the novel object suggest decreased anxiety-like behaviour with natural ageing. Interestingly, there was a trend for the *tert*$^{-/-}$ fish to display decreased anxiety-like behaviour at 14-17 months when compared with their WT counterpart, in both tests performed (OF: p=0.091; NO: p=0.072). However, this did not reach statistical significance.

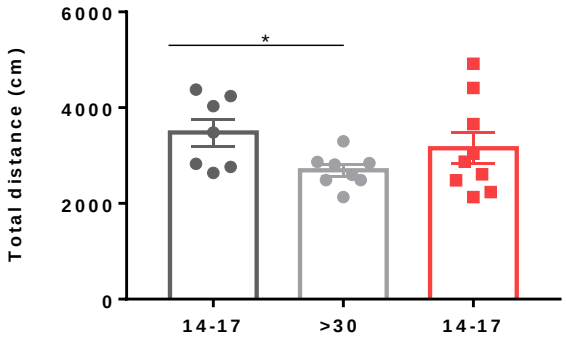


**Fig 5.11. Alterations in locomotion with ageing, in WT and *tert*$^{-/-}$ zebrafish.** Distance moved (cm) over-time in the WT and *tert*$^{-/-}$, accessed by OF test and analysed as described in *section 2.9.2*. N=7-9. Bar errors represent the SEM. Unpaired t-tests: * p<0.05; ** p<0.01; *** p<0.001

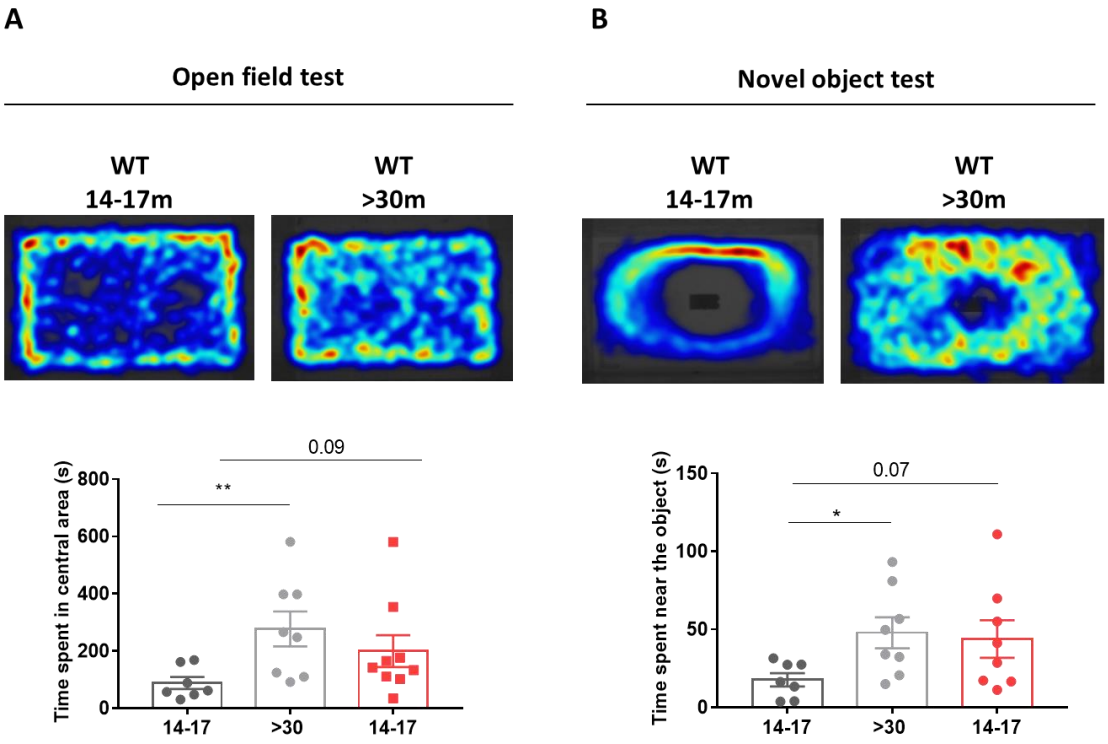


**Fig 5.12. Alterations in anxiety-like behaviour with ageing, in the presence and absence of telomerase. (A)** Anxiety-like behaviour assessed by OF test. Top: heatmap representing young vs old fish locomotion in the tank throughout the OF test**.** Bottom: time spent (s) in the central area of the tank, over-time, in the WT and *tert*$^{-/-}$ **(B)** Anxiety-like behaviour assessed by NO test. Top: heatmap representing young vs old fish locomotion in the tank throughout the NO test**.** Bottom: time spent (s) near the novel object, over-time, in the WT and *tert*$^{-/-}$ N=7-9. Bar errors represent the SEM. Mann-Whitney tests: * p<0.05; ** p<0.01; *** p<0.001

Short-term memory was assessed through a novel object recognition test. To test whether WT can discriminate between two objects to start with, as a baseline control, I tested whether young (4-6 months) WT fish display a preference for one of the objects. The data showed that the young WT tend to prefer the novel object, but this was just below statistical significance (p=0.078) (**Fig 5.13**). This suggests that WT fish are able to discriminate, at least partially, the two objects. With ageing, WT fish animals seem to lose this potential ability to discriminate between objects, as no preference was identified in middle aged or old WT groups (14-17m: p=0.094; >30m: p=0.313). The inability to discriminate the two objects at old ages, compared with young ages, would suggest reduced short-term memory with ageing. However, as it was not identified any statistically significant preference in the WT young fish, the results are inconclusive. Nevertheless, this non-statistically significant trend is accelerated in the absence of TERT, which display no preference already at young ages (p=0.297), warranting further investigation with a larger number of animals.

Overall, these data suggest that zebrafish display age-associated reduced locomotion and decreased anxiety-like behaviour. Nonetheless, it is unclear whether this is accompanied by cognitive impairment. Despite the great variability observed in *tert*$^{-/-}$ behaviour, the results suggest that anxiety-like behaviour might be, at least partially, affected by the absence of TERT.

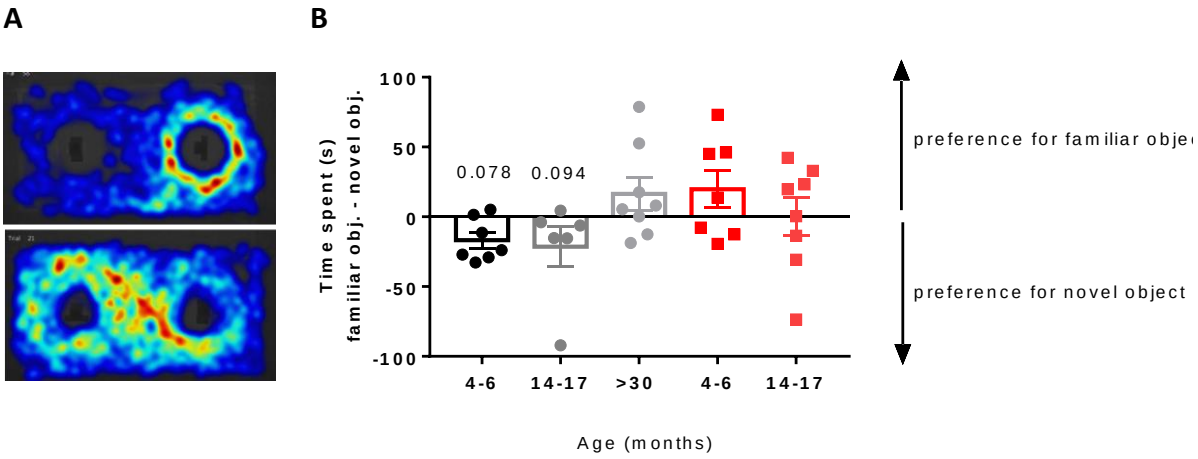


**Fig 5.13. Results from the NOR test. (A)** Heatmaps illustrating the locomotion of the fish during the test phase of the NOR test, when the fish discriminate the objects (top) and when it does not (bottom). **(B)** Assessment of object discrimination during the first 5 min of test phase, as described in *section 2.9.2*. N=6-8. Bar errors represent the SEM. Statistics: wilcoxon signed-ranked test against the hypothetical value of 0. * p<0.05; ** p<0.01; *** p<0.001

## 5.5 Assessing potential TERT-associated mechanisms of ageing in the zebrafish brain

My results so far show that the zebrafish brain accumulates cellular senescence with ageing and that this is accelerated in the absence of telomerase. Thus, I next set out to explore which TERT-associated molecular mechanisms could be associated with the ageing process in the brain, and how these mechanisms could be linked to cellular senescence. In order to test this, I performed RNA Sequencing in whole brain tissue from WT and *tert*$^{-/-}$ adult zebrafish, at different time-points throughout their lifespan, more specifically at the ages of 2, 9, 22 and >30 months in WT, and at the ages of 2, 9 and 22 months in *tert*$^{-/-}$ fish.

The first analysis of the RNA Sequencing data revealed a Q30-score (probability of having a wrong nucleotide is 1:1,000) of 92%, with all samples presenting a total of 14.4-17.3 million reads. In order to observe the distribution of the samples *per* age and genotype, a quality assessment was performed with unsupervised methods, including heatmap and principle component analysis (PCA). Both the heatmap (**Fig 5.14A**) and the PCA (**Fig 5.14B**) showed that different ages form individual clusters, suggesting that there are differences in gene expression with ageing. This was particularly visible in the WT at >30 months of age, the group with the greatest distance to all the other clusters. Whilst no obvious clusters were identified between WT and *tert*$^{-/-}$ fish at the ages of 9 or 22 months, at 2 months of age the two genotypes presented two distinguished clusters, with the 2 months old *tert*$^{-/-}$ samples being closer to the 9 months of age samples.

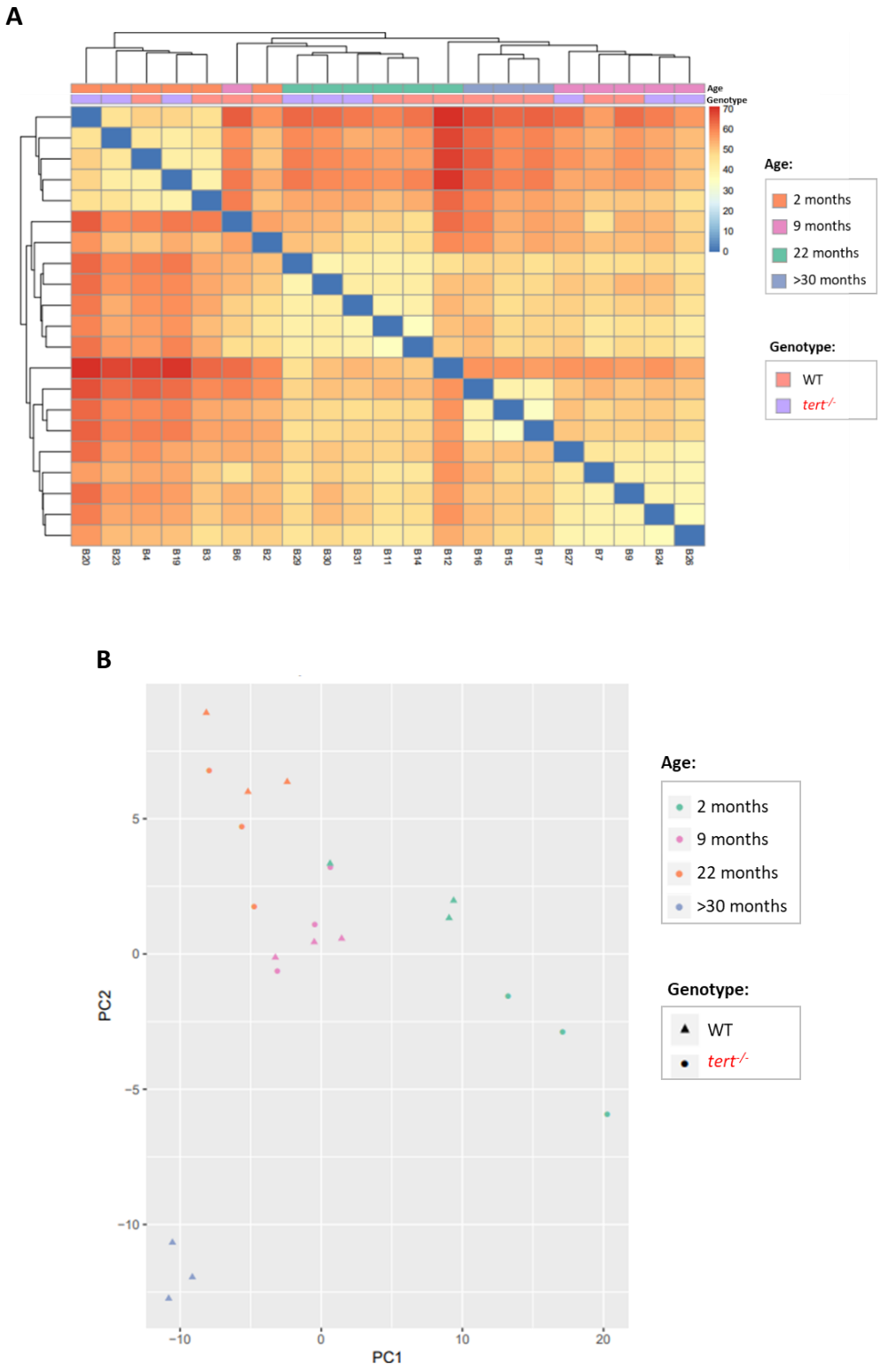


**Fig 5.14. Quality assessment of the RNA Sequencing data, using unsupervised methods. (A)** Heatmap showing the clustering of all samples from WT and *tert*$^{-/-}$ fish at different ages. **(B)** PCA representing the sample distribution by genotype (WT and *tert*$^{-/-}$) and age.

### 5.5.1 RNA Sequencing analysis of the aged brain, in the WT versus *tert*$^{-/-}$

In order to identify which genes are being up- and down- regulated over-time in a consistent way (i.e. constantly being up/down-regulated over-time), time-series analysis was performed using the STEM software, as described in *section 2.6*. This analysis was performed in each group separately: brain WT and brain *tert*$^{-/-}$.

Time-series analysis of the whole WT brain identified 11 different profiles with a total of 1,447 differentially expressed genes with ageing (**Fig 5.15A**). Within those, 6 profiles clustered a total of 645 up-regulated genes and 5 profiles grouped a total of 1,551 down-regulated genes. After identifying the differentially expressed genes in the ageing zebrafish brain, enrichment analysis was performed in order to test which functions these genes were associated with.

Enrichment analysis was performed as described in *section 2.6.* The results showed that the up-regulated genes were mostly associated with regulation of the immune system and immune response (**Fig 5.15B**). Within those, there were genes associated with antigen processing and presentation of peptide antigen via major histocompatibility complex (MHC) class I (GO: 0002474, enrichment: 25.183), leukocyte migration (GO: 0050900, enrichment: 4.197), regulation of cytokine production (GO: 0001817, enrichment: 4.361) and interleukin-1 family signalling (R:DRE-446652, enrichment: 6.769). Down-regulated genes, on the other hand, were mainly associated with proliferation and DNA repair (**Fig 5.15C**), including genes associated with cell cycle process (GO: 0022402, enrichment: 6.868), cell division (GO: 0051301, enrichment: 5.864), and double-strand break repair via break-induced replication (GO: 0000727, enrichment: 38.239).

**A**

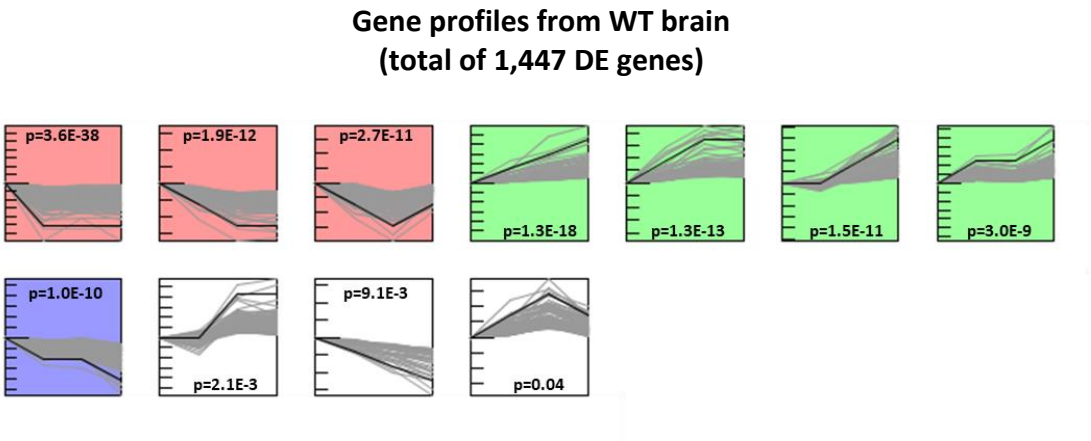


**B**

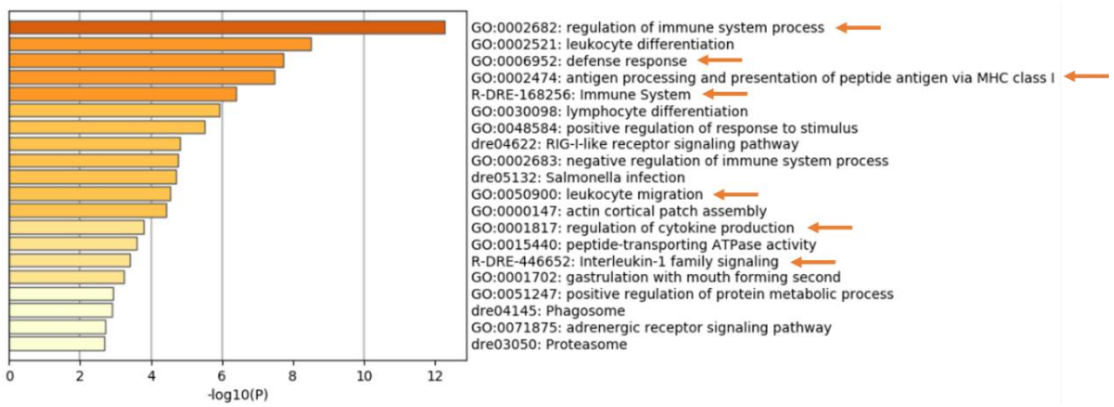


**C**

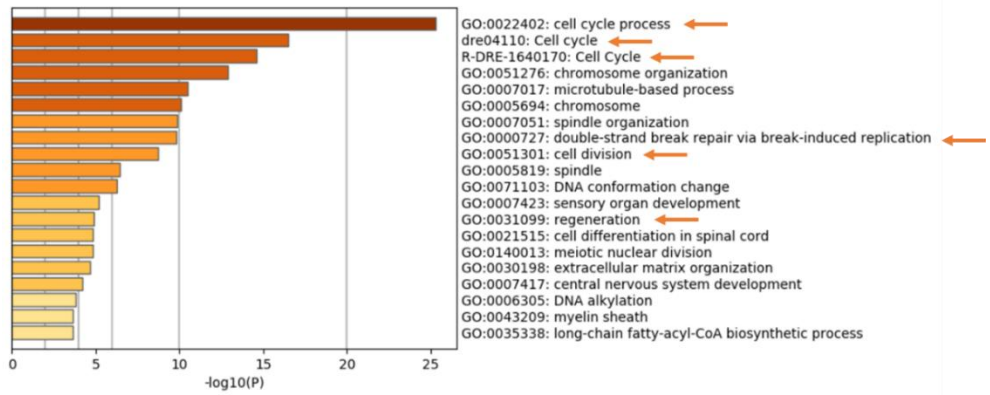


**Fig 5.15. Time-series and enrichment analysis in the whole WT brain, throughout the zebrafish life-course. (A)** Profiles with DE genes in the ageing WT brain, obtained after time-series analysis using STEM software, as described in *section 2.6*. Values were normalised for the 2 months time-point. Each colour represents a cluster of genes. **(B-C)** Enrichment analysis of **(B)** up- and **(C)** down-regulated genes in the natural aged brain. Enrichment analysis was performed using the Gorilla and Metascape software, and the graphs were generated by last software, as described in *section 2.6*. In the graphs, terms are ordered by log10(P). Orange arrows are highlighting the terms and/or pathways associated with immune response, proliferation, DNA repair and mitochondrial function.

In the absence of TERT, time-series analysis identified 4 different profiles of differentially expressed genes over-time, which included a total of 2,392 genes (**Fig 5.16A).** Half of the profiles consisted in a total of 841 up-regulated genes whereas the other half consisted in 1,551 down-regulated genes. Enrichment analysis showed that up-regulated genes were mostly related with immune response and mitochondria function (**Fig 5.16B**). These included regulation of innate immune response (GO: 0045089, enrichment: 8.0003), p38MAPK cascade (GO: 0038066, enrichment: 22.918), TNF receptor superfamily members mediating non-canonical NF-kB pathway (R-DRE-5676594, enrichment: 11.459) and nicotinamide adenine dinucleotide (NAD) : ubiquinone oxidoreductase (M00142, enrichment: 13.096). On the other hand, down-regulated genes were mostly associated with proliferation (**Fig 5.16C**), including functions such as mitotic cell cycle (GO:0000278, enrichment: 4.952), cell division (GO: 0051301, enrichment: 4.011) and regeneration (GO: 0031099, enrichment: 3.904).

**A**

**Gene profiles from *tert*$^{-/-}$ brain (total of 2,392 DE genes)**

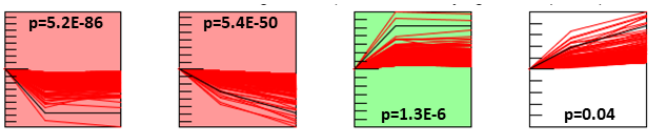


**B**

**Up-regulated genes in the ageing *tert*$^{-/-}$ brain (total of 841 DE genes)**

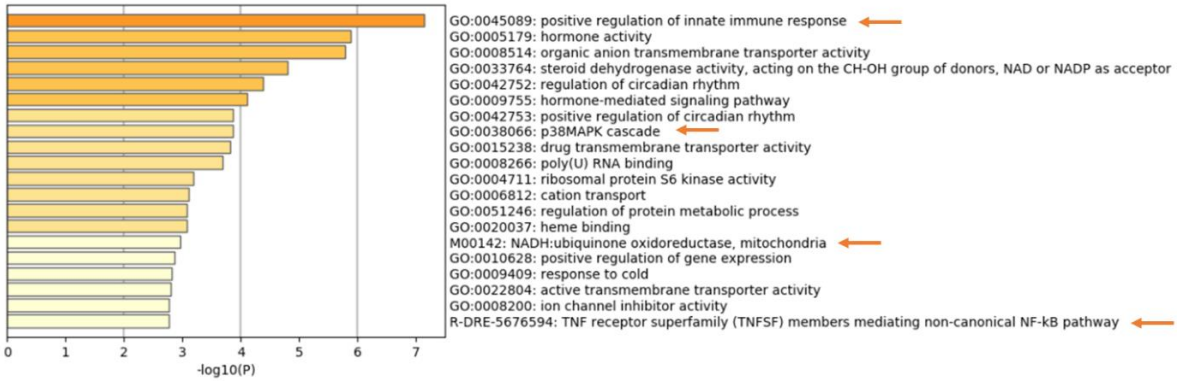


**C**

**Down-regulated genes in the ageing *tert*$^{-/-}$ brain (total of 1,551 DE genes)**

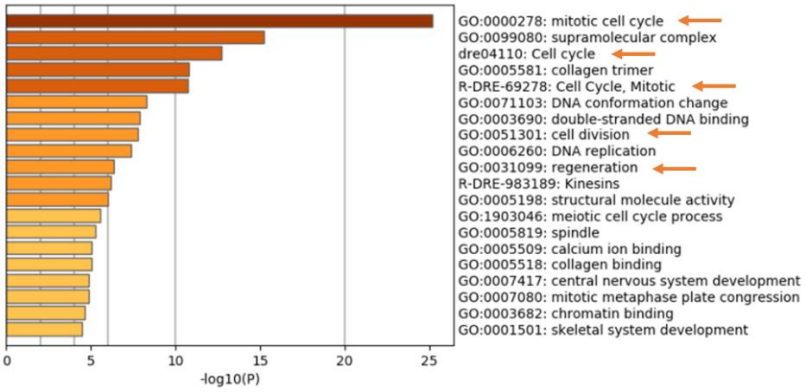


**Fig 5.16. Time-series and enrichment analysis in the whole *tert*$^{-/-}$ brain, throughout the zebrafish life-course.(A)** Profiles with DE genes in the ageing *tert*$^{-/-}$ brain, obtained after time-series analysis using STEM software, as described in *section 2.6*. Values were normalised for the 2 months time-point. Each colour represents a cluster of genes. **(B-C)** Enrichment analysis of **(B)** up- and **(C)** down-regulated genes in the natural aged brain. Enrichment analysis was performed using the Gorilla and Metascape software, and the graphs were generated by last software, as described in *section 2.6*. In the graphs, terms are ordered by log10(P). Orange arrows are highlighting the terms and/or pathways associated with immune response, proliferation, DNA repair and mitochondrial function.

To further confirm the previous analysis, I used an alternative method to identify differentially expressed genes common to both genotypes, WT and *tert*$^{-/-}$. These would likely represent TERT-dependent mechanisms. This analysis was performed after identifying the common genes being up- and down- regulated in both genotypes, after time-series analysis.

The results showed that there were 151 genes being up-regulated and 191 genes being down-regulated in both genotypes over-time (**Fig 5.17A**). Enrichment analysis of these genes revealed similar results as the previous ones. Whilst most of the up-regulated genes were associated with immune response (**Fig 5.17B**), most of the down-regulated genes are associated with cell cycle and DNA repair (**Fig 5.17C**).

**A**

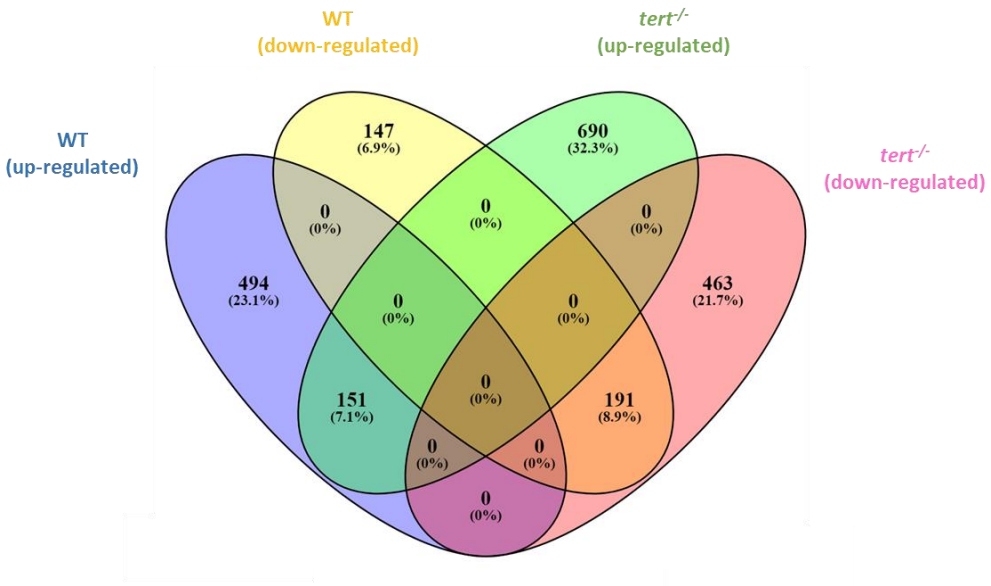


**B**

**Up-regulated genes in the ageing brain, in both WT and *tert*$^{-/-}$**

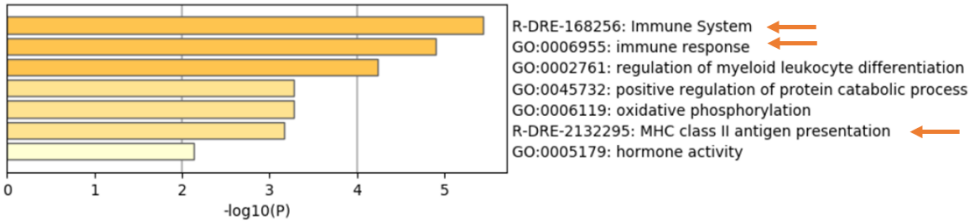


**C**

**Down-regulated genes in the ageing brain, in both WT and *tert*$^{-/-}$**

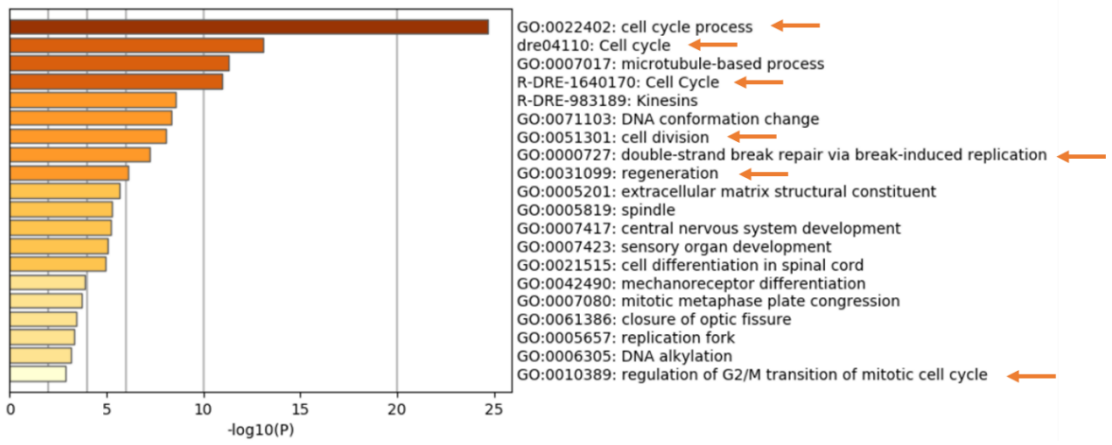


**Fig 5.17. Venn-diagram showing DE genes in the whole brain of WT and *tert*$^{-/-}$ zebrafish, and enrichment analysis of DE genes with ageing, common to both WT and *tert*$^{-/-}$ genotypes. (A)** Venn diagram showing the up- and down- regulated genes in both WT and *tert*$^{-/-}$ ageing brain. **(B-C)** Enrichment analysis of **(B)** up- and **(C)** down-regulated genes over-time, common to both genotypes. Venn diagram and enrichment analysis were performed as described in *section 2.6*.

#### 5.5.1.1 Network analysis in the WT versus *tert*$^{-/-}$ aged brain

Previously I identified the genes being consistently up- and down-regulated in the ageing brain, in the presence and absence of TERT. On one hand, the up-regulated genes in both WT and *tert*$^{-/-}$ ageing were mainly associated with immune response, supporting my previous findings that there is TERT-dependent increased number of immune cells and immune activation in the aged brain. On the other hand, the down-regulated genes in both genotypes are associated with proliferation capacity and DNA repair, which goes in hand with the previous observations that there is TERT-dependent accumulation of DNA damage and decreased proliferation in the ageing brain. Considering this, I then sought to determine which set of genes could be associated with TERT-dependent ageing that could potentially contribute to accumulation of senescence and/or inflammation in the ageing brain.

To do this, I performed network analysis on the DE genes previously identified by time-series analysis. Network analysis was performed as described in *section 2.6*. In order to identify small and strong networks, from all the up- or down-regulated genes, the 10 genes with the highest number of connections (or edges) were considered a tight, strong network. The connections between genes are recognised by the software based on the identification of previous experiments, online databases, co-expression, proximity in the genome and/or co-occurrence in publications. This approach was chosen because the genes with the highest number of connections are putative key players in the whole network, influencing and/or being influenced by many other genes. Of note, other approaches were tested, including analysis per clusters and analysis per functions (enrichment terms) (data not shown). Moreover, the data was also analysed considering up- and down-regulated genes together or separately. All the different analysis had similar results and therefore the first approach was considered consistent and appropriate to use.

Within the over-expressed genes with natural ageing, in the brain, I identified a set of genes with a total of 21 edges between them (**Fig 5.18A**). Consistently with the previous findings, all these genes were associated with immune response. Accordingly, proteasome activator complex subunit 2 (psme2), proteasome subunit beta type-8 (psmb8) and rac family small GTPase 1 (rac1l) are associated with MAPK6/MAPK4 signalling (DRE-5687128, FDR=0.00013) as well as with the AKT signalling (DRE-1257604< false discovery rate, FDR=0.0008). psme2, psmb8 and cluster of differentiation 40 (CD40) are associated with

tumour necrosis factor receptor 2 (TNFR2) non-canonical NF-kB pathway (DRE-5668541, FDR=0.00013). Moreover, psme2, psmb8, together with beta-2-microglobulin like (b2ml) and beta-2-microglobulin (b2m) seem to be involved in cytokine signalling (DRE-1280215, FDR=0.00013).

A more strongly connected network was identified within the genes being down-regulated with natural ageing, where the 10 genes formed a total of 45 edges between them (**Fig 5.18B**). All the genes from this network were associated with cell cycle and mitosis process. Indeed, budding uninhibited by benzimidazoles 1 (bub1), polo-like kinase 1 (plk1), mitotic arrest deficient 2 like-1 (mad2l1), cyclin a2 (ccna2), cell division cycle 20 (cdc20), cyclin dependent kinase 1 (cdk1) and cyclin b1 (ccnb1) are all associated with cell cycle (DRE-04110, FDR=1.31E-13).

In the *tert*$^{-/-}$ model, within the up-regulated genes I detected a network with 23 edges (**Fig 5.18C**). A large number of these genes was associated with antigen processing, involving ubiquitination and proteasome degradation (DRE-983168, FDR=1.05E-08). These included ankyrin repeat and couple suppressor of cytokine signalling (SOCS) box containing 4 (asb4), ankyrin repeat and SOCS box containing 15b (asb15b), ankyrin repeat and SOCS box containing 1 (asb1), ring finger and CHY finger domain containing protein 1 (rchy1), F-box protein 32 (fbxo32) and zinc finger and BTB domain-containing 16b (zbtb16b or LOC569773).

Importantly, the network identified within the down-regulated genes in *tert*$^{-/-}$ was quite similar to the one previously identified in natural ageing, with only one different node (ccnb2 instead of ccna2) (**Fig 5.18D**). Like what I found in natural ageing, the majority of these genes were associated with cell cycle and proliferation (DRE-04110, FDR=9.17E-14). These included mad2l1, cdk1, bub1, plk1, cdc20, ccnb1 and cyclin b2 (ccnb2).

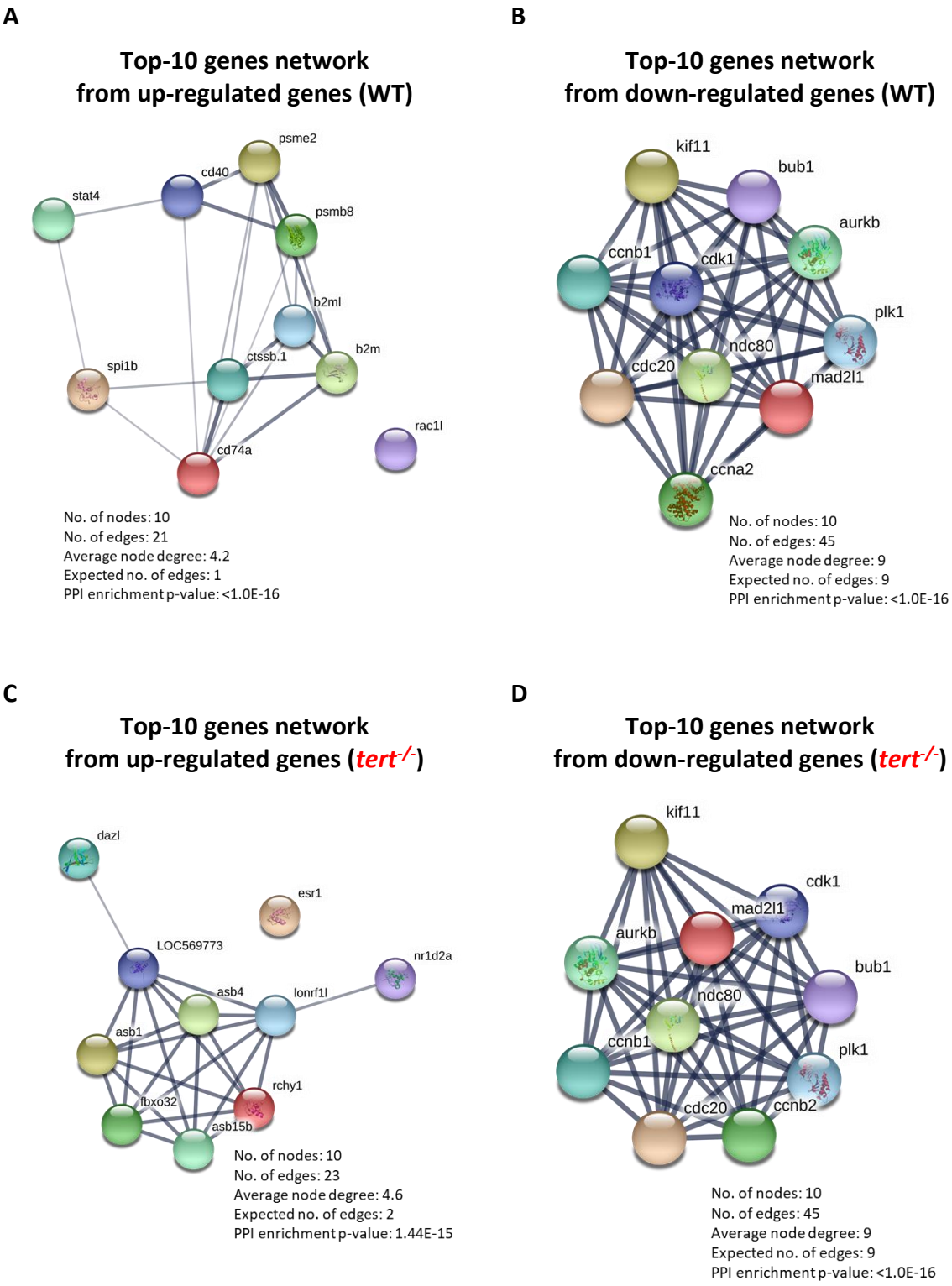


**Fig 5.18. Network analysis of the DE genes identified in the ageing zebrafish brain, in the presence and absence of TERT. (A-B)** Networks formed by the 10 genes with higher degree being: **(A)** up-regulated in natural ageing, **(B)** down-regulated in natural ageing, **(C)** up-regulated in the absence of TERT and **(D)** down-regulated in the absence of TERT. Networks were generated using the SRING software, as described in *section 2.6*. Thickness of the edges represents the confidence of the connections, with thicker stripes indicating that the evidence supporting it is stronger. Colour of the nodes do not have any meaning. PPI: protein-protein interaction.

#### 5.5.1.2 Analysing hand-picked senescence-associated genes in the ageing brain

When I had previously tested selected genes known to be senescence-associated markers, more specifically, known downstream effectors of the DNA damage response, I detected no differences with ageing. These included *p53*, *p21* and *p16-like* (see **Fig 4.5**). To confirm these results, I hand-picked these and other related genes from the RNA Sequencing data. To do this, Log2 values from young and old brains from WT and *tert*$^{-/-}$ fish were used to plot the heatmap.

The results showed only small, subtle changes in the expression of these genes with ageing, in both genotypes (**Fig 5.19**).

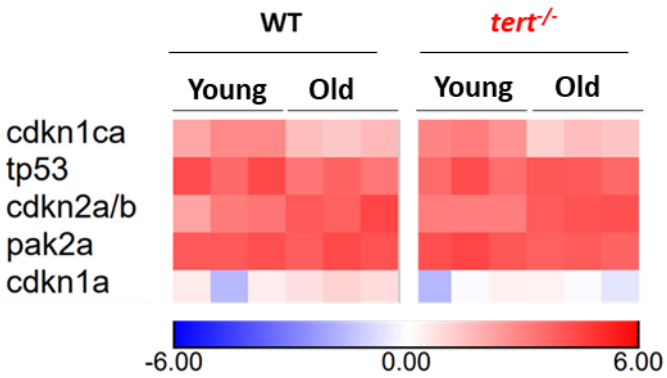


**Fig 5.19. Heatmap with hand-picked genes associated with senescence in young (2m) and old (>30m in WT, 23m in *tert*$^{-/-}$) whole brains.** Heatmap was generated using the Morpheus software: https://software.broadinstitute.org/morpheus/, using Log2 values.

## 5.6 Discussion

In this Chapter, I aimed to uncover some TERT-dependent mechanisms of ageing that could affect the zebrafish brain and contribute to accumulation of cellular senescence, which I showed to occur (see *Chapter 4*). Ultimately, this aimed to uncover some mechanisms that in the future could be further explored, aiming to develop targeted therapies for preventing or ameliorating cellular senescence in ageing. To do so, I firstly determined whether accumulation of cellular senescence in the aged brain was accompanied by increased inflammation in a telomerase-dependent manner. This was determined by measuring the number of immune cells as well as immune activation, in both WT and *tert*$^{-/-}$, at different ages. Secondly, I explored other potential TERT-dependent mechanisms of ageing affecting the zebrafish brain, through network analysis of RNA Seq data performed in whole brain of WT and *tert*$^{-/-}$ fish.

### The role of TERT in inflammation, in the aged zebrafish brain

This study identified an increased number of immune cells (L-plastin$^{+}$ cells) in the whole brain of old zebrafish; however, this was not accelerated in the *tert*$^{-/-}$ model, suggesting it to be telomerase-independent. Interestingly, though, I observed an increased number of microglia/ macrophages (Lplastin$^{+}$; mpeg$^{+}$ cells) in the brain, over-time, which was accelerated in the absence of TERT. Moreover, increased number of microglia/ macrophages with ageing was accompanied by increased levels of chitotriosidase activity, which again, was accelerated in the *tert*$^{-/-}$ in comparison to its WT counterpart. These findings are in agreement with the literature, as neuro-inflammation is a characteristic of the mammalian CNS (Popescu et al. 2016). Neuro-inflammation is known to involve increased number of microglia as well as increased immune activation, with ameboid-shaped microglia and increased levels of pro-inflammatory cytokines (Damani et al., 2011; Crowe et al., 2016). Similarly, two recent studies in zebrafish reported increased number of microglia/ macrophages in the aged brain, more specifically in the telencephalon and optic nerve (Van houcke et al., 2017; Zambusi et al., 2020). In the telencephalon, microglia were also shown to display an ameboid shape in the aged fish, suggesting to be more activated (Zambusi et al., 2020). Furthermore, chitotriosidase activity has been proposed as a putative marker of microglial/ macrophage

activation in mammals. In humans, increased levels of chitotriosidase activity have been reported to increase with normal ageing (in serum) (Ramanathan et al., 2013) and exacerbated in pathologies associated with chronic inflammation, including in ALS (in the spinal cord) (Steinacker et al., 2018). Hand in hand with the literature, the increased chitotriosidase activity identified in this project correlated with the increased number of microglia/macrophages.

Analysis per macroarea revealed that increased number of microglia/ macrophages with ageing occurs in the telencephalon, optic tectum, cerebellum, and medulla oblongata, but not in the diencephalon (**Table 5.1**). Nevertheless, it is important to mention that the lack of differences observed in the diencephalon may be due to the small sample size used. Power calculations showed that it would be required a minimum sample size of 22 animals to detect a 25% difference with 90% power between the groups. This experiment should therefore be repeated with more animals in order to strengthen the results. In addition, in comparison to the WT, increased number of microglia/ macrophages was only accelerated in the *tert*$^{-/-}$ in the diencephalon and medulla oblongata. If inflammation in the aged brain were associated with senescence, then I would expect to find increased number of immune cells in the same regions where I find accumulation of cellular senescence. Contrary to this prediction, the location of microglia/ macrophages does not correlate with location of senescence (see **Table 5.1**), suggesting that senescence is unlikely to be associated with increased number of microglia/ macrophages. Despite this and considering the unexpectedly insufficient sample sizes used in these experiments, it would be important to repeat these experiments with more animals to confirm the results.

**Table 5.1 Summary of the brain macroareas that accumulate senescence and increased number of immune cells with natural ageing and in the absence of TERT (in comparison with WT counterpart).** In WT, the age represents the time-point from which differences started being observed. In *tert*$^{-/-}$**,** the age represents the time-point where differences are detected in comparison with their WT counterpart. Age is represented in months. Tel: Telencephalon, OT: Optic tectum, Die: Diencephalon, Ce: Cerebellum, MO: Medulla oblongata.

| | **Senescence** | | **No. of L-plastin$^{+}$ cells** | | **No. of mpeg$^{+}$ cells** | |
|---|---|---|---|---|---|---|
| | **WT** | ***tert*$^{-/-}$** | **WT** | ***tert*$^{-/-}$** | **WT** | ***tert*$^{-/-}$** |
| Tel | - | - | ↑ >30m | - | ↑ >30m | - |
| OT | - | - | ↑ >30m | - | ↑ >30m | - |
| Die | ↑ >30m | ↑ 4-6m | ↑ >30m | - | - | ↑ 4-6m |
| Ce | ↑ >30m | ↑ 4-6m | ↑ >30m | - | ↑ >30m | - |
| MO | - | - | ↑ >30m | - | ↑ >30m | ↑ 4-6m |

It is interesting to note that the medulla oblongata was the macroarea with higher number of microglia/ macrophages. This is relevant because in *Chapter 4* I showed that the medulla oblongata was the region of the brain containing higher expression of SA-β-Gal. It remains unclear whether this is a real association between inflammation and senescence or if this reflects an artifact. This is because some immune cells, including macrophages, can express SA-β-Gal when activated (Hall et al., 2017). It would be important to confirm this by determining if most of the cells expressing SA-β-Gal staining are indeed immune cells (L-plastin$^+$ or mpeg$^+$ cells). I tried to test this by co-labelling cells with SA-β-Gal and anti-L-plastin antibody, in cryosections of the brain. Preliminary data (not shown) revealed that most of the L-plastin$^+$ cells are surrounding the blue staining, and not co-localising with it, suggesting that the immune cells are unlikely to be expressing SA-β-Gal themselves. Nonetheless, further experiments should confirm if this observation is real or if this represents an artifact. This is because in this experiment I did not test whether L-plastin staining would be affected by the incubation with X-gal, or vice-versa. To confirm this, I would need to use adjacent sections of the brain with the following staining conditions: (1) L-plastin; (2) SA-β-Gal, and (3) L-plastin and SA-β-Gal. If the distribution of immune cells and SA-β-Gal staining were identical in conditions 1 and 3 or in conditions 2 and 3, respectively, then I would be more confident about the results of this experiment. This extra test was not performed due to time constraints and lack of samples available.

As great part of the cranial nerves (with afferent and efferent innervations) are connected to the medulla oblongata, this macroarea is likely to affect and to be affected by peripheral tissues (see *section 5.6*). Assuming that the SA-β-Gal staining observed in the medulla oblongata is real cellular senescence, it would be plausible to hypothesise that inflammation in peripheral tissues may contribute to inflammation in this macroarea. In support of this hypothesis, it has been shown that peripheral inflammation (upon IP injection of TNFα or LPS) leads to increased inflammation in the brain. Moreover, this seems to occur through the vagus nerve, at least partially, as vagotomy or electric stimulation of this nerve decreased the inflammatory response in the brain (Bonaz et al., 2018; Meneses et al., 2016; Zielinski et al., 2013).

Additionally, it would be important to explore what accumulates first, if inflammation or cellular senescence, and whether one causes the other. One hypothesis is that immune cells

could be recruited to sites of cellular senescence, stimulated by SASP factors released by senescence cells themselves, based on what was previously described at wound site (Demaria et al., 2014). An alternative hypothesis is that the presence of pro-inflammatory factors in the environment could trigger cellular senescence, based on the evidences that SASP factors can lead to paracrine senescence (Acosta et al., 2013). As an example, it was recently shown in mice that macrophage-derived transforming growth factor β1 (TGFβ1) contributed to paracrine senescence and that inhibition of its receptor led to reduced accumulation of senescence (Bird et al., 2018).

## Possible routes for increasing number of immune cells in the aged brain

My results suggested that increased number of immune cells in the aged zebrafish brain was not associated with increased immune proliferation. Nonetheless, this was assessed in L-plastin$^{+}$ cells, representing all populations of immune cells. It remains unknown if microglia/ macrophages, specifically, increase their proliferation activity over-time. It would be important to assess proliferation levels specifically in microglia/ macrophages in order to confirm these results. This was not done in this project due to time constraints. Despite previous reports suggesting an increased number of microglia/ macrophages in the aged CNS in mammals and fish (Damani et al., 2011; Crowe et al., 2016; van houcke et al., 2017; Zambusi et al., 2020), the authors failed to clarify whether this were due to increased proliferation of this cell population. It is reasonable to hypothesise that immune proliferation contributes to it, at least partially, as increased microglial proliferation has been reported to occur in response to injury as well as in contexts where there is chronic damage, such as in AD and PD (Spittau, 2017). Moraga et al., (2015) have also reported higher microglial proliferation activity with ageing in a mice model of cerebral ischemia (Moraga et al., 2015). It remains unclear whether this reflects what happens in 'normal' ageing or if this observation is triggered by increased damage, in this case, due to permanent cerebral artery occlusion.

Apart from immune proliferation, there are other mechanisms that could contribute to the increased number of immune cells in the aged brain. The BBB constitutes a protective barrier between the blood and the CNS, avoiding the entrance of foreign molecules into the brain, including the entrance of peripheral immune cells. However, the BBB loses its integrity with

ageing (Pakulski et al., 2000), which can lead to the infiltration of peripheral immune cells in the brain (Deverman & Patterson, 2009). Moreover, the choroid plexus holds some populations of resident immune cells, mostly including T-cells and monocytes but also B-cells, dendritic cells and natural-killer cells (Meeker, et al., 2012). These resident immune cells are now thought to be able to invade the brain parenchyma, at least in response to inflammation (Strominger et al., 2018). Importantly, it has been described that with ageing auto-reactive T-cells (Coder et al. 2015) are capable of penetrating the brain, both through the bloodstream and lymphatic vessels (Louveau et al., 2015). These lymphatic-like vessels in the brain are in close contact with the meninges and carry cerebrospinal fluid as well as immune cells (Louveau et al., 2015). Additionally, circumventricular organs constitute another mechanism by which peripheral immune cells could invade the brain. These are brain structures that lack the classical BBB and display high permeability (Ganong, 2000), constituting vulnerable regions to the infiltration of large molecules and possibly, cells, into the brain parenchyma.

Therefore, increased number of immune cells in the aged brain is likely to be associated with the following mechanisms: (1) increased proliferation of immune cells, particularly of microglia; (2) recruitment of immune cells from the periphery, through the BBB; (3) crossing of resident immune cells from the cerebrospinal fluid (choroid plexus and meninges) into the brain parenchyma; and/or (4) infiltration of peripheral immune cells, through the circumventricular organs. Although the data found in this project does not support the first mechanism, it does support the second one. In fact, in this study I identified increased BBB permeability with natural ageing, in zebrafish, similarly to what has been reported to occur in mammals (Pakulski et al., 2000). Importantly, this project also identified that BBB permeability with ageing is accelerated in the absence of TERT. Thus, this project suggest that the increased number of immune cells found in the aged zebrafish brain might be due to BBB leakiness. The other potential mechanisms were not explored in this project.

## TERT-dependent mechanisms of brain ageing

In the second part of this Chapter, I explored other potential TERT-dependent mechanisms of ageing that may affect the zebrafish brain and that could be associated with accumulation of senescence. I did this through RNA Seq analysis of the whole zebrafish brain. The data

showed that most of the genes being up-regulated with ageing are associated with immune function, in both WT and *tert*$^{-/-}$. These observations strengthen my previous results showing that there is increased inflammation with ageing, in a telomerase-dependent manner. In addition, the data showed that most of the genes being down-regulated over-time are associated with proliferation and DNA repair, in both WT and *tert*$^{-/-}$. Once again, this strengthens the previous findings showing that there is increased DNA damage accompanied by decreased proliferation in the naturally aged brain (see *Chapter 4*). Moreover, in *Chapter 4* I had observed an accelerated accumulation of DNA damage in the *tert*$^{-/-}$, which goes hand in hand with the results obtained by RNA Seq. Despite this, reduced proliferation with ageing was not observed in the *tert*$^{-/-}$, which goes against the RNA Seq data. Further analysis showed that the experiment assessing PCNA staining by IF (*section 4.4.1*) was underpowered and it would be necessary a minimum of 12 animals per groups in order to detect any differences. Thus, it would be important to confirm this, by repeating the experiment by IF with a larger sample size and by analysing proliferation using an alternative technique, such as by RT-qPCR.

Furthermore, network analysis of differentially expressed genes in the ageing brain revealed that both genotypes have a set of 9 common down-regulated genes, with a very strong connection between them. These might be good candidates for TERT-dependent mechanisms of brain ageing and therefore it is important to further explore their potential roles on ageing. These genes include CDK1, bub 1, aurkb, plk1 mad2l1, ndc80, cdc20, ccnb1, and kif11, which are protein kinases involved in the regulation of different phases of mitosis, and therefore essential to maintain cell cycle and to secure chromosomal stability during cell division. To my knowledge, none of these genes have been associated with TERT; however, some of them are known to be associated with ageing.

Down-regulation of kif11 with ageing is not a zebrafish-specific phenotype, as reduced expression of this gene was recently identified in aged mice and humans. Although it is not known what the consequences of decreased expression of Kif11 are in aged mammals, the equivalent gene in *Caenorhabditis elegans* (*C. elegants*), Bim subfamily of kinesin-1 (bmk-1), has been shown to regulate lifespan. In *C. elegants*, inhibition of bmk-1 was shown to reduce lifespan, whereas over-expression of bmk-1 was shown to extend lifespan (Qian et al., 2015). It remains unknown whether reduced expression of kif11 also contributes to reduced lifespan in zebrafish and, if so, whether it occurs in a telomerase-dependent manner. Furthermore,

reduced levels of bub1 have been shown to contribute to age-related phenotypes, including accumulation of cellular senescence, being associated with shorter lifespan in mice (Baker et al., 2004). Not only senescent cells express low levels of bub1, but also silencing bub1 leads to premature senescence in both mice and human cells (Andriani et al., 2016; Gjoerup et al., 2007). Similarly to bub1, inhibition of aurkb, plk1 and mad2 have been reported to induce senescence in human cells, through a p53-dependent mechanism (Kim et al., 2013; Kim et al., 2011). It remains unknown whether TERT expression prevents and/or delays down-regulation of these genes in the aged zebrafish brain, and if so, whether it presents and/or delays senescence accumulation with ageing. My RNA Seq data suggests this to be the case; however, further experiments would be required to confirm this.

My RNA Seq data point to kif11, bub1, aurkb, plk1 and mad2 as potential TERT-dependent mechanisms of ageing affecting the zebrafish brain. In the future, it would be important to further explore this. To do so, firstly, it would be important to confirm the results from the RNA Seq using an alternative technique such as RT-qPCR. After confirmation, it would be important to test whether TERT expression regulates these genes. One way of testing this would be to cross mutants of these genes (i.e. kif11, bub1, aubkb, plk1 and mad2) with *tert*$^{-/-}$ fish, and then to assess whether the resultant mutants would display a worsened phenotype in comparison with the *tert*$^{-/-}$ (i.e. accelerated and/or exacerbated senescence and inflammation in the brain). A complementary way of testing this would be to rescue telomerase in the *tert*$^{-/-}$ model and measuring the expression of each target gene. Increased levels of the target genes after telomerase rescuing, in comparison with *tert*$^{-/-}$ alone, would suggest that TERT expression is involved in the regulation of these target genes. If this was to be confirmed, then further investigation would be necessary to explore what mechanisms of TERT regulate these genes.

## Conclusion

In summary, this Chapter shows that there is increased inflammation in the aged zebrafish brain, characterised by increased number of microglia/ macrophages and elevated levels of chitotriosidase activity. Moreover, this is accelerated in the *tert*$^{-/-}$ fish, suggesting that TERT

plays a protective role against accumulation of inflammation in the aged brain. Nonetheless, as the location of immune cells does not correlate with the location of cellular senescence, it remains unclear whether inflammation is associated with accumulation of senescence in the aged brain. Further investigation would be necessary to confirm this and to further determine whether inflammation causes cellular senescence or vice-versa. Additionally, RNA Seq analysis identified a tight cluster of genes being differentially expressed with ageing in both WT and *tert*$^{-/-}$, being potential TERT-dependent mechanisms of ageing. Hence, this work encourages further investigation to test the role of these genes in zebrafish ageing, aiming to unravel potential targets that can be used, in the future, to prevent or delay age-associated phenotypes including cellular senescence.

# Chapter 6.
# Comparing accumulation of senescence with ageing in high versus low proliferative tissues

## 6.1 Introduction

Since replicative senescence is linked to telomere shortening (Bodnar et al., 1998) and there is accelerated telomere erosion in tissues with higher cell turnover (Carneiro et al., 2016; Lee et al., 1998), high proliferative tissues are more likely to accumulate replicative senescence. In *Chapter 4*, I observed an accumulation of cellular senescence in the aged zebrafish brain, specifically in the diencephalon and cerebellum, which was anticipated in the absence of TERT (*tert*$^{-/-}$). It remained unclear whether, in comparison to the brain and within the same individual, high proliferative tissues display exacerbated and/or accelerated accumulation of cellular senescence and whether this accumulation is associated with telomere shortening (i.e. replicative senescence). This is relevant because understanding the mechanisms behind the accumulation of cellular senescence in different tissues may help to find more targeted therapies to prevent accumulation of senescent cells with ageing.

The gut is not only known to have a high proliferative capacity (Lee et al., 1998) but it is also known to accumulate cellular senescence and critically short telomeres with ageing, in zebrafish, in a telomerase-dependent manner (Carneiro et al., 2016; Henriques et al., 2013). However, accumulation of senescence in the aged zebrafish gut was never compared directly with the brain (i.e. in the same animals). Furthermore, determining whether accumulation of cellular senescence in the gut precedes the brain would be particularly interesting due to the recently discovered gut-brain axis (reviewed in Carabotti et al., 2015). If accumulation of senescence in the gut were to precede the brain, as expected, then it would be interesting to further explore whether this accumulation in the brain can somehow be influenced by the increased senescence in the gut, and which potential systemic mechanisms could be involved.

Thus, in this Chapter I set out to test whether there is accumulation of cellular senescence with ageing in the zebrafish gut, and whether this is accelerated in the absence of TERT (*tert*$^{-/-}$). More specifically, I aimed to determine whether accumulation of cellular senescence in the zebrafish gut precedes the brain, a low proliferative tissue. In order to do so, several senescence-associated markers were assessed by IHC and RT-qPCR, throughout WT and *tert*$^{-/-}$ zebrafish life-course. In order to make a directly comparison between high (i.e. gut) and low proliferative tissues (i.e. brain), cellular senescence in the gut was analysed in the same animals where I had assessed accumulation of senescence in the brain, in *Chapter 4*.

## 6.2 Assessing cellular senescence in the aged gut, in WT and *tert*$^{-/-}$ zebrafish

First, I sought to confirm that, in the animals in which I detected senescence in the brain, there is also accumulation of cellular senescence in the ageing gut, and whether this is accelerated in the absence of telomerase. To test this, several senescence-associated markers were analysed in young and old fish, in the presence (WT) and absence of TERT (*tert*$^{-/-}$).

Here, I measured the same senescence-associated markers previously assessed in the brain (see *Chapter 4*). These included expression of SA-β-Gal, DNA damage foci, key downstream effectors of γH2AX (p53, p21, p16 and cyclin g1) and proliferation, all associated with cellular senescence (Campisi & d'Adda di Fagagna, 2007; Dimri et al., 1995; van Deursen, 2014). Furthermore, relative telomere length was analysed *in situ,* to confirm that potential accumulation of cellular senescence in the gut is associated with telomere shortening and replicative cell exhaustion.

### 6.2.1 Measuring SA-β-Gal and DNA damage expression

In order to assess whether there is increased expression of SA-β-Gal in the ageing gut and whether this is accelerated in the absence of TERT, X-gal staining was performed in young (4-6 months) and old (>30 months) WT fish and compared with young *tert*$^{-/-}$ (4-6 months) fish. X-gal staining was performed as described in *section 2.4.2* and the percentage of blue areas was quantified as described in *section 2.4.4.*

Similarly to what was previously shown in the brain (*Chapter 4*), the chromogenic staining in the gut was only observed when the slices were incubated with X-gal solution (**Fig 6.1A**). Therefore, the blue staining observed seems to reflect the presence of galactosidase, as this enzyme is responsible for cleavaged of X-gal, which results in the blue colouration.

The results showed an increased percentage of SA-β-Gal-positive area in the gut with natural ageing ($p=0.0002$, **Fig 6.1B, C**). Moreover, in the *tert*$^{-/-}$ model there were already increased levels of blue staining in the gut at the young age of 4-6 months, in comparison to the WT of the same age ($p<0.0001$).

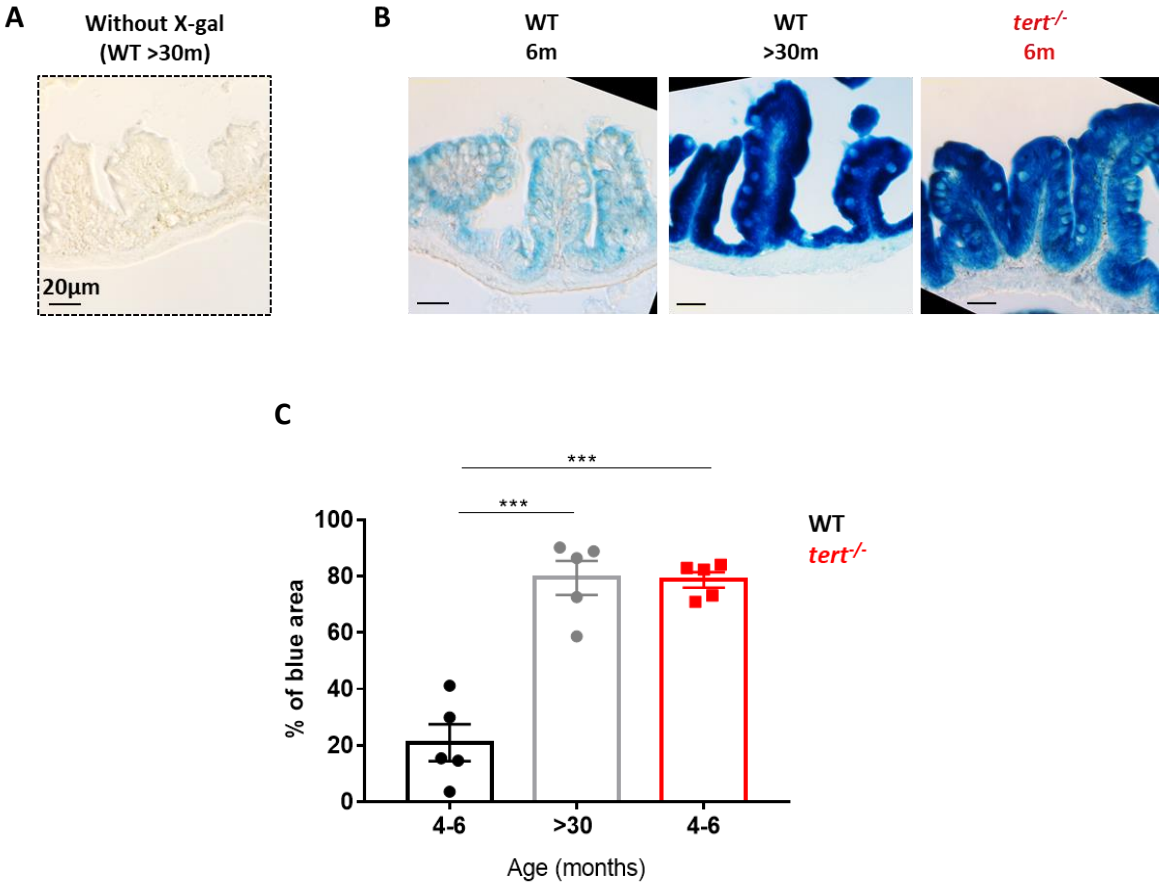


**Fig 6.1. SA-β-Gal expression in the zebrafish gut, with ageing, in the presence and absence of TERT.** **(A)** Representative image of the gut stained with solutions A and B but no X-gal solution (negative control). **(B)** Representative images of the SA-β-Gal staining (after staining with X-gal solution) in the gut of young (4-6 months) WT and *tert*$^{-/-}$, and old (>30 months) WT zebrafish. Scale bar: 20µm. **(C)** Quantifications of SA-β-Gal staining, in % of blue area, as described in *section 2.4.4*. Graphs: X-axis, age in months; Y-axis, % of blue area. N=5 per group. Each dot represents one animal. Error bars represent SEM. Unpaired t-test: * p<0.05; ** p<0.01; *** p<0.001.

In order to test whether accumulation of SA-β-Gal is accompanied by increased levels of DNA damage, DNA damage foci were measured in young (5-6 months), middle aged (12-17 months) and old (>30 months) WT fish, and compared with young (5-6 months) and old (12-17 months) *tert*$^{-/-}$ fish. To do this, I assessed γH2AX foci expression, by IF, as described in *section 2.3.2*. The percentage of cells containing >5 γH2AX foci in the zebrafish gut was then counted as described in *section 2.3.5*.

The results showed increased DNA damage with ageing in the WT gut ($p<0.001$), more specifically from 12-17 months onwards (5-6m vs 12-17m: $p=0.0013$; 5-6m vs >30m: $p=0.039$) (**Fig 6.2A, B**). Nonetheless, contrary to SA-β-Gal expression, no differences in DNA damage were identified between WT and *tert*$^{-/-}$ at 5-6 ($p=0.999$) or 12-17 months of age ($p=0.208$).

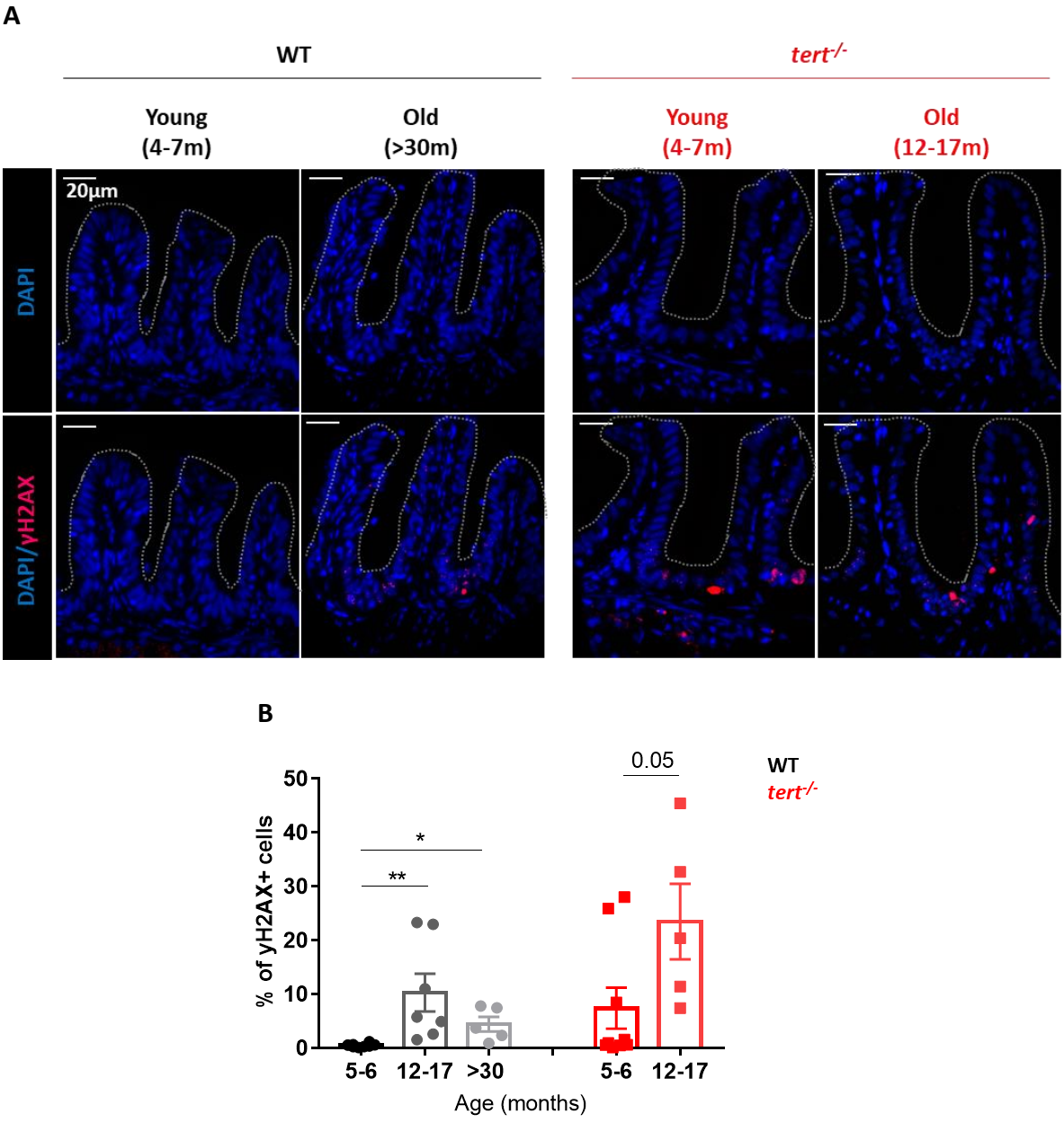


**Fig 6.2. DNA damage foci in the ageing zebrafish gut, in the presence and absence of TERT. (A)** Representative images of γH2AX staining by IF, in young (5-6 months) WT and *tert*$^{-/-}$, middle aged WT (12-17m), and old WT (>30 months) and *tert*$^{-/-}$ (12-17m) zebrafish gut. Scale bar: 20µm. **(C)** Quantification of the percentage of γH2AX$^{+}$ cells with ageing in the gut, as described in *section 2.3.7*. Graphs: X-axis, age in months; Y-axis, percentage of γH2AX$^{+}$. N=5-9 per group. Each dot represents one animal. Bar errors represent the SEM. Kruskal-Wallis (WT over-time) or two-way ANOVA (WT versus *tert*$^{-/-}$ at 5-6 versus 12-17m): * <0.05; ** <0.01; *** <0.001.

### 6.2.2 Measuring downstream effectors of γH2AX (*p53, p21, p16* and *cyclin g1*)

Given that I confirmed accumulation of DNA damage in the naturally aged gut, I then set out to measure gene expression of *p53*, *p21*, *p16* and *cyclin g1*, known to be key downstream effectors of γH2AX and markers associated with cellular senescence (Coppé et al., 2008; van Deursen, 2014). In order to determine whether there is differential expression of *p53*, *p21*, *p16* and *cyclin g1* with natural ageing, in the gut, and whether this is affected by TERT expression, the expression of these genes was measured in young (6-9 months) middle aged (22-24 months) and old (>30 months) WT fish, and compared with middle aged *tert*$^{-/-}$ (6-9 months) fish. To do so, RNA was extracted from the whole gut and mRNA expression of these genes was analysed by RT-qPCR, as described in *section 2.5.3*.

Similar to what was previously found in the brain (*Chapter 4*), no differences were detected in the expression of *p53* (p=0.832), *p21* (p=0.303), *p16-like* (p=0.629) and *cyclin g1* (p=0.695) in the natural aged gut (**Fig 6.3A-D**). Moreover, no differences were identified in the gut between WT and *tert*$^{-/-}$ at 6-9 months in any of the genes analysed (p53: p=0.240; p21: 0.714; cyclin g1: p=0.381).

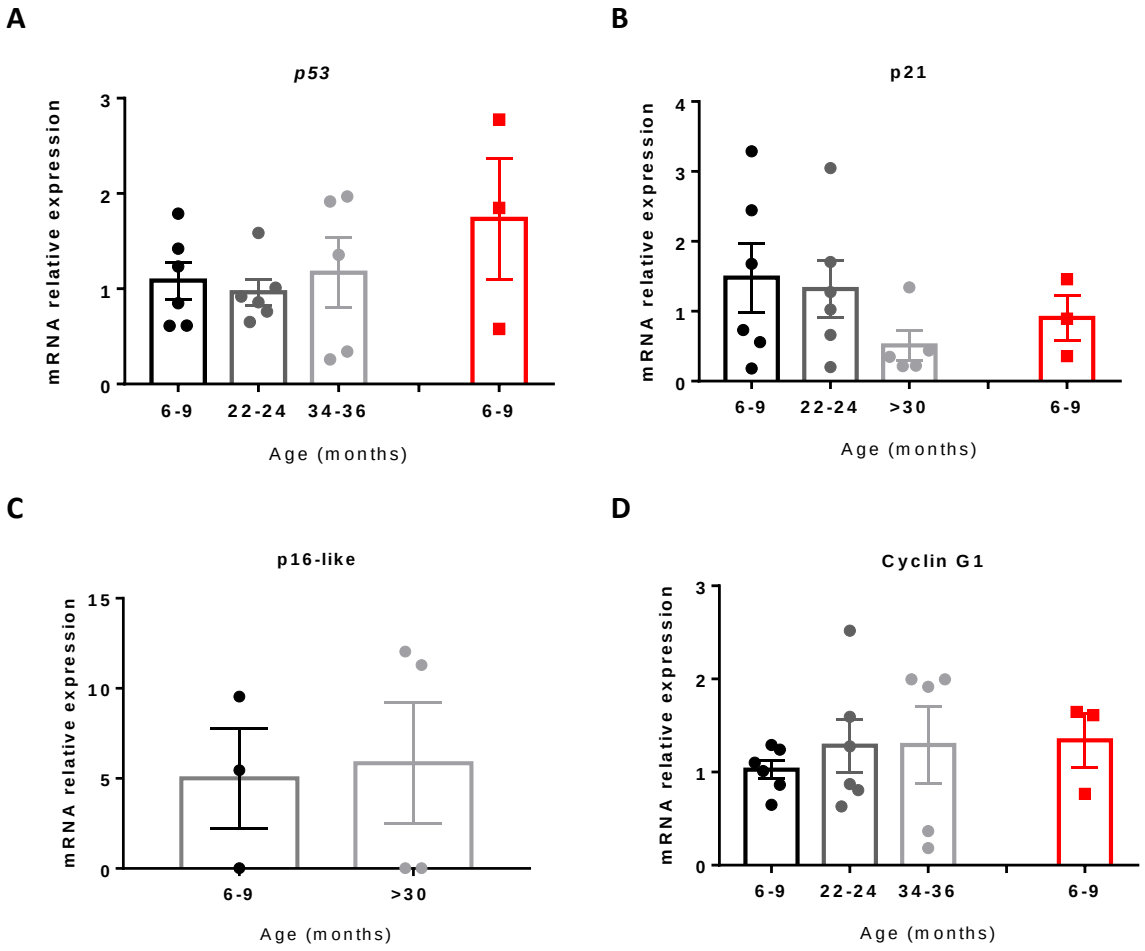


**Fig 6.3. mRNA relative expression of key downstream effectors of γH2AX in the ageing gut of WT and *tert*$^{-/-}$ zebrafish.** mRNA relative expression of (**A**) p53, (**B**) p21, (**C**) p16-like and (**D**) cyclin g1 genes, in the young (6-9 months) WT and *tert*$^{-/-}$, middle aged WT (22-24 months) and old WT (>30 months) zebrafish. Graphs: X-axis, age in months; Y-axis, mRNA relative expression normalised to the WT 6-9 months of age, as described in *section 2.5.3*. N=3-6 *per* group. Each dot represents one animal. Bar errors represent the SEM. (**A**) One-way ANOVA test (WT over-time) and unpaired t-test test (6-9 months WT versus *tert*$^{-/-}$);(**B-D**) Kruskal-Wallis and Mann-Whitney test (6-9 months WT versus *tert*$^{-/-}$): * <0.05; ** <0.01; *** <0.001.

### 6.2.3 Measuring proliferation

Senescent cells are characterised by being in a state of cell cycle arrest (Hayflick, 1965; Hayflick & Moorhead, 1961) and therefore proliferation activity was assessed as a marker of cellular senescence. In order to measure the percentage of cells proliferating, PCNA expression was assessed by IF, as described in *section 2.3.2*, in young (5-7 months), middle aged (12-17 months) and old (>22 months) WT fish, and compared with young (5-7 months) and old (12-17 months) *tert*$^{-/-}$ fish.

The results showed decreased levels of proliferation in the gut with natural ageing (p=0.001), more specifically at 22 months of age (5-7 vs 22m: p=0.008; 12 vs 22m: p=0.001) (**Fig 6.4A, B**). Additionally, the *tert*$^{-/-}$ model already presented decreased levels of proliferation at the age of 12-17 months, in comparison to its WT counterpart (12-17m WT vs *tert*$^{-/-}$: p=0.031).

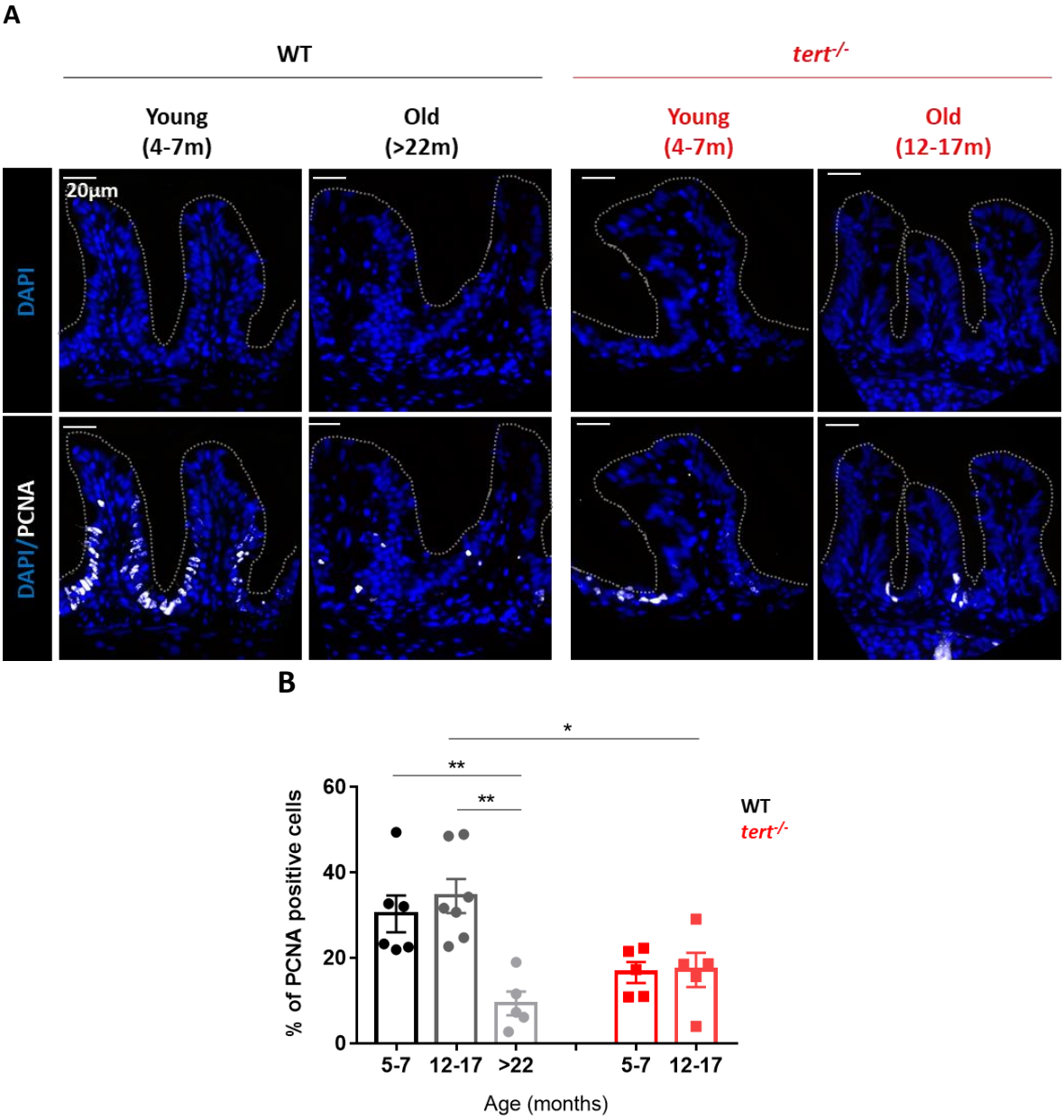


**Fig 6.4. Proliferation in the ageing zebrafish gut, in the presence and absence of TERT. (A)** Representative images of PCNA staining by IF, in young (5-7 months) WT and *tert*$^{-/-}$, middle aged WT (12-17m), and old WT (>22 months) and *tert*$^{-/-}$ (12-17m) zebrafish gut. **(B)** Quantifications of the percentage of PCNA-positive cells, counted as described in *section 2.3.7.* Graph: X-axis, age in months; Y-axis, % of PCNA-positive cells. N=5-7 per group. Each dot represents one animal. Bar errors represent the SEM. One-way ANOVA (WT over-time) and two-way ANOVA (WT versus *tert*$^{-/-}$ at 5-7 versus 12-17m): * <0.05; ** <0.01; *** <0.001.

### 6.2.4 Measuring relative telomere length *in situ*

Since I confirmed an accumulation of cellular senescence in the WT aged gut, characterised by increased levels of SA-β-Gal and DNA damage, and decreased levels of proliferation, I then sought to confirm whether this was due to replicative senescence. To do so, I tested whether there is telomere shortening in the gut with natural ageing and whether this is accelerated in the absence of TERT, as previously reported by TRF analysis in Southern blots (C. Carneiro et al., 2016; Henriques et al., 2013). I tested this by measuring relative telomere length in young (4-5 months), middle aged (14-17 months) and old (>22 months) WT fish, and comparing it with young (4-5 months) and old (14-17 months) *tert*$^{-/-}$ fish. Relative telomere length was assessed *in situ*, by telo-FISH, as described in *section 2.3.3*. Telo-FISH was the technique chosen to analyse telomere length in the gut in order to be consistent and comparable with the brain.

The results showed no significant difference in telomere length with natural ageing (4-5 vs 14-17m: p=0.925; 4-5 vs >22m: p=0.705) (**Fig 6.5A-B; Fig 6.6**). Furthermore, no differences in telomere length were detected between WT and *tert*$^{-/-}$ at 4-5 months (p=0.625) or 14-17 months of age (p=0.687).

**A**

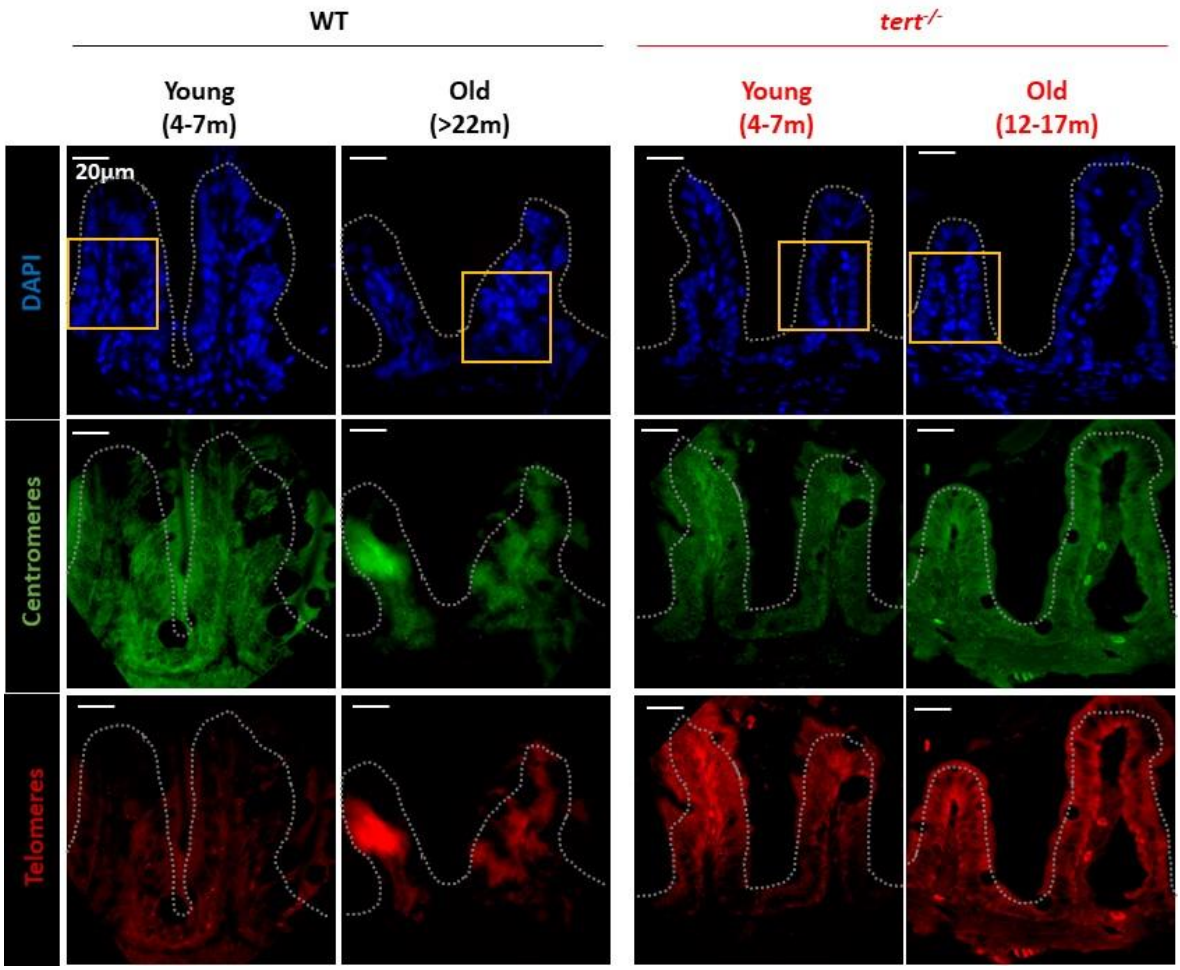


**B**

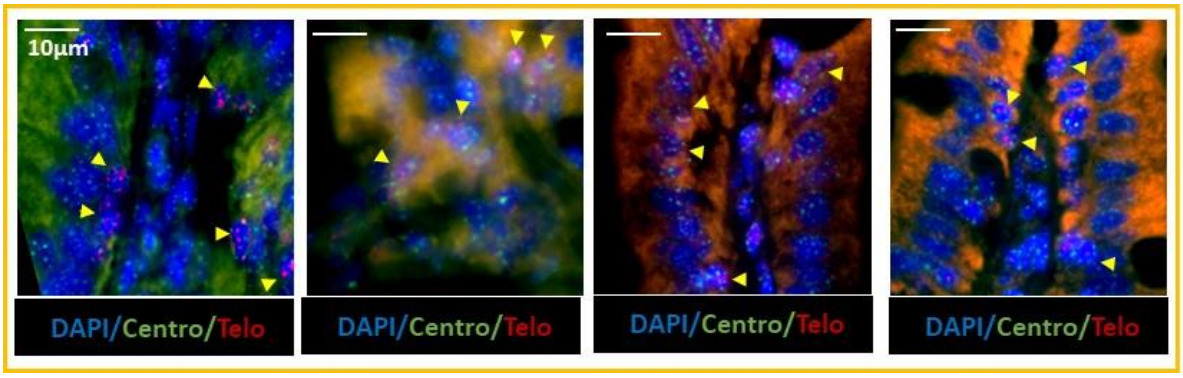


**Fig 6.5. Representative images of telomeres and centromeres in the gut of young and old WT and *tert*$^{-/-}$ zebrafish. (A)** Representative images of centromeres (green) and telomeres (red), in the gut of young (4-5 months) WT and *tert*$^{-/-}$, and old WT (>22 months) and *tert*$^{-/-}$ (12-17m) zebrafish. Grey dashed is delimiting the gut villi. line Scale bar: 20µm. **(B**) Amplification of the areas delimited by a yellow square in **A**. Yellow head arrows are pointing to the cell nuclei where longer telomeres are observed. Scale bar: 10µm.

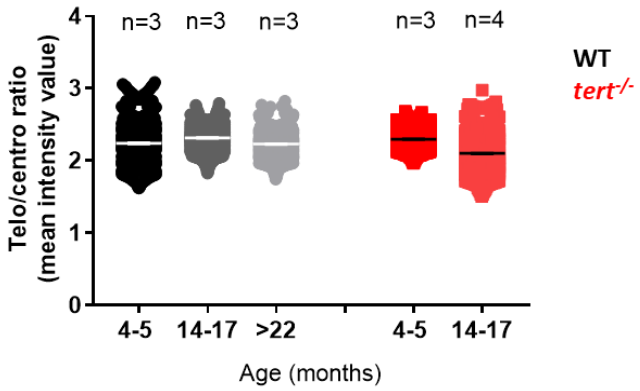


**Fig 6.6. Telomere length in the ageing gut of WT and *tert*$^{-/-}$ zebrafish.** Quantifications of telomere/centromere ratio, as described in *section 2.3.3.* Graph: X-axis, age in months; Y-axis, telomeres/centromeres ratio, expressed in mean Intensity value. N=3-4 per group. Each dot represents a cell. Bar errors represent the SEM. Random effects ANOVA: * <0.05; ** <0.01; *** <0.001.

## 6.3 Analysis of inflammation in the aged gut, in WT and *tert*$^{-/-}$ zebrafish

In some contexts, immune cells are known to be recruited to the sites of cellular senescence and clear them (Demaria et al., 2014; Krizhanovsky et al., 2008). Accordingly, even though I could not establish causality, I did observe increased inflammation in the brain at the same age as I observed increased senescence. Here, I set out to test whether accumulation of cellular senescence in the ageing gut is also accompanied by increased number of immune cells and immune activation. To test this, I counted the overall number of immune cells and measured chitotriosidase activity in the ageing gut, in the presence (WT) and absence of telomerase (*tert*$^{-/-}$).

If increased inflammation with ageing were to be a telomerase-dependent phenomenon, then removing telomerase would accelerate it and/or exacerbate it. I therefore counted the number of immune cells in the gut, throughout the zebrafish life-course, from young (4-7 months), to middle aged (12-17 months) and old (>22 months) in WT fish, and compared with young (4-7 months) and old (12-17 months) *tert*$^{-/-}$ fish. Immune cells were detected by IF, using the pan-leukocyte marker LCP1 (L-plastin), as described in *section 2.3.2*, and previously performed in the brain (see *Chapter 4*).

Contrary to what I observed in the brain, the results showed no differences in the number of immune cells in the naturally aged gut (4-7 vs >22m: p=0.248; 12-17 vs >22m: p=0.999) (**Fig 6.7**). Furthermore, there were no differences in the percentage of immune cells between WT and *tert*$^{-/-}$ at 5-7 (p=0.112) or 12-17 months of age (p=0.999).

Despite no differences in number, immune cells might become more activated with ageing. To test this hypothesis, I determined whether there is increased immune activation with natural ageing and whether this was accelerated in the absence of TERT. To do this, immune activation was assessed in young (4-6 months) and old (>23 months) WT fish and compared with young (4-6) *tert*$^{-/-}$ fish. Immune activation was assessed by measuring chitotriosidase activity in the whole gut, as described in *section 2.7.3*.

The results showed no differences in chitotriosidase levels in the WT gut over-time (p=0.167) (**Fig 6.8**). In addition, no differences were detected between WT and *tert*$^{-/-}$ at 4-7 (p=0.112) or 12-17 (p=0.999) months of age.

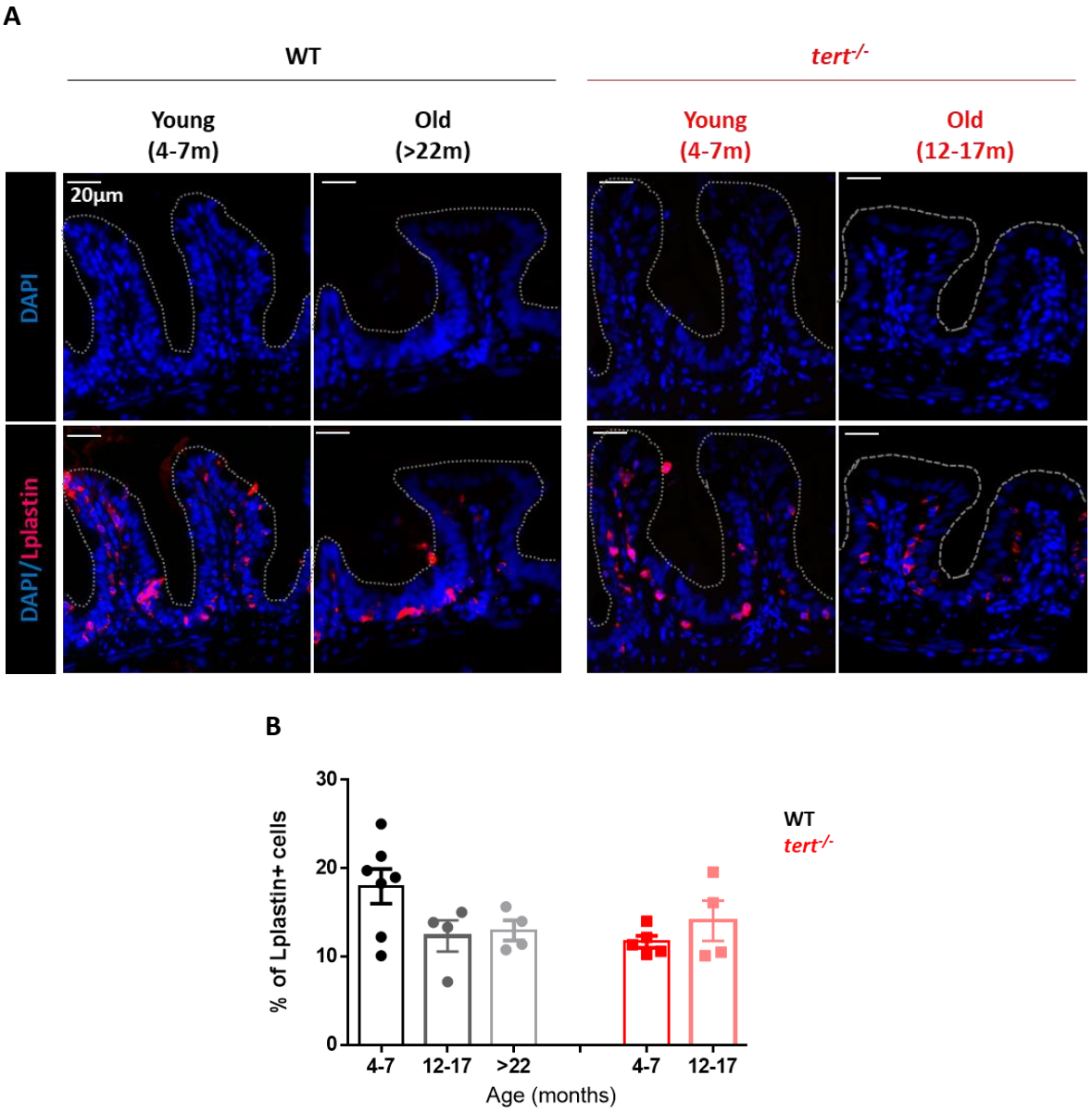


**Fig 6.7. Percentage of immune cells with the ageing gut, in WT and *tert*$^{-/-}$ zebrafish. (A)** Representative images of L-plastin staining in the gut of young (4-7 months) WT and *tert*$^{-/-}$, middle aged WT (12-17 months), and old WT (>22 months) and *tert*$^{-/-}$ (12-17m) zebrafish. Scale bar: 20µm. **(B)** Quantifications of percentage of L-plastin-positive cells, counted as described in *section 2.3.7.* Graph: X-axis, age in months; Y-axis, % of L-plastin-positive cells. N=4-7 per group. Each dot represents one animal. Error bars represent the SEM. One-way ANOVA (WT over-time) and two-way ANOVA (WT vs *tert*$^{-/-}$ at 5-7 vs 12-17m): * p<0.05; ** p<0.01; *** p<0.001.

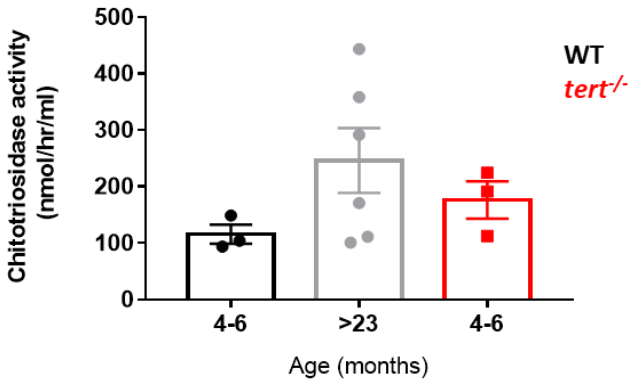


**Fig 6.8. Chitotriosidase activity in the ageing gut, in the presence and absence of telomerase.** Graphs: X-axis, age in months; Y-axis, chitotriosidase activity in nmol/h/ml, analysed as described in *section 2.7.3*. N=3-6 *per* group. Each dot represents one animal. Bar errors represent the SEM. Unpaired t-tests: * <0.05; ** <0.01; *** <0.001.

## 6.4 Assessing gut permeability with ageing in WT and *tert*$^{-/-}$ zebrafish

In order to test whether accumulation of cellular senescence in the gut was having any detrimental effect in the tissue, I sought to perform a functional assay. Gut permeability is known to increase with ageing, and it has been suggested to potentially contribute to a state of chronic inflammation with ageing. I therefore tested whether accumulation of cellular senescence in the gut, with natural ageing, is accompanied by increased gut permeability, and whether this is accelerated in the absence of telomerase. In order to do this, gut barrier permeability was assessed in young (3 months), middle aged (22 months) and old (>30 months) WT fish, and compared with young (3 months) and old (22 months) *tert*$^{-/-}$ fish. This was performed using the 'smurf' assay, described in *section 2.8.2*. Briefly, fish were immersed in water containing blue food colourant for 30 min. After rinsing the fish in clear water to remove the excess of blue colouration, it was assessed whether the colourant remained in the gut (absence of blue colouration in the skin, indicative of no gut permeability) or whether it diffused all the way into the skin (indicative of gut permeability).

The results showed increased blue colouration in the fish skin with natural ageing ($p=0.0036$), more specifically from 22 months of age onwards ($p=0.021$, **Fig 6.9**). Despite there was a mean difference of 11 units between young WT and *tert*$^{-/-}$ at the age of 3 months, suggesting that removing telomerase could accelerate this phenomenon, the differences between genotypes did not reach statistical significance at this time-point ($p=0.189$). No differences were observed at later ages either, between WT and *tert*$^{-/-}$ (at 22 months: $p=0.948$).

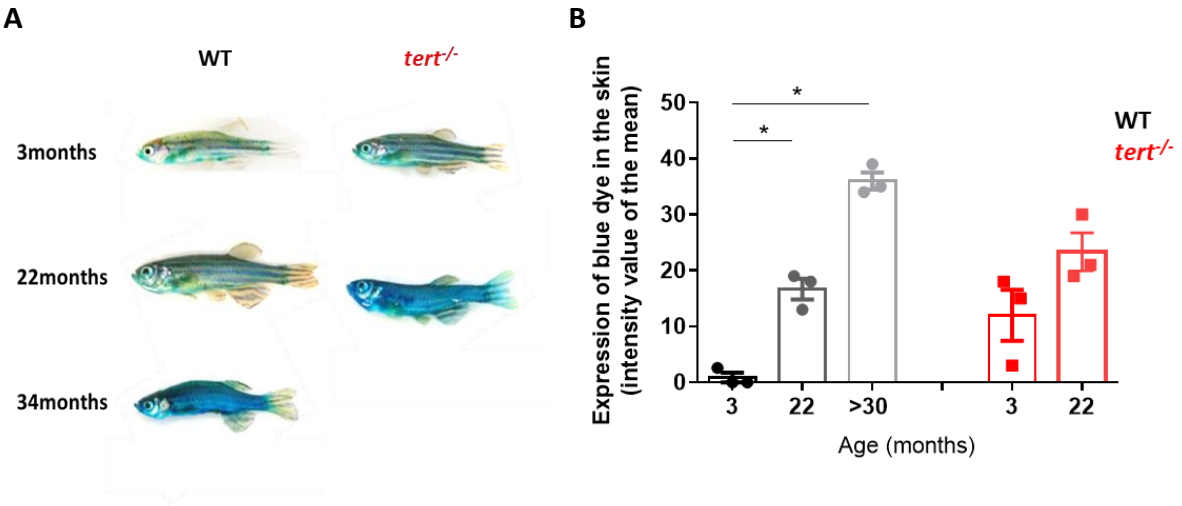


**Fig 6.9. Gut barrier permeability in the ageing zebrafish, in the presence and absence of TERT. (A)** Representative images of blue colouration in the skin of young (3 months) WT and *tert*$^{-/-}$, middle aged WT (22 months), and old WT (>30 months) and *tert*$^{-/-}$ (22 months) zebrafish, after exposure to the 'smurf' assay. **(B)** Quantifications of the expression of blue colouration in the skin, measured as described in *section 2.8.2.* Graph: X-axis, age in months; Y-axis, % of expression of blue dye in the skin, in intensity value of the mean. N=3 per group. Each dot represents one animal. Error bars represent the SEM. Kruskal-Wallis test (WT over-time) and two-way ANOVA (WT vs *tert*$^{-/-}$ at 3 vs 22m): * p<0.05; ** p<0.01; *** p<0.001.

## 6.5 Discussion

In this Chapter I aimed to test: (1) whether a high proliferative tissue, the gut, displayed exacerbated and/or accelerated accumulation of cellular senescence than a low proliferative tissue, the brain; and (2) whether accumulation of cellular senescence in the gut was associated with telomere shortening. This is because replicative senescence is more likely to accumulate in high turnover tissues, where there is rapid telomere erosion. To do this, I had to perform all assays in the guts of the same animals in which I studied the brain, in *Chapter 4*.

### The role of TERT in accumulation of senescence in the zebrafish aged gut

Firstly, to confirm whether there is accumulation of cellular senescence in the gut, with natural ageing, I assessed different markers of senescence in the WT zebrafish gut at different ages throughout their life course. I identified increased expression of SA-β-Gal (ca. 60%) and DNA damage (ca. 5-10%), accompanied by decreased levels of proliferation (ca. 20%) in the zebrafish gut at >30 months of age. These findings suggest that there is accumulation of cellular senescence in the zebrafish gut with natural ageing, in agreement with the literature. Indeed, Carneiro et al. (2016) had already shown increased expression of SA-β-Gal, accompanied by increased levels of γH2AX and decreased levels of proliferation, in the zebrafish gut, from 24 months of age onwards (Carneiro et al., 2016). Moreover, this does not seem to be a fish-specific phenotype as increased percentage of cells containing γH2AX foci had also been reported in the aged mice gut, at 42 months of age, particularly in epithelial cells near the crypts (Wang et al., 2009).

Secondly, to confirm whether accumulation of senescence was accelerated in the absence of telomerase, I compared WT versus *tert*$^{-/-}$ guts, at different ages throughout the zebrafish lifespan. Compared to their WT counterpart, *tert*$^{-/-}$ fish displayed increased SA-β-Gal expression (~60%) and reduced levels of proliferation (~15%), at 4-6 months and at 12 months, respectively. These findings support the literature as it had already been reported that *tert*$^{-/-}$ zebrafish accumulates cellular senescence in the gut at an earlier age that their WT siblings, displaying increased levels of SA-β-Gal (ca. 2.5x) at the age of 12 months (Carneiro et al., 2016; Henriques et al., 2013), and decreased proliferation levels (ca. 40% in WT VS 20% in *tert*$^{-/-}$)

from 6 months of age (Henriques et al., 2013). Again, this does not seem to be a unique characteristic of zebrafish, as the gut crypts of G4 TERT$^{-/-}$ mice model display increased levels of p53, one of the markers of senescence, when compared with TERT$^{+/+}$ age-matched controls (Jaskelioff et al., 2011). Apart from increased SA-β-Gal and decreased proliferation, Henriques et al. (2013) and Carneiro et al. (2016) have observed an accelerated accumulation of DNA damage in the *tert*$^{-/-}$ model, compared with WT siblings (ca. 10x of γH2AX$^{+}$ cells) (Carneiro et al., 2016; Henriques et al., 2013). In contrast, the present study failed to identify differences in DNA damage between the genotypes. In the absence of increased levels of DNA damage in the *tert*$^{-/-}$ (versus WT), it is not possible to conclude whether the absence of telomerase contributes to an accelerated accumulation of cellular senescence in the zebrafish gut, as it was previously described (Carneiro et al., 2016; Henriques et al., 2013). However, none of these studies had compared the gut with the brain within the same animals, which was what I aimed to do.

Despite partially going hand in hand with the literature, the results found in this study need to be interpreted with caution. This is because: (1) I observed a great discrepancy between percentage of cells expressing DNA damage and area of the tissue expressing SA-β-Gal staining, in both WT and *tert*$^{-/-}$ old guts; and (2) I did not identify accelerated accumulation of DNA damage response in the absence of telomerase, regardless of observing accelerated accumulation of SA-β-Gal and reduced proliferation activity.

(1) On one hand, Carneiro et al. (2016) had identified 10-18% of cells expressing γH2AX foci in fish of >24 months of age (Carneiro et al., 2016), which is the double of the percentage I identified in this study (5-10%) in >30 months old fish. This difference might either be associated with an inter-laboratory variability, or with an undetermined technical issue that may have led to the labelling of fewer cells with the anti-γH2AX antibody. On the other hand, as mentioned in *section 1.3.2*, SA-β-Gal can also be detected, at least transitory, in non-senescent cells, including in pro-inflammatory immune cells (Hall et al., 2017), quiescent and immortalised cells (Severino et al., 2000; Yang & Hu, 2005). Additionally, the SA-β-Gal staining is diffused throughout the tissue, and it is not cell specific, as observed in **Fig 6.1A**. This diffuse and non-specific staining can therefore lead to false-positives, which may be one of the reasons why I observed such a high percentage of the tissue expressing SA-β-Gal staining in the aged zebrafish gut. Further investigation would be required to determine this. More

specifically, it would be important to repeat the immuno-staining with anti-γH2AX, using a new batch of antibody, in order to test whether the few number of γH2AX-positive cells observed in this project is associated with a technical issue. Moreover, cells could be co-labelled with SA-β-Gal and other markers of senescence, such as γH2AX (by immunostaining) or p21 (by *in-situ* hybridisation). Despite being technically challenging, this co-labelling could help detecting and excluding potential non-senescent cells expressing SA-β-Gal.

(2) Regarding the lack of differences in the percentage of cells containing DNA damage observed between WT and *tert*$^{-/-}$ model, it remains unclear if this is real or if it reflects some experimental issues. It is reasonable to think that the lack of differences observed between genotypes may either be due to a possible technical problem during IF, as above mentioned, or due to the small sample size used in this study. Indeed, power calculations revealed that the γH2AX experiment would require a minimum of 22 animals per group in order to detect a 25% difference (with 90% power) between genotypes. This suggests that I would be likely to identify differences between WT and *tert*$^{-/-}$ if I were to expand the sample size of this experiment. Of note, accordingly to the power calculations, the number of fish required for these experiments are much higher than the ones reported in previous studies, where the sample size required was 3 to 6 animals per group (Carneiro et al., 2016; Henriques et al., 2013). The higher variability found in this study could well be because, contrary to the previous studies, I did not use siblings as I did not have animals enough from each given time-point to do so. Laboratory tert mutants are generated via the incross of heterogyzous fish (see *section 2.2.2*), and the parental telomere length influences the progeny telomere length. If, by chance, some tert$^{+/-}$ parents have longer telomeres, then their offspring will also have longer telomeres and will age slower. This is likely to contribute not only to a high inter-individual variability (between non-siblings) but also to a high inter-laboratory variability. In fact, this is likely to have affected some of the results obtained in this project as the laboratory had many tert$^{-/-}$ fish living until the age of 22 months, which had not been reported to happen in the previous studies (Carneiro et al., 2016; Henriques et al., 2013). In the future, the lab will aim to characterise telomere length in the parents before establishing crosses. However, this is technically challenging and time consuming as it involves to measure absolute telomere length in every parent.

Therefore, in order to strengthen the data, in the future, it would be important to repeat the immunolabelling with the anti-γH2AX antibody using a larger sample size. Additionally, in order to test whether the SA-β-Gal staining is over-representing the number of senescent cells present in the tissue, it would be important to test: (a) whether SA-β-Gal staining is showing a great number of false-positive cells due to, for example, transient expression of SA-β-Gal by activated immune cells (by determining if immune cells in the aged zebrafish gut are in a pro-inflammatory state and whether they express SA-β-Gal staining themselves); and (b) whether cells expressing γH2AX foci also express SA-β-Gal staining (by co-labelling cells with both staining at the same time). Moreover, apart from SA-β-Gal and DNA damage expression, it would be important to determine the presence of other markers of cellular senescence in the aged gut, such as, for example, the presence of SASP factors and p53 phosphorylation. The use of multiple markers would strengthen the confidence on whether there is telomerase-dependent accumulation of cellular senescence with ageing, in the zebrafish gut, as it was previously reported by others (Carneiro et al., 2016; Henriques et al., 2013).

## The role of TERT on telomere shortening in the ageing gut

After testing whether there is accumulation of cellular senescence in the aged zebrafish gut, I aimed to determine whether this accumulation was associated with telomere shortening, a characteristic of replicative senescence (Bodnar et al., 1998). In order to test this, I assessed relative telomere length over-time, in the zebrafish gut, by telo-FISH. Being a tissue with high cell turnover, where there is rapid telomere shortening (Bodnar et al., 1998; Lee et al., 1998), I would expect to see decreased telomere length over-time. Moreover, being telomerase the only enzyme known to be capable of elongating telomeres (Greider & Blackburn, 1985), I would expect that in its absence, telomere erosion was accelerated. Accordingly, telomere shortening had already been shown to occur with ageing in mice (Wang et al., 2009) and zebrafish gut (Carneiro et al., 2016; Henriques et al., 2013), in a telomerase-dependent manner (i.e. accelerated in the absence of telomerase). Contrary to what was expected, and in opposition to the previous reports, the present study did not identify decreased telomere length in the zebrafish gut, with natural ageing, neither it identified shorter telomeres in the *tert*$^{-/-}$, compared with the WT, at any time-point analysed. It is

unclear whether the lack of telomere shortening with ageing, or in the absence of telomerase, observed in this project, is real or it if reflects some technical issues.

It is important to note that in this study I measured relative telomere length by telo-FISH whereas in the previous studies performed in zebrafish the authors performed TRF analysis by Southern blotting, the gold standard technique to measure telomere length (Carneiro et al., 2016; Henriques et al., 2013). Telo-FISH was the technique chosen in this study to assess telomere shortening with ageing because, contrary to Southern blotting, it allows the measurement of relative telomere length in different cell populations and in different regions of the tissue, which was one of the aims of the project, particularly in the brain. This is because southern blotting requires large amounts of DNA, which makes it really challenging to obtain sufficient amounts of DNA from brain macroareas or specific cell populations after sorting. Hence, telo-FISH was used to assess relative telomere length in both brain (*Chapter 4*) and gut in order to maintain consistency and to be possible to make a direct comparison between the tissues. Nonetheless, telo-FISH also has some disadvantages and it is not as sensitive as Southern blotting. Besides telo-FISH does not allow the measurement of absolute telomere length, it may not allow the detection of critically short telomeres (Lai et al., 2017; Lai et al., 2018), and it is highly compromised by the amounts of background in the tissue. This is particularly relevant in a model species that has already naturally short, human-like size telomeres (~4-12kb) (Carneiro et al., 2016; Henriques et al., 2013). In mouse, this technique is highly use without such limitations because most of the mice strains used in laboratory present very long telomeres and thus their signal/background ratio is much higher and easy to detect. To overcome the challenge of detecting small differences in telomere length in zebrafish, over-time, after performing Southern blotting, in the previous studies, the authors used the median of telomere length (instead of mean) to assess telomere length, taking into consideration the critically short population of telomeres (Carneiro et al., 2016; Henriques et al., 2013). However, in this project, using telo-FISH, no differences were observed between analysis using the mean or the median (data not shown). It is therefore possible that telo-FISH, used in this project, was not sensitive enough to detect small differences in telomere length with ageing in the zebrafish gut. Particularly, given that the biggest difference in telomere length in the gut can be attributed to a small population of cells, that have longer telomere length in the WT. Unpublished data from the lab now shows that these cells with

longer telomeres are immune cells, and it is the changes in telomere length in these cells that makes the biggest difference between WT and *tert*$^{-/-}$.

Furthermore, telomere shortening in the zebrafish gut has been shown to occur mainly in the first 3 months of life (~3-4Kb), from which there is a small decrease (~1Kb) or a maintenance in telomere length (Carneiro et al., 2016; Henriques et al., 2013). In this project, I assessed telomere length from 4-5 months of age onwards, where only a small decrease in telomere length is expected to occur. Thus, it is likely that I have missed the critical period where telomere shortening is more prominent, and that telo-FISH lacked sensitivity to detect slight changes in telomere length at later ages. Of note, on top of this, a great variability in telomere length was observed between animals, within each experimental group. In fact, power calculations revealed that I would need a minimum of 22 animals per group in order to identify differences in telomere length between experimental groups.

So far, the results obtained in this project did not allow to confirm whether accumulation of senescence in the zebrafish gut, of the animals where I observed accumulation of senescence in the brain with natural ageing, is associated with telomere shortening. In the future, further investigation would be required to confirm this. In this regard, it would be crucial to repeat the experiment that aimed to measure telomere length by telo-FISH, increasing the sample size and adding earlier time-points than the ones analysed in this project (<4 months old fish). In parallel, it would be important to measure telomere length using an alternative technique, more specifically, TRF by Southern blotting. Apart from these experiments, it would be interesting to look at telomere-associated DNA damage foci or TAFs (i.e. DNA damage foci co-localising with telomeres), in order to detect DNA damage specifically at telomeres sites. Contrary to DNA damage that occur in non-telomeric regions, that is rapidly repaired and therefore is short-lived, TAFs are persistent, and therefore they are thought to contribute to the accumulation of DNA damage foci with ageing (Hewitt et al., 2012). Hence, TAFs constitute another important marker of cellular senescence. However, it is technically challenging to assess TAFs in tissues of animals with short telomeres, where the short telomeres are already barely detectable by telo-FISH. Therefore, it is challenging to analyse TAFs in zebrafish tissues and I would likely miss most TAFs that accumulate at critically short telomeres.

## The role of TERT in inflammation, in the aged zebrafish gut

In the second part of this Chapter, I aimed to test what are the consequences of accumulation of cellular senescence in the aged zebrafish gut, in terms of inflammation and tissue integrity. As immune cells are recruited to the sites of cellular senescence and are able to clear them, at least in some contexts (Demaria et al., 2014; Kang et al., 2011; Krizhanovsky et al., 2008), I would expect that accumulation of cellular senescence in the aged zebrafish gut to be associated with increased inflammation. Moreover, senescent cells are known to contribute to impairment of tissue homeostasis, due to their inability to proliferate, and to promote a chronic, low-level inflammation in the tissue, via releasing of SASP components (Franceschi & Campisi, 2014; Tchkonia et al. 2013; Freund et al. 2010; Campisi & d'Adda di Fagagna 2007). Together, this can lead to the loss of tissue integrity and contribute to disease (Ovadya & Krizhanovsky, 2014; van Deursen, 2014). Thus, I would expect that accumulation of cellular senescence in the aged zebrafish gut to be associated with increased inflammation and decreased tissue integrity. To test this, I determined whether cellular senescence was associated with increased number of immune cells and increased immune activation, as well as with increased gut-barrier permeability.

Contrary to what was observed in the brain (*Chapter 4*), this study did not show any differences in the number of immune cells or chitotriosidase activity, with ageing, in the zebrafish gut. Additionally, no differences were identified between WT and *tert*$^{-/-}$ model (i.e. in the absence of telomerase) in any of these assays. Despite little being known about age-associated alterations in the immune cells of the gut, it is thought that with advancing age, in mammals, there is decreased migration of immune cells from the Peyer's patches (mammalian gut structures formed by an agglomerate of lymphocytes). Whilst greater numbers of lymphocytes accumulate in these structures, the mouse lamina *propria* was reported to display reduced number of immune cells with ageing (Schmucke et al., 2003; Saffrey, 2014). Although zebrafish do not present Peyer's patches (Brugman, 2016), it is not known whether migration of immune cells is impaired in the aged zebrafish gut, preventing infiltration of immune cells from the bloodstream into the lamina *propria*, which could explain the results found in this project. Contrary to this hypothesis, Carneiro et al (2016) reported an infiltration of leukocytes in the lamina *propria*, with ageing, in the *tert*$^{-/-}$ (but not WT) zebrafish. This was assessed by haematoxylin/eosin (H&E) staining and qualitatively analysed

by a pathologist. However, the number of immune cells was not counted and the type of immune cells accumulating in this region with ageing was not analysed (Carnero et al., 2016). Therefore, further experiments should aim at confirming these results. Furthermore, it is important to note that this project only analysed the number of overall immune cells (L-plastin-positive cells). Hence, it remains unknown whether, with ageing, there is a shift in the proportion of the different immune cell populations in the gut, with an increased number of a specific immune cell type.

Independently of the number of immune cells, though, it may be that immune cells in the gut, with ageing, become more activated, expressing pro-inflammatory markers. For example, in humans, increased levels of IL6 were identified in the aged gut, specifically in dendritic cells (Man et al., 2015). In this project, I tested chitotriosidase activity as a marker of inflammation, but detected no differences with ageing, or in the absence of telomerase. Nonetheless, power calculations showed that it would be necessary a minimum of 16 animals per group in order to identify possible differences between the groups, and therefore these results remain inconclusive. In order to confirm these results, in the future it would be important to repeat the experiment with an increased sample size. Interestingly, Carneiro et al. (2016) reported decreased villi length and thickening of the gut lamina *propria*, accompanied by increased enteritis, with ageing, in the zebrafish gut (Carneiro et al., 2016; Henriques et al., 2013). This suggests that there may be inflammation in the aged zebrafish gut, associated with morphological changes in the tissue. Thus, it would also be important to use other methods to assess inflammation, such as measuring lamina propria width, localised infiltration of immune cells, and expression of pro-inflammatory signals such as IL6, IL1, TNFα or NFkB. It is important to note, though, that it remains a technical challenge to assess pro-inflammatory signals in the zebrafish gut due to the lack of specific antibodies available. Additionally, despite there are transgenic reporter lines available for IL6, IL1b, TNFα and NFkB, they do not enable an accurate quantitative assessment of the levels of expression of these molecules. This is because the reporter fluorescent proteins have different half-lives and because there is some uncertainty regarding the number of inserted copies of the transgene per animal (unpublished data from the lab).

Finally, I tested whether gut permeability was associated with increased cellular senescence in the aged zebrafish gut. In agreement with previous reports in mice

(Thevaranjan et al., 2017) and zebrafish (Dambroise et al., 2016; Martins et al., 2018), this study identified gut permeability in natural ageing. However, no differences were identified between WT and *tert*$^{-/-}$ model and therefore it is not clear whether gut permeability with ageing is accelerated in the absence of telomerase. Effect sizes showed that this experiment was underpowered and a minimum of 12 animals would be required to detect differences between genotypes. This suggests that I would be likely to detect differences between genotypes if I was to increase the sample size of the experiment. Hence, it would be important to repeat this experiment increasing the sample size.

## Conclusion

Overall, this Chapter aimed to test whether a high proliferative tissue, the gut, accumulates cellular senescence with ageing, whether this occurs in a telomerase-dependent manner, and whether it anticipates accumulation of senescence in the brain, a low-proliferative tissue. Several technical issues, mainly driven by the small sample sizes used, did not allow to take any conclusions, apart from that there is accumulation of cellular senescence in the zebrafish gut, with natural ageing. Therefore, the data found in this Chapter could not confirm whether accumulation of senescence in the gut is accelerated in the absence of TERT and whether this occurs in a telomere-dependent manner. Due to the uncertainty of the results, in the end, the data did not allow to determine whether accumulation of senescence in the gut precedes the brain. Further investigation is required to address all these questions in the future.

# Chapter 7.
# General Discussion

With ageing, the risk of developing chronic diseases increases dramatically. Age-related degenerative diseases affecting the CNS, including the retina and the brain, have an enormous negative impact on patient's quality of life, as well as respective care takers. Thus, it is urgent to develop new models and techniques that may help to unravel mechanisms underlying age-related diseases of CNS, aiming to identify therapeutic targets that promote healthy ageing.

In this project I used the zebrafish model to address specific questions regarding the accumulation of senescence and inflammation with ageing in the CNS (retina and brain), and how telomerase, a key molecule involved in many age-related conditions, may play a part on it.

In the first part of this project I tested whether the zebrafish retina undergoes degeneration with ageing and whether telomerase plays a role on it. This work showed that the zebrafish retina suffers several structural and morphological alterations over-time, resembling human retinal ageing. These include retina thinning, accompanied by increased cell death and reduced proliferation (Eriksson & Alm, 2009). In addition, there is loss of amacrine and bipolar neurons and disorganisation of the photoreceptors, which culminates in visual impairment (Marshall, 1987; Nian & Lo, 2019; Salvi et al., 2006). Reactivation of telomerase has been shown to ameliorate AMD in humans (Dow & Harley, 2016; Rowe-Rendleman & Randolph, 2004), suggesting that telomerase is crucial for retinal health. Surprisingly, none of the age-associated retinal phenotypes described were accelerated in the *tert*$^{-/-}$ model (versus counterpart WT), suggesting that telomerase is unlikely to contribute to zebrafish retinal ageing, at least in the retinal areas I focused on, and associated visual defects. Importantly, despite MG maintaining their regenerative capacity in response to acute damage until old ages, MG fail to proliferate in response to chronic, age-associated neurodegeneration. Instead of a regenerative response, the aged zebrafish retina displays a gliotic-like response, like in humans. Furthermore, although telomerase is known to play an essential role in proliferation and regeneration (Bednarek et al., 2015; Lin et al., 2018), the absence of telomerase did not worsen retina degeneration with ageing. This suggests that telomerase is unlikely to be a limiting factor for age-associated retinal degeneration in zebrafish. Reduced proliferation with ageing, in the zebrafish retina, is thus unlikely to be the driving mechanism for retinal degeneration, whereas cell death is likely to play a more important role.

Together, this part of project shows that zebrafish display several cellular and molecular alterations with ageing that mimic what happens in the human retina during ageing and disease, making it a suitable model to study human retinal ageing. Importantly, here I show that there are key differences in MG and microglia response to chronic versus acute damage. Gliosis is one of the main differences between acute and chronic damage, and therefore it constitutes a key target to further explore regenerative mechanisms in the human retina, in the future. Furthermore, this study highlights the relevance of studying regenerative mechanisms in the context of ageing and points to zebrafish as a good model to do so.

In the second part of this project I determined whether the zebrafish brain accumulates cellular senescence with ageing, in a TERT-dependent manner. The findings of this work suggested that there is accumulation of cellular senescence in the zebrafish brain, with ageing, specifically in the diencephalon and cerebellum. Importantly, accumulation of senescence was accelerated in the *tert*$^{-/-}$ fish model, suggesting that TERT exerts a protective effect against accumulation of senescence. In parallel, this project also suggested that there is increased inflammation in the aged zebrafish whole brain, as assessed by increased number of microglia/ macrophages and chitotriosidase activity. Once again, this was anticipated in the *tert*$^{-/-}$ fish model, suggesting that TERT plays a protective role against inflammation in the aged zebrafish brain. However, the macroareas where increased number of microglia/ macrophages were identified did not correlate with the macroareas where SA-β-Gal was observed. This particular inconsistency, together with the fact that some of these experiments were underpowered, makes it unclear whether inflammation in the aged brain is associated with accumulation of senescence.

It is important to mention that power calculations made before the starting of the project, based on laboratory data as well as on published data, had shown that most of the experiments required sample sizes of 3 to 6 fish (Carneiro et al., 2016; Henriques et al., 2013). Regarding the experiments that were never performed before, effect sizes were not possible to calculate beforehand, due to lack of data available, and therefore I used sample sizes identical to the rest of the experiments. Despite this first analysis, in the end, some of the experiments were showed to be underpowered (larger sample sizes would be required to detect a 25% difference with 90% power and 5% significance level between groups, using a two-sided test). This could be, in part, because contrary to the previous studies I did not use

siblings, which is likely to contribute to an increased inter-individual variability (see *section 6.5.1*). Nevertheless, it is important to note that the usage of non-siblings offers a better representation of the population, potentially presenting more meaningful results.

Immune cells are known to be recruited to sites of cellular senescence, at least in some contexts (Demaria et al., 2014; Krizhanovsky et al., 2008). In addition, senescent cells are known to release pro-inflammatory factors (part of SASP), contributing to inflammation (Franceschi & Campisi, 2014; Campisi & d'Adda di Fagagna 2007). Therefore, it is likely that cellular senescence can lead to increased inflammation and vice-versa. Nonetheless, the data found in this project do not allow discerning what happens first.

Curiously, within all the macroareas of the brain, the medulla oblongata was the one displaying the highest levels of SA-β-Gal from young ages. At the same time, this macroarea displayed the highest density of microglia/ macrophages from young ages, which became even more evident over-time. Nonetheless, there are some observations that should be confirmed in the future. Since DNA damage was not analysed in the medulla oblongata, due to a technical issue, and SA-β-Gal by itself cannot be used as a maker of senescence, it remains unclear whether the blue staining observed in this macroarea represents real cellular senescence. The main reason why SA-β-Gal staining is not considered a marker of senescence, *per se*, is that non-senescent cells can express it, in some contexts (Severino et al., 2000; Yang & Hu, 2005). For instance, macrophages have been shown to express SA-β-Gal, transiently, when activated (Hall et al., 2017). Given that the medulla oblongata was observed to have a considerable number of microglia/ macrophages from young ages, it is plausible to think that, at least part of the blue staining observed in this region, might be due to immune activation rather than senescence. Preliminary data suggested that most of the L-plastin$^{+}$ cells are surrounding the blue staining and not co-localising with it. Nonetheless, some controls are required to confirm these results (see *section 5.6.1*). Hence, it would be important to confirm whether the medulla oblongata displays high levels of senescence and whether this precedes accumulation of senescence in other macroareas of the brain.

Therefore, future work should aim to confirm some of the findings identified in this project, including the following:

(1) <u>To confirm whether there is accumulation of cellular senescence in the medulla oblongata with ageing and whether this accumulation precedes other macroareas of</u>

the brain. This could be tested by using a combination of markers of senescence, such as DNA damage and, particularly, DNA damage at telomeres (TAFs); γH2AX downstream effectors (for example, p21, p16 and p53); as well as the presence of SASP factors (for example, IL6, IL8, MCP-2, IGFBP, MMP-1, MMP-3). Since high expression of SA-β-Gal was already observed in 4-6 months old WT, it would be important to add an earlier time-point (less than 3 months of age) to the experiment. Nonetheless, it is important to note that these experiments are technically challenging. Firstly, because there is a lack of antibodies available in zebrafish to detect SASP components, and the transgenic reporter lines available are still limited and present several issues (see *section 6.5.3*). Secondly, since it is hard to detect short telomeres by telo-FISH, I would likely miss great part of the TAFs that accumulate in critically short telomeres (see *section 6.5.2*). After overcoming the technical challenges, these experiments would enable to confirm whether there is accumulation of senescence over-time, in the medulla oblongata, and whether it occurs earlier than in the other regions of the brain. This would be relevant because the medulla oblongata is a privileged bridge of contact between the brain and the periphery, as a great number of cranial nerves leave or enter the brain through this macroarea (Moens & Prince, 2002). Therefore, if it were to be confirmed that the medulla oblongata accumulates senescence in the brain before other macroareas, then it would be plausible to hypothesise that inflammation and/or senescence from peripheral tissues could contribute to the accumulation of senescence in this region of the brain. This could open an exciting new line of investigation on possible mechanisms driving accumulation of cellular senescence in the brain.

(2) To test whether senescence in the brain causes inflammation or whether, instead, increased inflammation in the brain leads to accumulation of senescence. These two hypotheses could be tested by treating two groups of fish with a senolytic drug (to kill the senescent cells, group 1) or an anti-inflammatory (to reduce inflammation, group 2) and observe whether this prevented and/or decreased inflammation or senescence, respectively. A low number of immune cells and reduced immune activation upon treatment with a senolytic (in group 1), would indicate that senescent cells contribute to inflammation in the aged brain. A reduced number of senescent cells upon

treatment with an anti-inflammatory (in group 2), would indicate that inflammation contribute to accumulation of cellular senescence in the brain. The findings of these experiments would enable to further explore mechanisms driving accumulation of cellular senescence in the ageing brain, aiming to uncover potential targets to prevent it. Nevertheless, it is important to note that before performing these experiments, it would be essential to test their feasibility, as so far it is not known whether senolytics cross the BBB. ABT-263 (Navitoclax) is a well-known senolytic that was previously administered in both mice and zebrafish (Bussian et al., 2018; Novoa et al., 2019). However, none of these studies looked at the brain and therefore it is unknown whether this drug crosses the zebrafish BBB and whether it exerts any effect on the brain. Despite it being reported that ABT-263 does not cross the BBB (Vogler et al., 2011; Yamaguchi & Perkins, 2012), Bussian et al. reported that treating mice with ABT-263, from weaning to 6 months of age, is enough to prevent the up-regulation of several senescent-associated genes in the brain (Bussian et al., 2018). Therefore, a pilot study would be crucial to test whether ABT-263 crosses the zebrafish BBB and to assess what is the best treatment to do it, by determining the dose and time of drug administration required.

If these experiments (1 and 2) were to confirm that there is accumulation of cellular senescence in the zebrafish brain, with ageing, including in the medulla oblongata, then it would be important to further confirm whether this happens in a TERT-dependent manner. In this project this was tested by using the *tert*$^{-/-}$ model zebrafish, that lacks TERT protein activity in zebrafish (Anchelin et al., 2013; Henriques et al., 2013). Nonetheless, it would be important to confirm these findings, in the future, by restoring TERT expression in the *tert*$^{-/-}$ model and testing whether this is enough to prevent and/or delay accumulation of cellular senescence in the aged brain. This could be done by generating a transgenic line expressing TERT and using it in the *tert*$^{-/-}$ background, where TERT expression would be restored from birth (now on-going in the lab). Alternatively, this could be done by generating an inducible transgenic line where TERT expression would be restored in a time-specific manner. Despite being technically more challenging, an inducible transgenic model would have the advantage of allowing the re-expression of TERT in early adulthood, in order to test whether TERT can

prevent accumulation of senescence; or in late ages, in order to test whether TERT can rescue the phenotype already observed.

Finally, exploratory experiments in this project also aimed at identifying potential mechanisms underlying the protective effect of TERT on accumulation of cellular senescence in the aged zebrafish brain. Within these experiments, it was observed that accumulation of TERT-dependent senescence not only occurs in proliferative areas of the brain, but also in non-proliferative ones, where it is unlikely to be due to replicative cell exhaustion. These findings hint that telomere-independent functions of telomerase (i.e. non-canonical functions of telomerase) may possibly be involved in this protective mechanism. Additionally, in a parallel experiment, I identified a set of tightly connected genes that are down-regulated with ageing in both WT and *tert*$^{-/-}$. Interestingly, some of these genes have been shown to be associated with cellular senescence (bub1, aurkb, mad2 and plk1). Hence, these genes might potentially be key TERT-dependent mechanisms of brain ageing involved in accumulation of senescence. Although these are preliminary data and require further confirmation, these results point to specific mechanisms that may be involved in the protective role of telomerase in the aged zebrafish brain, encouraging further investigation.

In conclusion, this study shows that zebrafish is a valuable model to study CNS ageing, in both the retina and brain. On one hand, thanks to its high regenerative capacity in the retina, at least in the context of acute injury, zebrafish was shown to be a unique model to explore new therapeutics aiming to prevent and/or delay degeneration of human retina. On the other hand, my data suggest that telomerase expression has a protective role against senescence accumulation in the aged zebrafish brain. This highlights the importance of investigating telomerase-dependent mechanisms of ageing in order to find potential therapeutic targets aiming to ameliorate brain health in ageing. Promisingly, this study opens new lines of investigation in both retina and brain ageing.

# Chapter 8.
# Bibliography

Acosta, J. C., Banito, A., Wuestefeld, T., Georgilis, A., Janich, P., Morton, J. P., … Gil, J. (2013). A complex secretory program orchestrated by the inflammasome controls paracrine senescence. *Nature Cell Biology*, *15*(8), 978–990. https://doi.org/10.1038/ncb2784

Aggarwal, P., Nag, T. C., & Wadhwa, S. (2007). Age-related decrease in rod bipolar cell density of the human retina: an immunohistochemical study. *J. Biosci.*, *32*(2), 293–298.

Ahmed, S., Passos, J. F., Birket, M. J., Beckmann, T., Brings, S., Peters, H., … Saretzki, G. (2008). Telomerase does not counteract telomere shortening but protects mitochondrial function under oxidative stress. *Journal of Cell Science*, *121*, 1046–1053. https://doi.org/10.1242/jcs.019372

Ain, Q., Schmeer, C., Penndorf, D., Fischer, M., Bondeva, T., Förster, M., … Kretz, A. (2018). Cell cycle-dependent and -independent telomere shortening accompanies murine brain aging. *Aging*, *10*(11), 3397–3420.

Alcaraz-pe, F., Garcia-Castillo, J., Garcia-Moreno, D., López-Muñoz, A., Anchelin, M., Angosto, D., … Cayuela, M. L. (2014). A non-canonical function of telomerase RNA in the regulation of developmental myelopoiesis. *Nature Communications*, *5*(3228), 1–11. https://doi.org/10.1038/ncomms4228

Allsopp, R. C., Chang, E., Kashefi-Aazam, M., Rogaev, E. I., Piatyszek, M. a, Shay, J. W., & Harley, C. B. (1995). Telomere shortening is associated with cell division in vitro and in vivo. *Experimental Cell Research*. https://doi.org/10.1006/excr.1995.1306

Allsopp, R. C., & Harley, C. B. (1995). Evidence for a critical telomere length in senescent human fibroblasts. *Experimental Cell Research*. https://doi.org/10.1006/excr.1995.1213

Altun, M., Bergman, E., Edström, E., Johnson, H., & Ulfhake, B. (2007). Behavioral impairments of the aging rat. *Physiology & Behavior*, *92*, 911–923. https://doi.org/10.1016/j.physbeh.2007.06.017

Alupei, M. C., Maity, P., Esser, P. R., Montanaro, L., Scharffetter-kochanek, K., Alupei, M. C., … Parlato, R. (2018). Loss of Proteostasis Is a Pathomechanism in Cockayne Syndrome Report Loss of Proteostasis Is a Pathomechanism in Cockayne Syndrome. *CellReports*, *23*(6), 1612–1619. https://doi.org/10.1016/j.celrep.2018.04.041

Anchelin, M., Alcaraz-Pérez, F., Martínez, C. M., Bernabé-García, M., Mulero, V., & Cayuela, M. L. (2013). Premature aging in telomerase-deficient zebrafish. *Disease Models & Mechanisms*, *6*(5), 1101–1112. https://doi.org/10.1242/dmm.011635

Anchelin, M., Murcia, L., Alcaraz-Pérez, F., García-Navarro, E. M., & Cayuela, M. L. (2011). Behaviour of telomere and telomerase during aging and regeneration in zebrafish. *PLoS ONE*, *6*(2). https://doi.org/10.1371/journal.pone.0016955

Andriani, G. A., Almeida, V. P., Faggioli, F., Mauro, M., Tsai, W. L., Santambrogio, L., … Montagna, C. (2016). Whole Chromosome Instability induces senescence and promotes SASP. *Scientific Reports*, *6*(October), 1–17. https://doi.org/10.1038/srep35218

Angele, S. (2018). Living longer: how our population is changing and why it matters. Retrieved from https://www.ons.gov.uk/peoplepopulationandcommunity/birthsdeathsandmarriages/ageing/articles/livinglongerhowourpopulationischangingandwhyitmatters/2018-08-13

Armanios, M. (2010). Syndromes of telomere shortening. *Annu Rev Genomics Hum Genet*, *40*(45), 1–21. https://doi.org/10.1146/annurev-genom-082908-150046.Syndromes

Armanios, M., Alder, J. K., Parry, E. M., Karim, B., Strong, M. A., & Greider, C. W. (2009). Short Telomeres are Sufficient to Cause the Degenerative Defects Associated with Aging. *American Journal of Human Genetics*, *85*(6), 823–832.

https://doi.org/10.1016/j.ajhg.2009.10.028
Armbruster, B. N., Banik, S. S. R., Guo, C., Smith, A. C., & Counter, C. M. (2001). N-Terminal Domains of the Human Telomerase Catalytic Subunit Required for Enzyme Activity in Vivo. *Molecular and Cellular Biology*, *21*(22), 7775–7786. https://doi.org/10.1128/MCB.21.22.7775
Arslan-Ergul, A., Erbaba, B., Karoglu, E. T., Halim, D. O., & Adams, M. M. (2016). Short-term dietary restriction in old zebrafish changes cell senescence mechanisms. *Neuroscience*, *334*, 64–75. https://doi.org/10.1016/j.neuroscience.2016.07.033
Baker, D. J., Childs, B. G., Durik, M., Wijers, M. E., Sieben, C. J., Zhong, J., … Van Deursen, J. M. (2016). Naturally occurring p16 Ink4a -positive cells shorten healthy lifespan. *Nature*, *530*(7589), 1–5. https://doi.org/10.1038/nature16932
Baker, D. J., Jeganathan, K. B., Cameron, J. D., Thompson, M., Juneja, S., Kopecka, A., … Deursen, J. M. Van. (2004). BubR1 insufficiency causes early onset of aging-associated phenotypes and infertility in mice. *Nature Genetics*, *36*(7), 744–749. https://doi.org/10.1038/ng1382
Baker, D. J., Perez-terzic, C., Jin, F., Pitel, K., Niederländer, N. J., Jeganathan, K., … Deursen, J. M. Van. (2008). Opposing roles for p16Ink4a and p19Arf in senescence and ageing caused by BubR1 insufficiency. *Nature Cell Biology*, *10*(7), 825–836. https://doi.org/10.1038/ncb1744.Opposing
Baltanás, F. C., Casafont, I., Lafarga, V., Weruaga, E., Alonso, J. R., Berciano, M. T., & Lafarga, M. (2011). Purkinje cell degeneration in pcd mice reveals large scale chromatin reorganization and gene silencing linked to defective DNA repair. *Journal of Biological Chemistry*, *286*(32), 28287–28302. https://doi.org/10.1074/jbc.M111.246041
Barnett, K., Mercer, S. W., Norbury, M., Watt, G., Wyke, S., & Guthrie, B. (2012). Epidemiology of multimorbidity and implications for health care, research, and medical education: A cross-sectional study. *The Lancet*, *380*(9836), 37–43. https://doi.org/10.1016/S0140-6736(12)60240-2
Bassi, G. S., Kanashiro, A., Santin, F. M., Souza, G. E. P. De, Nobre, M. J., & Coimbra, N. C. (2012). Lipopolysaccharide-Induced Sickness Behaviour Evaluated in Different Models of Anxiety and Innate Fear in Rats. *Basic & Clinical Pharmacology & Toxicology*, *110*, 359–369. https://doi.org/10.1111/j.1742-7843.2011.00824.x
Bednarek, D., González-rosa, J. M., Guzmán-martínez, G., Aguado, T., Sánchez-ferrer, C., Marques, I. J., … Flores, I. (2015). Telomerase Is Essential for Zebrafish Heart Regeneration. *Cell Reports*, *12*(10), 1691–1703. https://doi.org/10.1016/j.celrep.2015.07.064.Telomerase
Bernard, J. A., & Seidler, R. D. (2014). Moving Forward: Afe Effects on the Cerebellum Underlie Cognitive and Motor Decline. *Neuroscience & Biobehavioral Reviews*, *0*, 193–207. https://doi.org/10.1016/j.neubiorev.2014.02.011.Moving
Bernardos, R. L., Barthel, L. K., Meyers, J. R., & Raymond, P. A. (2007). Late-Stage Neuronal Progenitors in the Retina Are Radial Müller Glia That Function as Retinal Stem Cells. *The Journal of Immunology*, *27*(26), 7028–7040. https://doi.org/10.1523/JNEUROSCI.1624-07.2007
Bhat, R., Crowe, E. P., Bitto, A., Moh, M., Katsetos, C. D., Garcia, F. U., … Torres, C. (2012). Astrocyte Senescence as a Component of Alzheimer's Disease. *PLoS ONE*, *7*(9), 1–10. https://doi.org/10.1371/journal.pone.0045069
Bird, T. G., Müller, M., Boulter, L., Vincent, D. F., Ridgway, R. A., Lopez-Guadamillas, E., … Forbes, S. J. (2018). TGFβ inhibition restores a regenerative response in acute liver

injury by suppressing pracrine senescence. *Sci Transl Med.*, *10*(454), 1–30.
Bitto, A., Sell, C., Crowe, E., Lorenzini, A., Malaguti, M., Hrelia, S., & Torres, C. (2010). Stress-induced senescence in human and rodent astrocytes. *Experimental Cell Research*, *316*(17), 2961–2968. https://doi.org/10.1016/j.yexcr.2010.06.021
Bodnar, A. G., Ouellette, M., Frolkis, M., Holt, S. E., Chiu, C. P., Morin, G. B., … Wright, W. E. (1998). Extension of life-span by introduction of telomerase into normal human cells. *Science*, *279*(5349), 349–352. https://doi.org/10.1126/science.279.5349.349
Bonaz, B., Bazin, T., & Pellissier, S. (2018). The Vagus Nerve at the Interface of the Microbiota-Gut-Brain Axis. *Frontiers in Neuroscience*, *12*(49), 1–9. https://doi.org/10.3389/fnins.2018.00049
Boyer, N. P., Higbee, D., Currin, M. B., Blakeley, L. R., Chen, C., Ablonczy, Z., … Koutalos, Y. (2012). Lipofuscin and N-Retinylidene-N -Retinylethanolamine (A2E) Accumulate in Retinal Pigment Epithelium in Absence of Light Exposure. *The Journal of Biological Chemistry*, *287*(26), 22276–22286. https://doi.org/10.1074/jbc.M111.329235
Bringmann, A., Iandiev, I., Pannicke, T., Wurm, A., Hollborn, M., Wiedemann, P., … Reichenbach, A. (2009). Cellular signaling and factors involved in Müller cell gliosis: Neuroprotective and detrimental effects. *Progress in Retinal and Eye Research*, *28*(6), 423–451.
Brockerhoff, S. E., Hurleyt, J. B., Janssen-bienholdt, U., Neuhauss, S. C. F., Driever, W., & Dowling, J. E. (1995). A behavioral screen for isolating zebrafish mutants with visual system defects. *Proc. Matl. Acad. Sci. USA*, *92*, 10545–10549.
Brugman, S. (2016). The zebrafish as a model to study intestinal inflammation. *Developmental and Comparative Immunology*, *64*, 82–92. https://doi.org/10.1016/j.dci.2016.02.020
Burtner, C. R., & Kennedy, B. K. (2010). Progeria syndromes and ageing: what is the connection? *Nature Reviews. Molecular Cell Biology*, *11*(8), 567–578. https://doi.org/10.1038/nrm2944
Bussian, T. J., Aziz, A., Meyer, C. F., Swenson, B. L., van Deursen, J. M., & Baker, D. J. (2018). Clearance of senescent glial cells prevents tau-dependent pathology and cognitive decline. *Nature*, *562*, 578–599. https://doi.org/10.1038/s41586-018-0543-y
Cameron, D. A. (2000). Cellular proliferation and neurogenesis in the injured retina of adult zebrafish. *Visual Neuroscience*, *17*, 789–797.
Campisi, J., & d'Adda di Fagagna, F. (2007). Cellular senescence: when bad things happen to good cells. *Nature Reviews. Molecular Cell Biology*, *8*(9), 729–740. https://doi.org/10.1038/nrm2233
Cao, Y., Li, H., Deb, S., & Liu, J. (2002). TERT regulates cell survival independent of telomerase enzymatic activity. *Oncogene*, *21*, 3130–3138. https://doi.org/10.1038/sj/onc/1205419
Caporaso, G. L., Lim, D. A., Alvarez-Buylla, A., & Chao, M. V. (2003). Telomerase activity in the subventricular zone of adult mice. *Molecular and Cellular Neuroscience*, *23*(4), 693–702. https://doi.org/10.1016/S1044-7431(03)00103-9
Capper, R., Britt-Compton, B., Tankimanova, M., Rowson, J., Letsolo, B., Man, S., … Baird, D. M. (2007). The nature of telomere fusion and a definition of the critical telomere length in human cells. *Genes and Development*, *21*(19), 2495–2508. https://doi.org/10.1101/gad.439107
Carabotti, M., Scirocco, A., Maselli, M. A., & Severi, C. (2015). The gut-brain axis: Interactions between enteric microbiota, central and enteric nervous systems. *Annals*

*of Gastroenterology*, *28*(2), 203–209. https://doi.org/10.1038/ajgsup.2012.3
Carneiro, C., Henriques, C. M., Nabais, J., Ferreira, T., Carvalho, T., & Ferreira, M. G. (2016). Short Telomeres in Key Tissues Initiate Local and Systemic Aging in Zebrafish. *PLoS Genetics*, *12*(1), 1–31. https://doi.org/10.1371/journal.pgen.1005798
Carneiro, T., Khair, L., Reis, C. C., Borges, V., Moser, B. A., Nakamura, T. M., & Ferreira, M. G. (2010). Telomeres avoid end detection by severing the checkpoint signal transduction pathway. *Nature*, *467*(7312), 228–232. https://doi.org/10.1038/nature09353
Cheng, Y., Liu, P., Zheng, Q., Lu, Z., Guan, J., Wang, G., … Xie, L. (2018). Mitochondrial Trafficking and Processing of Report Mitochondrial Trafficking and Processing of Telomerase RNA TERC. *Cell Reports*, *24*(10), 2589–2595. https://doi.org/10.1016/j.celrep.2018.08.003
Childs, B. G., Baker, D. J., Wijshake, T., & Conover, C. A. (2016). Senescent intimal foam cells are deleterious at all stages of atherosclerosis. *Science*, *354*(6311), 472–477. https://doi.org/10.1126/science.aaf6659.Senescent
Choi, J., Southworth, L. K., Sarin, K. Y., Venteicher, A. S., Ma, W., Chang, W., … Artandi, S. E. (2008). TERT Promotes Epithelial Proliferation through Transcriptional Control of a Myc- and Wnt-Related Developmental Program. *PLoS Genetics*, *4*(1), 0124–0138. https://doi.org/10.1371/journal.pgen.0040010
Chu, C., Qu, K., Zhong, F., Artandi, S. E., & Chang, H. Y. (2012). Genomic maps of lincRNA occupancy reveal principles of RNA-chromatin interactions. *Molecular Cell*, *44*(4), 667–678. https://doi.org/10.1016/j.molcel.2011.08.027.Genomic
Coder B, Wang H, Ruan L, S. D. (2015). Thymic Involution Perturbs Negative Selection Leading to Autoreactive T Cells That Induce Chronic Inflammation. *Journal of Immunology*, *194*(12), 5825–5837. https://doi.org/10.1038/nbt.3121.ChIP-nexus
Collins, C. A., Zammit, P. S., Ruiz, A. P., Morgan, J. E., & Partridge, T. A. (2007). Population of Myogenic Stem Cells That Survives Skeletal AND. *Stem Cells*, *25*, 885–894. https://doi.org/10.1634/stemcells.2006-0372
Commission, E. (2018). Horizon 2020 Work Programme 2018-2020. Health, demographic change and wellbeing. https://doi.org/https://ec.europa.eu/research/participants/data/ref/h2020/wp/2018-2020/main/h2020-wp1820-health_en.pdf
Conedera, F. M., Pousa, A. M., Mercader, N., Tschopp, M., & Enzmann, V. (2019). Retinal microglia signaling affects Müller cell behavior in the zebrafish following laser injury induction. *Glia*, *67*(4).
Coppé, J.-P., Desprez, P.-Y., Krtolica, A., & Campisi, J. (2010). The senescence-associated secretory phenotype: the dark side of tumor suppression. *Annual Review of Pathology*, *5*, 99–118. https://doi.org/10.1146/annurev-pathol-121808-102144
Coppé, J.-P., Patil, C. K., Rodier, F., Sun, Y., Muñoz, D. P., Goldstein, J., … Campisi, J. (2008). Senescence-associated secretory phenotypes reveal cell-nonautonomous functions of oncogenic RAS and the p53 tumor suppressor. *PLoS Biology*, *6*(12), 2853–2868. https://doi.org/10.1371/journal.pbio.0060301
Counter, C. M., Hahn, W. C., Wei, W., Caddle, S. D., Beijersbergen, R. L., Lansdorp, P. M., … Weinberg, R. A. (1998). Dissociation among in vitro telomerase activity, telomere maintenance, and cellular immortalization. *Proc. Natl. Acad. Sci.*, *95*, 14723–14728.
Crowe, E. P., Tuzer, F., Gregory, B. D., Donahue, G., Gosai, S. J., Cohen, J., … Torres, C. (2016). Changes in the transcriptome of human astrocytes accompanying oxidative stress-induced senescence. *Frontiers in Aging Neuroscience*, *8*(AUG), 1–13.

https://doi.org/10.3389/fnagi.2016.00208
Cutler, R. G., & Mattson, M. P. (2006). Introduction: The adversities of aging. *Ageing Research Reviews*, *5*(3), 221–238. https://doi.org/10.1016/j.arr.2006.05.002
Da, S., Álvarez, S., Guerra, J., Cameán, D. S., Quelle, A., Barreiro, A., … Manuel, S. (2019). Cell senescence contributes to tissue regeneration in zebrafish, (July), 1–5. https://doi.org/10.1111/acel.13052
Damani, M. R., Zhao, L., Fontainhas, A. M., Amaral, J., Fariss, R. N., & Wong, W. T. (2011). Age-related Alterations in the Dynamic Behavior of Microglia. *Aging Cell*, *10*(2), 263–276. https://doi.org/10.1111/j.1474-9726.2010.00660.x.Age-related
Dambroise, E., Monnier, L., Ruisheng, L., Aguilaniu, H., Joly, J., Tricoire, H., & Rera, M. (2016). Two phases of aging separated by the Smurf transition as a public path to death. *Scientific Reports*, (March), 1–7. https://doi.org/10.1038/srep23523
Danilova, N., Kumagai, A., & Lin, J. (2010). p53 Upregulation Is a Frequent Response to Deficiency of Cell-Essential Genes, *5*(12). https://doi.org/10.1371/journal.pone.0015938
Deacon, K., & Knox, A. J. (2018). PINX1 and TERT Are Required for TNF-α–Induced Airway Smooth Muscle Chemokine Gene Expression. *The Journal of Immunology*, *200*, 1283–1294.
De Felice, B., Annunziata, A., Fiorentino, G., Manfellotto, F., D'Alessandro, R., Marino, R., … Biffali, E. (2014). Telomerase expression in amyotrophic lateral sclerosis (ALS) patients. *Journal of Human Genetics*, *59*(10), 555–561. https://doi.org/10.1038/jhg.2014.72
de Jong, P. R., González-Navajas, J. M., & Jansen, N. J. G. (2016). The digestive tract as the origin of systemic inflammation. *Critical Care (London, England)*, *20*(1), 279. https://doi.org/10.1186/s13054-016-1458-3
Demaria, M., Ohtani, N., Youssed, S., Rodier, F., Toussaint, W., Mitchell, J. R., … Campisi, J. (2014). An Essential Role for Senescent Cells in Optimal Wound Healing through Secretion of PDGF-AA. *Dev Cell*, *31*(6), 722–733. https://doi.org/10.1016/j.devcel.2014.11.012.An
Desgarnier, M. D., Zinflou, C., Mallet, J. D., Gendron, S. P., Méthot, S. J., & Rochette, P. J. (2016). Telomere Length Measurement in Different Ocular Structures: A Potential Implication in Corneal Endothelium Pathogenesis. *Biochemistry and Molecular Biology*, *57*(13), 5547–5555. https://doi.org/10.1167/iovs.16-19878
Deverman, B. E., & Patterson, P. H. (2009). Cytokines and CNS Development. *Neuron*, *64*(1), 61–78. https://doi.org/10.1016/j.neuron.2009.09.002
Dey, A., & Chakrabarti, K. (2018). Current Perspectives of Telomerase Structure and Function in Eukaryotes with Emerging Views on Telomerase in Human Parasites. *International Journal of Molecular Sciences*, *19*(333), 1–28. https://doi.org/10.3390/ijms19020333
Dimri, G. P., Lee, X., Basile, G., Acosta, M., Scott, G., Roskelley, C., … O, P.-S. (1995). A biomarker that identifies senescent human cells in culture and in aging skin in vivo. *Proc Natl Acad Sci*, *92*(20), 9363–9367. https://doi.org/10.1073/pnas.92.20.9363
Dow, C. T., & Harley, C. B. (2016). Evaluation of an oral telomerase activator for early age-related macular degeneration - a pilot study. *Clinical Ophtalmology*, *10*, 243–249.
*Clark DT (1981) Visual responses in the developing zebrafish (Brachydanio rerio) [Ph D].* Eugene: Univ. of Oregon.
Eastlake, K., Heywood, W. E., Tracey-white, D., Erika, A., Bliss, E., Vasta, G. R., … Limb, G. A. (2017). Comparison of proteomic profiles in the zebrafish retina during experimental

degeneration and regeneration. *Scientific Reports*, *7*(44601), 1–13. https://doi.org/10.1038/srep44601
Eden, E., Navon, R., Steinfeld, I., Lipson, D., & Yakhini, Z. (2009). GOrilla: a tool for discovery and visualization of enriched GO terms in ranked gene lists. *BMC Bioinformatics*, *10*(48), 1–7. https://doi.org/10.1186/1471-2105-10-48
Egan, E. D., & Collins, K. (2012). An Enhanced H/ACA RNP Assembly Mechanism for Human Telomerase RNA. *Molecular and Cellular Biology*, *32*(13), 2428–2439. https://doi.org/10.1128/MCB.00286-12
Eitan, E., Tichon, A., Gazit, A., Gitler, D., Slavin, S., & Priel, E. (2012). Novel telomerase-increasing compound in mouse brain delays the onset of amyotrophic lateral sclerosis. *EMBO Molecular Medicine*, *4*(4), 313–329. https://doi.org/10.1002/emmm.201200212
Ellett, F., Pase, L., Hayman, J. W., Andrianopoulos, A., & Lieschke, G. J. (2011). mpeg1 promoter transgenes direct macrophage-lineage expression in zebrafish. *Blood*, *117*(4), 49–57. https://doi.org/10.1182/blood-2010-10-314120.The
Eriksson, U., & Alm, A. (2009). Macular thickness decreases with age in normal eyes: a study on the macular thickness map protocol in the Stratus OCT. *British Journal of Ophtalmology*, *93*(11).
Ernst, J., & Bar-joseph, Z. (2006). STEM : a tool for the analysis of short time series gene expression data. *BMC Bioinformatics*, *11*, 1–11. https://doi.org/10.1186/1471-2105-7-191
European Commission Directorate-General for Economic and Financial Affairs. (2015). *The 2015 Ageing Report Economic and budgetary projections for the 28 EU Member States (2013-2060)* (Vol. 2015 (3)). https://doi.org/10.2765/877631
Evans, R. J., Wyllie, F. S., Wynford-thomas, D., Kipling, D., & Jones, C. J. (2003). A P53-dependent , Telomere-independent Proliferative Life Span Barrier in Human Astrocytes Consistent with the Molecular Genetics of Glioma Development 1. *American Association for Cancer Research*, *63*, 4854–4861.
Farmen, E., Hultman, M. T., Anglès, M., & Erik, K. (2014). Development of a Screening System for the Detection of Chemically Induced DNA Methylation Alterations in a Zebrafish Liver Cell Line. *Journal of Toxicology and Environmental Health, Part A*, *77*(9--11), 587–599. https://doi.org/10.1080/15287394.2014.887423
Ferreira, M. G., Miller, K. M., Cooper, J. P., & Fields, I. (2004). Indecent Exposure: When Telomeres Become Uncapped. *Molecular Cell*, *13*, 7–18.
Ferron, S. R., Marques-Torrejon, M. A., Mira, H., Flores, I., Taylor, K., Blasco, M. A., & Farinas, I. (2009). Telomere Shortening in Neural Stem Cells Disrupts Neuronal Differentiation and Neuritogenesis. *Journal of Neuroscience*, *29*(46), 14394–14407. https://doi.org/10.1523/JNEUROSCI.3836-09.2009
Fischer, A. J., & Reh, T. A. (2001). Müller glia are a potential source of neural regeneration in the postnatal chicken retina. *Nature Neuroscience*, *4*, 247–252.
Flanary, B. E., & Streit, W. J. (2004). Progressive Telomere Shortening Occurs in Cultured Rat Microglia, but Not Astrocytes. *Glia*, *45*(1), 75–88. https://doi.org/10.1002/glia.10301
Fleming, A., Diekmann, H., & Goldsmith, P. (2013). Functional Characterisation of the Maturation of the Blood-Brain Barrier in Larval Zebrafish, *8*(10), 1–12. https://doi.org/10.1371/journal.pone.0077548
Forsyth, N. R., Wright, W. E., & Shay, J. W. (2002). Telomerase and differentiation in multicellular organisms: Turn it off, turn it on, and turn it off again. *Differentiation*, *69*(4–5), 188–197.

Fortin, M., Lapointe, L., Hudon, C., Vanasse, A., Ntetu, A. L., & Maltais, D. (2004). Multimorbidity and quality of life in primary care: a systematic review. *Health and Quality of Life Outcomes*, *2*(1), 51-. https://doi.org/10.1186/1477-7525-2-51

Franceschi, C., & Campisi, J. (2014). Chronic inflammation (Inflammaging) and its potential contribution to age-associated diseases. *Journals of Gerontology - Series A Biological Sciences and Medical Sciences*, *69*, S4–S9. https://doi.org/10.1093/gerona/glu057

Freund A, Orjalo A, Desprez P, C. J. (2010). Inflammatory Networks during Cellular Senescence: Causes and Consequences. *Trends of Molecular Medicine*, *16*(5), 238–246. https://doi.org/10.1016/j.immuni.2010.12.017.Two-stage

Fu, J., Nagashima, M., Guo, C., Raymond, P. A., & Wei, X. (2018). Novel Animal Model of Crumbs-Dependent Progressive Retinal Degeneration That Targets Specific Cone Subtypes. *Retinal Cell Biology*, *59*, 505–518.

Fülöp, T., Dupuis, G., Witkowski, J. M., & Larbi, A. (2016). The role of immunosenescence in the development of age-related diseases. *Revista de Investigacion Clinica*, *68*(2), 84–91.

Gabriel, D., Gordon, L. B., & Djabali, K. (2016). Temsirolimus Partially Rescues the Hutchinson-Gilford Progeria Cellular Phenotype, 1–25. https://doi.org/10.1371/journal.pone.0168988

Gage, F. H. (2000). Mammalian Neural Stem Cells. *Science*, *287*(5457), 1433–1438. https://doi.org/10.1126/science.287.5457.1433

Ganong, W. (2000). Circumventricular Organs: Definition And Role In The Regulation Of Endocrine And Autonomic Function. *Clinical and Experimental Pharmacology and Physiology*, *27*, 422–247.

Gao, H., & Hollyfield, J. (1992). Aging of the human retina. Differential loss of neurons and retinal pigment epithelial cells. *Invest Ophthalmol Vis Sci.*, *33*(1), 1–17.

Ghosh, A., Saginc, G., Leow, S. C., Khattar, E., Shin, E. M., Yan, T. D., … Tergaonkar, V. (2012). Telomerase directly regulates NF- κ B-dependent transcription. *Nature Cell Biology*, *14*(12), 1270–1281. https://doi.org/10.1038/ncb2621

Gizard, F., Heywood, E. B., Findeisen, H. M., Zhao, Y., Karrie, L., Cudejko, C., … Staels, B. (2011). Telomerase Activation in Atherosclerosis and Induction of Telomerase Reverse Transcriptase Expression by Inflammatory Stimuli in Macrophages. *Arterioscler Thromb Vasc Biol.*, *31*(2), 245–252. https://doi.org/10.1161/ATVBAHA.110.219808.Telomerase

Gjoerup, O. V, Wu, J., Chandler-militello, D., Williams, G. L., Zhao, J., Schaffhausen, B., … Roberts, T. M. (2007). Surveillance mechanism linking Bub1 loss to the p53 pathway. *PNAS*, *104*(20), 8334–8339.

Goodman, W. A., & Jain, M. K. (2011). Length Does Not Matter. *Arterioscler Thromb Vasc Biol.*, *31*(2), 235–236. https://doi.org/10.1161/ATVBAHA.110.220343

Grandel, H., Kaslin, J., Ganz, J., Wenzel, I., & Brand, M. (2006). Neural stem cells and neurogenesis in the adult zebrafish brain : Origin , proliferation dynamics , migration and cell fate. *Developmental Biology*, *295*, 263–277. https://doi.org/10.1016/j.ydbio.2006.03.040

Greider, C. W., & Blackburn, E. H. (1985). Identification of a Specific Telomere Terminal Transferase Activity in Tetrahymena Extracts. *Cell*, *43*(December), 405–413.

Gross, N. E., Aizman, A., Brucker, A., Klancnik, J. J., & Yannuzzi, L. A. (2005). Nature and risk of neovascularization in the fellow eye of patients with unilateral retinal angiomatous proliferation. *The Journal of Retinal and Vitreous Diseases*, *25*(6), 713–718.

Haendeler, J., Dro, S., Bu, N., Jakob, S., Altschmied, J., Goy, C., … Dimmeler, S. (2009). Mitochondrial Telomerase Reverse Transcriptase Binds to and Protects Mitochondrial

DNA and Function From Damage. *Arterioscler Thromb Vasc Biol.*, *29*, 929–935. https://doi.org/10.1161/ATVBAHA.109.185546

Hall, B. M., Balan, V., Gleiberman, A. S., Strom, E., Krasnov, P., Virtuoso, L. P., … Gudkov, A. V. (2017). p16(Ink4a) and senescence-associated β-galactosidase can be induced in macrophages as part of a reversible response to physiological stimuli. *Aging*, *9*(8), 1867–1884.

Hanovice, N. J., Leach, L. L., Slater, K., Gabriel, A. E., Romanovicz, D., Shao, E., … Gross, J. M. (2019). Regeneration of the zebrafish retinal pigment epithelium after widespread genetic ablation. *PLoS Genetics*, 1–35.

Hayflick, L. (1965). The limited in vitro lifetime of human diploid cell strains. *Experimental Cell Research*, *37*(3), 614–636. https://doi.org/10.1016/0014-4827(65)90211-9

Hayflick, L., & Moorhead, P. S. (1961). The serial cultivation of human diploid cell strains. *Experimental Cell Research*, *25*(3), 585–621. https://doi.org/10.1016/0014-4827(61)90192-6

Heidinger, B. J., Blount, J. D., Boner, W., Griffiths, K., Metcalfe, N. B., & Monaghan, P. (2012). Telomere length in early life predicts lifespan. *Proceedings of the National Academy of Sciences of the United States of America*, *109*(5), 1743–1748. https://doi.org/10.1073/pnas.1113306109

Hemann, M. T., & Greider, C. W. (2000). Wild-derived inbred mouse strains have short telomeres. *Nucleic Acids Research*, *28*(22), 4474–4478. https://doi.org/10.1093/nar/28.22.4474

Henriques, C. M., Carneiro, M. C., Tenente, I. M., Jacinto, A., & Ferreira, M. G. (2013). Telomerase Is Required for Zebrafish Lifespan. *PLoS Genetics*, *9*(1). https://doi.org/10.1371/journal.pgen.1003214

Henriques, C. M., & Ferreira, M. G. (2012). Consequences of telomere shortening during lifespan. *Current Opinion in Cell Biology*, *24*(6), 804–808.

Hernandez-Segura, A., de Jong, T. V., Melov, S., Guryev, V., Campisi, J., & Demaria, M. (2017). Unmasking Transcriptional Heterogeneity in Senescent Cells. *Current Biology*, *27*(17), 2652–2660.e4. https://doi.org/10.1016/j.cub.2017.07.033

Hernandez-Segura, A., Nehme, J., & Demaria, M. (2018). Hallmarks of Cellular Senescence. *Trends in Cell Biology*, *xx*, 1–18. https://doi.org/10.1016/j.tcb.2018.02.001

Hewitt, G., Jurk, D., Marques, F. D. M., Correia-Melo, C., Hardy, T., Gackowska, A., … Passos, J. F. (2012). Telomeres are favoured targets of a persistent DNA damage response in ageing and stress-induced senescence. *Nature Communications*, *3*. https://doi.org/10.1038/ncomms1708

Heyn, H., Moran, S., & Esteller, M. (2013). Aberrant DNA methylation profiles in the premature aging disorders Hutchinson-Gilford Progeria and Werner syndrome. *Epigenetics*, *8*(1), 28–33.

Hickson, L. J., Langhi, L. G. P., Bobart, S. A., Evans, T. K., Giorgadze, N., Hashmi, S. K., … Kirkland, J. L. (2019). Senolytics decrease senescent cells in humans: Preliminary report from a clinical trial of Dasatinib plus Quercetin in individuals with diabetic kidney disease. *EBioMedicine*, *47*, 446–456. https://doi.org/10.1016/j.ebiom.2019.08.069

Hiyama, K., Hirai, Y., Kyoizumi, S., Akiyama, M., Hiyama, M., Piatyszek, M., … Yamakido, M. (1995). Activation of telomerase in human lymphocytes and hematopoietic progenitor cells. *Journal of Immunology*, *155*(8), 3711–3715.

Holz, F. G., Bellman, C., Staudt, S., & Schu, F. (2001). Fundus Autofluorescence and Development of Geographic Atrophy in Age-Related Macular Degeneration.

*Investigative Ophthalmology & Visual Science*, *42*(5), 1051–1056.
Howe, K., Clark, M., Torroja, C., Torrance, J., Berthelot, C., Muffato, M., Collins J., Humphray, S. … Stemple, D. (2013). The zebrafish reference genome sequence and its relationship to the human genome.*Nature, 496*, 498-503. https://doi.org/10.1038/nature12111
Hudson, G., Faini, D., Stutt, A., Eccles, M., Robinson, L., Burn, D. J., & Chinnery, P. F. (2011). No evidence of substantia nigra telomere shortening in Parkinson's disease. *Neurobiology of Aging*, *32*(11), 172–175. https://doi.org/10.1016/j.neurobiolaging.2011.05.022
Imamura, S., Uchiyama, J., Koshimizu, E., Hanai, J., Raftopoulou, C., Murphey, R. D., … Kishi, S. (2008). A Non-Canonical Function of Zebrafish Telomerase Reverse Transcriptase Is Required for Developmental Hematopoiesis. *Plos ONE*, *3*(10), 1–20. https://doi.org/10.1371/journal.pone.0003364
Iribarne, M., Hyde, D. R., Masai, I. & Roger, J. E. (2019). TNFα Induces Müller Glia to Transition From Non-proliferative Gliosis to a Regenerative Response in Mutant Zebrafish Presenting Chronic Photoreceptor Degeneration. *Frontiers in Cell and Developmental Biology*, *7*(296), 1–14. https://doi.org/10.3389/fcell.2019.00296
Itou, J., Kawakami, H., Burgoyne, T., & Kawakami, Y. (2012). Life-long preservation of the regenerative capacity in the fin and heart in zebrafish. *Biology Open*, *1*, 739–746. https://doi.org/10.1242/bio.20121057
Jackson, S. P., & Bartek, J. (2010). The DNA-damage response in human biology and disease. *Nature*, *461*(7267), 1071–1078. https://doi.org/10.1038/nature08467.The
Jadhav, A. P., Roesch, K., & Cepko, C. L. (2009). Development and Neurogenetic Potential of Müller Glial Cells in the Vertebrate Retina. *Prog Retin Eye Res.*, *28*(4), 249–262. https://doi.org/10.1016/j.preteyeres.2009.05.002.DEVELOMENT
Jaskelioff, M., Muller, F. L., Paik, J., Thomas, E., Jiang, S., Sahin, E., … Depinho, R. a. (2011). Telomerase reactivation reverses tissue degeneration in aged telomerase deficient mice. *Nature*, *469*(7328), 102–106. https://doi.org/10.1038/nature09603.Telomerase
Jeck, W. R., Siebold, A. P., & Sharpless, N. E. (2012). Review: A meta-analysis of GWAS and age-associated diseases. *Aging Cell*, *11*(5), 727–731. https://doi.org/10.1111/j.1474-9726.2012.00871.x
Jeong, J.-Y., Kwon, H.-B., Ahn, J.-C., Kang, D., Kwon, S.-H., Park, J. A., & Kim, Kyu, W. (2008). Functional and developmental analysis of the blood-brain barrier in zebrafish. *Brain Research Bulletin*, *75*(5), 619–628.
Jeyapalan. (2007). Accumulation of Senescent Cells in Mitotic Tissue of Aging Primates. *Biophysical Chemistry*, *128*(1), 36–44. https://doi.org/10.1016/j.immuni.2010.12.017.Two-stage
Johns, P. F., & Fernald, R. D. (1981). Genesis of rods in teleost fish retina. *Nature*, *293*, 141–142.
Jorstad, N. L., Wilken, M. S., Gimes, W. N., Wohl, S. G., VandenBosh, L. S., Yoshimatsu, T., … Reh, T. A. (2017). Stimulation of functional neuronal regeneration from Müller glia in adult mice. *Nature*, *548*(7665), 103–107. https://doi.org/10.1038/nature23283.Stimulation
Jorstad, N. L., Wilken, M. S., Todd, L., Wilkerson, B. A., Rieke, F., Reh, T. A., … Radulovich, N. (2020). STAT Signaling Modifies Ascl1 Chromatin Binding and Limits Neural Regeneration from Muller Glia in Adult Mouse Retina. *Cell Reports*, *30*, 2195–2208. https://doi.org/10.1016/j.celrep.2020.01.075
Jose, S. S., Tidu, F., Burilova, P., Kepak, T., Bendickova, K., & Fric, J. (2018). The Telomerase

Complex Directly Controls Hematopoietic Stem Cell Differentiation and Senescence in an Induced Pluripotent Stem Cell Model of Telomeropathy. *Frontiers in Genetics*, *9*(August), 1–19. https://doi.org/10.3389/fgene.2018.00345

Julian, D., Ennis, K., & Korenbrot, J. I. (1998). Birth and fate of proliferative cells in the inner nuclear layer of the mature fish retina. *Journal of Comparative Neurology*, *394*(3), 271–282.

Jurk, D., Wang, C., Miwa, S., Maddick, M., Korolchuk, V., Tsolou, A., … von Zglinicki, T. (2012). Postmitotic neurons develop a p21-dependent senescence-like phenotype driven by a DNA damage response. *Aging Cell*, *11*(6), 996–1004. https://doi.org/10.1111/j.1474-9726.2012.00870.x

Justice, J. N., Nambiar, A. M., Tchkonia, T., Lebrasseur, N. K., Pascual, R., Hashmi, S. K., … Kirkland, J. L. (2019). Senolytics indidiopathic pulmonary fibrosis: Results from a first-in-human, open-label, pilot study. *EBioMedicine*, *40*, 554–563. https://doi.org/10.1016/j.ebiom.2018.12.052

Kalueff, A., & Cachat, J. (2011). *Zebrafish Models in Neurobehavioral Research*. https://doi.org/10.1016/S1573-4285(04)80400-9

Kalueff, A., Gebhardt, M., Stewart, A. M., Cachat, J. M., Brimmer, M., Chawla, J. S., … Schneider, and the Zebrafish Neuros, H. (2013). Towards a Comprehensive Catalog of Zebrafish Behavior 1.0 and Beyond. *Zebrafish*, *10*(1), 70–86. https://doi.org/10.1089/zeb.2012.0861

Kang, T.-W., Yevsa, T., Woller, N., Hoenicke, L., Wuestefeld, T., Dauch, D., … Zender, L. (2011). Senescence surveillance of pre-malignant hepatocytes limits liver cancer development. *Nature*, *479*(7374), 547–551. https://doi.org/10.1038/nature10599

Karl, M. O., Hayes, S., Nelson, B. R., Tan, K., Buckingham, B., & Reh, T. A. (2008). Stimulation of neural regeneration in the mouse retina. *PNAS*, *9*, 19508–19513.

Keatinge, M., Bui, H., Menke, A., Chen, Y., Sokol, A. M., Bai, Q., … Bandmann, O. (2015). Glucocerebrosidase 1 de fi cient Danio rerio mirror key pathological aspects of human Gaucher disease and provide evidence of early microglial activation preceding alpha-synuclein-independent neuronal cell death. *Human Molecular Genetics*, *24*(23), 6640–6652. https://doi.org/10.1093/hmg/ddv369

Kim, C., Sung, S., & Lee, J. (2016). Internal genomic regions mobilized for telomere maintenance in *C. elegans*. *Worm*, *5*(1), e1146856. https://doi.org/10.1080/21624054.2016.1146856

Kim, H., Cho, J. H., & Kim, J. (2013). Downregulation of Polo-Like Kinase 1 Induces Cellular Senescence in Human Primary Cells Through a p53-Dependent Pathway. *Journal of Gerontology: Biological Sciences*, *68*(10), 1145–1156. https://doi.org/10.1093/gerona/glt017

Kim, H., Cho, J. H., Quan, H., & Kim, J. (2011). Down-regulation of Aurora B kinase induces cellular senescence in human fibroblasts and endothelial cells through a p53-dependent pathway. *FEBS Letters*, *585*(22), 3569–3576. https://doi.org/10.1016/j.febslet.2011.10.022

Kim, N., Piatyszek, M., Prowse, K., Harley, C., West, M., Ho, P., … Shay, J. (1994). Specific association of human telomerase activity with immortal cells and cancer. *Science*, *Vol. 266*(5193), 2011–2015.

Kishi, S., Bayliss, P. E., Uchiyama, J., Koshimizu, E., Qi, J., Nanjappa, P., … Roberts, T. M. (2008). The identification of zebrafish mutants showing alterations in senescence-associated biomarkers. *PLoS Genetics*, *4*(8).

https://doi.org/10.1371/journal.pgen.1000152
Knogler, L. D., Kist, A. M., & Portugues, R. (2019). Motor context dominates output from purkinje cell functional regions during reflexive visuomotor behaviours. *eLife*, *8*(42138), 1–36.
Koga, H., Kaushik, S., & Cuervo, a M. (2012). Protein Homeostasis and Aging: the importance of exquisite quality control. *Ageing Res. Rev.*, *10*(2), 205–215. https://doi.org/10.1016/j.arr.2010.02.001.Protein
Kokkinopoulos, I., Shahabi, G., Colman, A., & Jeffrery, G. (2011). Mature Peripheral RPE Cells Have an Intrinsic Capacity to Proliferate; A Potential Regulatory Mechanism for Age-Related Cell Loss. *Plos ONE*, *6*(4), 1–10. https://doi.org/10.1371/journal.pone.0018921
Krishnamurthy, J., Torrice, C., Ramsey, M. R., Kovalev, G. I., Al-regaiey, K., Su, L., & Sharpless, N. E. (2004). Ink4a/Arf expression is a biomarker of aging. *Journal of Clinical Investigation*, *114*(9), 1299–1307. https://doi.org/10.1172/JCI200422475.The
Krizhanovsky, V., Yon, M., Dickins, R. A., Hearn, S., Simon, J., Miething, C., … Lowe, S. W. (2008). Senescence of Activated Stellate Cells Limits Liver Fibrosis. *Cell*, *134*(4), 657–667. https://doi.org/10.1016/j.cell.2008.06.049
Lai, C. K., Mitchell, J. R., & Collins, K. (2001). RNA Binding Domain of Telomerase Reverse Transcriptase. *Molecular and Cellular Biology*, *21*(4), 990–1000. https://doi.org/10.1128/MCB.21.4.990
Lai, T., Wright, W. E., Shay, J. W., & Shay, J. W. (2018). Comparison of telomere length measurement methods. *Phil. Trnas. R. Soc.*, *373*, 1–10.
Lai, T., Zhang, N., Noh, J., Mender, I., Tedone, E., Huang, E., … Shay, J. W. (2017). A method for measuring the distribution of the shortest telomeres in cells and tissues. *Nature Communications*, *8*(1356), 1–13. https://doi.org/10.1038/s41467-017-01291-z
Lange, T. de. (2004). T-loops and the origin of telomeres. *Nature Reviews. Molecular Cell Biology*, *5*, 3–9.
Lawrence, C. (2007). The husbandry of zebrafish (Danio rerio): A review. *Aquaculture*, *269*(1–4), 1–20. https://doi.org/10.1016/j.aquaculture.2007.04.077
Le, O., Palacio, L., Bernier, G., Batinic-Haberle, I., Hickson, G., & Beauséjour, C. (2018). INK4a/ARF Expression Impairs Neurogenesis in the Brain of Irradiated Mice. *Stem Cell Reports*, *10*(6), 1721–1733. https://doi.org/10.1016/j.stemcr.2018.03.025
Lee, B. Y., Han, J. A., Im, J. S., Morrone, A., Johung, K., Goodwin, E. C., … Hwang, E. S. (2006). Senescence-associated β-galactosidase is lysosomal β-galactosidase. *Aging Cell*, *5*(2), 187–195. https://doi.org/10.1111/j.1474-9726.2006.00199.x
Lee, H.-W., Blasco, M. A., Gottlieb, G. J., II, J. W. H., Greider, C. W., & DePinho, R. A. (1998). Essential role of mouse telomerase in highly proliferative organs. *Nature*, *392*, 569–574.
Lee, J., Jo, Y. S., Sung, Y. H., Hwang, I. K., Kim, H., Kim, S. Y., … Lee, H. W. (2010). Telomerase deficiency affects normal brain functions in mice. *Neurochemical Research*, *35*(2), 211–218. https://doi.org/10.1007/s11064-009-0044-3
Lenkowski, J. R., & Raymond, P. A. (2014). Müller glia: Stem cells for generation and regeneration of retinal neurons in teleost fish Jenny. *Prog Retin Eye Res.*, *0*, 94–123. https://doi.org/10.1016/j.preteyeres.2013.12.007.M
Lessieur, E. M., Id, P. S., Nivar, G. C., Piccillo, E. M., Fogerty, J., Rozic, R., & Id, B. D. P. (2019). Ciliary genes arl13b, ahi1 and cc2d2a differentially modify expression of visual acuity phenotypes but do not enhance retinal degeneration due to mutation of cep290 in zebrafish. *Plos ONE*, *14*(4), 1–26.

Levy, M. Z., Allsopp, R. C., Futcher, A. B., Greider, C. W., & Harley, C. B. (1992). Telomere end-replication problem and cell aging. *Journal of Molecular Biology*, *225*(4), 951–960. https://doi.org/10.1016/0022-2836(92)90096-3

Lin, S., Nascimento, E. M., Gajera, C., Chen, L., Garbuzov, A., Wang, S., … Program, B. (2018). Distributed hepatocytes expressing telomerase repopulate the liver in homeostasis and injury. *Nature*, *556*(7700), 244–248. https://doi.org/10.1038/s41586-018-0004-7.Distributed

Linkus, B., Wiesner, D., Mebner, M., Karabatsiakis, A., Scheffold, A., Rudolph, K. L., … Danzer, K. M. (2016). Telomere shortening leads to earlier age of onset in ALS mice. *Aging*, *8*(2), 382–393. https://doi.org/10.18632/aging.100904

Livak, K. J., & Schmittgen, T. D. (2001). Analysis of Relative Gene Expression Data Using Real-Time Quantitative PCR and the 2 Χ  C T Method, *408*, 402–408. https://doi.org/10.1006/meth.2001.1262

López-Otín, C., Blasco, M. A., Partridge, L., & Serrano, M. (2013). The Hallmarks of Aging. *Cell*, *153*(6), 1194–1217. https://doi.org/10.1016/j.cell.2013.05.039.The

Louveau, A., Smirnov, I., Keyes, T. J., Eccles, J. D., Rouhani, S. J., Peske, J. D., … Kipnis, J. (2015). Structural and functional features of central nervous system lymphatic vessels. *Nature*, *523*(7560), 337–341. https://doi.org/10.1038/nature14432

Lukens, J. N., Deerlin, V. Van, Clark, C. M., Xie, S. X., & Johnson, F. B. (2009). Comparisons of telomere lengths in peripheral blood and cerebellum in Alzheimer's disease. *Alzheimers Dement*, *5*(6), 463–469. https://doi.org/10.1111/j.1743-6109.2008.01122.x.Endothelial

Maciejowski, J., & Lange, T. De. (2017). Telomeres in cancer: tumour suppression and genome instability. *Nature Reviews Molecular Cell Biology*, *18*, 175–187. https://doi.org/10.1038/nrm.2016.171

Majji, A. B., Cao, J., Chang, K. Y., Hayashi, A., & Aggarwal, S. (2000). Age-Related Retinal Pigment Epithelium and Bruch's Membrane Degeneration in Senescence-Accelerated Mouse. *Investigative Ophthalmology & Visual Science*, *41*(12), 3936–3942.

Man, A. L., Bertelli, E., Rentini, S., Regoli, M., Briars, G., Marini, M., … Nicoletti, C. (2015). Age-associated modifications of intestinal permeability and innate immunity in human small intestine. *Clinical Science*, *129*, 515–527. https://doi.org/10.1042/CS20150046

Marazita, M. C., Dugour, A., Marquioni-ramella, M. D., Figueroa, J. M., & Suburo, A. M. (2016). Redox Biology Oxidative stress-induced premature senescence dysregulates VEGF and CFH expression in retinal pigment epithelial cells: Implications for Age-related Macular Degeneration. *Redox Biology*, *7*, 78–87. https://doi.org/10.1016/j.redox.2015.11.011

Marengoni, A., Pasina, L., Concoreggi, C., Martini, G., Brognoli, F., Nobili, A., … Bettoni, D. (2014). Understanding adverse drug reactions in older adults through drug-drug interactions. *European Journal of Internal Medicine*, *25*(9), 843–846. https://doi.org/10.1016/j.ejim.2014.10.001

Marengoni, A., Rizzuto, D., Wang, H. X., Winblad, B., & Fratiglioni, L. (2009). Patterns of chronic multimorbidity in the elderly population. *Journal of the American Geriatrics Society*, *57*(2), 225–230. https://doi.org/10.1111/j.1532-5415.2008.02109.x

Marshall, J. (1987). The Ageing Retina: Physiology or Pathology. *Eye*, *1*, 282–295. https://doi.org/10.1038/eye.1987.47

Marshall, J. C., Christou, N. V, Horn, R., & Meakins, J. L. (1988). Microbiology of Multiple Organ Failure Occult Reservoir of Pathogens. *Analysis*, *132*, 309–315.

Martins, R., McCracken, A., Simons, M., Henriques, C., & Rera, M. (2018). How to Catch a

Smurf? – Ageing and Beyond…In vivo Assessment of Intestinal Permeability in Multiple Model Organisms. *Bio-Protocol*, *7*(3), 1–13. https://doi.org/10.21769/BioProtoc.2722
Mason, A. (2012). Responses of Human Embryonic Stem Cells and Their Differentiated Progeny to Ionizing Radiation. *Biochem Biophys Res Commun.*, *426*(1), 100–105. https://doi.org/10.1016/j.asieco.2008.09.006.EAST
Matsui, H., Namikawa, K., Babaryka, A., & Köster, R. W. (2014). Functional regionalization of the teleost cerebellum analyzed in vivo. *PNAS*, *111*(32), 11846–11851. https://doi.org/10.1073/pnas.1403105111
Matsunaga, H., Handa, J. T., Aotaki-keen, A. A., Sherwood, S. W., West, M. D., & Hjelmeland, L. M. (1999). B-Galactosidase Histochemistry and Telomere Loss in Senescent Retinal Pigment Epithelial Cells. *Invest Ophthalmol Vis Sci.*, *40*(1), 197–202.
Matteoli, G., Gomez-Pinilla, P. J., Nemethova, A., Di Giovangiulio, M., Cailotto, C., van Bree, S. H., … Boeckxstaens, G. E. (2014). A distinct vagal anti-inflammatory pathway modulates intestinal muscularis resident macrophages independent of the spleen. *Gut*, *63*, 938–948. https://doi.org/10.1136/gutjnl-2013-304676
Mattiussi, M., Tilman, G., Lenglez, S., & Decottignies, A. (2012). Human telomerase represses ROS-dependent cellular responses to Tumor Necrosis Factor-α without affecting NF-κB activation. *Cellular Signalling*, *24*, 708–717.
McClure, M. M., McIntyre, P. B., & McCune, A. R. (2006). Notes on the natural diet and habitat of eight danionin fishes, including the zebrafish Danio rerio. *Journal of Fish Biology*, *69*(2), 553–570. https://doi.org/10.1111/j.1095-8649.2006.01125.x
Meeker, R. B., Williams, K., Killebrew, D. A., & Hudson, L. C. (2012). Cell trafficking through the choroid plexus. *Cell Adhesion & Migration*, *6*(5), 390–396.
Meneses, G., Bautista, M., Florentino, A., Díaz, G., Acero, G., Besedovsky, H., … Sciutto, E. (2016). Electric stimulation of the vagus nerve reduced mouse neuroinflammation induced by lipopolysaccharide. *Journal of Inflammation*, *13*(33), 1–11. https://doi.org/10.1186/s12950-016-0140-5
Michael, M., Jessica, A., Tammy, B., Peter, G., & Joana, M. (2020). *Health equity in England: The Marmot Review 10 years on. London: Institute of Health Equity*.
Ming, G., & Song, H. (2011). Adult Neurogenesis in the Mammalian Brain: Significant Answers and Significant Questions. *Neuron*, *70*(4), 687–702. https://doi.org/10.1016/j.neuron.2011.05.001.Adult
Mishima, K., Handa, J. T., Aotaki-keen, A., Lutty, G. A., Morse, L. S., & Hjelmeland, L. M. (1999). Senescence-Associated B-Galactosidase Histochemistry for the Primate Eye. *IOVS*, *40*(7), 1590–1593.
Mitchell, D. M., Sun, C., Hunter, S. S., New, D. D., & Stenkamp, D. L. (2019). Regeneration associated transcriptional signature of retinal microglia and macrophages. *Scientific Reports*, *9*(4768), 1–17. https://doi.org/10.1038/s41598-019-41298-8
Mitchell, J. R., Cheng, J., & Collins, K. (1999). A Box H/ACA Small Nucleolar RNA-Like Domain at the Human Telomerase RNA 3' End. *Molecular and Cellular Biology*, *19*(1), 567–576.
Mitchell, J. R., Collins, K., & Rnas, T. (2000). Human Telomerase Activation Requires Two Independent Interactions between Telomerase RNA and Telomerase Reverse Transcriptase. *Molecular Cell*, *6*, 361–371.
Moens, C. B., & Prince, V. E. (2002). Constructing the Hindbrain: Insights From the Zebrafish. *Developmental Dynamics*, *224*, 1–17. https://doi.org/10.1002/dvdy.10086
Molofsky, A. V, Slutsky, S. G., Joseph, N. M., He, S., Krishnamurthy, J., Sharpless, N. E., & Morrison, S. J. (2006). Increasing p16INK4a expression decreases forebrain progenitors

and neurogenesis during ageing. *Nature*, *443*(7110), 448–452. https://doi.org/10.1038/nature05091.Increasing

Montgomery, J. E., Parsons, M. J., & Hyde, D. R. (2010). A Novel Model of Retinal Ablation Demonstrates That the Extent of Rod Cell Death Regulates the Origin of the Regenerated Zebrafish Rod Photoreceptors. *Journal of Comparative Neurology*, *518*(6), 800–814. https://doi.org/10.1002/cne.22243.A

Moraga, A., Pradillo, J. M., García-culebras, A., Palma-tortosa, S., Ballesteros, I., Hernández-jiménez, M., … Lizasoain, I. (2015). Aging increases microglial proliferation , delays cell migration , and decreases cortical neurogenesis after focal cerebral ischemia. *Journal of Neuroinflammation*, *12*(87), 1–12. https://doi.org/10.1186/s12974-015-0314-8

Moskalev, A. A., Shaposhnikov, M. V., Plyusnina, E. N., Zhavoronkov, A., Budovsky, A., Yanai, H., & Fraifeld, V. E. (2013). The role of DNA damage and repair in aging through the prism of Koch-like criteria. *Ageing Research Reviews*, *12*(2), 661–684. https://doi.org/10.1016/j.arr.2012.02.001

Mostoslavsky, R., Chua, K. F., Lombard, D. B., Pang, W. W., Fischer, M. R., Gellon, L., … Alt, F. W. (2006). Genomic instability and aging-like phenotype in the absence of mammalian SIRT6. *Cell*, *124*(2), 315–329. https://doi.org/10.1016/j.cell.2005.11.044

Moyzis, R. K., Buckingham, J. M., Cram, L. S., Dani, M., Deaven, L. L., Jones, M. D., … Wu, J. R. (1988). A highly conserved repetitive DNA sequence, (TTAGGG)n, present at the telomeres of human chromosomes. *Proceedings of the National Academy of Sciences of the United States of America*, *85*(18), 6622–6626. https://doi.org/10.1073/pnas.85.18.6622

Mueller, T. (2012). What is the thalamus in zebrafish? *Frontiers in Neuroscience*, *6*(64), 1–14. https://doi.org/10.3389/fnins.2012.00064

Mueller, T., Dong, Z., Berberoglu, M. A., & Guo, S. (2011). The Dorsal Pallium in Zebrafish, Danio rerio (Cyprinidae, Teleostei). *Brain Research*, *1381*, 95–105. https://doi.org/10.1016/S0006-8993(00)03174-7

Mukherjee, S., Firpo, E. J., Wang, Y., & Roberts, J. M. (2011). Separation of telomerase functions by reverse genetics. *PNAS*, *108*(50), 1363–1371. https://doi.org/10.1073/pnas.1112414108

Nakamura, K. I., Takubo, K., Izumiyama-Shimomura, N., Sawabe, M., Arai, T., Kishimoto, H., … Ishikawa, N. (2007). Telomeric DNA length in cerebral gray and white matter is associated with longevity in individuals aged 70 years or older. *Experimental Gerontology*, *42*(10), 944–950. https://doi.org/10.1016/j.exger.2007.05.003

Nasrabady, S. E., Rizvi, B., Goldman, J. E., & Brickman, A. M. (2018). White matter changes in Alzheimer's disease: a focus on myelin and oligodendrocytes. *Acta Neuropathologica Communications*, *6*(22), 1–10. https://doi.org/10.1016/j.neuron.2014.01.045

Neuhauss, S. C. F., Biehlmaier, O., Seeliger, M. W., Das, T., Kohler, K., Harris, W. A., & Baier, H. (1999). Genetic Disorders of Vision Revealed by a Behavioral Screen of 400 Essential Loci in Zebrafish. *The Journal of Neuroscience*, *19*(19), 8603–8615.

Nian, S., & Lo, A. C. Y. (2019). Protecting the Aging Retina, Neuroprotection. In *Protecting the Aging Retina, IntechOpen* (pp. 1–20).

Novoa, B., Pereiro, P., López-Munõz, Varela, M., Forn-Cuní, G., Anchelin, M., … Figueras, A. (2019). Rag1 immunodeficiency-induced early aging and senescence in zebrafish are dependent on chronic inflammation and oxidative stress. *Aging Cell*, *18*, 1–17. https://doi.org/10.1111/acel.13020

O'Connell, L. A., & Hofmann, H. A. (2011). The Vertebrate Mesolimbic Reward System and

Social Behavior Network: A Comparative Synthesis. *The Journal of Comparative Neurology*, *519*, 3599–3639. https://doi.org/10.1002/cne.22735
Ohtani, N., & Hara, E. (2013). Roles and mechanisms of cellular senescence in regulation of tissue homeostasis. *Cancer Science*, *104*(5), 525–530. https://doi.org/10.1111/cas.12118
Ooto, S., Akagi, T., Kageyama, R., Akita, J., Mandai, M., Honda, Y., & Takahashi, M. (2004). Potential for neural regeneration after neurotoxic injury in the adult mammalian retina. *PNAS*, *101*(37), 13654–13659.
Otteson, D. C., Costa, A. R. D., & Hitchcock, P. F. (2001). Putative Stem Cells and the Lineage of Rod Photoreceptors in the Mature Retina of the Goldfish. *Developmental Biology*, *232*, 62–76. https://doi.org/10.1006/dbio.2001.0163
Ovadya, Y., & Krizhanovsky, V. (2014). Senescent cells: SASPected drivers of age-related pathologies. *Biogerontology*, *15*(6), 627–642. https://doi.org/10.1007/s10522-014-9529-9
Pakulski, C., Drobnik, L., & Millo, B. (2000). Age and sex as factors modifying the function of the blood-cerebrospinal fluid barrier. *Medical Science Monitor*, *6*(2), 314–318.
Palm, W., & Lange, T. de. (2008). How Shelterin Protects Mammalian Telomeres. *Annual Review of Genetics*, *42*, 301–334.
Park, J., Venteicher, A. S., Hong, J. Y., Choi, J., Jun, S., Chang, W., … Program, A. T. (2015). Telomerase modulated Wnt signalling by association with target gene chromatin. *Nature*, *460*(7251), 66–72. https://doi.org/10.1038/nature08137.Telomerase
Partnership for Solution. (2004). Chronic Conditions : Making the Case for Ongoing Care. *Robert Wood Johnson Foundation*, (September), 69. https://doi.org/http://www.partnershipforsolutions.org/statistics/reports.html
Pérez-Mancera, P. A., Young, A. R. J., & Narita, M. (2014). Inside and out: the activities of senescence in cancer. *Nature Reviews. Cancer*, *14*(8), 547–558. https://doi.org/10.1038/nrc3773
Pinto-teixeira, F., Viader-llargue, O., & Torres-mej, E. (2015). Inexhaustible hair-cell regeneration in young and aged zebrafish. *Biology Open*, *4*, 903–909. https://doi.org/10.1242/bio.012112
Powers, E. T., Morimoto, R. I., Dillin, A., Kelly, J. W., & Balch, W. E. (2009). Biological and chemical approaches to diseases of proteostasis deficiency. *Annual Review of Biochemistry*, *78*(August), 959–991. https://doi.org/10.1146/annurev.biochem.052308.114844
Qian, H., Xu, X., & Niklason, L. E. (2015). Bmk-1 regulates lifespan in Caenorhabditis elegans by activating hsp-16. *Oncotarget*, *6*(22), 18790–18799.
Rahman, R., Latonen, L., & Wiman, K. G. (2005). hTERT antagonizes p53-induced apoptosis independently of telomerase activity. *Oncogene*, *24*, 1320–1327. https://doi.org/10.1038/sj.onc.1208232
Raj, D. D. A., Moser, J., van der Pol, S. M. A., van Os, R. P., Holtman, I. R., Brouwer, N., … Boddeke, H. W. G. M. (2015). Enhanced microglial pro-inflammatory response to lipopolysaccharide correlates with brain infiltration and blood-brain barrier dysregulation in a mouse model of telomere shortening. *Aging Cell*, *14*(6), 1003–1013. https://doi.org/10.1111/acel.12370
Ramanathan, R., Kohli, A., Ingaramo, M. C., Jain, A., Leng, S. X., Punjabi, N. M., … Fedarko, N. S. (2013). Serum Chitotriosidase, a Putative Marker of Chronically Activated Macrophages, Increases With Normal Aging. *Journals of Gerontology: Medical Sciences*,

*68*(10), 1303–1309. https://doi.org/10.1093/gerona/glt022
Ranski, A. H., Kramer, A. C., Morgan, G. W., Perez, J. L., & Thummel, R. (2018). Characterization of retinal regeneration in adult zebrafish following multiple rounds of phototoxic lesion. *PeerJ*, *6*, 1–21. https://doi.org/10.7717/peerj.5646
Rao, M. B., Didiano, D., & Patton, J. G. (2017). Neurotransmitter-Regulated Regeneration in the Zebrafish Retina. *Stem Cell Reports*, *8*, 831–842. https://doi.org/10.1016/j.stemcr.2017.02.007
Raymond, P. A., Barthel, L. K., Bernardos, R. L., & Perkowski, J. J. (2006). Molecular characterization of retinal stem cells and their niches in adult zebrafish. *BMC Developmental Biology*, *6*(36), 1–17. https://doi.org/10.1186/1471-213X-6-36
Reichenbach, A., & Bringmann, A. (2013). New functions of Müller cells. *Glia*, *61*(5), 651–678.
Rera, M., Clark, R. I., & Walker, D. W. (2012). Intestinal barrier dysfunction links metabolic and inflammatory markers of aging to death in Drosophila. *Proceedings of the National Academy of Sciences of the United States of America*, *109*(52), 21528–21533. https://doi.org/10.1073/pnas.1215849110/-/DCSupplemental.www.pnas.org/cgi/doi/10.1073/pnas.1215849110
Richardson, R., Webster, A., & Moosajee, M. (2017). The zebrafish eye - a paradigm for investigating human ocular genetics. *Eye*, *31*, 68–86. https://doi.org/10.1038/eye.2016.198
Rink, E., & Wullimann, M. F. (2001). The teleostean (zebrafish) dopaminergic system ascending to the subpallium (striatum) is located in the basal diencephalon (posterior tuberculum). *Brain Research*, *889*(1–2), 316–330.
Romaniuk, A., Paszel, A., Ewa, J., Natalia, T., Hanna, L., & Anna, H. (2019). The non-canonical functions of telomerase: to turn off or not to turn off. *Molecular Biology Reports*, *46*(1), 1401–1411. https://doi.org/10.1007/s11033-018-4496-x
Roos, W. P., & Kaina, B. (2006). DNA damage-induced cell death by apoptosis, *12*(9). https://doi.org/10.1016/j.molmed.2006.07.007
Rossiello, F., Herbig, U., Longhese, M. P., Fumagalli, M., & d'Adda di Fagagna, F. (2014). Irreparable telomeric DNA damage and persistent DDR signalling as a shared causative mechanism of cellular senescence and ageing. *Current Opinion in Genetics and Development*, *26*, 89–95. https://doi.org/10.1016/j.gde.2014.06.009
Rowe-Rendleman, C., & Randolph, D. G. (2004). Possible therapy for age-related macular degeneration using human telomerase. *Brain Research Bulletin*, *62*(6), 549–553.
Ryu, S. J., Oh, Y. S., & Park, S. C. (2007). Failure of stress-induced downregulation of Bcl-2 contributes to apoptosis resistance in senescent human diploid fibroblasts. *Cell Death and Differentiation*, *14*(5), 1020–1028. https://doi.org/10.1038/sj.cdd.4402091
Sagiv, A., & Krizhanovsky, V. (2013). Immunosurveillance of senescent cells: The bright side of the senescence program. *Biogerontology*, *14*(6), 617–628. https://doi.org/10.1007/s10522-013-9473-0
Sahin, E., & Depinho, R. a. (2010). Linking functional decline of telomeres, mitochondria and stem cells during ageing. *Nature*, *464*(7288), 520–528. https://doi.org/10.1038/nature08982
Salech, F., Ponce, D. P., Sanmartín, C. D., Rogers, N. K., Chacón, C., Henríquez, M., & Behrens, M. I. (2017). PARP-1 and p53 Regulate the Increased Susceptibility to Oxidative Death of Lymphocytes from MCI and AD Patients. *Frontiers in Aging Neuroscience*, *9*(310), 1–10. https://doi.org/10.3389/fnagi.2017.00310

Salero, E., Blenkinsop, T. A., Corneo, B., Harris, A., Rabin, D., Stern, J. H., & Temple, S. (2012). Adult Human RPE Can Be Activated into a Multipotent Stem Cell that Produces Mesenchymal Derivatives. *Cell Stem Cell*, *10*(1), 88–95. https://doi.org/10.1016/j.stem.2011.11.018

Salvi, S. M., Akhtar, S., & Currie, Z. (2006). Ageing changes in the eye. *Postgrad Med J*, *82*, 581–587. https://doi.org/10.1136/pgmj.2005.040857

Sampson, T. R., Debelius, J. W., Thron, T., Wittung-stafshede, P., Knight, R., Mazmanian, S. K., … Chesselet, M. (2016). Gut Microbiota Regulate Motor Deficits and Neuroinflammation in a Model of Parkinson ' s Disease. *Cell*, 1–12. https://doi.org/10.1016/j.cell.2016.11.018

Santos, J. H., Meyer, J. N., & Houten, B. Van. (2006). Mitochondrial localization of telomerase as a determinant for hydrogen peroxide-induced mitochondrial DNA damage and apoptosis. *Human Molecular Genetics*, *15*(11), 1757–1768. https://doi.org/10.1093/hmg/ddl098

Santos, J. H., Meyer, J. N., Skorvaga, M., Annab, L. A., & Houten, B. Van. (2004). Mitochondrial hTERT exacerbates free-radical-mediated mtDNA damage. *Aging Cell*, *3*, 399–411.

Sarin, K. Y., Cheung, P., Gilison, D., Lee, E., Tennen, R. I., Wang, E., … Artandi, S. E. (2005). Conditional telomerase induction causes proliferation of hair follicle stem cells. *Nature Letters*, *436*, 1048–1052. https://doi.org/10.1038/nature03836

Sassen, W. A., & Köster, R. W. (2015). A molecular toolbox for genetic manipulation of zebrafish. *Advances in Genomics and Genetics*, *5*, 151–163. https://doi.org/10.2147/AGG.S57585

Schafer, M. J., White, T. A., Iijima, K., Haak, A. J., Ligresti, G., Atkinson, E. J., … Lebrasseur, N. K. (2017). Cellular senescence mediates fibrotic pulmonary disease. *Nature Communications*, *8*(14532), 1–11. https://doi.org/10.1038/ncomms14532

Schmidt, R., Strähle, U., & Scholpp, S. (2013). Neurogenesis in zebrafish - from embryo to adult. *Neural Development*, *8*(1), 1–13. https://doi.org/10.1186/1749-8104-8-3

Schmucker, D. L., Owen, R. L., Outenreath, R., & Thoreux, K. (2003). Basis for the Age-related Decline in Intestinal Mucosal Immunity. *Clininal & Developmental Immunology*, *10*(2–4), 167–172. https://doi.org/10.1080/10446670310001642168

Ségal-bendirdjian, E., & Geli, V. (2019). Non-canonical Roles of Telomerase: Unraveling the Imbroglio. *Frontiers in Cell and Developmental Biology*, *7*(332), 1–12. https://doi.org/10.3389/fcell.2019.00332

Serrano, M., Lin, A. W., McCurrach, M. E., Beach, D., & Lowe, S. W. (1997). Oncogenic ras provokes premature cell senescence associated with accumulation of p53 and p16(INK4a). *Cell*, *88*(5), 593–602. https://doi.org/10.1016/S0092-8674(00)81902-9

Severino, J., Allen, R., Balin, S., Balin, A., & Cristofalo, V. J. (2000). Is β-Galactosidase Staining a Marker of Senescence in Vitro and in Vivo? *Experimental Cell Research*, *257*(1), 162–171.

Shaerzadeh, F., Phan, L., Miller, D., Dacquel, M., Hachmeister, W., Hansen, C., … Khoshbouei, H. (2020). Microglia senescence occurs in both substantia nigra and ventral tegmental area. *Glia*.

Shannon, P., Markiel, A., Ozier, O., Baliga, N. S., Wang, J. T., Ramage, D., … Ideker, T. (2003). Cytoscape: A Software Environment for Integrated Models of Biomolecular Interaction Networks. *Cold Spring Harbor Laboratory Press*, *13*, 2498–2504. https://doi.org/10.1101/gr.1239303.metabolite

Shoji, H., Takao, K., Hattori, S., & Miyakawa, T. (2016). Age-related changes in behavior in C57BL/6J mice from young adulthood to middle age. *Molecular Brain*, *9*(11), 1–18. https://doi.org/10.1186/s13041-016-0191-9

Sparrow, J. R., Fishkin, N., Zhou, J., Cai, B., Jang, Y. P., Krane, S., … Nakanishi, K. (2003). A2E, a byproduct of the visual cycle. *Vision Research*, *43*, 2983–2990. https://doi.org/10.1016/S0042-6989(03)00475-9

Spence, R., Fatema, M. K., Reichard, M., Huq, K. A., Wahab, M. A., Ahmed, Z. F., & Smith, C. (2006). The distribution and habitat preferences of the zebrafish in Bangladesh. *Journal of Fish Biology*, *69*(5), 1435–1448. https://doi.org/10.1111/j.1095-8649.2006.01206.x

Spence, R., Gerlach, G., Lawrence, C., & Smith, C. (2008). The behaviour and ecology of the zebrafish, Danio rerio. *Biological Reviews*, *83*(1), 13–34. https://doi.org/10.1111/j.1469-185X.2007.00030.x

Spittau, B. (2017). Aging Microglia — Phenotypes, Functions and Implications for Age-Related Neurodegenerative Diseases. *Frontiers in Aging*, *9*(194), 1–9. https://doi.org/10.3389/fnagi.2017.00194

Sprungala, S. (2009). *Telomere length, telomerase and maintenance of stem cells in the adult zebrafish brain*.

Steinacker, P., Verde, F., Fang, L., Feneberg, E., Oeckl, P., Roeber, S., … Otto, M. (2018). Chitotriosidase ( CHIT1 ) is increased in microglia and macrophages in spinal cord of amyotrophic lateral sclerosis and cerebrospinal fluid levels correlate with disease severity and progression, 239–247. https://doi.org/10.1136/jnnp-2017-317138

Stenkamp, D. L. (2015). Development of the Vertebrate Eye and Retina. *Prog Mol Biol Transl Sci.*, *134*, 397–414. https://doi.org/10.1016/bs.pmbts.2015.06.006.Development

Sterba, G. (1962). *Freshwater Fishes of the World.* (London: Vi).

Strominger, I., Elyahu, Y., Berner, O., Reckhow, J., Mittal, K., Nemirovsky, A., & Monsonego, A. (2018). The choroid plexus functions as a niche for T-cell stimulation Within the central nervous system. *Frontiers in Immunology*, *9*(1066), 1–15. https://doi.org/10.3389/fimmu.2018.01066

Sullivan, R. J. O., & Karlseder, J. (2010). Telomeres: protecting chromosomes against genome instability. *Nature Reviews Molecular Cell Biology*, *11*(3), 171–181. https://doi.org/10.1038/nrm2848.Telomeres

Sung, Y. H., Ali, M., & Lee, H. (2014). Extracting Extra-Telomeric Phenotypes from Telomerase Mouse Models. *Yonsei Med J*, *55*(1), 1–8.

Suriyampola, DS, S., R, S., T, R., A, B., & EP, M. (2016). Zebrafish Social Behavior in the Wild. *Zebrafish*, *13*(1), 1–8.

Szklarczyk, D., Gable, A. L., Lyon, D., Junge, A., Wyder, S., Huerta-cepas, J., … Mering, C. Von. (2019). STRING v11: protein – protein association networks with increased coverage , supporting functional discovery in genome-wide experimental datasets. *Nucleic Acids Research*, *47*, 607–613. https://doi.org/10.1093/nar/gky1131

Talens, R. P., Christensen, K., Putter, H., Willemsen, G., Christiansen, L., Kremer, D., … Heijmans, B. T. (2012). Epigenetic variation during the adult lifespan: Cross-sectional and longitudinal data on monozygotic twin pairs. *Aging Cell*, *11*(4), 694–703. https://doi.org/10.1111/j.1474-9726.2012.00835.x

Tappeiner, C., Gerber, S., Enzmann, V., Balmer, J., Jazwinska, A., & Tschopp, M. (2012). Visual acuity and contrast sensitivity of adult zebrafish. *Frontiers in Zoology*, *9*(10), 1–6.

Tarr, A. J., Chen, Q., Wang, Y., Sheridan, J. F., & Quan, N. (2012). Neural and behavioral responses to low-grade iflammation. *Behav Brain Res.*, *235*(2), 334–341.

https://doi.org/10.1016/j.bbr.2012.07.038.NEURAL
Tchkonia, T., Zhu, Y., Deursen, J. Van, Campisi, J., & Kirkland, J. L. (2013). Cellular senescence and the senescent secretory phenotype therapeutic opportunities. *The Journal of Clinical Investigation*, *123*(3), 966–972. https://doi.org/10.1172/JCI64098.966
Telegina, D. V, Kozhevnikova, O. S., & Kolosova, N. G. (2018). Changes in Retinal Glial Cells with Age and during Development of Age-Related Macular Degeneration. *Biochemistry*, *83*(9), 1009–1017.
Thevaranjan, N., Puchta, A., Schulz, C., Naidoo, A., Szamosi, J. C., Verschoor, C. P., … Bowdish, D. M. (2017). Age-Associated Microbial Dysbiosis Promotes Intestinal Permeability, Systemic Inflammation, and Macrophage Dysfunction. *Cell Host & Microbe*, *21*, 455–466. https://doi.org/10.1016/j.chom.2017.03.002
Thomas, J. L., Nelson, C. M., Luo, X., Hyde, D. R., & Thummel, R. (2012). Characterization of Multiple Light Damage Paradigms Reveals Regional Differences in Photoreceptor Loss. *Exp. Eye Res.*, *97*(1), 105–116. https://doi.org/10.1016/j.exer.2012.02.004.Characterization
Thomas, J. L., Ranski, A. H., Morgan, G. W., & Thummel, R. (2016). Reactive gliosis in the adult zebrafish retina. *Experimental Eye Research*, *143*, 98–109.
Thummel, R., Kassen, S. C., Enright, J. M., Nelson, C. M., Montgomery, J. E., & Hyde, D. R. (2008). Characterization of Müller glia and neuronal progenitors during adult zebrafish retinal regeneration. *Experimental Eye Research*, *87*(5), 433–444. https://doi.org/10.1016/j.exer.2008.07.009.Characterization
Tinetti, M.; Fried, T.; Boyd, C. (2012). Designing Health Care for the Most Common Chronic Condition —Multimorbidity. *JAMA*, *257*(5), 2432–2437. https://doi.org/10.1016/j.immuni.2010.12.017.Two-stage
Unit, G., & Health, D. of. (2014). *DH Corporate Plan 2014-2015*. *Corporate Report*. https://doi.org/https://assets.publishing.service.gov.uk/government/uploads/system/uploads/attachment_data/file/320698/DH_corporate_plan.pdf
van Deursen, J. M. (2014). The role of senescent cells in ageing. *Nature*, *509*(7501), 439–446. https://doi.org/10.1038/nature13193
Van houcke, J., Bollaerts, I., Geeraerts, E., Davis, B., Beckers, A., Van Hove, I., … Moons, L. (2017). Successful optic nerve regeneration in the senescent zebrafish despite age-related decline of cell intrinsic and extrinsic response processes. *Neurobiology of Aging*, *60*, 1–10. https://doi.org/10.1016/j.neurobiolaging.2017.08.013
Van Houcke, J., Geeraerts, E., Vanhunsel, S., Beckers, A., Noterdaeme, L., Christiaens, M., … Groef, L. De. (2019). Extensive growth is followed by neurodegenerative pathology in the continuously expanding adult zebrafish retina. *Biogerontology*, *20*(1), 109–125. https://doi.org/10.1007/s10522-018-9780-6
Vogeli, C., Shields, A. E., Lee, T. A., Gibson, T. B., Marder, W. D., Weiss, K. B., & Blumenthal, D. (2007). Multiple chronic conditions: Prevalence, health consequences, and implications for quality, care management, and costs. *Journal of General Internal Medicine*, *22*(SUPPL. 3), 391–395. https://doi.org/10.1007/s11606-007-0322-1
Vogler, M., Dickens, D., Dyer, M. J. S., Owen, A., Pirmohamed, M., & Cohen, G. M. (2011). The B-cell lymphoma 2 (BCL2)-inhibitors, ABT-737 and ABT-263, are substrates for P-glycoprotein. *Biochemical and Biophysical Research Communications*, *408*(2), 344–349. https://doi.org/10.1016/j.bbrc.2011.04.043
Wagner, K. D., Ying, Y., Leong, W., Jiang, J., Hu, X., Chen, Y., … Ye, J. (2017). The differential spatiotemporal expression pattern of shelterin genes throughout lifespan. *Aging*, *9*(4),

1219–1232. https://doi.org/10.18632/aging.101223
Wan, J., & Goldman, D. (2016). Retina regeneration in zebrafish. *Current Opinion in Genetics and Development*, *40*, 41–47. https://doi.org/10.1016/j.gde.2016.05.009.Retina
Wang, C., Jurk, D., Maddick, M., Nelson, G., Martin-ruiz, C., & Von Zglinicki, T. (2009). DNA damage response and cellular senescence in tissues of aging mice. *Aging Cell*, *8*(3), 311–323. https://doi.org/10.1111/j.1474-9726.2009.00481.x
Wang, J., Feng, Y., Han, P., Wang, F., Luo, X., Liang, J., … Sun, X. (2018). Photosensitization of A2E triggers telomere dysfunction and accelerates retinal pigment epithelium senescence. *Cell Death and Disease*, *9*(178), 1–14. https://doi.org/10.1038/s41419-017-0200-7
White, D. T., Sengupta, S., Saxena, M. T., Xu, Q., Hanes, J., Ding, D., … Mumm, J. S. (2017). Immunomodulation-accelerated neuronal regeneration following selective rod photoreceptor cell ablation in the zebrafish retina. *PNAS*, 719–728. https://doi.org/10.1073/pnas.1617721114
Wiemann, S. U., Satyanarayana, A., Tsahuridu, M., Tillmann, H. L., Zender, L., Klempnauer, J., … Rudolph, K. L. (2019). Hepatocyte telomere shortening and senescence are general markers of human liver cirrhosis. *FASEB Journal*, *16*(9), 935–942.
Wing, G. L., Blanchard, G. C., & Weiter, J. J. (1978). The topography and age relationship of lipofuscin concentration in the retinal pigment epithelium. *Invest Ophthalmol Vis Sci.*, *17*(7), 601–607.
Wright, W., Piatyszek, M., Rainey, W., Byrd, W., & Shay, J. (1996). Telomerase activity in human germline and embryonic tissues and cells. *Dev Genet.*, *18*(2), 173–179.
Wui-Man Lau, B., On-Lam Wong, A., Sai-Wah Tsao, G., So, K.-F., & Ka-Fun Yip, H. (2008). Molecular Cloning and Characterization of the Zebrafish (Danio rerio) Telomerase Catalytic Subunit (Telomerase Reverse Transcriptase, TERT). *Journal of Molecular Neuroscience*, *34*, 63–75.
Xue W., Zender L., Miething C., Dickins R., Hernando R., Krizhanovsky V., Cordon-Cardo C., L. S. (2007). Senescence and tumour clearance is triggered by p53 restoration in murine liver carcinomas. *Nature*, *445*(7128), 656–660. https://doi.org/10.1177/1043454210368532.Analysis
Yamaguchi, R., & Perkins, G. (2012). Finding a Panacea Among Combination Cancer Therapies. *Cancer Research*, *72*(1), 18–23. https://doi.org/10.1158/0008-5472.CAN-11-3091.Finding
Yamazaki, Y., Baker, D., Tachibana, M., Liu, C., van Deursen, J., Brott, T., … Kanekiyo, T. (2016). Vascular Cell Senescence contributes to Blood-Brain Barrier Breakdown. *Stroke*, *47*, 1068–1077. https://doi.org/10.1161/STROKEAHA.115.010835
Yang, N.-C., & Hu, M.-L. (2005). The limitations and validities of senescence associated-β-galactosidase activity as an aging marker for human foreskin fibroblast Hs68 cells. *Experimental Gerontology*, *40*(10), 813–819.
Yousefzadeh, M. J., Zhao, J., Bukata, C., Wade, E. A., Mcgowan, S. J., Angelini, L. A., … Niedernhofer, L. J. (2020). Tissue specificity of senescent cell accumulation during physiologic and accelerated aging of mice. *Aging Cell*, 1–13. https://doi.org/10.1111/acel.13094
Yu, L., Tucci, V., Kishi, S., & Zhdanova, I. V. (2006). Cognitive aging in zebrafish. *PLoS ONE*, *1*(1). https://doi.org/10.1371/journal.pone.0000014
Zambusi, A., Burhan, Ö. P., Giaimo, R. Di, Schmid, B., & Ninkovic, J. (2020). Granulins Regulate Aging Kinetics in the Adult Zebrafish Telencephalon. *Cells*, *9*(350), 1–25.

Zhang, C., Zhu, Q., & Hua, T. (2010). Aging of cerebellar Purkinje cells. *Cell Tissue Res*, *341*, 341–347. https://doi.org/10.1007/s00441-010-1016-2

Zhang, X., Ye, C., Sun, F., Wei, W., Hu, B., & Wang, J. (2016). Both complexity and location of DNA damage contribute to cellular senescence induced by ionizing radiation. *PLoS ONE*, *11*(5), 1–16. https://doi.org/10.1371/journal.pone.0155725

Zheng, Q., Liu, P., Gao, G., Yuan, J., Wang, P., Huang, J., … Wang, G. (2019). Mitochondrion-processed TERC regulates senescence without affecting telomerase activities. *Protein & Cell*, *10*(9), 631–648. https://doi.org/10.1007/s13238-019-0612-5

Zhong, F., Savage, S. A., Shkreli, M., Giri, N., Jessop, L., Myers, T., … Artandi, S. E. (2011). Disruption of telomerase trafficking by TCAB1 mutation causes dyskeratosis congenita. *Genes and Development*, *25*(1), 11–16. https://doi.org/10.1101/gad.2006411

Zhou, Y., Zhou, B., Pache, L., Chang, M., Benner, C., Chanda, S. K., … Tanaseichuk, O. (2019). Metascape provides a biologist-oriented resource for the analysis of systems-level datasets. *Nature Communications*, *10*(1523), 1–10. https://doi.org/10.1038/s41467-019-09234-6

Zhu, S., & Coffman, J. A. (2017). Simple and fast quantification of DNA damage by real-time PCR, and its application to nuclear and mitochondrial DNA from multiple tissues of aging zebrafish. *BMC Research Notes*, *10*(1), 1–6. https://doi.org/10.1186/s13104-017-2593-x

Zhu, X., Ji, M., Li, S., Li, B., Mei, L., & Yang, J. (2019). Systemic Inflammation Impairs Mood Function by Disrupting the Resting-State Functional Network in a Rat Animal Model Induced by Lipopolysaccharide Challenge. *Hindawi - Mediators of Inflammation*, *2019*, 1–11. https://doi.org/10.1155/2019/6212934 Research

Zielinski, M. R., Dunbrasky, D. L., Taishi, P., Souza, G., & Krueger, J. M. (2013). Vagotomy Attenuates Brain Cytokines and Sleep Induced by Peripherally Administered Tumor Necrosis Factor-α and Lipopolysaccharide in Mice. *Sleep*, *36*(8), 1227–1238.